

THE EFFECTS OF ELEVATED ULTRAVIOLET-B RADIATION
ON THE GROWTH AND DEVELOPMENT OF THE PRIMARY
LEAF OF WHEAT (TRITICUM AESTIVUM L. CV MARIS
HUNTSMAN)

Laura Hopkins

A Thesis Submitted for the Degree of PhD
at the
University of St Andrews



1997

Full metadata for this item is available in
St Andrews Research Repository
at:
<http://research-repository.st-andrews.ac.uk/>

Please use this identifier to cite or link to this item:
<http://hdl.handle.net/10023/13563>

This item is protected by original copyright

**The Effects of Elevated Ultraviolet-B Radiation
on the Growth and Development
of the Primary Leaf of Wheat
(*Triticum aestivum* L. cv Maris Huntsman)**

**By
Laura Hopkins**

**Submitted in Accordance with the Requirements of the Degree
Doctor of Philosophy**

**The University of St. Andrews
School of Biological and Medical Sciences
Department of Plant Sciences**

July 1997



ProQuest Number: 10167204

All rights reserved

INFORMATION TO ALL USERS

The quality of this reproduction is dependent upon the quality of the copy submitted.

In the unlikely event that the author did not send a complete manuscript and there are missing pages, these will be noted. Also, if material had to be removed, a note will indicate the deletion.



ProQuest 10167204

Published by ProQuest LLC (2017). Copyright of the Dissertation is held by the Author.

All rights reserved.

This work is protected against unauthorized copying under Title 17, United States Code
Microform Edition © ProQuest LLC.

ProQuest LLC.
789 East Eisenhower Parkway
P.O. Box 1346
Ann Arbor, MI 48106 – 1346

TR C 320

For
Mum, Dad and Anita
and
In memory of
Win and John Spencer
and
Ev and Ken Hopkins

DECLARATIONS

(i) I, Laura Hopkins, hereby certify that this thesis, which is approximately 45,000 words in length, has been written by me, that it is the record of work carried out by me and that it has not been submitted in any previous application for a higher degree.

date 1/7/97..... signature of candidate

(ii) I was admitted as a research student in October 1993 and as a candidate for the degree of Doctor of Philosophy in October 1993; the higher study for which this is a record was carried out in the School of Biological Sciences at the University of Manchester between 1993 and 1994, and at the University of St. Andrews between 1994 and 1996.

date 1/7/97..... signature of candidate

(iii) I hereby certify that the candidate has fulfilled the conditions of the Resolution and Regulations appropriate for the degree of Doctor of Philosophy in the University of St. Andrews and that the candidate is qualified to submit this thesis in application for that degree.

date 30/6/97..... signature of supervisor,

COPYRIGHT

In submitting this thesis to the University of St. Andrews I understand that I am giving permission for it to be made available for use in accordance with the regulations of the University Library for the time being in force, subject to any copyright vested in the work not being affected thereby. I also understand that the title and abstract will be published, and that a copy of the work may be made and supplied to any *bona fide* library or research worker.

date 1/7/97..... signature of candidate

ABSTRACT

Seedlings of *Triticum aestivum* L. cv. Maris Huntsman were grown for 7 days in a controlled environment chamber (16 hour photoperiod: PAR - photosynthetically active radiation), in the presence and absence of ultraviolet-B (UV-B: 280-320nm) radiation (+30% increase on ambient). UV-B resulted in a 17% reduction in leaf length due to changes in both the rate and duration of cell division and elongation. Measurements of the spatial distribution of cell division and elongation within the primary leaf were used to determine the temporal distribution of cells (*i.e.* cell age). The cell age gradient allows for the comparison of direct, and indirect UV-B responses, which result from the altered growth. Direct effects of UV-B included a reduction in chloroplast and mitochondrial transverse area, and an increase in chloroplast number, which suggests that UV-B affects organelle division. The developmental changes in protein content and amino acid free pools were increased as a direct result of UV-B treatment. In contrast, increases in chlorophyll content were due to an indirect effect of UV-B via altered growth. UV-B had no effect on the developmental changes in photosynthetic capacity and efficiency, and carbohydrate status of the primary leaf. The primary leaf of wheat has provided a model system in which to examine the effects of UV-B on leaf development. This study highlights the need to consider cell age when determining the response of plants to UV-B.

ACKNOWLEDGEMENTS

I would like to thank my supervisor Dr. Alyson Tobin for advice, encouragement and above all, patience during the past 4 years of this study. Thanks are also due to Harry Hodge and John Mackie for their technical advice and expertise.

A big thank you must go to all those resident in the basement of the Harold Mitchell Building 1994-1997, including Lucy Peat, Jonathan Howarth, Neil Harris, Mike Ward and Urte Schlürter for many a 'ground hog' like Friday night out, Lisa Smith and Pam Gray for help in preparing this thesis, and Mark Bond who shared in the never ending saga of the growth cabinet!

Finally, I would like to thank my mum, dad, sister, Jon Tonge, and my nephew Connell-Patrick for their constant encouragement and support.

TABLE OF CONTENTS

Declarations.....	i
Copyright.....	ii
Abstract.....	iii
Acknowledgements.....	iv
Contents.....	v
List of Figures.....	xvi
List of Plates.....	xxiii
Abbreviations.....	xxiv

CHAPTER 1:

General Introduction.....	1
1.1 Plants and Light.....	2
1.2 The Solar Spectrum.....	2
1.3 UV-B Radiation and Stratospheric Ozone.....	3
1.3.1 The Stratospheric Ozone Layer.....	3
1.3.2 The History of Stratospheric Ozone Depletion.....	4
1.3.3 How Does Stratospheric Ozone Layer Depletion Occur?.....	6
1.3.4 Increases in UV-B Radiation Reaching The Earth's Surface.....	7
1.4 Biological Consequences of Increased UV-B Radiation.....	9
1.5 Biological Weighting of UV-B Measurements.....	9
1.6 Effects of UV-B Radiation on Plants.....	10
1.6.1 Plant Growth and Morphology.....	10
1.6.2 Photosynthetic Targets.....	12

1.6.3 DNA Damage and Repair.....	14
1.7 Why are Plant Responses to UV-B Radiation so Variable?.....	15
1.7.1 Environmental Factors.....	15
1.7.1.1 Light.....	15
1.7.1.2 Water Stress.....	16
1.7.1.3 Temperature.....	17
1.7.2 Developmental Stage of the Plant.....	17
1.8 Aims of Thesis.....	19
 CHAPTER 2:	
Materials and Methods.....	23
2.1 Materials.....	24
2.2 Plant Material and Growth Conditions.....	24
2.3 Selection of Plant Tissue.....	25
2.4 Statistical Analysis.....	25
2.5 Primary Leaf Development.....	26
2.5.1 Growth Rate Determination.....	26
2.5.2 Fresh and Dry Weight Determination.....	26
2.5.3 Leaf Area and Width.....	26
2.5.4 Mitotic Index.....	26
2.5.5 Cell Doubling Time.....	27
2.5.6 Leaf Elongation.....	28
2.5.7 Cell Age Determination.....	29
2.5.8 Epidermal Cell Length.....	30

2.5.9 Mesophyll Cell Number.....	31
2.6 Transmission Electron Microscopy.....	31
2.6.1 Fixation.....	31
2.6.2 Post Fixation.....	31
2.6.3 Dehydration.....	32
2.6.4 Embedding.....	32
2.6.5 Ultrathin Sectioning.....	32
2.6.6 Heavy Metal Staining.....	33
2.6.7 Examination of Tissue.....	33
2.6.8 Printing.....	33
2.7 Light Microscopy.....	34
2.7.1 Thick Sectioning.....	34
2.7.2 Staining.....	34
2.7.3 Examination of Tissue.....	34
2.8 Leaf and Cell Structure.....	34
2.9 Determination of Chloroplast Number per Mesophyll Cell.....	37
2.9.1 Preparation of Tissue.....	37
2.9.2 Preparation of Slides.....	37
2.9.3 Confocal Microscopy.....	37
2.9.4 Printing Confocal Images.....	38
2.10 Chlorophyll Determination.....	38
2.11 Photosynthesis Measurements Using the Leaf Disc Electrode.....	39
2.11.1 Leaf Disc Electrode.....	39
2.11.1.1 Calibration.....	39

2.11.2	Photosynthesis Measurements.....	39
2.11.3	Dark Respiration.....	40
2.12	Carbohydrate Determination.....	40
2.12.1	Glucose Standard Curve.....	40
2.12.2	Preparation of Samples.....	40
2.12.3	Total Soluble Carbohydrates.....	41
2.12.4	Total Insoluble Carbohydrates.....	41
2.13	Protein Analysis.....	42
2.13.1	Soluble Protein Determination.....	42
2.13.2	Protein Extraction.....	42
2.14	Determination of Amino Acid Free Pools.....	42
2.14.1	Preparation of Tissue.....	42
2.14.2	Preparation of Standards.....	43
2.14.3	High Pressure Liquid Chromatography.....	43
2.14.3.1	Gradient Solvents and Programme.....	43
2.14.4	Pre-column Derivatisation of Amino Acids and Detection.....	44
2.14.5	Amino Acid Determination.....	45
2.14.6	Amino Acid Quantification.....	45
2.15	¹⁴ C CO ₂ Pulse-chase Labelling of Amino Acids.....	45
2.15.1	¹⁴ C Labelling.....	45
2.15.2	Determination of ¹⁴ C in Amino Acid Fractions.....	46
2.15.2.1	Scintillation Counter.....	47

CHAPTER 3:

Effects of UV-B Radiation on The Morphology of The Primary Leaf of Wheat.....	57
INTRODUCTION.....	58
3.1 Plant Growth.....	58
3.1.1 What is Growth?.....	58
3.1.2 Plant Growth Analysis.....	59
3.2 Control of Plant Growth.....	59
3.3 Chapter Aims.....	60
RESULTS.....	61
3.4 Effects of UV-B on Wheat Leaf Growth.....	61
3.4.1 Total Leaf Growth.....	61
3.4.2 Primary Leaf Growth.....	61
3.4.3 Primary Leaf Width.....	62
3.4.4 Primary Leaf Area.....	63
3.4.5 Primary Leaf Fresh and Dry Weight.....	63
3.4.6 Specific Primary Leaf Area.....	63
3.4.7 Primary Leaf Thickness.....	63
DISCUSSION.....	71
3.5 Growth of The Primary Leaf of Wheat.....	71
3.6 Changes in Primary Leaf Growth Under UV-B.....	72

CHAPTER 4:

Effects of UV-B Radiation on Primary Leaf Cell Development in Wheat.....	75
INTRODUCTION.....	76
4.1 Leaf Development.....	76
4.1.1 Dicotyledon Leaf.....	77
4.1.2 Monocotyledon Leaf.....	77
4.1.2.1 Grass Leaf Development - a Model System.....	78
4.2 Mechanisms and Regulation of Cell Division and Expansion.....	78
4.2.1 Cell Division.....	78
4.2.2 Cell Expansion.....	79
4.3 Chapter Aims.....	80
RESULTS.....	83
4.4 Effects of UV-B on Cell Division in the Primary Leaf Basal Meristem.....	83
4.4.1 Mitotic Index.....	83
4.4.2 Cell Doubling Time.....	84
4.5 Effects of UV-B on Cell Elongation.....	85
4.5.1 Mesophyll Cell Numbers.....	85
4.5.2 Epidermal Cell Length.....	85
4.5.3 Spatial Distribution of Segmental Elongation Rates (SER) Within the Cell Elongation Zone.....	86
4.5.4 Spatial Distribution of Vertical Displacement Velocity (V_D) Within the Cell Elongation Zone.....	86
4.6 Effects of UV-B on Cellular Differentiation.....	87
4.6.1 Tissue Preservation and Structure.....	87

4.6.2 Volume Fractions of Tissue Types in the Primary Leaf.....	87
4.6.3 Frequency of Cell Types in the Primary Leaf.....	88
4.7 Cell Age Determination.....	88
DISCUSSION.....	106
4.8 Effects of UV-B on Cell Division.....	106
4.9 Effects of UV-B on Cell Elongation.....	109
4.10 Consequences of Altered Cell Division and Elongation on the Growth of the Primary leaf.....	112
4.11 Effects of UV-B on Cellular Differentiation.....	113
4.12 Effect of Growth Under UV-B on the Cell Age Gradient Within the Primary Leaf of Wheat.....	114

CHAPTER 5:

Effects of UV-B Radiation on the Ultrastructural Development of Mesophyll Cells In the Primary Leaf of Wheat.....	116
--	------------

INTRODUCTION.....	117
--------------------------	------------

5.1 Mesophyll Cell Ultrastructure.....	117
--	-----

5.1.1 The Chloroplast.....	118
----------------------------	-----

5.1.1.1 Structure.....	118
------------------------	-----

5.1.1.2 Biogenesis.....	119
-------------------------	-----

5.1.1.3 Changes in Chloroplast Populations During Leaf Development.....	119
---	-----

5.1.2 The Mitochondria.....	120
-----------------------------	-----

5.1.2.1 Structure.....	120
------------------------	-----

5.1.2.2 Biogenesis.....	121
5.1.2.3 Changes in Mitochondria Populations During Leaf Development.....	121
5.1.3 Effects of UV-B on Cell Ultrastructure.....	122
5.2 Quantitative Analysis of Subcellular Compartmentation Using Stereology.....	123
5.2.1 Stereological Principles.....	123
5.2.1.1 Volume Fraction.....	123
5.2.1.2 Sampling.....	124
5.2.1.3 Errors.....	125
5.3 Chapter Aims.....	126
RESULTS.....	129
5.4 Effects of UV-B on Mesophyll Cell Structure.....	129
5.5 LM Analysis.....	129
5.5.1 Mesophyll Cell Transverse Area.....	129
5.5.2 Vacuole Volume Fraction.....	130
5.6 TEM Analysis.....	130
5.6.1 Tissue Preservation.....	130
5.6.2 Effects of UV-B on Mesophyll Cell Ultrastructure.....	130
5.6.2.1 Chloroplast Volume Fraction.....	131
5.6.2.2 Chloroplast Transverse Area.....	131
5.6.2.3 Mitochondrial Volume Fraction.....	132
5.6.2.4 Mitochondrion Transverse Area.....	132
5.6.3 Effects of UV-B on Chloroplast Ultrastructure.....	133
5.6.3.1 Granal Thylakoid Volume Fraction.....	133

5.6.3.2 Stromal Thylakoid Volume Fraction.....	133
5.6.3.3 Granal Sac Number Per Granum.....	133
5.7 Effect of UV-B on Chloroplast Number Per Mesophyll Cell.....	134
DISCUSSION.....	160
5.8 Mesophyll Cell Development In the Wheat Primary.....	160
5.9 Changes In Mesophyll Cell Development Under UV-B.....	164
5.10 Summary.....	169
CHAPTER 6:	
Effects of UV-B Radiation on the Metabolism of the Developing Primary Leaf of Wheat.....	171
INTRODUCTION.....	172
6.1 Changes In Metabolism During Leaf Development.....	173
6.1.1 Photosynthesis.....	173
6.1.2 Photorespiration.....	174
6.1.3 Respiration.....	174
6.1.4 Amino Acid Metabolism.....	175
6.2 Interaction Between Different Metabolic Pathways During Leaf Development.....	176
6.3 Cell Ultrastructure and Metabolism.....	177
6.4 Chapter Aims.....	178
RESULTS.....	179
6.5 Effect of UV-B on the Chlorophyll Content of the Primary Leaf.....	179
6.6 Effect of UV-B on Photosynthesis in the Primary Leaf.....	180
6.6.1 Photosynthetic Rate.....	180

6.6.2 Photosynthetic Efficiency.....	180
6.7 Effect of UV-B on Dark Respiration in the Primary Leaf.....	180
6.8 Effect of UV-B on the Carbohydrate Content of the Primary Leaf.....	181
6.8.1 Total Soluble Carbohydrate.....	181
6.8.2 Total Insoluble Carbohydrate.....	181
6.9 Effect of UV-B on the Soluble Protein Content of the Primary Leaf.....	182
6.10 Effect of UV-B on the Free Amino Acid Pools of the Primary Leaf.....	183
6.10.1 Total Free Amino Acid Pool.....	183
6.10.2 Abundant Amino Acid Pools.....	183
6.10.3 Other Protein Amino Acid Pools.....	184
6.11 Effect of UV-B on the Incorporation of ¹⁴ C Into The Abundant Amino Acid Pools.....	185
DISCUSSION.....	209
6.12 Changes in Carbon Metabolism During Leaf Development.....	209
6.13 Effects of UV-B on Carbon Metabolism During Leaf Development.....	216
6.14 Changes in Amino Acid Free Pools During Leaf Development.....	223
6.15 Effect of UV-B on Amino Acid Free Pools During Leaf Development.....	225
6.15.1 The Incorporation of ¹⁴ C Into Amino Acid Free Pools.....	227
6.15.1.1 Glycine and Serine.....	227
6.15.1.2 Aspartate.....	228
6.15.1.3 Glutamate.....	228
6.15.1.4 Asparagine.....	229
6.15.1.5 Glutamine.....	229

6.15.1.6 Consequences of UV-B Radiation on the Flow of Carbon Into Amino Acid Free Pools.....	229
6.16 Summary.....	230
 CHAPTER 7:	
General Discussion.....	233
7.1 Changes in Leaf Morphology in Response to UV-B.....	234
7.2 UV-B Induced Changes in Cell Division and Elongation Alter Leaf Morphology.....	235
7.3 Changes in the Development of Cell Structure in Response to UV-B.....	237
7.4 Changes in Metabolic Development in Response to UV-B.....	239
7.5 Conclusions.....	241
 CHAPTER 8:	
References.....	242

LIST OF FIGURES

Fig. 1.1 Solar Spectrum (λ 290-1100nm) at the Earth's Surface.....	20
Fig 1.2 Reactions Representing Photochemical Loss of Ozone in the Polar Vortex.....	21
Fig. 1.3 UV Action Spectra.....	22
Fig. 2.1 Spectral Distribution of UV-B in Plant Growth Cabinet.....	48
Fig. 2.2 An Example of the Progressive Sampling Technique Used to Estimate the Number of Micrographs for Stereological Determination.....	49
Fig. 2.3 Glucose Standard Curve.....	52
Fig. 2.4 Thyroglobulin Standard Curve.....	53
Fig. 2.5 HPLC Trace of Amino Acid Standards.....	54
Table 2.1 Breakpoints for the HPLC Solvent Gradient.....	55
Fig. 2.6 Diagrammatic Representation of Experimental Apparatus Used for $^{14}\text{CO}_2$ Pulse-chase Study.....	56
Fig. 3.1 Effect of UV-B radiation on (a) total plant height, and (b) meristem displacement.....	64
Fig. 3.2 Effect of UV-B radiation on primary leaf length (a) and growth rate (b).....	65
Fig. 3.3 Effect of UV-B radiation on the width of 7-d-old primary leaves.....	66
Fig. 3.4 Effect of UV-B radiation on primary leaf area.....	67

Fig. 3.5 Effect of UV-B radiation on primary leaf (a) fresh weight , and (b) dry weight.....	68
Fig. 3.6 Effect of UV-B radiation on specific leaf area.....	69
Fig. 3.7 Effect of UV-B radiation on the average (a) maximum, and (b) minimum thickness of 7-d-old primary leaves.....	70
Fig. 4.1 The Cell Cycle.....	82
Fig. 4.2 Effect of UV-B radiation on the mitotic index of basal cells of 7-d-old primary leaves.....	91
Fig. 4.3 Effect of UV-B radiation on the frequency of cells in (a) interphase, (b) prophase, (c) metaphase, (d) anaphase and (e) telophase in 7-d-old primary leaves.....	92
Fig. 4.4 Effect of UV-B radiation on the accumulation of meristematic cells in metaphase after colchicine treatment (a), and the linear regression of accumulation (b).....	95
Fig. 4.5 Effect of UV-B radiation on mesophyll cell numbers along the length of 7-d-old primary leaves.....	96
Fig. 4.6 Effect of UV-B radiation on the length of epidermal cells in the cell elongation zone of 7-d-old primary leaves.....	97
Fig. 4.7 Effect of UV-B radiation on the spatial distribution of segmental elongation rates (a) and velocity of displacement (b), within the cell elongation zone of 7-d-old primary leaves.....	98
Fig. 4.8 Effect of UV-B radiation on the volume fraction of leaf tissue occupied by (a) mesophyll tissue, (b) vascular tissue, (c) epidermal tissue and (d) air spaces along the	

length of 7-d-old primary leaves.....	101
Fig. 4.9 Effect of UV-B radiation on the average volume fraction of tissue types within the 7-d-old primary leaf.....	102
Fig. 4.10 Effect of UV-B radiation on the frequency of (a) mesophyll cells, (b) vascular cells and (c) epidermal cells in transverse sections along the length of 7-d-old primary leaves.....	103
Fig. 4.11 Effect of UV-B radiation on the average frequency of cell types in the 7-d-old primary leaf.....	104
Fig. 4.12 Growth trajectory showing changes in cell age with distance from the leaf base of 7-d-old primary leaves.....	105
Fig. 5.1 Chloroplast Ultrastructure.....	127
Fig. 5.2 Chloroplast Development.....	128
Fig. 5.3 Effect of UV-B radiation on mesophyll cell transverse area along the length of 7-d-old primary leaves, expressed on a (a) spatial and (b) temporal scale.....	137
Fig. 5.4 Effect of UV-B radiation on the volume fraction of mesophyll cell occupied by vacuole along the length of 7-d-old primary leaves, expressed on a (a) spatial and (b) temporal scale.....	138
Fig. 5.5 Effect of UV-B radiation on the volume fraction of mesophyll cell cytoplasm occupied by chloroplasts along the length of 7-d-old primary leaves, expressed on a (a) spatial and (b) temporal scale.....	144
Fig. 5.6 Effect of UV-B radiation on mesophyll cell chloroplast transverse area along the length of 7-d-old primary leaves, expressed on a (a) spatial and (b) temporal	

scale.....	145
Fig. 5.7 Effect of UV-B radiation on the volume fraction of mesophyll cell cytoplasm occupied by mitochondria along the length of 7-d-old primary leaves, expressed on a (a) spatial and (b) temporal scale.....	146
Fig. 5.8 Effect of UV-B radiation on mesophyll cell mitochondrial transverse area along the length of the 7-d-old primary leaves, expressed on a (a) spatial and (b) temporal scale.....	147
Fig. 5.9 Effect of UV-B radiation on the volume fraction of mesophyll cell chloroplast occupied by granal thylakoids along the length of 7-d-old primary leaves, expressed on a (a) spatial and (b) temporal scale.....	151
Fig. 5.10 Effect of UV-B radiation on the volume fraction of mesophyll cell chloroplast occupied by stromal thylakoids along the length of 7-d-old primary leaves, expressed on a (a) spatial and (b) temporal scale.....	152
Fig. 5.11 Effect of UV-B radiation on the number of granal sacs per granum of mesophyll cell chloroplasts along the length of 7-d-old primary leaves, expressed on a (a) spatial and (b) temporal scale.....	153
Fig. 5.12 Effect of UV-B radiation on chloroplast number per mesophyll cell along the length of 7-d-old primary leaves, expressed on a (a) spatial and (b) temporal scale.....	159
Fig. 6.1 Effect of UV-B radiation on the chlorophyll concentration along the length of 7-d-old primary leaves, expressed on a (a) spatial and (b) temporal scale.....	186
Fig. 6.2 Effect of UV-B radiation on the concentration of chlorophyll a and chlorophyll b, per g. fwt of tissue (a,b), and per chloroplast (c,d) in relation to cell age along the	

length of 7-d-old primary leaves.....	187
Fig. 6.3 Effect of UV-B radiation on the ratio of chlorophyll a:b, in relation to cell age along the length of the 7-d-old primary leaf.....	188
Fig. 6.4 Light response curve of photosynthetic O ₂ evolution of leaf sections taken along the length of 7-d-old control-grown primary leaves (a), and the linear regression to the initial slope of the light response curves (b).....	189
Fig. 6.5 Light response curve of photosynthetic O ₂ evolution of leaf sections taken along the length of 7-d-old UV-B-grown primary leaves (a), and the linear regression to the initial slope of the light response curves (b).....	190
Fig. 6.6 Effect of UV-B radiation on the relative quantum yield along the length of 7-d-old primary leaves, expressed on a (a) spatial, and (b) temporal scale.....	191
Fig. 6.7 Effect of UV-B radiation on the rate of CO ₂ - dependent O ₂ evolution along the length of 7-d-old primary leaves, at a PPFD of (a) 79, (b) 262 and (c) 915 μmole m ⁻² s ⁻¹	192
Fig. 6.8 Effect of UV-B radiation on the rate of CO ₂ - dependent O ₂ evolution per mesophyll cell (a), and per chloroplast (b), in relation to cell age along the length of 7-d-old primary leaves, at a PPFD of 915 μmole.m ⁻² .s ⁻¹	193
Fig. 6.9 Effect of UV-B radiation on the rates of dark respiration in relation to cell age along the length of 7-d-old primary leaves.....	194
Fig. 6.10 Effect of UV-B radiation on the concentration of soluble carbohydrates per g. fresh weight tissue (a), and per cell (b), in relation to cell age along the length of 7-d-old primary leaves.....	195
Fig. 6.11 Effect of UV-B radiation on the concentration of insoluble carbohydrates per	

g. fresh weight tissue (a), and per cell (b), in relation to cell age along the length of 7-d-old primary leaves.....	196
Fig. 6.12 Effect of UV-B radiation on the total soluble protein concentration per g. fresh weight tissue (a), and per cell (b), in relation to cell age along the length of 7-d-old primary leaves.....	197
Fig. 6.13 Effect of UV-B radiation on the total free amino acid* pool per g. fresh weight tissue (a), and per cell (b), in relation to cell age along the length of 7-d-old primary leaves.....	198
Fig. 6.14 Effect of UV-B radiation on (a) glutamate as a percentage of the total free amino acid pool, and (b) the concentration of the free glutamate pool, in relation to cell age along the length of 7-d-old primary leaves.....	199
Fig. 6.15 Effect of UV-B radiation on (a) glutamine as a percentage of the total free amino acid pool, and (b) the concentration of the free glutamine pool, in relation to cell age along the length of 7-d-old primary leaves.....	200
Fig. 6.16 Effect of UV-B radiation on (a) aspartate as a percentage of the total free amino acid pool, and (b) the concentration of the free aspartate pool, in relation to cell age along the length of 7-d-old primary leaves.....	201
Fig. 6.17 Effect of UV-B radiation on (a) asparagine as a percentage of the total free amino acid pool, and (b) the concentration of the free asparagine pool, in relation to cell age along the length of 7-d-old primary leaves.....	202
Fig. 6.18 Effect of UV-B radiation on (a) glycine as a percentage of the total free amino acid pool, and (b) the concentration of the free glycine pool, in relation to cell age along the length of 7-d-old primary leaves.....	203
Fig. 6.19 Effect of UV-B radiation on (a) serine as a percentage of the total free amino	

acid pool, and (b) the concentration of the free serine pool, in relation to cell age along the length of 7-d-old primary leaves.....	204
Table 6.1 Changes in Amino Acids as a Percentage of the Total Free Amino Acid Pool.....	205
Table 6.2 Changes in Amino Acids (nmol.g ⁻¹ .fwt) in the Total Free Amino Acid Pool.....	206
Fig. 6.20 Changes in the ¹⁴ C post-labelling content of the (a) aspartate, (b) glutamate and (c) asparagine free pools.....	207
Fig. 6.21 Changes in the ¹⁴ C post-labelling content of the (a) serine, (b) glutamine and (c) glycine free pools.....	208
Fig. 6.22 Carbon Flow in Amino Acid Biosynthesis.....	232

LIST OF PLATES

Plate 2.1 Examples of Micrographs Used for Stereological Analysis.....	50
Plate 4.1 Light Micrograph of Meristematic Cells Undergoing Mitosis.....	89
Plate 4.2 Light Micrographs of Meristematic Cells in Metaphase, From Control (a) and Colchicine Treated Tissue (b).....	93
Plate 4.3 Light Microscopy of Primary Leaf Development.....	99
Plate 5.1 Light Microscopy of Mesophyll Cell Development.....	135
Plate 5.2 General Cell Ultrastructure Under the Transmission Electron Microscope.....	139
Plate 5.3 (i,ii) Transmission Electron Microscopy of Mesophyll Cell Development.....	141
Plate 5.4 (i,ii) Transmission Electron Microscopy of Chloroplast Development.....	148
Plate 5.5 (i,ii) Confocal Microscopy Z Series Through a Mesophyll Cell.....	154
Plate 5.6 Merged Confocal Images From a Z Series Through a Mesophyll Cell.....	157

ABBREVIATIONS

A -	absorbance
AABA -	L- α -amino butyric acid
ANOVA -	analysis of variance
cab -	chlorophyll a/b binding protein
<i>cab</i> -	mRNA encoding cab protein
CCCP -	carbonyl cyanide m-chlorophenylhydrazone
CDT -	cell doubling time
CFCs -	chlorofluorocarbons
Chl -	chlorophyll
Chl a -	chlorophyll a
Chl b -	chlorophyll b
Ci -	curie
CPD -	cyclobutane pyrimidine dimer
DCMU -	3-(3,4 dichlorophenyl) dimethylurea
DPM -	disintegrations per minute
EDTA -	ethylenediaminetetra-acetic acid
EM -	electron microscope
FCCP -	carbonyl cyanide p-trifluoromethoxyphenyl-hydrazone
Fd _{red} -	reduced ferredoxin
fw -	fresh weight
G6PDH -	glucose 6-phosphate dehydrogenase
<i>g</i> -	relative centrifugal force
GS -	glutamine synthetase

GOGAT -	glutamate synthase (glutamine : oxoglutarate amino transferase)
HPLC -	high pressure liquid chromatography
<i>i</i> -	integer
IAA -	indole - acetic acid
LER -	leaf elongation rate
LHCI -	light harvesting chlorophyll complex of PSI
LHCII -	light harvesting chlorophyll complex of PSII
LM -	light microscopy
LSU -	large subunit of Rubisco
mag -	magnification
MI-	mitotic index
MSX -	L methionine sulphoximine
NAT -	nitric acid trihydrate
NiR -	nitrite reductase
NR -	nitrate reductase
OAA -	oxaloacetate
OPA -	o-Phthaldialdehyde
OPPP -	oxidative pentose phosphate pathway
PAR -	photosynthetically active radiation (400-700nm)
PEP -	phospho <i>enol</i> pyruvate
PFK -	phosphofructokinase
6-4 photoproduct -	pyrimidine (6-4) pyrimidone photoproduct
PPFD -	photosynthetically active photon flux density
PSI -	photosystem I

PSII -	photosystem II
PSI-LHCI -	photosystem I - light harvesting complex I
PSII-LHCII -	photosystem II - light harvesting complex II
<i>psb A</i> -	mRNA encoding psb protein
PSCs -	polar stratospheric clouds
QY -	quantum yield
<i>rbc S</i> -	mRNA encoding small subunit of Rubisco
<i>rbc L</i> -	mRNA encoding large subunit of Rubisco
rpm -	revolutions per minute
RSE -	relative segmental elongation
Rubisco -	ribulose 1,5-bisphosphate carboxylase oxygenase
S.E. -	standard error of the mean
SER -	segmental elongation rate
SSU -	small subunit of Rubisco
TA -	transverse area
TCA cycle -	tricarboxylic acid cycle
TEM -	transmission electron microscopy
TFAA -	total free amino acid pool
TIC -	total insoluble carbohydrate
TOMS -	total ozone mapping spectrometer
TSC -	total soluble carbohydrate
UV -	ultraviolet
UV-A -	ultraviolet -A
UV-B -	ultraviolet-B

UV-C -	ultraviolet-C
V_D -	vertical displacement rate
v/v -	volume/volume
V_v -	volume fraction
W -	watts
w/v -	weight/volume

CHAPTER 1
General Introduction

1.1 Plants and Light

Solar radiation is essential for all plant life, controlling both growth and development (Hart, 1988). The light a plant receives is not only a source of energy for photosynthesis, but also triggers and regulates a number of morphological responses. The light used to drive photosynthesis, photosynthetically active radiation (PAR) is within the range of visible light from 400-700nm. The radiant energies on either side of the visible range (λ 290-400nm, λ 700-1100nm) are involved in photomorphogenic responses, which in higher plants are under the control of one of three signal transducing photoreceptors: phytochrome - absorbs red/far red light (λ 660-770nm); cryptochrome - absorbs blue light/ ultraviolet-A (UV-A: 320-400nm); UV-B photoreceptor - absorbs ultraviolet-B (UV-B: 280-320nm). As photosynthesis and photomorphogenesis are mediated by the selective absorption of different wavelengths of light, any change in the light regime a plant receives may therefore result in altered growth and development.

1.2 The Solar Spectrum

The sun emits a continuous spectrum of solar radiation, of which only *c.* 50% (λ 290-1100nm) reaches the Earth's surface, as a result of the attenuating effects of the atmosphere (see Fig. 1.1)(Attridge, 1990). The longer wavelength limit is determined by the water vapour and carbon dioxide (CO₂) content of the atmosphere, while radiation at shorter wavelength is absorbed by atmospheric oxygen (O₂) and ozone (O₃). Approximately 90% of atmospheric O₃ is located in the stratosphere (10-50km above sea level), and is the primary attenuator of UV-B radiation. Depletion of the stratospheric O₃ layer recorded over the past 30 years has led to concern about increased

levels of UV-B radiation reaching the Earth's surface.

1.3 UV-B Radiation and Stratospheric Ozone

1.3.1 The Stratospheric Ozone Layer

Ozone is a trace gas found at concentrations of *c.* 3 parts per ten million in the Earth's atmosphere (Gribben, 1989). The majority of O₃ (*c.* 90%) is located within the stratosphere (10-50km above sea level), and is highly concentrated in a layer between 15-25km known as the ozone layer, while the remaining 10% is located in the troposphere (0-10km altitude)(see Larcher, 1995). Ozone is produced via the action of sunlight on O₂ to produce O atoms which then combine with O₂ to form O₃, a process that is in a continual state of flux with O₃ molecules continuously being destroyed and regenerated by photochemical reaction. The production of O₃ is greatest over tropical latitudes, and is distributed around the globe by winds in the upper atmosphere, producing an O₃ layer that is in constant motion, changing in depth both latitudinally and seasonally, with the highest O₃ concentrations normally occurring at the poles and higher latitudes (Brasseur & Solomon, 1986) during late winter and early spring (McFarland & Kaye, 1992).

Although O₃ only constitutes a minute part of the atmosphere, it is the only gas to absorb appreciably at wavelengths below 300nm (Solomon, 1988). The ozone layer therefore serves an important function in the Earth's ecological balance, reducing the amount of biologically damaging shortwave radiation reaching the Earth's surface. UV-A (λ 320-400nm) radiation is not absorbed by O₃ and passes unaffected to the Earth's surface, whilst UV-C (λ <280nm) radiation is completely excluded due to its absorption by atmospheric O₂ and O₃. UV-B radiation is attenuated solely by O₃, and therefore the

amount of UV-B radiation reaching the Earth's surface is dependent upon the status of the stratospheric ozone layer.

Stratospheric O₃ levels recorded since 1957 from 'local' ground-based measurements (Farman, Gardiner, Shanklin, 1985) and from satellite monitors since the late 1970s (Stolarski *et al.*, 1986; Proffitt *et al.*, 1990), have shown a depletion in the stratospheric O₃ layer between 1979-1990 of 3-5% in mid-latitudes and 6-8% at higher latitudes (Gleason *et al.*, 1993). This reduction in stratospheric O₃ has been linked to increased anthropogenic emissions, *e.g.* chlorine-containing chlorofluorocarbons (CFCs) and bromine-containing halons (Reviews: Solomon, 1990; Abbatt & Molina, 1993; Prather *et al.*, 1996), which increase the rate at which O₃ is destroyed, thus upsetting the natural balance of ozone production and destruction (see Section 1.3.3). Neither CFCs nor halons occur naturally, however since their industrial production began in the 1930s their widespread use in aerosol propellants, refrigerants and the manufacture of foam, coupled to their atmospheric stability and long-lifetimes, *e.g.* CFCs have an estimated atmospheric lifetime of 120 years, has resulted in their increased concentrations in the atmosphere. For example, the concentration of CFCs in the stratosphere approximately tripled between 1960 and 1985 (Kerr, 1988).

The cause for concern over a reduction in stratospheric O₃ levels is due to the fact that a 1% decrease in total O₃ equates to a *c.* 2% increase in UV-B radiation reaching the Earth's surface, which has a disproportionately large biological effect as discussed in Section 1.4.

1.3.2 The History of Stratospheric Ozone Depletion

The potential depletion of the stratospheric O₃ layer as a result of increased concentrations of CFCs in the atmosphere was first predicted by Molina and Rowland

(1974), who suggested that the photodissociation of CFCs in the stratosphere would produce chlorine atoms capable of O₃ destruction. It was not until 1985, however, that long term ground-based measurements (1957-1984) taken by the British Antarctic Survey confirmed a depletion in the Antarctic O₃ layer, termed the 'ozone-hole', during the Austral Spring (Farman *et al.*, 1985). Farman *et al.*, (1985) proposed that it was a combination of increased anthropogenic O₃ depleting substances, *e.g.* CFCs, and the special meteorological conditions that occur over the Antarctic that led to the *c.* 40% reduction in O₃ density within the column of the Antarctic vortex. The discovery of the ozone-hole led to the production of the Montreal Protocol (1987) which requires emission reductions of CFCs by 50% by the year 2000 and halon use to be kept at 1996 levels. It has since been revised (London, 1990; Copenhagen, 1992) as additional data on the status of the stratospheric O₃ layer on a global scale have become available. Further evidence confirming the existence of the Antarctic ozone-hole came from data taken between 1979-1985 by the NASA Total Ozone Mapping Spectrometer (TOMS) aboard the Nimbus 7 satellite (Stolarski *et al.*, 1986). Data from TOMS also show that the O₃ depletion is not confined to the Antarctic polar vortices, and a reduction in total column O₃ at mid-latitudes of the Southern hemisphere have been recorded (Stolarski *et al.*, 1991).

The meteorological conditions in the Arctic are different from those found in the Antarctic essential for the CFC-induced O₃ destruction, and were therefore originally regarded as being unsuitable for O₃ destruction (see Section 1.3.3). By the late 1980s, however, it was becoming increasingly evident that a similar pattern of stratospheric O₃ depletion was developing over the Arctic. Data from the Airborne Arctic Stratospheric Expedition (AASE I) during the Winter of 1989/90 found a reduction of *c.* 6% in

column O₃ in the Arctic vortex (Proffitt *et al.*, 1990). The total column O₃ over the Arctic during Winter has been reported to be depleted annually by *c.* 5%, from a loss of *c.* 15% in 1991/92, to a *c.* 40% loss in 1995/96 (Salawitch *et al.*, 1993; Manney *et al.*, 1994; Chipperfield, Lee & Pyle, 1996; Wirth & Renger, 1996). The 40% reduction in column O₃ found in 1996 extended out to mid-latitudes, including Britain which experienced a 50% O₃ column loss in March (Pearce, 1996). Recent data from the NASA TOMS aboard NASA's Earth Probe satellite have shown that the total column O₃ over the Arctic during late March - early April 1997 are the lowest on record (www.nasa.gov, unpublished).

1.3.3 How Does Stratospheric Ozone Layer Depletion Occur?

The overall rate of O₃ loss is lower in the Arctic compared to the Antarctic, despite the fact that both the amount of O₃ destroying halogen oxides (ClO_x, BrO_x) formed within the polar vortex, and the overall chemical reactions leading to O₃ destruction (net reaction: 2O₃ ⇒ 3O₂) are virtually identical over both hemispheres. This difference in O₃ loss is the result of differences in the geographical position of the Antarctic, which is isolated from land masses, as compared to the Arctic which is surrounded by the land masses of Northern America and Asia. The high mountain ranges of N.America and Asia disturb the polar vortex motion, producing weaker short-lived vortices and a warmer climate less favourable for O₃ destruction compared to the colder, long-lived vortices of the Antarctic (Schoeberl & Hartmann, 1991).

A polar vortex forms over the pole of the Winter hemisphere, which effectively isolates stratospheric air over the polar region during the polar night (Schoebel & Hartmann, 1991). With the onset of the polar night, temperatures in the stratosphere decrease (< -78°C)(McFarland & Kaye, 1992) and this allows for the formation of polar

stratospheric clouds (PSCs)(Solomon, 1990). The type of PSC formed is temperature dependent, with clouds of nitric acid trihydrate (NAT) forming at $< -78^{\circ}\text{C}$, and water-ice clouds forming at $< -88^{\circ}\text{C}$ (Webster *et al.*, 1993). The formation of PSCs is an essential component in the process of O_3 destruction and these compounds serve two primary functions. Firstly, PSCs provide a surface on which reactions can occur between compounds that do not normally take place in the gas-phase, termed heterogeneous reactions (McFarland & Kaye, 1992). This group of reactions liberates active species of chlorine (ClO - chlorine monoxide) from the inactive reservoir compounds (HCl - hydrochloric acid; ClONO_2 - chlorine nitrite). Secondly, PSCs remove nitrogen oxides and nitric acid, released from both natural and anthropogenic processes, from the stratospheric gas-phase, and thus inhibit the conversion of ClO back into the inert reservoirs of HCl and ClONO_2 (Webster *et al.*, 1993).

Once the active chlorine is released from the stratospheric reservoirs, the polar vortex is primed for photolysis of O_3 on the return of sunlight to the vortex in early spring. Three catalytic cycles have been shown to account for *c.* 95% of photochemical loss of O_3 in the vortex (see Fig 1.2), with each Cl atom and ClO molecule having the potential to destroy up to 100,000 O_3 molecules. With the return of the polar spring the PSCs evaporate with the increased vortex temperature $> -78^{\circ}\text{C}$. The nitrogen oxides are returned to the stratospheric gas-phase which promotes the conversion of ClO and NO_2 back into their inert reservoir forms of HCl and ClONO_2 . Ozone destruction is therefore reduced until the conditions of the next polar Winter favour chlorine activation.

1.3.4 Increases In UV-B Radiation Reaching the Earth's Surface

In general terms, each 1% reduction in stratospheric O_3 equates to a *c.* 2%

increase in UV-B radiation reaching the Earth's surface (Blumthaler & Ambach, 1990). As a result of the natural variation in the levels of UV-B radiation, *e.g.* seasonal changes, long-term monitoring of ground-level UV-B radiation has been required to determine whether O₃ depletion has caused an increase in UV-B radiation reaching the Earth's surface.

Blumthaler & Ambach (1990) monitored surface UV-B radiation at an Alpine site from 1979-1990, and reported a $1.1 \pm 0.4\%$ increase per annum in UV-B radiation. Increased ground-levels of UV-B radiation of *c.* 18% reported by Ambach *et al.*, (1991) over the Arctic during Spring, and an annual increase of *c.* 35% between 1989-1993 reported by Kerr & McElroy (1993) over Toronto during Winter, both coincide with the annual period of maximum O₃ depletion. Sekneyer & McKenzie (1992) compared UV-B levels in the mid-latitudes of the Northern (48°N, Germany) and Southern (45°S, New Zealand) hemispheres during the Summer. The results showed UV-B radiation was approximately a factor of two greater in New Zealand, which was correlated to a greater decrease in stratospheric O₃ over New Zealand.

In order to predict future changes in the amount of UV-B radiation reaching the Earth's surface, changes in the stratospheric O₃ layer need to be taken into account. Despite recent measures to eliminate anthropogenic emissions of O₃ destroying substances, the stability and long retention times of these compounds in the atmosphere makes it difficult to predict future changes in stratospheric O₃ levels (Prather & Watson, 1990). A continued reduction in the stratospheric O₃ layer is expected into the next century (Soloman & Albritton, 1992), and therefore an understanding of the potential effects of increased UV-B radiation on biological systems is required.

1.4 Biological Consequences of Increased UV-B

Although UV-B radiation only constitutes *c.* 0.5% of the total solar irradiance reaching the Earth's surface, many biologically important molecules, such as nucleic acids and proteins, absorb strongly within the UV-B region of the solar spectrum. The potential consequences of future increases in UV-B radiation reaching the Earth's surface, have been reported in micro-organisms (Witkin, 1976), plants (Caldwell, Teramura & Tevini, 1989) and animals, including humans (Kripke, 1994; Madronich & Gruijl, 1994). Due to their static nature, and the fact that plants need to intercept solar energy for both photosynthesis and photomorphogenesis, plants are, and will be in the future, exposed to the elevated levels of UV-B radiation reaching the Earth's surface.

1.5 Biological Weighting of UV-B Measurements

The biological effectiveness of UV radiation depends on the particular biological process of interest, and in many cases the response is a strong function of the wavelength. The relative biological effectiveness of different wavelengths is described by 'action spectra' (Caldwell *et al.*, 1986; Coohill, 1989, 1991). A number of action spectra have been described for plant response to UV, including general plant impact (Caldwell, 1971) and plant growth (Steinmüller, 1986)(see Fig. 1.3). Action spectra serve as spectral weighting functions which can be used to determine the biological consequences of changes in solar UV-B radiation, resulting from a given change in O₃. A common characteristic of most action spectra is a decreasing effect with increasing wavelength (see Fig. 1.3), and therefore a slight shift in the spectrum towards shorter wavelengths may have significant biological effects.

1.6 Effects of UV-B Radiation on Plants

Numerous studies have investigated the effects of elevated UV-B on plants, and have shown a diverse ranges of responses, including changes at the physiological, morphological, biochemical and molecular levels (Reviews: Teramura, 1983; Caldwell, Teramura & Tevini, 1989; Tevini & Teramura, 1989; Teramura & Sullivan, 1991; Tevini, 1994; Caldwell *et al.*, 1995; Jordan, 1996). The sensitivity of plants to UV-B, defined as any morphological, physiological or biochemical change induced by UV-B, varies between both species and cultivars (Tevini & Teramura, 1989), and of the 300+ species studied, approximately two-thirds are UV-B sensitive (Caldwell *et al.*, 1989; Teramura & Sullivan, 1991).

1.6.1 Plant Growth and Morphology

Changes in plant growth and morphology associated with increased UV-B include alterations in the yield, biomass, plant height and leaf area (Tevini, Iwanzik, Thoma, 1981; Barnes *et al.*, 1990, 1996), and occur in a variety of species including *Triticum aestivum* (wheat; Barnes *et al.*, 1988), *Raphanus sativus* (radish; Tevini *et al.*, 1981), *Cucumis sativus* (cucumber; Takeuchi *et al.*, 1989) and *Phaseolus vulgaris* (bean; Deckmyn & Impens, 1995).

Altered leaf development, *e.g.* reduced leaf length and area, reported in a range of species including *T.aestivum* (Barnes *et al.*, 1988, 1990), *Avena sativa* (oat; Barnes *et al.*, 1990), *Oryza sativa* (rice; Teramura, Ziska & Szein, 1991) and *R.sativus* (Tevini *et al.*, 1981) is a common response to elevated UV-B (discussed in Chapter 3). The extent of the response varies within and between species. In more sensitive species, *e.g.* *P.vulgaris*, leaf area may be reduced by up to *c.* 60%, as compared to a reduction of *c.* 10% in less sensitive species, *e.g.* *Zea mays* (maize; Tevini *et al.*, 1981). Large

differences in cultivar sensitivity have been reported, for example in a study by Teramura *et al.*, (1991) a reduction in leaf area in response to UV-B was found in only a quarter of the 16 *O.sativa* cultivars tested. Changes in leaf development in response to UV-B have been attributed to alterations in both cell division (Dickson & Caldwell, 1978) and expansion (Steinmetz & Wellmann, 1986), and is discussed in more detail in Chapter 4.

An increase in leaf thickness has been found in a number of species grown under UV-B, including *Glycine max* (soybean; Mirecki & Teramura, 1983), *Brassica campestris* (Bornman & Vogelmann, 1991), *T.aestivum*, *O.sativa*, *Z.mays* (Barnes *et al.*, 1990) and the arctic grass, *Calamagrostis purpurea* (Gwynn-Jones & Johanson, 1996). Thicker leaves lengthen the optical path between the epidermis and potential sensitive cellular sites, such as the mesophyll tissue, resulting in a lower internal UV-B fluence (Bornman & Vogelmann, 1991; Teramura, 1983). This has been suggested to be a protective response, reducing UV-B penetration into the leaf tissue (Flint, Jordan & Caldwell, 1985; Bornman & Vogelmann, 1991). The epidermis of plant leaves selectively filters sunlight, removing the majority of the damaging UV-B radiation and transmitting most of the PAR (Caldwell *et al.*, 1983). A common response to elevated UV-B is the epidermal accumulation of flavonoids, non-photosynthetic pigments that absorb within the UV-B region of the spectrum, and has been reported in a range of species including *Pisum sativum* (pea; Strid & Porra, 1992), *Vicia faba* (faba bean; Flint *et al.*, 1985), *Silene vulgaris* (van de Staaij *et al.*, 1995) and *Hordeum vulgare* (barley; Liu *et al.*, 1995). The accumulation of epidermal flavonoids in response to UV-B, has been suggested to be another UV-B induced protective mechanism, increasing the attenuating capacity of the epidermis to UV-B and therefore reducing UV-B penetration

(Caldwell *et al.*, 1983; Cen & Bornman, 1993).

1.6.2 Photosynthetic Targets

Photosynthesis is one of the most important processes influencing plant productivity, and the potential effects of elevated UV-B have therefore been extensively studied (Reviews: Bornman, 1989; Jordan, 1993; Bornman & Sundby-Emanuelsson, 1995). In many of the plant species investigated, for example *G.max* (Teramura *et al.*, 1984) and *P.sativum* (Day & Vogelmann, 1995), a reduction in photosynthetic capacity was observed in response to UV-B (as discussed in Chapter 6). Various factors have been identified as being UV-B sensitive, that may either directly or indirectly affect photosynthesis. The indirect effects of UV-B on photosynthesis include changes in leaf morphology (see Section 1.6.1), stomatal conductance (Day & Vogelmann, 1995), and a reduction in stomatal number (Tevini & Iwanzik, 1986; Dai *et al.*, 1995). The direct effects of UV-B on photosynthesis include changes in photosynthetic enzymes and pigments, and the disruption of the photosystem II (PSII) complex.

Photosystem II has been identified as one of the primary photosynthetic targets to UV-B (Bornman, 1989). A reduction in PSII activity has been demonstrated in leaf tissue (Strid, Chow & Anderson, 1990), isolated chloroplasts (Noorudeen & Kulandaivelu, 1982), isolated thylakoids (Bornman *et al.*, 1984) and PSII membrane fragments (Renger *et al.*, 1989). A number of different sites of PSII inhibition have been identified, including a reduction in oxidative capacity (Renger *et al.*, 1989), photoreduction of plastoquinone (Melis *et al.*, 1992) and photodegradation of the D1 reaction centre (Jansen *et al.*, 1993). Photosystem I (PSI) appears to be much more resistant to UV-B radiation (Renger *et al.*, 1989; Prasil *et al.*, 1992). The role of PSII in the inhibition of CO₂ assimilation induced by exposure to UV-B was assessed by

Nogués & Baker (1995) in the mature leaves of *P.sativum*. It was concluded that although exposure to UV-B ultimately results in the photodamage of PSII reaction centres, this is not the primary cause of inhibition of CO₂ assimilation, and that other factors determine the loss of the ability to assimilate CO₂. In a recent study, Allen *et al.*, (1997) concluded that in *Brassica napus* L. cv. Bristol, the loss of Rubisco is a primary factor in the inhibition of CO₂ assimilation, and that the photoinhibitory damage to PSII appears to be a secondary effect of the UV-B induced stress.

Ribulose 1,5-bisphosphate carboxylase (Rubisco, EC 4.1.1.39), the primary CO₂ fixing enzyme of C₃ photosynthesis has also been identified as a UV-B sensitive target. The activity of Rubisco has been shown to decline in response to UV-B (Vu, Allen & Garrard, 1984; Strid, Chow & Anderson, 1990). In the study by Vu *et al.*, (1984) on *G.max* and *P.sativum*, the decline in Rubisco activity was attributed primarily to a loss of Rubisco protein. However, in another study on *P.sativum*, Jordan *et al.*, (1992) found that Rubisco activity declined more rapidly than the Rubisco protein. Recent studies at the molecular level have shown UV-B to affect the gene expression of both the nuclear encoded small-subunit (SSU) and the chloroplast encoded large-subunit (LSU) of Rubisco, with a severe reduction in both *rbcS* and *rbcL* mRNA transcripts upon exposure to elevated UV-B (Jordan *et al.*, 1991,1992). Changes in photosynthetic pigments, both quantitative and qualitative, have been reported in a number of species in response to elevated UV-B, including *C.sativus* (Takeuchi *et al.*, 1989), *P.sativum* (Strid *et al.*, 1990) and *P.vulgaris* (Deckmyn *et al.*, 1994). The gene expression of the nuclear encoded chlorophyll a/b binding protein (*cab*) has been reported to be severely inhibited by UV-B radiation (Jordan *et al.*, 1991). However, as with other UV-B induced responses, the extent to which UV-B alters gene expression has been shown to vary

between species. For example, only minor UV-B effects were found on the expression of *cab* in *T.aestivum* (Taylor *et al.*, 1996).

In addition to these biochemical and molecular changes in the photosynthetic apparatus, UV-B has also been reported to directly affect chloroplast ultrastructure (Brandle *et al.*, 1977; He, Huang & Whitecross, 1994). In the study by Brandle *et al.*, (1977) the effects of UV-B on *P.sativum* chloroplast ultrastructure, *i.e.* dilation followed by disruption of thylakoids, could be detected within 15 minutes of exposure to UV-B, and was suggested to be closely associated to PSII inhibition. This highlights the close co-ordination of cell ultrastructure and metabolism, and is discussed in more detail in Chapters 5 and 6.

1.6.3 DNA Damage and Repair

DNA is one of the primary UV-B absorbing chromophores in the cell. A number of DNA lesions have been identified in the nucleus, chloroplasts and mitochondria of plants exposed to enhanced UV-B (Britt, 1996; Stapleton, Thornber & Walbot, 1997). The majority of these lesions are dimeric photoproducts; cyclobutane pyrimidine dimers (CPDs) and pyrimidine (6-4) pyrimidone photoproducts ([6-4] photoproducts), with monomeric photoproducts, strand and chromosomal breakages making up the minor fraction of other DNA lesions (Reviews: Britt, 1995; Taylor, Tobin and Bray, in press). Other major cellular chromophores, such as RNA and proteins can be replaced by new synthesis, whereas DNA has to be repaired. Plants have therefore evolved mechanisms by which they can either shield their DNA from UV-B damage, *e.g.* by producing UV-B absorbing compounds such as flavonoids (see Section 1.6.1), or repair the UV-B induced DNA damage. In plants, three main UV-B repair mechanisms have been found to exist; excision repair, photoreactivation and recombinational repair (Kornberg & Baker, 1992).

The extent of DNA damage and subsequent repair may therefore alter a plants sensitivity to enhanced UV-B radiation, although this has not been studied in any great detail to date.

1.7 Why are Plant Responses to UV-B Radiation So Variable?

Considerable variation in plant response to elevated UV-B radiation has been reported between both species and cultivars (see Section 1.6). This variation can, in part, be explained by differences in growth conditions, for example light levels (Photosynthetically active photon flux density - PPF), water stress and temperature have all been shown to alter plant sensitivity to UV-B (Reviews: Teramura, 1983; Tevini, 1993).

1.7.1 Environmental Variation

1.7.1.1 Light

UV-B sensitivity is affected by both the quantity and quality of light levels (PPFD) under which plants are grown. High PPF, both before (preconditioned), and during (concomitant) exposure to UV-B radiation has frequently been shown to ameliorate the effects of elevated UV-B (Warner & Caldwell, 1983; Mirecki & Teramura, 1984; Cen & Bornman, 1990; Jordan *et al.*, 1992). The investigations of Warner & Caldwell (1983), and Mirecki & Teramura (1984) into the effects of UV-B on *G.max* photosynthesis, showed plants preconditioned with high PPF to have increased UV-B resistance. Preconditioned plants were found to have thicker leaves and increased levels of UV-B absorbing compounds. It was therefore suggested that the UV-B protection induced by high PPF preconditioning was an indirect effect of changes in leaf morphology and pigmentation, which offer a degree of protection from UV-B (see Section 1.6.1)(Flint *et al.*, 1985; Bornman & Vogelmann, 1991). More recently,

molecular studies on *P.sativum* have shown that the UV-B induced down regulation of photosynthetic genes, e.g. *rbcS*, *rbcL*, *cab* and *psbA* (Jordan *et al.*, 1991, 1992), can be partially ameliorated by concomitant high PPFD (Jordan *et al.*, 1992; Mackerness *et al.*, 1996). The protection of gene expression by high PPFD occurred within a few hours, indicating the rapid induction of a protective mechanism, different from the high PPFD induced changes in leaf morphology and pigmentation. In their study on *P.sativum* plants, Mackerness *et al.*, (1996) found that the high PPFD induced protection of photosynthetic gene expression under UV-B was lost in the presence of the photosynthesis inhibitors CCCP and DCMU. It was concluded, therefore, that photosynthesis, or a related process, plays a key role in the amelioration of UV-B induced reductions in gene expression. Light quality has also been shown to alter the sensitivity of plants to UV-B. Caldwell, Flint & Searles (1994) found that at low PPFD, UV-A played a significant role in ameliorating the UV-B response in *G.max*. This may be the result of increased photoactivated DNA repair, involving the enzyme DNA photolyase which utilizes photons of light in the UV-A and blue light (300-500nm) region of the spectrum as an energy source (Sancar, 1994).

1.7.1.2 Water Stress

Studies into the effects of water stress in combination with enhanced UV-B, on plant growth, suggests that a complex interaction exists between the two variables. As with many other UV-B induced effects, the response of a plant to water stress and elevated UV-B varies between species. In a study by Tevini *et al.*, (1983), the sensitivity of *R.sativus* seedlings to UV-B was reduced under water stress as a result of increased flavonoid production (see Section 1.6.1). Balakumar, Vincent & Paliwal (1993) have also reported an accumulation of UV-B protecting compounds (antioxidants and

phenolics) in *Vigna unguiculata* (cowpea) in response to the combination of water stress and elevated UV-B, as compared to UV-B alone. In *C.sativus* seedlings, however, the combined effect of water stress and UV-B, as compared to the effect of UV-B alone, has been found to be deleterious, as a result of the prevention of stomatal closure leading to increased water loss (Teramura *et al.*, 1983).

1.7.1.3 Temperature

The effect of temperature on plant response to elevated UV-B has been shown to differ considerably between species. In a study by Tevini (1993), the effects of elevated UV-B on the growth (plant height, leaf area and dry weight) of *Z.mays*, *A.sativa*, *Secale cereale* (rye), and *Helianthus annuus* (sunflower) was investigated at 28°C and 32°C. The growth of seedlings under UV-B was greater at 32°C than 28°C, for all species except *A.sativa*. The growth of *H.annuus* seedlings was significantly reduced under UV-B at both temperatures, whereas in both *Z.mays* and *S.cereale* seedlings the reduction in growth under UV-B was ameliorated at the higher temperature. The interaction between temperature and UV-B is complex, and in a recent study, Caldwell (1994) found that the growth of *C.sativus* under enhanced UV-B increased the plants ability to withstand elevated temperatures. The influence of temperature on the sensitivity of plants to UV-B may be mediated by changes in enzyme activities. For example, photolyase which is involved in the light repair of DNA damage has been shown to be inhibited by increased temperature (Pang & Hays, 1991).

1.7.2 Developmental Stage of the Plant

The developmental stage of a plant at the time of exposure to elevated UV-B has been shown to affect UV-B sensitivity in a number of plants including, *G.max* (Teramura & Caldwell, 1981), *Arabidopsis thaliana* (Giller, 1991), *H.vulgare*, and

P.sativum (Jordan *et al.*, 1994; Day, Howells & Ruhland, 1996). Teramura & Caldwell (1981) found that the leaves of *G.max* were more sensitive to UV-B radiation, measured as a reduction in net photosynthesis, prior to leaf expansion. The effect of UV-B on plastid pigment content of *A.thaliana* leaves, was also shown to be dependent upon leaf age (Giller, 1991). In this study, Giller (1991) found that although the initial reduction in chlorophyll a content of younger leaves exposed to UV-B was greater than that of older leaves, the effect of enhanced UV-B on the chlorophyll a content of younger plants was reversible. A possible explanation for the increased effect of UV-B in younger leaf tissue, may be related to the UV-B sensitivity of DNA. As DNA is a target for UV-B damage (see Section 1.6.3), the actively dividing and expanding cells of younger leaf tissue may be more susceptible to UV-B damage than the non-dividing cells of older leaf tissue. Older plants may also be more resistant to UV-B, as a result of changes during normal development, *e.g.* increased leaf thickness, that may convey a certain amount of protection against UV-B (see Section 1.6.1). In a recent study, Day *et al.*, (1996) concluded that the sensitivity of *P.sativum* plants to elevated UV-B was lower than had been reported in previous studies, because leaf age effects had not been previously considered. In this study, only one parameter, the ratio of UV-B absorbing compound to total chlorophyll, out of a total of 12 measured, including leaf area and the concentration of UV-B absorbing compounds, was significantly affected by elevated UV-B. The differences found in the other parameters were the result of leaf-age effects, *i.e.* UV-B altered leaf age and the reported affects were as an indirect result of this.

One of the most common responses to elevated UV-B is a reduction in plant growth and development (see Section 1.6.1). Many of the parameters whose response to elevated UV-B is frequently measured, *e.g.* leaf morphology and photosynthetic

capacity, show marked changes during normal plant development. If UV-B alters plant growth, are the observed changes in, for example, photosynthetic capacity, direct effects of elevated UV-B, or indirect effects as a result of UV-B altered growth?

1.8 Aims of Thesis

The many studies investigating plant responses to elevated UV-B have shown a wide variety of effects, including changes in leaf morphology, photosynthetic capacity and gene expression. The sensitivity of plants to UV-B varies between species and cultivars, and is also highly dependent on the interaction of UV-B with other environmental factors, such as light levels and water availability. Furthermore, plant sensitivity to UV-B has also been shown to vary with the developmental stage of the plant, and data from the recent study of Day *et al.*, (1996), highlight the importance of the need to consider leaf age in UV-B experimental design.

The aim of this thesis is to analyse the effects of elevated UV-B radiation on leaf development, at the cellular (see Chapter 3 + 4), subcellular (see Chapter 5), and metabolic (see Chapter 6) levels. The primary leaf of wheat (*T. aestivum* L. cv. Maris Huntsman), which is a model developmental system, as described in Section 4.1.2.1, has been used in this study. The gradient of cell age and development found in the primary leaf provides a system in which the effects of UV-B on a specific developmental stage can be examined, and also allows for the distinction of direct effects of UV-B, from the indirect effects of UV-B, *e.g.* changes mediated by altered growth under UV-B.

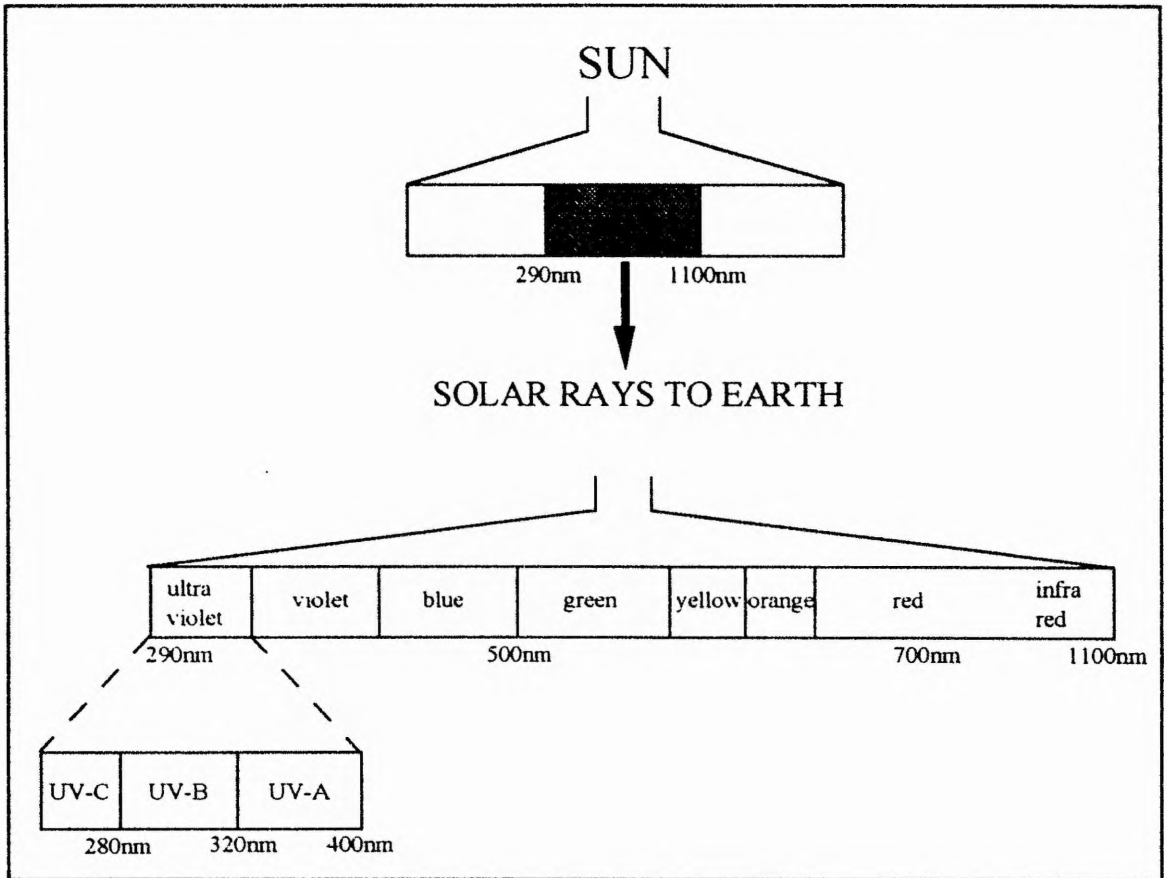


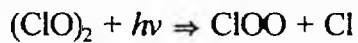
Fig. 1.1 Solar Spectrum (λ 290-1100nm) at the Earth's Surface

Inset represents the subdivision of UV radiation, of which only $\lambda \geq 290\text{nm}$ reaches the Earth's surface (After Salisbury & Ross, 1985).

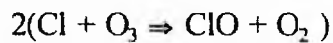
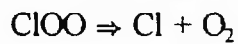
(1)



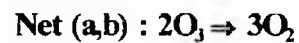
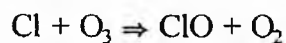
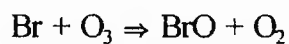
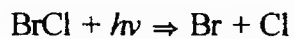
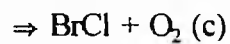
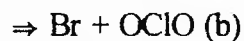
M = molecular nitrogen



$h\nu$ = light energy



(2)



(3)

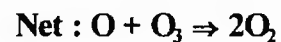
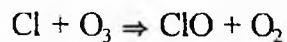
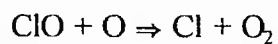


Fig. 1.2 Reactions Representing Photochemical Loss of Ozone in the Polar Vortex

Photolysis occurs after the release of active chlorine on PSCs in Spring at the polar vortices (taken from Salawitch *et al.*, 1993).

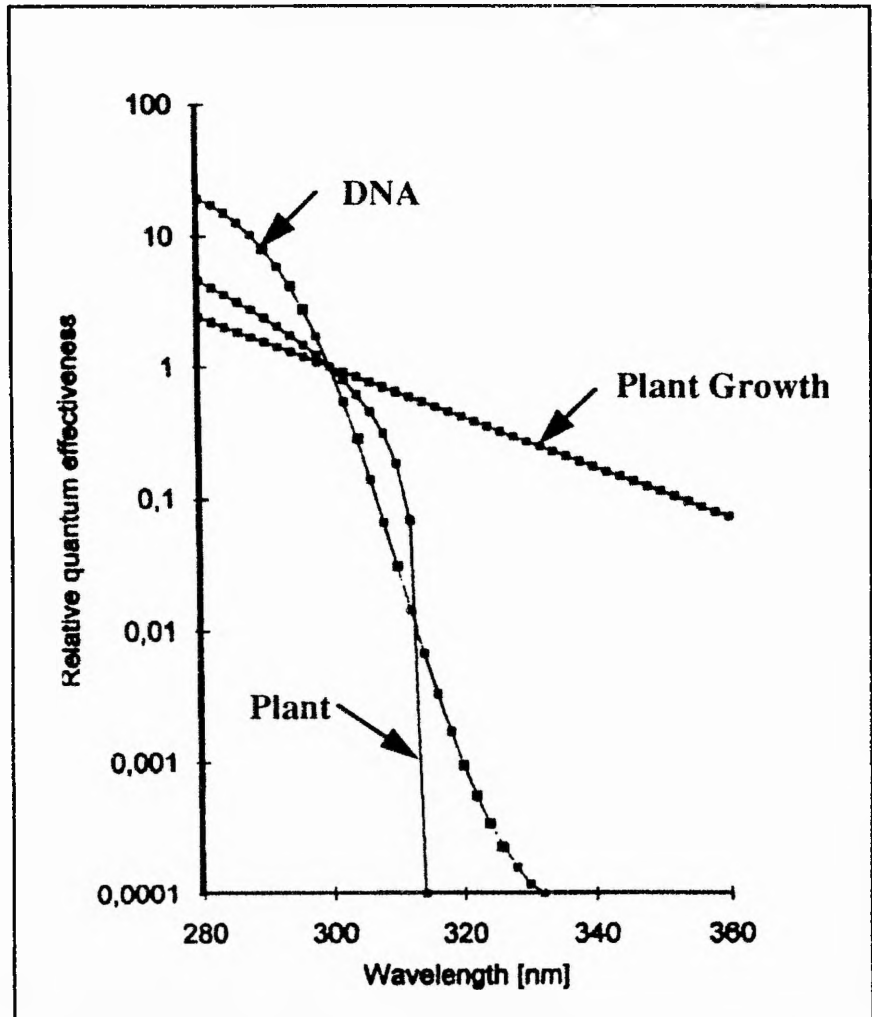


Fig . 1.3 UV Action Spectra

The figure shows action spectra for DNA damage (Setlow, 1974), general plant impact (Caldwell, 1971) and plant growth (Steinmüller, 1986) (see Section 1.5).

CHAPTER 2

Materials and Methods

2.1 Materials

The majority of chemicals used were from one of the following companies : Sigma Chemical Company Ltd, Poole, Dorset, UK; British Drug House Ltd, Poole, Dorset, UK; TAAB Laboratories Equipment Ltd, Reading, Berkshire, UK. All chemicals used were Analytical Grade, except those for electron microscopy and HPLC analysis which were EM and HPLC Grade respectively. Sodium bicarbonate [¹⁴C] was obtained from ICN Biomedicals Ltd, Thame, Oxfordshire, UK.

2.2 Plant Material and Growth Conditions

Winter wheat (*Triticum aestivum* L. cv Maris Huntsman) seeds from Plant Breeding International, Cambridge, UK, were imbibed for 16 hours in aerated tap water at 20°C. Seeds were sown at a density of 25g (pre-imbibition weight) per 30 x 44cm tray in Levingtons M2 medium nutrient potting compost (Levington Horticulture Ltd, Ipswich, UK), covered with fine grade vermiculite (Dupre, Hertford, UK). Plants were grown in a controlled environment chamber (Fi-totron PG1400: Sanyo-Gallenkamp, Loughborough, UK) with a 16 hour photoperiod at 20/10°C and a constant humidity of 70%. Incident irradiation was provided by 6 x HQI-TS 250W/NDL elements and 8 x 60W pearl tungsten bulbs (Sanyo-Gallenkamp, Loughborough, UK). Quantum flux density was measured daily 2 hours into the photoperiod using a Skye Light meter (Skye Instruments, Wales) and ranged between 232-348 μmoles m⁻² s⁻¹ photosynthetic photon flux (PPFD; λ 400-700nm). Additional UV-B was supplied during the photoperiod by 4 x 4ft UV-B tubes (Philips TL-40-12-RS: Starna Ltd, Romford, UK) covered in 0.13mm thick cellulose acetate (Gift from Dr.N.Paul, University of Lancaster) to eliminate radiation below 292nm (Strid *et al.*, 1990). The cellulose acetate was replaced

daily to minimise effects of deterioration. Due to the gradient of light intensity inside the chamber trays of plants were arranged in a diamond shape in the centre of the chamber. The spectral distribution of UV-B radiation in this central region of the cabinet is shown in Fig. 2.1. The incident dose rate was determined with a Macam SR991 double monochromator scanning spectroradiometer (Macam Photometrics, Livingston, UK). This spectroradiometer was calibrated using deuterium and tungsten calibration lamps traceable to national standards. Using this equipment the incident dose rate was estimated to be equivalent to a dose of $2.34 \times 10^{-1} \text{ W m}^{-2}$ (Caldwell weighting using a reference wavelength of 300nm). This level of UV-B approximates to a 30% increase in ambient levels of UV-B in natural sunlight measured on a summer's day in the north of England. UV-B levels were measured daily 2 hours into the photoperiod at 310nm with a UVX Radiometer (UVP Ltd, Cambridge, UK) and ranged between 150-206 W m^{-2} . Under control growth conditions background UV-B levels averaged 15 W m^{-2} .

2.3 Sampling of Plant Tissue

Unless specified all experiments used 7-d-old plants with a primary leaf length +/- 5mm about the mean and five replicates per treatment were used. Plants were harvested 2 hours into the photoperiod, and the seed, roots, coleoptile and secondary leaf removed, leaving the primary leaf.

2.4 Statistical Analysis

All data sets were correlated to confirm normal distribution, and statistical analysis performed by oneway analysis of variance (ANOVA) for paired-comparisons, using the Minitab programme (Minitab Inc, USA).

2.5 Primary Leaf Development

2.5.1 Growth Rate Determination

Thirty plants were randomly selected 4 days post-imbibition and leaf length measured twice daily for 6 days, 2 and 10 hours into the photoperiod. Primary leaf length was taken as the distance between the intercalary basal meristem and the developing leaf tip.

2.5.2 Fresh and Dry Weight Determination

The fresh and dry weight of 10 primary leaves were measured 4-7 days post-imbibition. Fresh weights were recorded using a fine balance, the leaves were then wrapped in absorbant paper and dried at 60°C for 72 hours. Dried tissue was cooled to room temperature in a dessicator and the dry weight recorded.

2.5.3 Leaf Area and Width

The area of 10 primary leaves were measured 4-7 days post-imbibition. Leaves were mounted flat onto graph paper with clear tape and photocopied. The photocopied leaves were then cut out and weighed on a fine balance and a piece of the same paper (1cm²) was weighed as a reference. Leaf areas were then calculated using the relationship between area and weight. The width of the leaf blade was measured from the leaves mounted onto the graph paper, using a ruler.

2.5.4 Mitotic Index

Mitotic index was determined using a modified method from Ougham, Jones & Evans (1987). Transverse sections of 1mm were taken at 0-4mm above the intercalary basal meristem of five primary leaves and fixed in 3:1 (v/v) ethanol to acetic acid at 4°C for 24 hours. Samples were hydrolysed in 1M hydrochloric acid (HCl) at 60°C for 8min and stained with Feulgens reagent (0.5% (w/v) basic fuchsin, 0.55% (w/v)

potassium metabisulphite, in 0.15M HCl, kept in the dark at 4°C for 30 min. Sections were squashed in 45% (v/v) acetic acid and viewed under oil at x 500 magnification with a Nikon light microscope (Nikon, Kingston-Upon-Thames, UK). The mitotic index was calculated as the percentage of total cells in metaphase, anaphase and telophase. Eight random counts of 200 cells were taken for each section.

2.5.5 Cell Doubling Time

The cell doubling time was determined using a modified method from Evans, Neary & Tonkinson (1957). This involves treating the leaf material with colchicine, which inhibits spindle formation so that actively dividing cells arrest in metaphase. Linear regression analysis of the accumulation of cells in metaphase (%) over time (h) generates a regression equation of the form :

$$y = a + b(x) \quad \text{where } y = \text{accumulation of cells in metaphase (\%)} \\ x = \text{time (h)} \\ a = \text{intercept on y axis} \\ b = \text{regression co-efficient (i.e. the slope of the line)}$$

The regression co-efficient can be used to calculate the cell doubling time (CDT) using the following formula :

$$\text{CDT (h)} = \ln 2 \cdot 100 \div b$$

Six day old plants were used for colchicine treatment over a 12 hour growing period. A vertical segment of the coleoptile (approximately 1mm wide) was removed

with a single edged razor blade to reveal the primary leaf base. 0.2ml, 1% (w/v) colchicine was applied to the leaf base with a hypodermic needle at the start of the light period, and reapplied at intervals of 2 hours. As a control, colchicine was replaced with dH₂O. Two plants were harvested every 2 hours from 0-12 hours, and the intercalary basal meristem fixed and processed as in section 2.4.4. Eight random counts of 200 cells were taken for each section and the proportion of metaphase cells (%) calculated.

2.5.6 Leaf Elongation

Leaf elongation rates were determined using a modified method of Schnyder and Nelson (1988). Ten primary leaves were selected 2 hours into the light period on day-6 and the leaf length measured. Each leaf was pierced at 2mm intervals from the leaf base (through the intact coleoptile) to the leaf tip with a needle constructed from a 0.2mm diameter steel guitar wire with a sharpened end. The plants were then returned to the growth cabinet for 24 hours, after which the leaf length was measured again. The average growth over this period of marked leaves was reduced by < 10% as compared to unmarked leaves. The plants were harvested, the coleoptile and secondary leaf removed, and the primary leaf mounted flat onto paper with clear tape. The distance between needle holes was measured with a ruler and the segmental elongation rate (SER *i.e.* rate of elongation of a leaf segment relative to the rate of elongation of the whole leaf blade) and vertical displacement rate (V_D *i.e.* the velocity at which a segment is moving up the leaf blade) determined using the following equations :

1. Relative segmental elongation (RSE_i) for the i th segment was calculated as

$$RSE_i = 2 (D_{i, m} - D_{i, t_0}) \cdot (D_{i, m} + D_{i, t_0})^{-1}$$

where D_{i, t_0} = the initial distance between neighbouring holes (*i.e.* 2mm)

$D_{i, m}$ = the distance between these same holes after a period of $(t_m - t_0)$ of growth

2. Segmental elongation rate (SER [mm.mm leaf length⁻¹. h⁻¹]) during undisturbed growth was calculated as

$$SER_i = LER \cdot RSE_i \cdot (RSE_1 + RSE_2 + \dots + RSE_n)^{-1} \cdot L^{-1}$$

where LER (mm.h⁻¹) = the average undisturbed leaf elongation rate (corrects for the effect of the hole reducing leaf elongation)

$RSE_i \cdot (RSE_1 + RSE_2 + \dots + RSE_n)^{-1}$ = the fractional contribution of segment *i* to LER

L = length of the segment (mm)(converts elongation rate per segment to elongation rate per mm of leaf length)

3. Vertical displacement rate (V_D [mm.h⁻¹])

$$V_{Di} = 2 \cdot (SER_1 + SER_2 \dots SER_{n-1}) + SER_n$$

2.5.7 Cell Age Determination

The gradient of cell age along the primary leaf blade was determined using the V_D data (see Section 2.5.6) to calculate a growth trajectory as first described by Silk & Wagner (1980). The following calculations (personal communication W.K.Silk, University of California) were made to estimate the growth trajectory for cells within the primary leaf :

1. Multiply the V_D found 2mm from the leaf base (*i.e.* the first mark position) by a set time increment, *e.g.* 0.25 hours. Add the resulting increment of distance to the former mark position to find the new mark position.

2. Repeat step (1) using the V_D from 2mm and the time interval of 0.25 hours until the new mark position is more than halfway to the next tabulated mark position at 4mm. Once the new mark position is ≥ 3 mm, multiply the V_D found 4mm from the leaf base by 0.25 hours and add this to the former mark position. This is repeated until the new mark position is ≥ 5 mm, after which the V_D found 6mm from the leaf base is used.
3. Repeat steps (1) and (2) up until the mark position at 14mm (the distal limit of the elongation zone), after which the V_D remains constant and the increase in distance over time is linear.
4. The growth trajectory of cell age along the leaf can be plotted as distance from the leaf base (mm) versus time (hours)

2.5.8 Epidermal Cell Length

To determine epidermal cell lengths a nail varnish impression of the abaxial epidermis was taken from five 7-d-old primary leaves. The abaxial side of the primary leaf was painted with a thin layer of clear nail varnish and allowed to dry for at least 20min. Once dried, a piece of clear tape was placed on top of the painted leaf, and a gentle pressure applied to ensure that there were no air bubbles between the tape and the varnish. The tape was then removed from the leaf, and an impression in varnish of the developing epidermis was left on the tape. The tape was mounted onto a microscope slide and examined at x 250 magnification with a Nikon light microscope (Nikon, Kingston-Upon-Thames, UK). The cell length, of epidermal cells adjacent to stomatal guard cells, was measured along 3 cell columns per leaf in 2.5mm sections, from 0 - 2.5mm up to 27.5 - 30mm and an average per section calculated. As cell length was measured up to 30mm above the leaf base, it included both elongating and mature epidermal cells.

2.5.9 Mesophyll Cell Number

Mesophyll cell number was determined using a method modified after Dean & Leech (1982a). Transverse sections were taken at 5mm intervals along the length of five primary leaves. The sections were added to 500 μ l, 5% (w/v) chromium trioxide and stored in the dark at 4°C for 7 days. Cells were released by gentle flushing of the sections through a Pasteur pipette followed by vortexing. Mesophyll cells were counted in a 0.2mm depth haemocytometer (Hawksley, UK), viewed at x 40 magnification with a Nikon light microscope (Nikon, Kingston-Upon-Thames, UK). Six counts per section were recorded.

2.6 Transmission Electron Microscopy

2.6.1 Fixation

Transverse sections of 1mm were taken along the length of ten primary leaves, 0, 1, 5, 10, 15, 20 and then every 10mm, above the intercalary basal meristem. The sections were floated on fixative (2.5% (v/v) glutaraldehyde in 0.1M sodium cacodylate, pH 7.3) and cut into squares (approximately 1mm²). The tissue was then vacuum infiltrated with fresh fixative for 10min and left on a rotator (TAAB, Berkshire, UK) at 2rpm overnight at room temperature.

2.6.2 Post Fixation

The tissue was washed in four changes of 0.1M sodium cacodylate (pH 7.3) and then incubated for 2 hours in 1% (w/v) osmium tetroxide in 0.1M sodium cacodylate (pH 7.3) on a rotator (2rpm) at room temperature. The tissue was then washed in 0.1M sodium cacodylate (pH 7.3) for 2 x 5 minutes.

2.6.3 Dehydration

The tissue was dehydrated sequentially in 30, 50, 70, 90 and 100% (v/v) ethanol for a period of 1 hour in each dilution at room temperature. Tissue was en-bloc stained in the dark in 2% (w/v) uranyl acetate in 100% ethanol, on a rotator (2rpm) overnight at room temperature. The tissue was washed in 100% ethanol for 1 hour.

2.6.4 Embedding

Tissue was embedded in Spurr's (1969) medium grade epoxy resin. The tissue was taken through the following series for a period of 1 hour in each dilution at room temperature

- (i) 2:1 ethanol to Spurr's resin
- (ii) 1:1 ethanol to Spurr's resin
- (iii) 1:2 ethanol to Spurr's resin
- (iv) Spurr's resin

The tissue was put in fresh resin and left overnight on a rotator (2rpm). Tissue was put in fresh resin for a further 1 hour before being polymerised at 60°C for 24 hour. Polymerisation was in flat agar moulds (TAAB, Berkshire, UK) which allowed orientation of the tissue, and eased subsequent sectioning of the tissue in transverse.

2.6.5 Ultrathin Sectioning

Transverse sections were taken from the blocks using glass knives (LKB Knifemaker 7801B: Leica UK Ltd, Milton Keynes, UK)(Hayat, 1989) on a ultramicrotome (Reichert-Jung Ultracut: Leica UK Ltd)(knife angle = 4°, cutting angle = 0°, cutting speed = 2mm s⁻¹). Ultrathin sections (60-90nm) showing copper/gold interference when cut onto distilled H₂O were expanded using 100% chloroform. Sections were mounted onto 200 mesh copper grids (AGAR Scientific, Essex, UK) that

had been coated with 2% (w/v) formvar in chloroform and carbon (Carbon Turbocoater: BIO-RAD Microscience Division, Herfordshire, UK).

2.6.6 Heavy Metal Staining

Staining was carried out on a piece of Nesco film in a petri dish and all solutions used were centrifuged at 10,000g for 10min in an MSE micro-centaur centrifuge (Scotlab, Coatbridge, UK), followed by filtration through a 2µm Millipore filter. Grids were stained in 2% (w/v) uranyl acetate in 70% (v/v) ethanol for 20min in the dark. Grids were then rinsed five times in distilled H₂O before staining in a CO₂ free environment (produced by the incorporation of NaOH pellets within the petri dish) with 0.3% (w/v) lead citrate (Reynold, 1963) in 0.1M sodium hydroxide for 5min. Grids were rinsed again in distilled H₂O, dried on hardened filter paper (Whatman No.50) and stored in a dust free environment.

2.6.7 Examination of Tissue

Sections were examined on a Philips 301 TEM at 60kV (Philips, Cambridge, UK) and photographed with Agfa Scientia EM Film. Negatives were developed in Ilford Phenisol at 20°C for 3.5min, washed in running water for 2 min, fixed in Ilford Hypham for 5min, washed in running water for a further 20 min and left to air dry.

2.6.8 Printing

Negatives were printed onto Ilford Multigrade IV RC Deluxe photographic paper. Plates were developed in 1:9 Ilford multigrade to water for 1min, washed in running water for 2min, fixed in 1:9 Ilford paper fixer to water for 2min, washed in running water for 2min and left to air dry.

2.7 Light Microscopy

The tissue blocks prepared for TEM were used for light microscopy and the negatives were printed in the same way.

2.7.1 Thick Sectioning

Transverse thick sections (0.5 μ m) were taken from the same blocks used for TEM as described in section 2.6.5. The sections were expanded and dried in distilled water on microscope slides at 80°C on a hot plate.

2.7.2 Staining

Contrast of tissue was obtained by staining with methylene blue (1% (w/v) methylene blue, 1% (w/v) sodium tetraborate in distilled H₂O) on a hot plate at 80°C for 1min and washed in running water.

2.7.3 Examination of Tissue

Thick sections were examined with a Leitz Laborlux 12 microscope fitted with a Pentax LX 35mm camera (Leica UK Ltd, Milton Keynes, UK). Photographs were taken using automatic exposure and Agfapan 25 film.

2.8 Leaf and Cell Structure

Quantification of leaf and cell structure was determined using stereological and morphometrical methodology as described in Section 5.2. These methods are based on estimates of probability, and therefore rigorous sampling procedures are required at all stages of analysis to ensure randomness (see Section 5.2.2).

Leaf tissue from ten 7-d-old primary leaves was fixed and processed as described in Section 2.6-2.7. Twenty random tissue blocks were selected for each developmental stage along the leaf blade (see Section 2.6.1) from both control and UV-B-grown plants.

The number of randomly selected micrographs required to be taken at each level of study, *i.e.* LM mag x 250, 500; TEM mag x 5000, 29000, to make the analysis significant was estimated by using the progressive sampling technique of Bolender (1978)(see Section 5.2.2). From a trial sample of random micrographs (*e.g.* 20) the cumulative standard error (expressed as a % of the mean), of increasing numbers of micrographs *e.g.* 1-20, was calculated (see Fig. 2.2). A constant standard error at a level $\leq 10\%$ of the mean gives an estimate of the number of micrographs needed for significant analysis. This corresponds to 15-20 micrographs per sample (see Fig. 2.2), and 20 micrographs per developmental stage along the leaf were taken at all levels of the study. Images of the micrographs were captured onto an AnalySIS image-analyser equipped with a mono-chrome CCD camera (Norfolk Analytical Ltd, Hilgay, UK), and parameters such as distances, *e.g.* leaf thickness, and areas of regions of interest, *e.g.* chloroplast and mitochondrion, determined utilizing the AnalySIS software programme. The area measurements (transverse areas - TA) were used to estimate volume fractions (V_v)(see Section 5.2.1.1). For example:

$$\text{Area}_{\text{compartment}} / \text{Area}_{\text{total}} = \text{Volume}_{\text{compartment}} / \text{Volume}_{\text{total}}$$

$$\text{Chloroplast Area} / \text{Cytoplasm Area} = V_v \text{ of cytoplasm occupied by chloroplasts}$$

Leaf and cell structure was analysed at four different levels (see Plate 2.1).

Level I and II: LM mag x 250 and x 500

Twenty tissue blocks (Section 2.6.1-2.6.4) at each developmental stage along the length of control and UV-B-grown plants were randomly selected for thick sectioning and staining (Sections 2.7.1-2.7.2). One micrograph per block was

photographed at x 250 and x 500 magnification using a Leitz microscope (Section 2.7.3).

Level I: Light micrographs (x 250 mag) of transverse sections through the leaf were used to estimate

- the average maximum and minimum transverse leaf thickness
- the ratio of different cell types in the leaf blade
- V_V of leaf occupied by different cell types

Level II: Light micrographs (x 500 mag) of transverse sections through the leaf were used to estimate:

- V_V of mesophyll cell occupied by vacuole

Level III and IV: TEM x 5000 and x 29000

Twenty tissue blocks (Section 2.6) at each developmental stage along the length of control and UV-B-grown plants were randomly selected for ultrathin sectioning and heavy metal staining (Sections 2.6.5-2.6.6). One micrograph per block was photographed at x 5000 and x 29000 magnification using a Philips 301 TEM (Section 2.6.7).

Level III: TEM micrographs (x 5000 mag) of transverse sections through mesophyll cells of the leaf were used to estimate

- V_V of cytoplasm occupied by chloroplasts and mitochondria
- Average chloroplast and mitochondrial TA

Level IV: TEM micrographs (x 29000 mag) of transverse sections through mesophyll cell chloroplasts were used to estimate

- V_V of chloroplast occupied by granal and stromal thylakoids
- number of grana per granal stack

2.9 Determination of Chloroplast Numbers per Mesophyll Cell

Chloroplast numbers per mesophyll cell were determined using the tissue preparation method of Dean and Leech (1982b), followed by confocal microscopy. This method uses the natural fluorescence of chlorophyll as a means of visualising individual chloroplasts within the mesophyll cell.

2.9.1 Preparation of Tissue

Transverse sections of 1mm were taken along the length of five 7-d-old primary leaves, 10, 20, 40, 60 and 80mm above the basal meristem, and fixed in 3.5% (v/v) glutaraldehyde in 0.1M EDTA (pH 9.0) for 1 hour in the dark. The tissue was washed in three changes of 0.1M EDTA (pH 9.0) and then incubated in fresh 0.1M EDTA (pH 9.0) for 3 hours at 60°C in a shaking water bath. Samples were kept (for up to 1 month) at 4°C prior to processing.

2.9.2 Preparation of Slides

Sections were put onto a drop of 0.1M EDTA (pH 9.0) on a microscope slide and gently squashed with the flattened end of a spatula, to release the cells. A coverslip was carefully placed on top of the cell suspension and sealed with nail varnish.

2.9.3 Confocal Microscopy

Fluorescent images of cells were observed under oil at a magnification of x 600, using a Nikon inverted microscope, Diaphot Model TMD (Nikon, Kingston-Upon-Thames, UK). The Bio-Rad MRC-600 series laser scanning confocal imaging system (Bio-Rad Microscience, Hertfordshire, UK) was used to generate confocal images of the cells. With the excitor filter set at 0, and the ND filter set at 1, 2µm optical sections were taken through the cell, at a scanning speed of 2 and a rate of 5 scans per section, and collected using the Kalmen filter (average 15 sections per cell). The set of images

through the cell (Z series) were recorded and stored on optical disc (Philips Magneto Optical Disk: Philips, Cambridge, UK) via a DPL optical drive (BIO-RAD, UK). Using COMOS 603 software these images were subsequently merged to give 3 representative sections per cell from which the chloroplast number per cell could be estimated. A total of 20 cells were counted for each position along the leaf blade.

2.9.4 Printing Confocal Images

Images were relayed to a colour video monitor (Sony Trinitron, PYM-1444QM: McMillan UK Ltd) and printed onto Sony UPC-5010P paper using a colour video printer (Sony Mavigraph UP-5000P: McMillan UK Ltd).

2.10 Chlorophyll Determination

The chlorophyll (Chl) concentration was determined according to the method of Arnon (1949). Transverse sections (5mm wide) were taken along the length of five primary leaves. The sections were ground in 1.5ml of 80% (v/v) acetone and centrifuged at 10,000g for 2min in an MSE micro-centaur centrifuge (Scotlab, Coatbridge, UK). The resulting supernatant was made up to 3ml with 80% (v/v) acetone and the absorbance of chlorophyll a and b measured against an acetone blank at 663 and 645nm respectively, in a Pye Unicam SP1800 Ultraviolet spectrophotometer (Pye Unicam, Cambridge, UK).

Chlorophyll concentrations were calculated using the following equations:

$$(i) \text{ Chl a } (\mu\text{g/ml}) = (12.7 \times A_{663}) - (2.69 \times A_{645})$$

$$(ii) \text{ Chl b } (\mu\text{g/ml}) = (22.9 \times A_{645}) - (4.68 \times A_{663})$$

2.11 Photosynthesis Measurements Using The Leaf Disc Electrode

2.11.1 Leaf Disc Electrode

The rates of O₂ consumption/evolution were measured using whole leaf tissue sections in a Hansatech Leaf-Disc Electrode (Hansatech, King-Lynn, Norfolk, UK) linked via a control box to a chart recorder. A constant temperature of 20°C was maintained in the leaf-disc chamber by circulating water from a temperature controlled water bath (Grant Cambridge Ltd, Hertfordshire, UK) through the surrounding water jacket. The leaf-disc electrode was assembled and maintained according to manufacturers instructions (Hansatech, UK)(Walker, 1990).

2.11.1.1 Calibration

The leaf-disc electrode was calibrated before each set of measurements. A gas-tight syringe containing 1ml of air is attached to the leaf-disc chamber and the voltage output (mV) recorded from the attached control box (= R1). The 1ml of air is then introduced into the leaf disc chamber and the new voltage output (mV) recorded (= R2). The voltage generated when the 1ml of air is introduced into the chamber, *i.e.* R2-R1, is used to calculate the relationship between mV (voltage output on chart recorder) and O₂ concentration. At standard pressure and 20°C, 1ml of air (*c.*21% O₂) contains 8.73µmole O₂. Therefore, $8.73 / (R2-R1)$ µmoles O₂ would generate a 1mV change on the chart recorder.

2.11.2 Photosynthesis Measurements

The rate of CO₂ - dependent O₂ evolution was measured in transverse leaf sections of 1cm from 10 primary leaves, taken at 0, 20, 40, 60 and 80mm above the leaf base. The fresh weight of the leaf sections was recorded before placing the leaf tissue into the leaf-disc chamber, to which 500µl of 1M potassium bicarbonate was added to

generate a CO₂ concentration of 5% (v/v). The chamber was sealed and left for 2 minutes before beginning CO₂ - dependent O₂ evolution measurements at 20°C and a range of PPFD levels from 79 - 915 μmoles m⁻² s⁻¹ .

2.11.3 Dark Respiration

The leaf-disc electrode was used to determine the rates of O₂ uptake in the dark using a similar procedure to that outlined in Section 2.11.2.

2.12 Carbohydrate Determination

The total soluble and total insoluble carbohydrate content of primary leaf tissue was determined colorimetrically using Dreywoods anthrone reagent (Morris, 1948). Anthrone reagent (8.6mM anthrone in 80% (v/v) H₂SO₄) is made fresh and must be kept in the dark at 4°C. This assay is based on the principle that when anthrone reagent and carbohydrates are heated together at 80°C, anthrone, a yellow solution, is converted into anthronol, a blue/green solution which absorbs at 623nm.

2.12.1 Glucose Standard Curve

Glucose standards were made in distilled H₂O and ranged from 0-200 μg ml⁻¹. To 1ml of each standard, 3ml of anthrone reagent was added and vortexed to ensure mixing of the two phases. The standards were heated in a water bath at 80°C for 10min and then kept on ice for 30min. The absorbance of each standard was read against an anthrone/water blank at 623nm in a Pye Unicam SP1800 Ultraviolet spectrophotometer (Pye Unicam, Cambridge, UK). Fig. 2.3 shows the glucose calibration curve.

2.12.2 Preparation of Samples

For carbohydrate analysis, transverse sections (1cm wide) were taken along the length of thirty primary leaves and weighed (approximately 0.2g fresh weight). Tissue

was boiled in 5 ml 40% (v/v) ethanol for 30min, the resulting extract removed and tissue re-extracted twice in 4ml distilled H₂O for 30min at 100°C. The combined ethanol/water extract was analysed for total soluble carbohydrates and the extracted tissue for total insoluble carbohydrate analysis.

2.12.3 Total Soluble Carbohydrates

The combined ethanol/water extract was dried by vortex evaporation at 40°C in a Searle Vortex-Evaporator (Buchler Instruments, Division of Searle Analytical Inc, New Jersey, USA) and redissolved in 250µl distilled H₂O. An 80µl aliquot of the extract was mixed with 920µl distilled H₂O, 3ml anthrone reagent and heated at 80°C for 10min. The mixture was kept on ice for 30min after which the absorbance at 623nm measured (see section 2.12.1) and the total soluble carbohydrate concentration calculated from the glucose calibration curve (Fig. 2.3).

2.12.4 Total Insoluble Carbohydrates

Extracted tissue was ground in liquid nitrogen and freeze dried overnight in an Edwards Modulyo Freeze Dryer (Edwards High Vacuum Int, BOC Ltd, Sussex, UK). Dried tissue was resuspended in 1ml, 1.6M Perchloric acid, vortexed and heated at 70°C for 2 hours. Samples were vortexed and centrifuged (10,000g, 10min) in an MSE micro-centaur centrifuge. A 40µl aliquot of the supernatant was mixed with 960µl distilled H₂O, 3ml anthrone reagent and heated at 80°C for 10min. The mixture was kept on ice for 30min and the absorbance at 623nm measure (see section 2.12.1) and the insoluble carbohydrate concentration calculated from the glucose calibration curve (Fig. 2.3).

2.13 Protein Analysis

2.13.1 Soluble Protein Determination

Soluble protein was measured using the Bio-Rad Protein Microassay (0-25µg protein/ml; Bio-Rad, Hertfordshire, UK). This assay is based on the colourimetric method of Bradford (1976), the principle of which is that when an acidic solution of Coomassie Brilliant Blue G-250 binds to protein, there is a shift in the absorbance maximum from 465 to 595nm. A standard curve was produced using thyroglobulin at concentrations of 0 - 25µg/ml (see Fig. 2.4), each time an assay was carried out.

2.13.2 Protein Extraction

Transverse sections were taken at 10mm intervals along the length of 10 primary leaves, and the fresh weight (per 10 leaf sections) recorded before freezing the leaf tissue in liquid N₂. Frozen tissue samples were ground up in 0.5ml extraction buffer (72mM Na₂HPO₄, 28mM NaH₂PO₄, 0.5mM EDTA, 1µM leupeptin, 0.007% (v/v) β-mercaptoethanol) and centrifuged at 10,000g for 10 mins at 4°C in a MSE micro-centaur centrifuge (Scotlab, Coatbridge, UK). The protein extract was diluted with distilled H₂O (200 - 500 fold dilution), to give a final volume of 800µl and mixed with 200µl of Bio-Rad Protein Assay reagent concentrate. The mixture was vortexed and left for between 20 - 60 minutes, in which time the dark-blue protein precipitate forms. The absorbance of the protein-dye complex was read in triplicate at 595nm on a microplate reader (MR5000, Dynatech Laboratories Ltd, Billingshurst, UK).

2.14 Determination of Amino Acid Free Pools

2.14.1 Preparation of Tissue

Sequential transverse sections of 1cm were taken from five primary leaves and

weighed. Tissue was frozen in liquid N₂ and ground to a fine powder using a mortar and pestle. The powder was ground in 1ml 80% (v/v) ethanol, the extract vortexed and left to stand at 4°C for 30min. The extract was then vortexed and centrifuged at 10,000g for 10min, and the resulting supernatant re-spun twice under the same conditions. The pooled supernatant was frozen in liquid N₂ and freeze dried overnight in an Edward Modulyo Freeze Dryer (BOC Ltd, Sussex, UK). The extract was redissolved in 1ml, 12.5µM L-α-aminobutyric acid (AABA) and centrifuged at 10,000g for 10 min. A 250µl aliquot of the sample was mixed with 250µl of 12.5µM AABA and centrifuged at 10,000g for 10min. The supernatant was kept at 4°C and was centrifuged at 10,000g for 10min immediately prior to HPLC analysis.

2.14.2 Preparation of Standards

The HPLC column was calibrated before each set of runs with a range of 12.5µM amino acids standards (Sigma Chemical Company)(see Fig. 2.5). Due to its lack of stability in solution the internal standard AABA and glutamine was added fresh to the standards.

2.14.3 High Pressure Liquid Chromatography

To determine the free pools of amino acids, the samples were subjected to HPLC (LKB Bromma 2156 Solvent Controller, 2152 LC Controller, 2159 HPLC Pump. LKB-Produkter AB, Bromma, Sweden). This was equipped with a 3.9mm x 150mm, Resolve C18 90Å 5µm reverse phase column (Waters Chromatography, Division of Millipore, Kent, UK) with a LDC Analytical-FluoroMonitor III fluorescence detector (LDC Analytical Inc, Florida, USA).

2.14.3.1 Gradient Solvents and Programme

The separation of amino acids using reverse phase HPLC works on the principle

that non-polar functional groups (C18 hydrocarbons) which are bonded to the silica particles within the column, makes them less polar than the solvent in which the amino acids are dissolved. These non polar components interact more strongly with the substrate than polar components and are eluted from the column at later times. By altering the composition of the solvent from polar (aqueous) to non polar (organic) over time, the separation of different amino acids can be enhanced.

The aqueous phase used in the gradient contained 50mM sodium acetate (pH 5.9) containing 19% (v/v) methanol and 1% (v/v) tetrahydrofuran, and the methanol phase, 50mM sodium acetate (pH 5.9) in methanol (1:4[v/v]). The gradient was run at 0.8ml. min⁻¹ and the breakpoints for the gradient programming are shown in Table 2.1.

2.14.4 Precolumn derivatisation of amino acids and detection

The samples were prederivatized before injection into the HPLC apparatus with o-phthalaldehyde (OPA) reagent (0.625ml 0.3M OPA in methanol, 25μl 2-mercaptoethanol, 5.6 ml 0.4M sodium borate, pH 9.5). The OPA reagent must be prepared at least 24 hours before use and will last for 2 weeks if kept in the dark at room temperature with N₂ over it.

The reaction was carried out in an eppendorf tube and the following mixed in order, 10μl sample (as prepared in section 2.14.1), 10μl 2% sodium dodecyl sulphate (SDS) in 0.4M sodium borate (pH 9.5) and 10μl OPA reagent. After exactly 1 min, 20μl of 0.1M potassium phosphate (pH 4.0) was added and mixed for 6 seconds before injecting 40μl into the Rheodyne valve which is connected to a 20μl loop. To standardise runs, the time between addition of potassium phosphate and injection was 30 seconds.

2.14.5 Amino Acid determination

The OPA-tagged amino acids within the solvent gradient are eluted from the column and passed through a fluorescence detector cell illuminated by UV light at 318nm. Fluorescence emission produced at 420nm passes through a cut-off filter and is detected by a photomultiplier tube. The resulting electrical impulses are quantified using a Chromjet integrator SP440 (Spectra-Physics Inc, California, USA).

2.14.6 Amino acid quantification

Absolute amounts of amino acids in samples were calculated by comparing the fluorescence readings of the samples with those of the standards. Differences in the fluorescence of the internal standard, AABA, corrects for differences in detector sensitivity between runs. Each standard consists of 50pmol, so that pmol/4µl of sample is given by:

$$\frac{\text{Fluorescence of sample}}{0.005 \times \text{Fluorescence of standard}} \times \frac{\text{Fluorescence of AABA sample}}{\text{Fluorescence of AABA standard}}$$

2.15 ¹⁴CO₂ Pulse-chase Labelling of Amino Acids

In order to determine the incorporation of ¹⁴C into the amino acids - aspartate, glutamate, asparagine, serine, glutamine, glycine - three replicate pulse-chase experiments were carried out for control and UV-B-grown plants. The experimental system used is outlined in Fig. 2.6. To estimate the amount of ¹⁴C in the amino acids of interest, the samples were subjected to HPLC, fractions were collected off the column and passed through a scintillation counter.

2.15.1 ¹⁴C Labelling

The top 3cm of the primary leaf blade was harvested from 18 average plants, 2

hours into the photoperiod on day-7. Each leaf tip was placed upright in 100 μ l of distilled H₂O in microtitre plate wells and returned to the growth cabinet for 30 minutes to allow recovery from cutting. Before labelling, 3 x 3cm leaf tips were taken as a control and frozen in liquid nitrogen. The microtitre plate was then put on a perspex tray inside a polythene bag and 100 μ l of NaHCO₃ containing 50 μ Ci of ¹⁴C (ICN-17441H, 1mCi (500 μ l) sodium bicarbonate [¹⁴C]) introduced into the large central well. The plate was then covered by a bottomless box (perspex sides, cellulose acetate lid), giving the plants a PPFD of 185 μ moles m⁻² s⁻¹ and UV-B of 122.3W m⁻². To release ¹⁴CO₂ into the environment surrounding the leaf tissue, 100 μ l of 1M HCl was injected through the cellulose acetate into the NaHCO₃. The syringe was removed and the hole sealed with tape, the whole system was then sealed within the polythene bag. After 10 minutes of labelling the plants were removed from the ¹⁴CO₂ , and 3 x 3cm leaf tips sampled and frozen in liquid nitrogen at 0, 30, 60, 90 and 120 minutes post-labelling. All frozen samples were then processed for HPLC analysis of amino acids as described in Section 2.14.

2.15.2 Determination of ¹⁴C in Amino Acid Fractions

The ¹⁴C labelled samples and the control sample were loaded onto the HPLC column as described in Section 2.14.4-2.14.5. For the labelled samples the asp, glu, asn, ser, gln and gly fractions were collected as they came off the column and all other fractions pooled together as one. For the control sample, everything coming off the column was collected as one fraction. The volume of each fraction was estimated, and a 500 μ l aliquot mixed with 2ml of Ready-Solv HP scintillation fluid (Beckman, USA) in a 6ml scintillation vial .

2.15.2.1 Scintillation Counter

The samples were run through a Packard 1600 computer assisted liquid scintillation analyser (Canberra Packard, Berkshire, UK). The counter was automatically calibrated for ^{14}C , with a preset count time of 10 minutes per sample, quench correction was automatic and gave a final DPM reading per sample. The average amount of ^{14}C label incorporated into the plants was *c.*10% for both control and UV-B experiments. The percentage of total label in each of the amino acids of interest was calculated as a percentage of the total label in these amino acids, over the 120 minutes post-labelling.

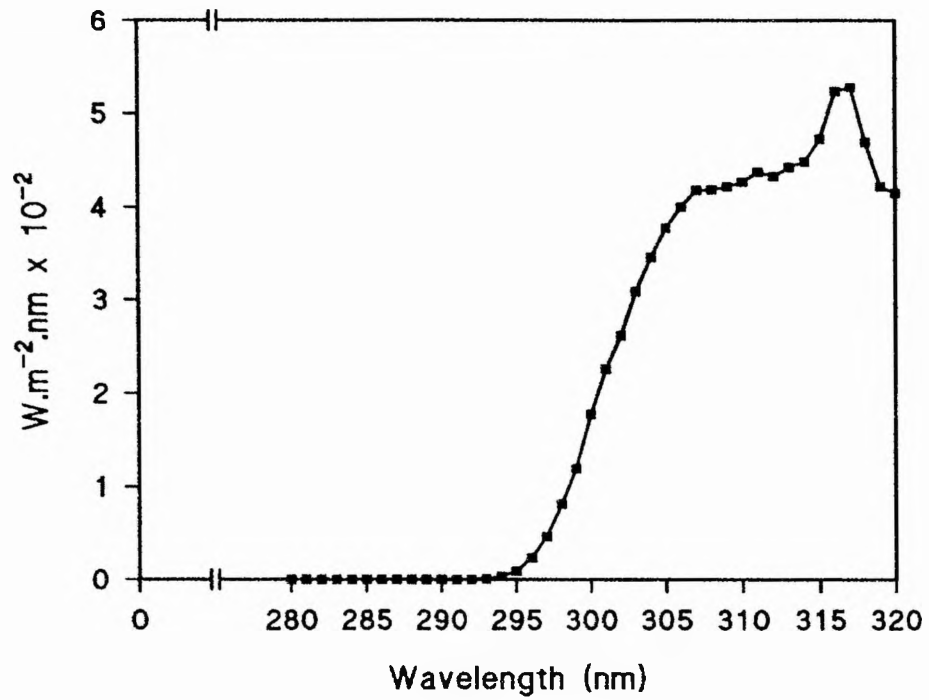


Fig 2.1 Spectral Distribution of UV-B in Plant Growth Cabinet

UV-B radiation was measured at plants height (see Section 2.2).

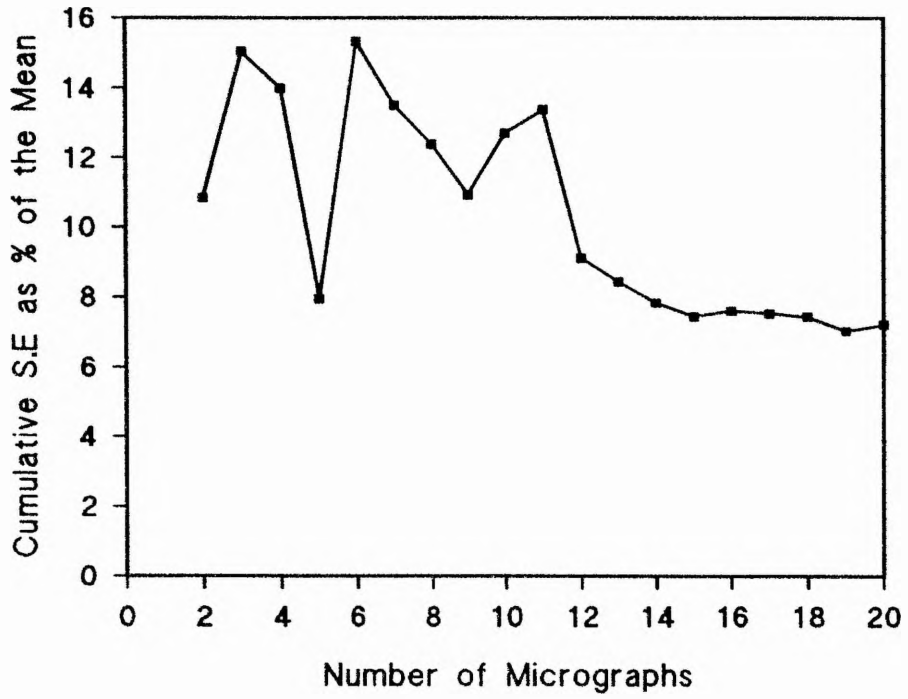
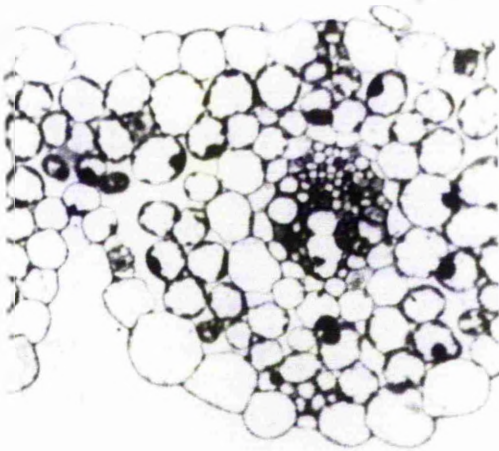


Fig. 2.2 An Example of the Progressive Sampling Technique used to Estimate the Number of Micrographs for Stereological Determination

See Section 2.8.

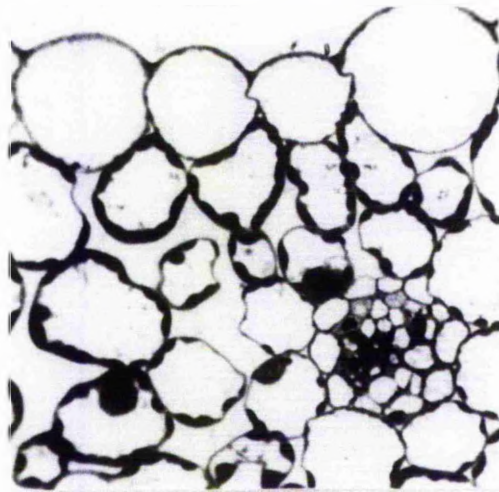
Plate 2.1 Examples of Micrographs Used for Stereological Analysis

Transverse sections taken at 40mm above the leaf base (see Section 2.6-2.8).



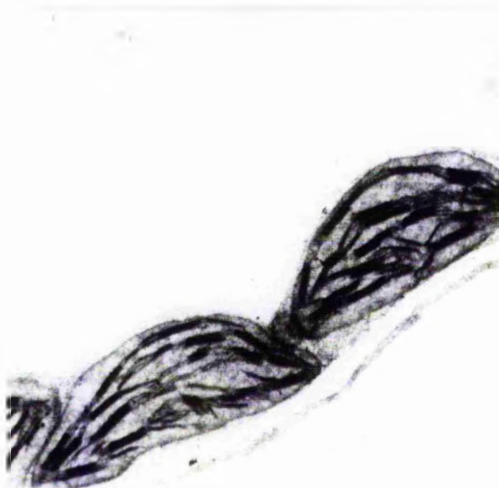
LM x 250

- leaf thickness
- V_V (%) of leaf occupied by
 - epidermal cells
 - mesophyll cells
 - vascular cell
 - air spaces
- ratio of epidermal : mesophyll : vascular cells



LM x 500

- V_V (%) of mesophyll cell occupied by
 - vacuole



TEM x 5000

- V_V (%) of mesophyll cell cytoplasm occupied by
 - chloroplasts
 - mitochondria
- TA of
 - chloroplast
 - mitochondrion



TEM x 29000

- V_V (%) of chloroplast occupied by
 - granal thylakoids
 - stromal thylakoids
- average no. of granal sacs per granum

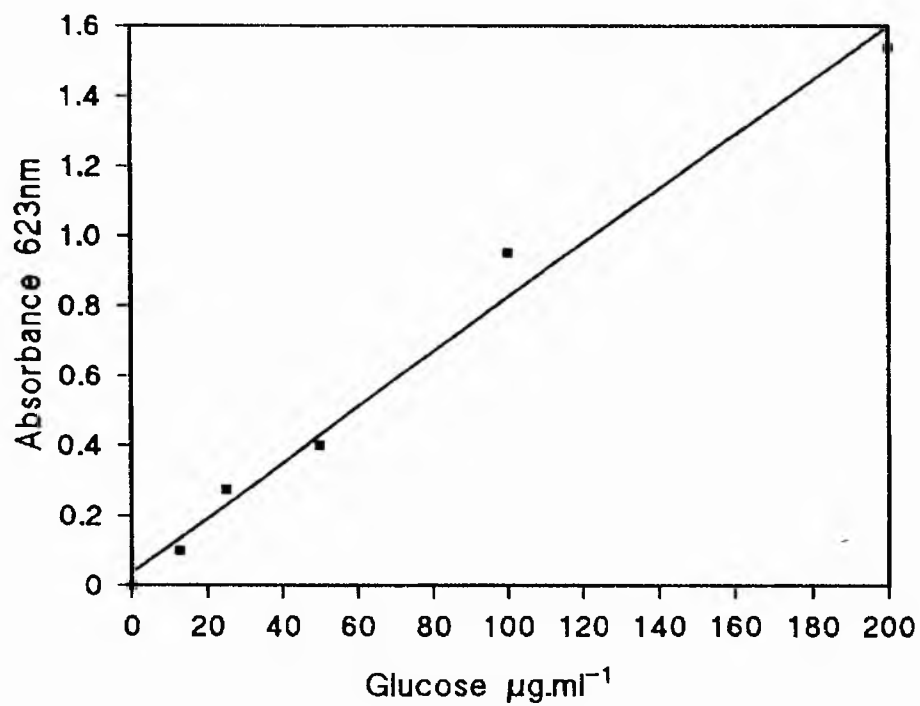


Fig. 2.3 Glucose Standard Curve

Absorbance (623nm) of glucose standards, using the Morris (1948) method (Section 2.12.1).

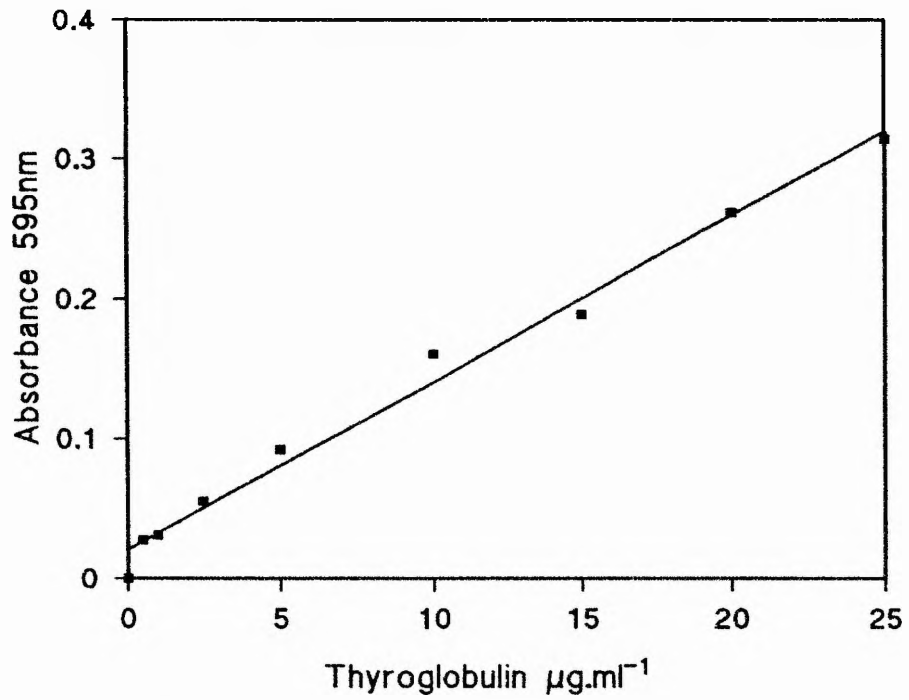


Fig. 2.4 Thyroglobulin Standard Curve

Absorbance (595nm) of thyroglobulin standards, using the Bradford (1976) method (Section 2.13.1).

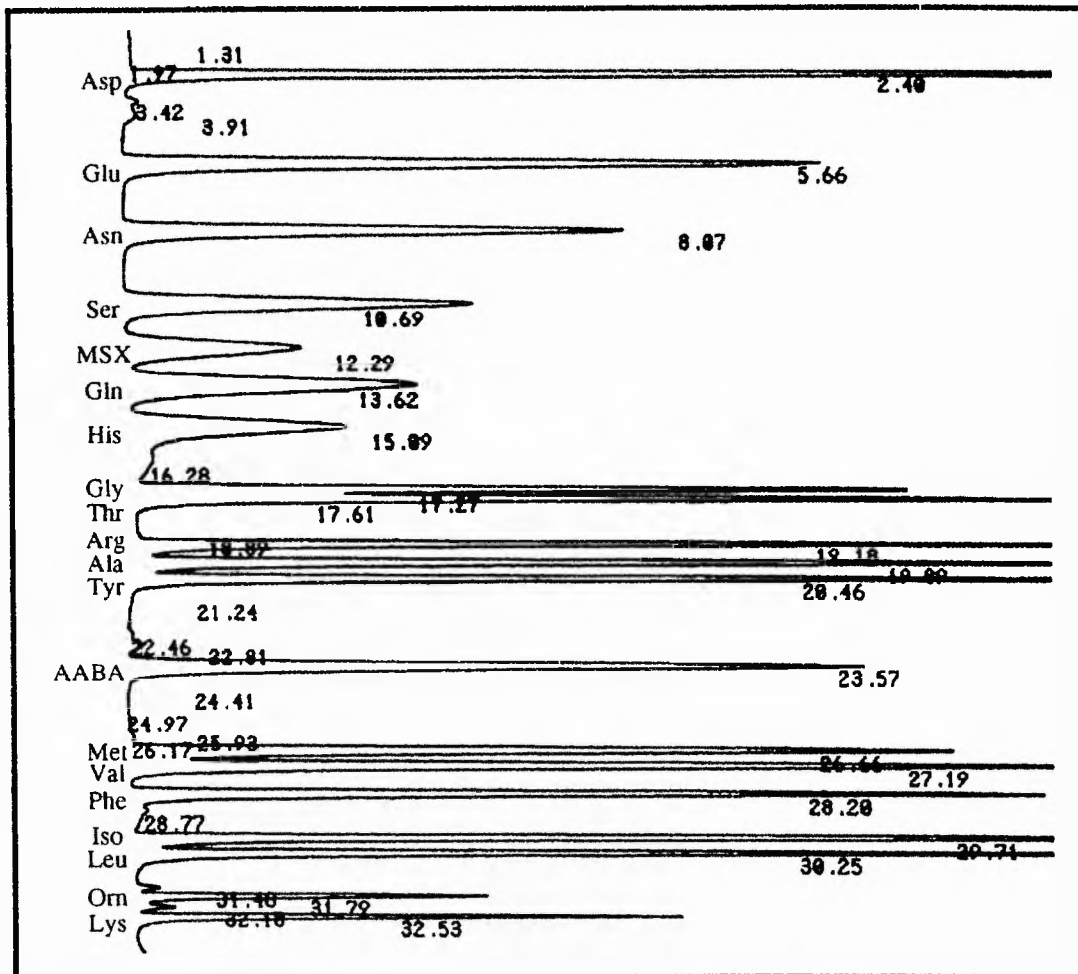


Fig. 2.5 HPLC Trace of Amino Acid Standards

Amino acid standards were analysed using HPLC (Section 2.14.2). Numbers refer to retention time of each amino acid passing through the HPLC column.

Time (Minutes)	% Methanol Phase
0	0
1	0
6	14
11	14
16	50
20	50
32	100
34	100
40	0

Table 2.1 Breakpoints for the HPLC solvent gradient

(see Section 2.14.3.1)

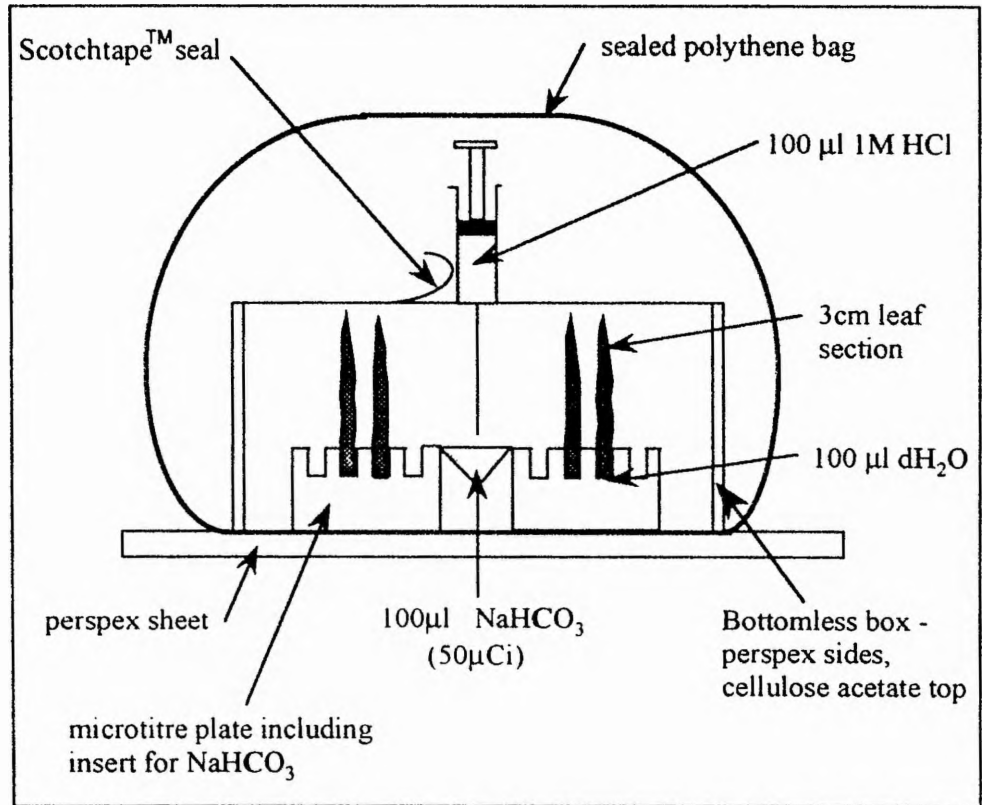


Fig. 2.6 Diagrammatic Representation of Experimental Apparatus Used for $^{14}\text{CO}_2$ Pulse-Chase Study

(see Section 2.15)

CHAPTER 3

Effects of UV-B Radiation on The Morphology of The Primary Leaf of Wheat

INTRODUCTION

Previous studies have shown UV-B radiation to cause a range of responses in plants as discussed in Chapter 1 (Reviews: Caldwell, 1971; Teramura, 1983; Tevini & Teramura, 1989; Jordan, 1993). These responses vary between both species (Barnes *et al.*, 1988), and also varieties of the same species (*G.max*; Teramura *et al.*, 1990; *O.sativa*, Teramura, Ziska & Szein, 1991). A major factor determining the effect of UV-B is the interaction of other environmental parameters, for example light (Teramura, 1980; Cen & Bornman, 1990; Deckmyn *et al.*, 1994) and temperature (Tevini, 1993; Caldwell, 1994) (Section 1.7.1).

Changes in plant morphology, including plant height, leaf area and biomass production have been found in a wide range of species from temperate crops - *T.aestivum* and *Avena sativa* (Barnes *et al.*, 1988), tropical crops - *O.sativa* (Teramura *et al.*, 1991), to subarctic grasses - *C.purpurea* (Gwynn-Jones & Johanson, 1996). The morphology of wheat has been shown to be both sensitive (Teramura, 1983) and tolerant (Krizek, 1975) to UV-B. These differences in the response of wheat grown under UV-B highlight the fact that the effects of UV-B on a single species can vary, and may be the result of differences in growth conditions. It is therefore important to characterise the growth of the primary wheat leaf under the conditions specific to this study.

3.1 Plant Growth

3.1.1 What is Growth?

Plant growth can be defined as an irreversible increase in size (Milthorpe & Moorby, 1974). At the cellular level growth can be divided into morphogenesis and

differentiation, both of which can overlap in space and time. Morphogenesis is the development of form and shape, in cells and organs, and occurs via orderly cell divisions, followed by strictly orientated cell expansion. Differentiation may refer to the development of specialized types of mature cells or to the changes occurring in development from meristematic to mature cell (Steeves & Sussex, 1989; Lyndon, 1990).

3.1.2 Plant Growth Analysis

At the whole plant level there are two principal methods for determining growth, changes in size (volume) or weight (Salisbury & Ross, 1985). Size changes involve measuring expansion in one or two directions and in the case of leaf growth include leaf length, width, thickness and area. Changes in both fresh and dry weight can be measured, although dry weight is usually used as it avoids any short-term fluctuations in water content.

Leaf morphology can affect the interception of light, temperature regulation, water balance and CO₂ diffusion (Fitter & Hay, 1987). This close relationship between morphology and factors affecting metabolism highlights the importance of measuring basic growth parameters. Effects of UV-B on plant growth therefore need to be considered when discussing the effects of UV-B on processes such as carbon and nitrogen metabolism (Chapter 6).

3.2 Control of Plant Growth

The growth of a plant is in part genetically determined (Grime *et al.*, 1990), and regulated by a complex array of endogenous factors as well as by a number of environmental signals (Review: Dale, 1988).

Of the many environmental factors which influence growth, light is probably one

of the most important, as in addition to its requirement for photosynthesis it also regulates morphogenesis (Hart, 1988). Light is also an important factor to consider regarding the work described in this chapter, as differences in light quality and quantity have been shown to modify the response of plants to UV-B (Teramura, 1980).

3.3 Chapter Aims

The effects of UV-B depend not only on the species, but also on the growth conditions. The aim of this chapter was therefore to firstly characterise the growth of the primary wheat leaf under the control and UV-B conditions used; and secondly, to investigate the effect, if any, of UV-B radiation on the morphology of the primary leaf of wheat. Changes in growth in response to UV-B could indicate alterations at the cellular and subcellular levels, and it is therefore important to understand the effects on growth before attempting to interpret such responses.

RESULTS

3.4 Effect of UV-B on Wheat Leaf Growth

3.4.1 Total Leaf Growth

Fig. 3.1a shows the increase in total plant height over the first 10 days of growth. In control-grown wheat, the total plant height increases at a linear rate up until day 9 to give a final height of *c.* 135mm. UV-B significantly reduces ($p \leq 0.05$) the total plant height from day 5 onwards. Under UV-B a final plant height of *c.* 95mm is reached on day 8, one day earlier than controls and is a reduction of *c.* 30% by comparison to the final plant height in controls.

In both control and UV-B grown plants the intercalary basal meristem begins to be displaced vertically on day 7 (Fig. 3.1b), as the meristem splits into two, the distal (basal intercalary) meristem having given rise to the leaf blade, and the proximal (sheath) meristem forming the sheath. This indicates the end of primary leaf growth from the basal intercalary meristem and the start of sheath growth from the sheath meristem. In control plants, meristem displacement, and therefore sheath growth, continues up to day 10, and may account for the increasing total plant height up until this time (Fig. 3.1a). Meristem displacement in UV-B grown plants increases up to day 9 and then ceases, signifying the end of sheath growth. This earlier cessation of sheath growth under UV-B may account for the final total plant height occurring earlier under UV-B (Fig. 3.1a).

3.4.2 Primary Leaf Growth

UV-B significantly reduces ($p \leq 0.05$) the growth of the primary leaf from day 4 onwards (Fig. 3.2a) by reducing the growth rate primarily during the light period (Fig.

3.2b).

Both control and UV-B grown plants show a diurnal fluctuation in growth rate, with maximum growth during the light period and minimum during the dark period. In control-grown plants the growth rate increases to a maximum of *c.* 1.7mm hr⁻¹, during the light period of day 5, after which it declines, and a final primary leaf length of *c.* 110mm is reached on day 9. The growth rate of UV-B treated plants in the light period is significantly lower ($p \leq 0.05$) than the control, although a similar trend is seen with the initial rate increasing to a maximum on day 5 and 6, of *c.* 1.1mm hr⁻¹, a reduction of *c.* 35 % as compared to the control. The growth rate then rapidly decreases, and a final leaf length of *c.* 75mm is reached on day 7.

In both control and UV-B-grown plants, growth of the primary leaf from cell division in the basal intercalary meristem ends 7 days post-imbibition when the sheath meristem becomes active (Section 3.4.1), any subsequent increase in primary leaf length after this will be due to cell elongation alone. Control primary leaves continue to grow at a reduced rate by cell elongation alone up until day 9 to give a final maximum primary leaf length of *c.* 110mm. Under UV-B, a maximum primary leaf length of *c.* 75mm, a reduction of *c.* 30% by comparison to controls is reached on day 7.

3.4.3 Primary Leaf Width

UV-B significantly increased ($p \leq 0.05$) the width throughout the length of the 7-d-old primary wheat leaf. (Fig. 3.3). Both control and UV-B grown leaves showed a similar distribution of width along the leaf blade, with the width increasing from the leaf base to a maximum level, 3/4 of the way along the leaf before decreasing towards the tip. The average leaf width of the 7-d-old primary leaf grown under UV-B was *c.* 10% greater than the control.

3.4.4 Primary Leaf Area

Primary leaf area increased at a linear rate between days 4-7 post-imbibition (Fig. 3.4). UV-B had no effect on the primary leaf area on days 4-5, but was significantly reduced ($p \leq 0.05$) on days 6-7. The average leaf area of 7-d-old primary leaves was reduced by *c.* 18% under UV-B as compared to the control.

3.4.5 Primary Leaf Fresh and Dry Weight

The mean fresh and dry weight of the primary leaf increased at a linear rate between days 4 -7 post-imbibition (Fig. 3.5). UV-B had no significant effect on either the fresh or dry weight over this period. The dry weight of the primary leaf was maintained at *c.* 10% of the fresh weight over the whole growing period, *i.e.* the water content of the leaf at the time of harvest was a constant *c.* 90% .

3.4.6 Specific Primary Leaf Area

The specific leaf area (ratio of leaf area to leaf dry weight) of the primary leaf increased slightly between days 4-7 post-imbibition (Fig. 3.6). UV-B had no significant effect on the specific leaf area on days 4-5, but was significantly reduced ($p \leq 0.05$) on days 6-7. The specific leaf area of 7-d-old primary leaves was reduced by *c.* 15% compared to the control.

3.4.7 Primary Leaf Thickness

UV-B significantly increased ($p \leq 0.05$) both the average maximum and minimum thickness of the middle section (15-40mm) of the 7-d-old primary leaf blade (Fig 3.7 a, b).

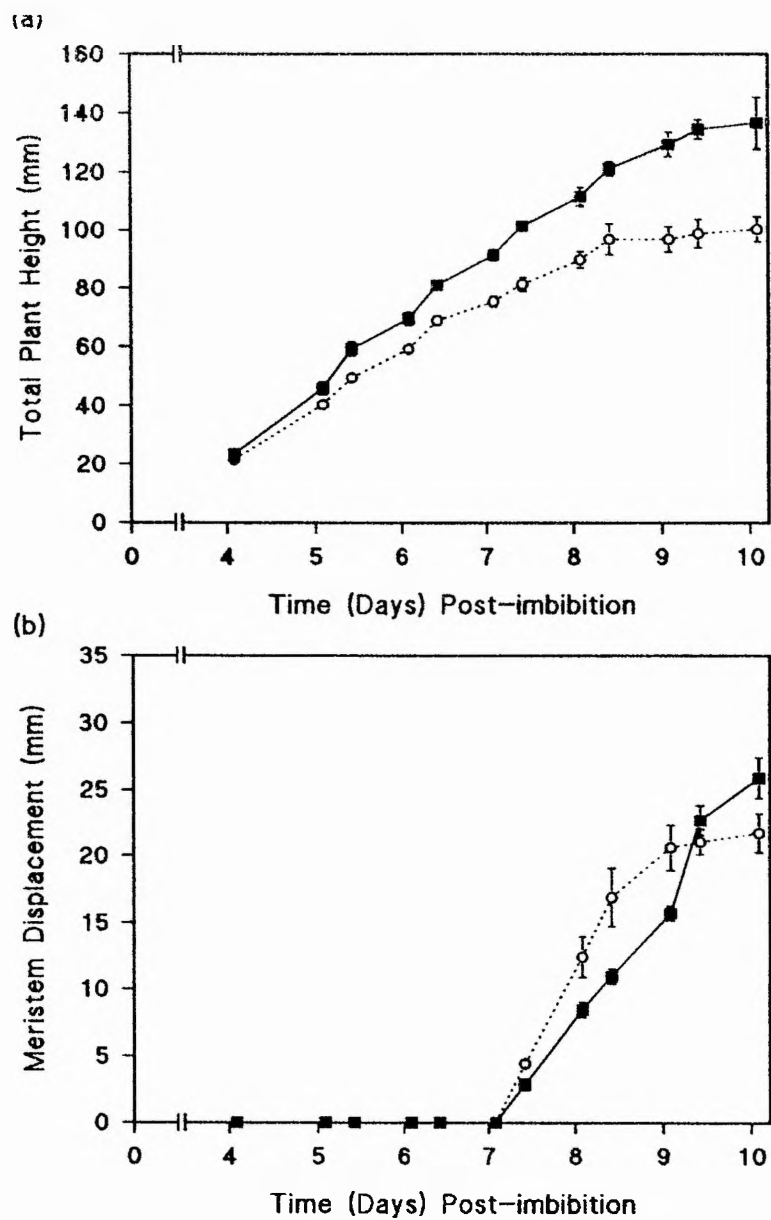


Fig. 3.1 Effect of UV-B radiation on (a) total plant height, and (b) meristem displacement

Plants were grown under control (■) and UV-B (○) conditions (Section 2.2). Total plant height and meristem displacement (*i.e.* distance between leaf base and the basal intercalary meristem) was measured as described in Section 2.5.1. Data points represent the mean of 5 independent growth studies, sampling 30 seedlings per replicate. Error bars show \pm one standard error of the mean.

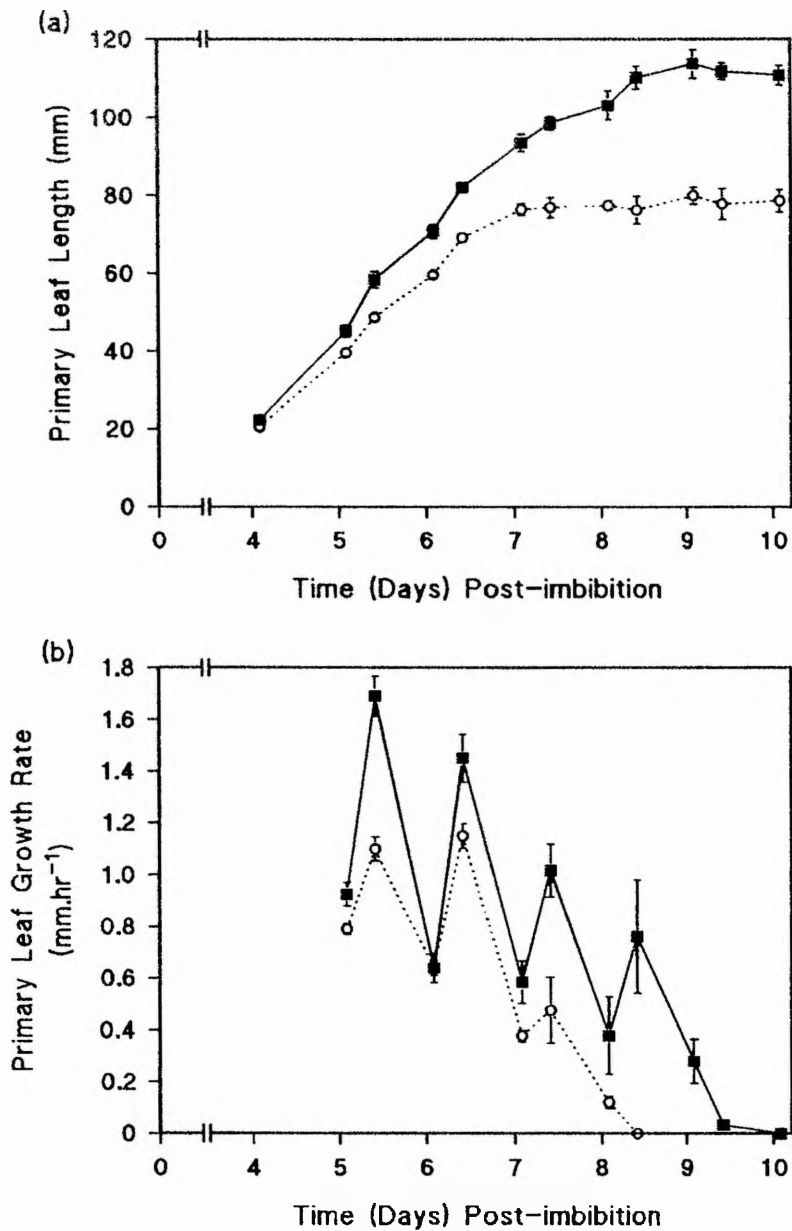


Fig. 3.2 Effect of UV-B radiation on primary leaf length (a) and growth rate (b) Plants were grown under control (■) and UV-B (○) conditions (Section 2.2). Primary leaf length was measured as described in Section 2.5.1. Data points represent the mean of 5 independent growth studies, sampling 30 seedlings per replicate. Error bars show \pm one standard error of the mean.

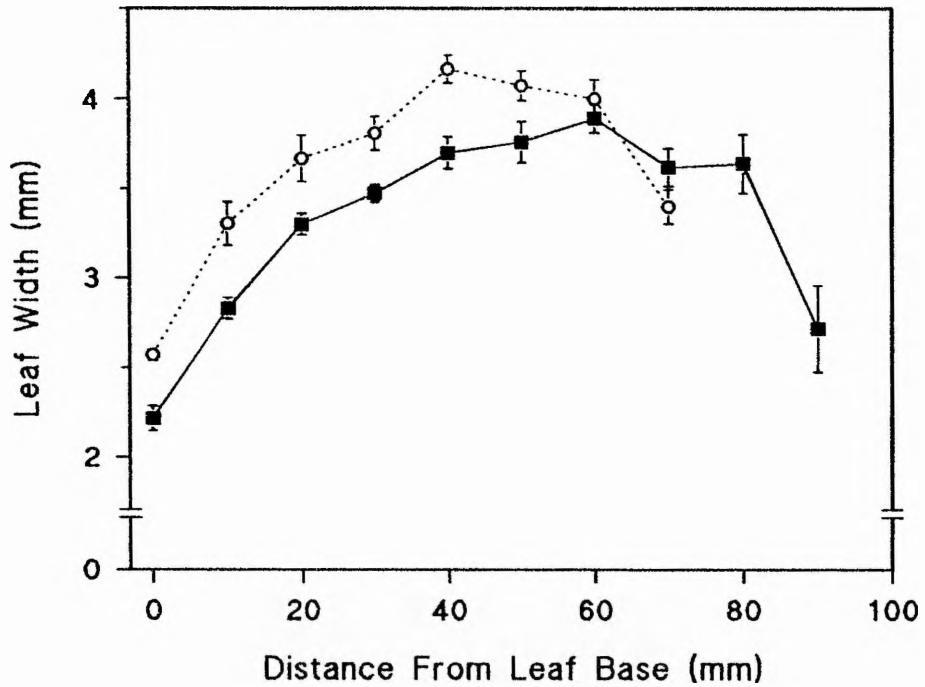


Fig. 3.3 Effect of UV-B radiation on the width of 7-d-old primary leaves

Plants were grown under control (■) and UV-B (○) conditions (Section 2.2). Leaf width was measured as described in Section 2.5.3. Data points represent the mean of 5 independent growth studies, sampling 10 seedlings per replicate. Error bars show \pm one standard error of the mean.

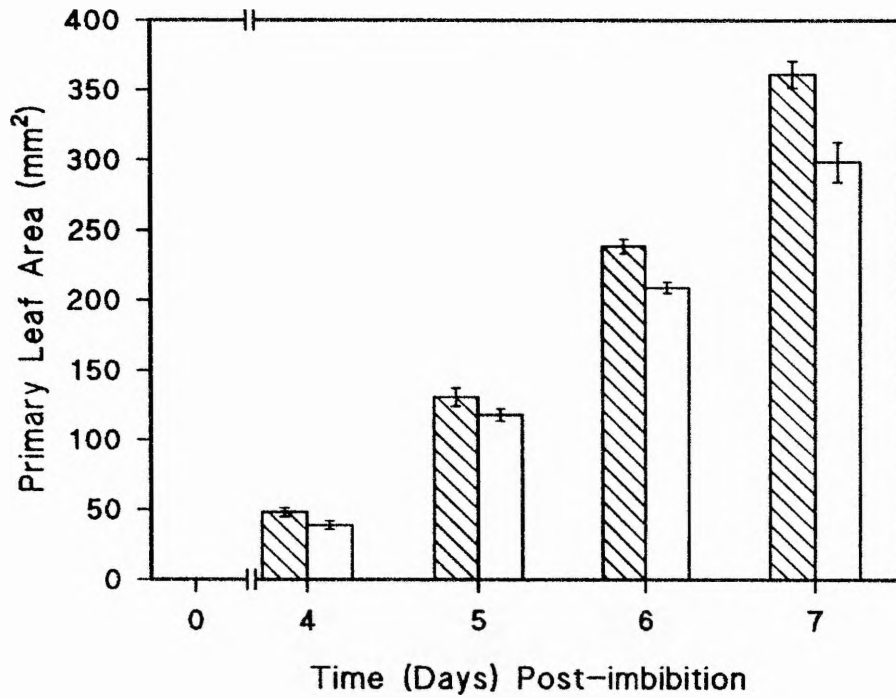


Fig. 3.4 Effect of UV-B radiation on primary leaf area

Plants were grown under control (▨) and UV-B (□) conditions (Section 2.2). Primary leaf area was measured as described in Section 2.5.3. Data points represent the mean of 5 independent growth studies, sampling 10 seedlings per replicate. Error bars show \pm one standard error of the mean.

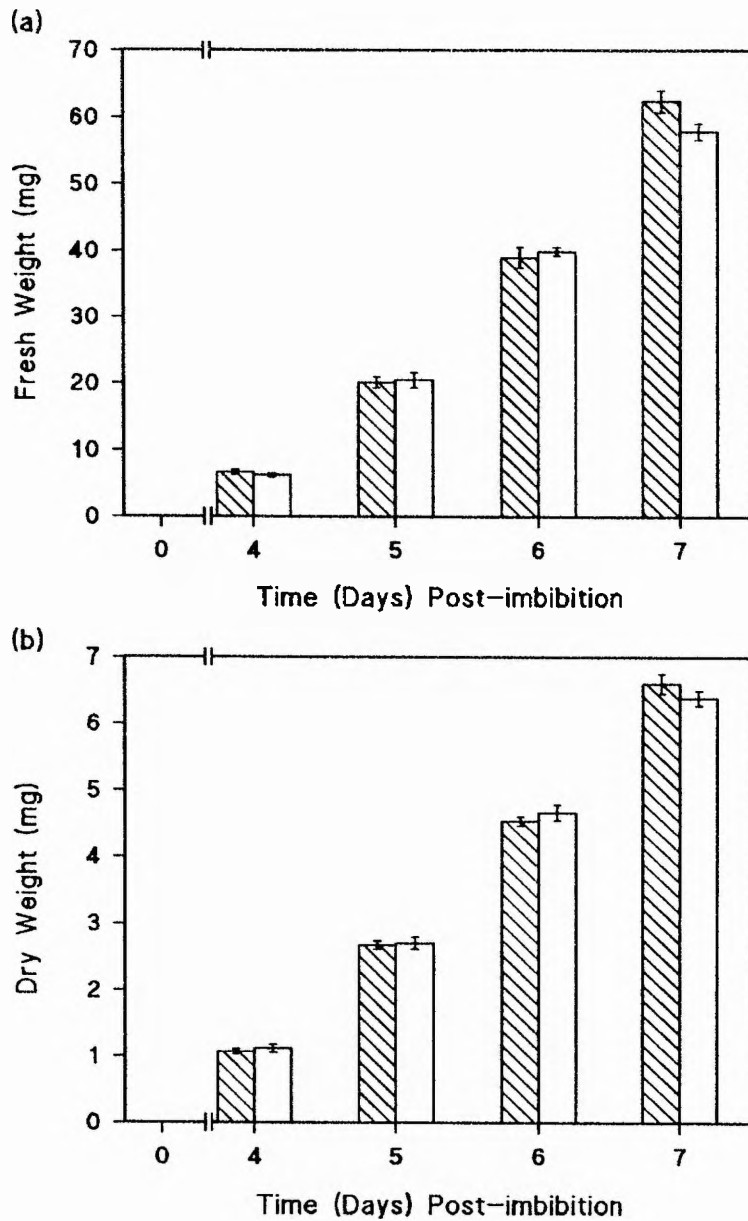


Fig. 3.5 Effect of UV-B radiation on primary leaf (a) fresh weight , and (b) dry weight. Plants were grown under control (▨) and UV-B (□) conditions (Section 2.2). Fresh and dry weights were measured as described in Section 2.5.2. Data points represent the mean of 5 independent growth studies, sampling 10 seedlings per replicate. Error bars show \pm one standard error of the mean.

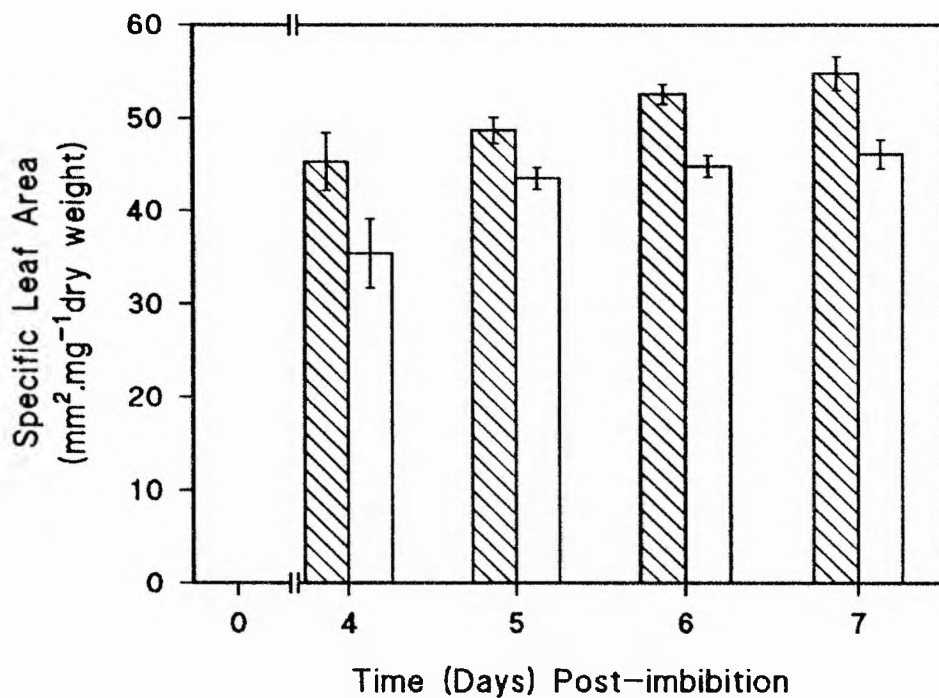


Fig. 3.6 Effect of UV-B radiation on specific leaf area

Plants were grown under control (▨) and UV-B (□) conditions (Section 2.2). Specific leaf area was calculated from primary leaf dry weight (Fig.3.5b) and leaf area (Fig 3.4) as described in Section 3.4.6. Data points represent the mean of 5 independent growth studies. Error bars show \pm one standard error of the mean.

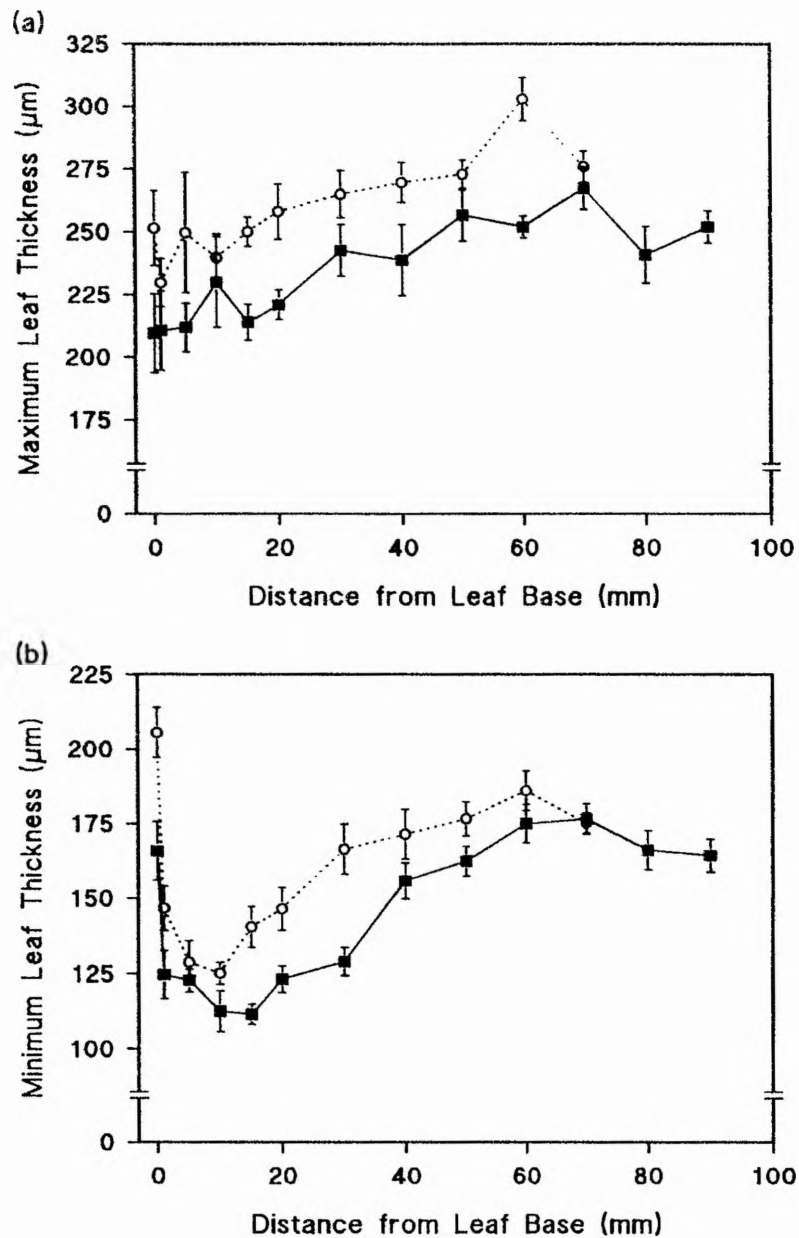


Fig. 3.7 Effect of UV-B on the average (a) maximum, and (b) minimum thickness of 7-d-old primary leaves

Plants were grown under control (■) and UV-B (○) conditions (Section 2.2). The average maximum and minimum leaf thickness was measured as described in Section 2.8. Data points represent the mean of 5 independent growth studies, sampling 10 seedlings per replicate. Error bars show \pm one standard error of the mean.

DISCUSSION

3.5 Growth of the Primary Leaf of Wheat

The growth of the primary leaf of wheat is a well characterised system (Reviews: Leech & Pyke, 1988; Tobin & Rogers, 1992), and in this study the leaf length, width, area and thickness of control grown plants were comparable to those of previous studies on wheat (Boffey *et al.*, 1979; Dean & Leech, 1982; Jellings & Leech, 1984; Pyke & Leech, 1985). Both the control and UV-B-grown leaves showed a typical sigmoidal growth curve, with slow growth at first, increasing at a linear rate before reaching a final constant level. The basal intercalary meristem was displaced from the leaf base on day 7 in both treatments, signifying the end of primary leaf growth by both cell division and elongation. The leaf on day 7, therefore, comprises a maximum range of cell ages between the leaf base and tip and unless specified otherwise primary leaf tissue was harvested on day 7.

The size and shape of a leaf is dependent upon the shape of the primordium, the frequency, distribution and orientation of cell division and the amount and distribution of cell expansion (Wareing & Phillips, 1981). These are in part genetically determined (Grime *et al.*, 1990) and regulated by a complex array of endogenous factors and environmental signals. In a study on the primary leaf of *H.vulgare*, Albrechtová and Kubínova (1991) proposed that the anatomy and morphology of the first leaf was primarily dependent on internal factors of plant development, such as seed nutrition. The following results, however, show that the development of the primary wheat leaf is not simply pre-determined and can be influenced by external factors such as UV-B.

3.6 Changes in Primary Leaf Growth Under UV-B

A reduction in leaf length is a common response to UV-B and has been demonstrated in a variety of species including *A.sativa* (Barnes *et al.*, 1988), *Lycopersicon esculentum* (tomato; Ballaré *et al.*, 1995a) and *Liquidambar styraciflua* (Dillenburg, Sullivan & Teramura, 1995). Work described in this chapter shows that 7-d-old primary leaves grown under UV-B were *c.*17% shorter than controls. A similar reduction in leaf length was found in *Triticum aestivum* L. cv. Bannock (Barnes, Flint & Caldwell, 1990). As well as reducing primary leaf length, the maximum length of the primary leaf is reached earlier when grown under UV-B. This is consistent with the work of Teramura and Caldwell (1981) on leaf expansion in *G.max*, in which leaves grown under UV-B were fully expanded at an earlier time than controls, but in contrast with the present study the final size of the UV-B-grown soybean leaves was greater than the control.

The changes observed in the growth of the primary wheat leaf can be related to the lower growth rate and earlier decline in growth found under UV-B. Similar reductions in growth rate (leaf elongation) have been observed in *Lepidum sativum* seedlings (cress; Steinmetz & Wellmann, 1986) and *L.esculentum* seedlings (Ballaré *et al.*, 1995a). Steinmetz and Wellmann (1986) found the inhibition of seedling elongation in *L.sativum* increased with decreasing UV wavelength, and it has been suggested (Ballaré *et al.*, 1996) that this could be due to direct effects, for example damage to proteins or cellular signals from DNA damage (Beggs, Stolzer-Jehle & Wellmann, 1985), or oxidative stress (Strid, 1993). In the case of reduced *L.esculentum* seedling emergence and hypocotyl elongation, the maximum inhibition occurred at a wavelength of 300nm suggesting that the response is triggered by a specific UV-B receptor (Ballaré

et al., 1995a). It was concluded that such a response may play a protective role, as a delay of a few hours in seedling emergence was sufficient to allow the synthesis of flavonoids, increasing the screening capacity of the tissue and protecting the sensitive sites from UV-B induced damage (Ballaré *et al.*, 1995b).

The width of the primary leaf was significantly increased under UV-B, with an average width *c.*10% greater than controls. In grasses, however, leaf area is primarily determined by vertical rather than horizontal cell expansion, Nelson *et al.*, (1977) calculated that in *Festuca arundinacea* (tall fescue) the leaf elongation rate was 1.7 times more influential than leaf width in modifying leaf area expansion. In the UV-B-grown plants of this study, the reduction of leaf length will therefore have a greater influence in determining the leaf area than the increased leaf width and this is confirmed by the observed *c.*18% reduction in primary leaf area of UV-B-grown plants compared to controls. Significant reductions in the leaf area of a range of species have also been reported by Barnes *et al.*, (1990).

In many studies, morphological changes in size, for example, leaf length and area appear to be more sensitive to UV-B than total biomass production (Gold & Caldwell, 1983; Barnes *et al.*, 1988, 1990). Work described in this chapter shows UV-B to have no significant effect on the fresh or dry weight of the primary leaf, despite the significant reduction in both leaf length and area when grown under UV-B. A similar response of reduced leaf area and length, with no changes in leaf dry weight was found in *Triticum aestivum* L. cv Bannock grown under UV-B (Barnes *et al.*, 1990).

Changes in the ratio of leaf area to dry weight, the specific leaf area (inverse of specific leaf weight) can be a reflection of both leaf density (dry mass per unit volume) and leaf thickness (Witkowski & Lamont, 1991). In wheat there is a negative

relationship between specific leaf area and leaf thickness (Kaminski *et al.*, 1990). In the present study UV-B significantly reduced the specific leaf area of the primary wheat leaf. A similar response (increased specific leaf weight) has been found before in *T.aestivum* L. cv Bannock (Barnes *et al.*, 1990) and a variety of other species including *C.sativus* (Takeuchi *et al.*, 1989), *Datura ferox* (Ballaré *et al.*, 1996) and the subarctic grass, *C. purpurea* (Gwynn-Jones & Johanson, 1996).

The decreased specific leaf area found in the primary wheat leaf could be accounted for by the significant increase in thickness of the leaf blade. Increased leaf thickness is a common response to UV-B (Cen & Bornman, 1990, 1993; Day, 1993), and it has been suggested to be a possible protective mechanism against the effects of UV-B by reducing light penetration into the leaf (Warner & Caldwell, 1983; Flint, Jordan & Caldwell, 1985). As well as lowering the internal UV-B fluence within the leaves, thicker leaves may also reduce penetration of visible light. It has been suggested that leaves may compensate for UV-B stress by increasing leaf thickness and controlling simultaneously the internal light gradient through modification of pigment content (Bornman & Vogelmann, 1991). Increases in leaf thickness have been found to be positively correlated to increased concentrations of flavonoids per leaf area (Cen & Bornman, 1993; Gwynn-Jones & Johanson, 1996).

The major aim of this chapter was to determine the effect, if any, of UV-B on the morphology of the primary wheat leaf. UV-B affects leaf morphology, resulting in a shorter, broader, thicker leaf blade. This altered growth under UV-B may be the result of alterations in cell division and/ or cell elongation, and the effects of UV-B on these processes will be investigated in the following chapter.

CHAPTER 4

Effects of UV-B Radiation on Primary Leaf Cell Development in Wheat

INTRODUCTION

Plant growth and development comprises three fundamental processes which can overlap in both space and time; those of cell division, expansion and differentiation (Dale, 1988). Changes in plant growth rates may be the result of alterations in cell division and/or cell expansion. Growth studies by Nelson and co-workers on *F.arundinacea* have shown that altered growth may be the result of different combinations in responses of cell division and elongation. For example, differences in growth between genotypes were found to be the result of altered cell division and expansion (Volenec & Nelson, 1981); differences in growth due to the application of nitrogen were the result of altered cell division alone (Volenec & Nelson, 1983); and changes under high and low irradiance were the result of altered cell expansion rates (Schnyder & Nelson, 1989). The purpose of this chapter is to investigate the effects of UV-B on cell division and expansion of the primary wheat leaf in order to explain the leaf growth responses observed in the previous chapter.

4.1 Leaf Development

All leaves, irrespective of their final size and form, have similar origins (Lyndon, 1983), arising from primordia produced by the shoot apical meristem at specific positions and in a regular sequence characteristic of the species (Cutter, 1971; Dale, 1988,1992).

The shoot apical meristem is classically considered to consist of two zones, the tunica (outer layers of cells) in which cell division is predominantly anticlinal, and the corpus (inner region of cells) in which cell division occurs in both the anticlinal and

periclinal planes (Lyndon, 1983). The earliest sign of leaf initiation is the formation of the leaf buttress from periclinal divisions in the tunica. In dicotyledonous species this division occurs in the lower layers of cells, in contrast to monocotyledonous species where division occurs within the outermost layer of cells, forming the epidermis. Growth continues as the cells in the corpus start to divide to form the leaf primordia. Once the primordium is *c.* 80-200 μ m in length, both marginal and submarginal meristems are established along the lateral flanks of dicot leaves. In monocot leaves however, marginal growth is absent and there is the establishment of a region of cell division in the leaf base (Cutter, 1971; Dale, 1988).

4.1.1 Dicotyledon Leaf

In dicots, clusters of cell division (intercalary meristems) occur throughout the leaf blade (Maksymowych, 1973). This pattern of growth makes it difficult to separate areas where cell division, expansion and differentiation are occurring within the leaf, making dicot leaf development extremely complex to model.

4.1.2 Monocotyledon Leaf

In monocot leaves, the region of cell division is located within the leaf base (basal intercalary meristem) and produces a developmental gradient of cells along the length of the leaf. Cell division and expansion occur in specific zones of the leaf blade and provide a simple model in which to study development. The growth of monocot leaves, especially those of the grasses (Poaceae), for example, *Triticum aestivum* and *F.arundinacea* have been extensively studied and developmental changes are well characterised (Leech & Baker, 1983; Nelson & MacAdam, 1989; Tobin & Rogers, 1992).

4.1.2.1 Grass leaf development - a model system

The developing grass leaf provides a simple model in which to study cell division and expansion. In the leaf blade cell division and expansion occur within specific zones located in the basal region of the blade, which is enclosed by the sheath of subtending leaves, or in the case of the primary leaf, the coleoptile (Nelson & MacAdam, 1989). Cell division is largely unidirectional, with the basal intercalary meristem producing parallel files of cells (Sharman, 1942; Robertson & Laetsch, 1974). Cells within a file then expand and are displaced away towards the leaf tip as a result of continued cell division and expansion of younger cells within the same file. In the grass leaf *c.* 85% of cell expansion occurs along the longitudinal axis of the leaf blade and is usually referred to as elongation (Schnyder & Nelson, 1987). This produces a gradient along the leaf blade in which both the age and developmental stage of a cell are a function of its position relative to the origin (*i.e.* basal meristem).

Both cell division and elongation contribute to leaf growth, and the temporal and spatial separation of these processes within the grass leaf provide a simple model in which to determine the cause of reduced growth in UV-B-grown plants.

4.2 Mechanism and Regulation of Cell Division and Expansion

4.2.1 Cell Division

Actively dividing cells, as found within the basal meristem of the grass leaf, pass through a regular sequence of events known as the cell cycle (Reviews : Francis, 1992; Doerner, 1994; Francis & Halford, 1995). The cell cycle comprises 4 phases : pre-synthetic interphase (G_1); DNA synthesis and replication (S); post-synthetic interphase (G_2); and mitosis (M) (Quastler & Sherman, 1959) (see Fig. 4.1)

Progression through the cell cycle is driven by a cascade of protein phosphorylation and dephosphorylation reactions (Pines, 1994). Two principal checkpoints of the cell cycle have been identified at the transition of G₁ - S, and G₂ - M, and are controlled by a number of proteins, of which p34^{cdc2} and cyclins are of primary importance (John, Sek & Lee, 1989).

4.2.2 Cell Expansion

Cell expansion is constrained by the primary cell wall, which is a rigid structure with the capacity to undergo both elastic (reversible) and plastic (irreversible) deformation (Brett & Waldron, 1996). The driving force for cell expansion is osmotic water uptake into the cell which causes a hydrostatic pressure to be exerted against the cell wall (turgor pressure) resulting in wall extension (Lockhart, 1965). The increased turgor pressure promotes cell wall extension but at the same time opposes the continued uptake of water. Therefore to expand, the cell must continually adjust its turgor pressure in order to balance its conflicting roles in water uptake and cell wall extension. This process, known as stress relaxation, is the result of wall-loosening events (Cosgrove, 1987).

Alteration in wall structure that may regulate cell expansion involves the breaking and reforming of cross linkages. Changes in phenolic cross-links between polymers, for example, between tyrosine residues within extensin and between ferulic acid in substituents in pectin, may control wall extensibility (Brett & Waldron, 1996). Both bonds are formed by the action of peroxidase, the concentration of which has been shown to be inversely related to wall extensibility. MacAdam, Nelson and Sharp (1992a) found that an increase in peroxidase activity in epidermal cell walls was directly correlated to the cessation of elongation along the leaf blade of *F.arundinacea*. In an

accompanying paper, MacAdam, Sharp and Nelson (1992b) found that it was the secretion of cationic isoforms of peroxidase into the cell wall that was linked to cessation of elongation, and suggested that the peroxidase was attracted to the net negative charge of the cell wall, resulting in the oxidation of ferulic acid and the covalent binding of hemicellulose and pectins into the wall.

A variety of growth substances, including auxin, gibberellins and ethylene have also been shown to regulate cell expansion (Reviewed: Brett & Waldron, 1996). The mechanism by which auxin stimulates cell wall extensibility has been the subject of much research. In the long-term, auxin stimulates the synthesis of wall polysaccharides (Brett & Waldron, 1996). However, it also acts rapidly on wall extensibility and more direct mechanisms are involved. One of the most well established theories for the rapid effects of auxin is the acid growth theory (Rayle & Cleland, 1977), although recent evidence would suggest that this generally only regulates growth when it is limiting (Brett & Waldron, 1996). The regulation of cell wall extensibility by auxin involves a complex control system, which is only partially understood at this time (Estelle, 1992).

4.3 Chapter Aims

Leaf growth originates from the two fundamental processes of cell division and elongation - either, or both of which may be targets for UV-B. This chapter aims to explain the growth changes reported in the previous chapter in relation to the observed effects of UV-B on cell division and elongation. Secondly, data of the spatial distribution of growth velocities within the zone of cell elongation will be used to calculate the gradient of cell age along the leaf blade. In the following chapters the

effects of UV-B at the ultrastructural and biochemical levels can therefore be compared directly in cells of the same age.

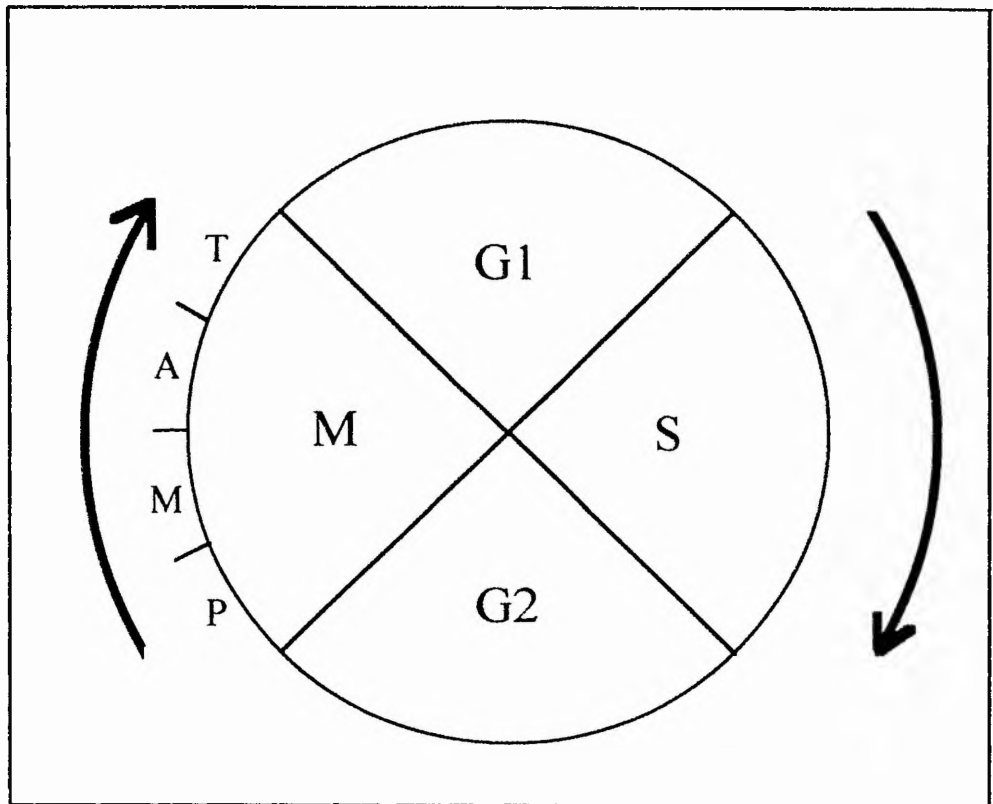


Fig. 4.1 The Cell Cycle

The diagram highlights the pre-synthetic interphase (G1), DNA synthesis (S), post-synthetic interphase (G2) and mitosis (M). Prophase (P) indicates initiation of mitosis (M) which consists of metaphase (M), anaphase (A) and telophase (T) states. Arrows indicate direction of cell division cycle (After Francis, 1992).

RESULTS

4.4 Effect of UV-B on Cell Division in the Primary Leaf Basal Meristem

4.4.1 Mitotic Index

The zone of cell division in both 7-d-old control and UV-B-grown plants, is located within the basal 5mm of the primary leaf, and within this zone UV-B significantly reduced ($p \leq 0.05$) the percentage of mitotically active cells, *i.e.* the mitotic index (Fig. 4.2).

In control plants a maximum mitotic index of *c.* 5% occurs within the basal intercalary meristem and decreases with distance, so that mitotic activity is absent from cells at and beyond 5mm from the leaf base. A similar pattern in mitotic activity is found within UV-B grown plants, with a maximum of *c.* 4% occurring within the basal intercalary meristem. The rate at which the mitotic index decreases with distance from the leaf base is increased under UV-B. This is the result of a significant reduction ($p \leq 0.05$) in the mitotic index of cells 1-3mm above the leaf base, but there was no difference in the mitotic index of cells at 0 and 5mm above the leaf base.

Plate 4.1 shows a tissue squash of cells in different mitotic stages from the basal intercalary meristem. The percentage of cells in the different stages of mitosis varies within the zone of division, with the percentage of cells in interphase increasing (Fig. 4.3a), while those in the other stages of mitosis decrease with distance from the leaf base (Fig.4.3 b-e). The reduction in the mitotic index in UV-B-grown plants can be attributed to the increased percentage of cells in interphase (Fig. 4.3a) and decreased percentage of cells in all other mitotic stages (Fig. 4.3 b-e). This reduction in mitotic index appears not to affect any particular stage more than another and in all of these

stages the greatest effect of UV-B occurs 2mm above the leaf base, with no change within the basal, 0mm section.

4.4.2 Cell Doubling Time

To determine cell doubling times (CDT), leaf material was treated with colchicine (Section 2.5.5). This inhibits spindle formation so that actively dividing cells arrest in metaphase (Utrilla, Sans & De la Torre, 1989). These cells are characterised by the presence of un-orientated chromosomes (Plate 4.2b), as compared to control metaphase (*i.e.* minus colchicine) in which the chromosomes align at the central plate (Plate 4.2a).

The pattern of metaphase accumulation over time is sigmoidal (Fig. 4.4a) with an initial lag (0-2 hours) in accumulation before colchicine starts to act, then increasing for a time at a linear rate (2-10 hours), after which the rate of accumulation is reduced (10-12 hours). This reduction may be due to the phenomenon of reconstituted nuclei, which form in cells after prolonged exposure to colchicine (Utrilla *et al.*, 1989). In these cells the spindle and chromosomes collapse into a ball structure resembling prophase, so that the true proportion of cells arrested in metaphase will be underestimated. Cell doubling times were calculated by regression analysis (Section 2.5.5) from the linear portion (2-10 hours) of the metaphase accumulation curve. Linear regression analysis of each of the 3 replicates per treatment gave regression co-efficients (*i.e.* the slope of the line) of 2.1, 2.67, 1.95 for control, and 1.53, 1.26, 1.05 for UV-B-grown plants. The CDT was calculated as described in Section 2.5.5, and showed UV-B significantly increased ($p \leq 0.05$) the CDT to 55.6 ± 2.85 hours, compared to 31.5 ± 6.02 hours in control-grown plants.

4.5 Effect of UV-B on Cell Elongation

4.5.1 Mesophyll Cell Numbers

Changes in mesophyll cell number along the length of the primary leaf blade provides an indication of the zone of mesophyll cell elongation (Fig. 4.5). In control-grown plants the number of mesophyll cells is highest in the basal 5mm of the leaf blade (*c.* 11×10^7 cells g^{-1} fwt), cell numbers then rapidly decrease to a constant level (*c.* 2×10^7 cells g^{-1} fwt) from 20mm onwards. This indicates that mesophyll cell elongation of control-grown plants occurs within the basal 20mm of the leaf. A similar distribution is found in UV-B-grown plants, with the highest number of cells in the basal 5mm of the leaf (*c.* 9×10^7 cells g^{-1} fwt), decreasing to a constant level (*c.* 2×10^7 cells g^{-1} fwt) at 20mm. UV-B therefore appears to have no effect on the size of the zone of mesophyll elongation.

4.5.2 Epidermal Cell Length

Changes in epidermal cell length along the length of the leaf blade provide an estimate of the zone of epidermal elongation. The relationship between epidermal cell length and the position within the basal region of the leaf blade was similar in both control and UV-B grown plants (Fig. 4.6). In control plants, cells were *c.* $40\mu\text{m}$ in length close to the leaf base and reached a final cell length of *c.* $170\mu\text{m}$. This constant epidermal cell length was reached 14mm from the leaf base, indicating this to be the region of epidermal elongation. UV-B significantly increased ($p \leq 0.05$) the length of cells close to the leaf base, to *c.* $50\mu\text{m}$, however the final cell length, *c.* $140\mu\text{m}$, was significantly smaller ($p \leq 0.05$) than in the control plants. UV-B also reduced the distance in which a constant cell length was achieved to 12mm, therefore reducing the zone of epidermal elongation.

4.5.3 Spatial Distribution of Segmental Elongation Rates (SER) Within the Cell Elongation Zone

Fig. 4.7a shows the spatial distribution of SER (*i.e.* the rate of expansion of each segment relative to itself) within the basal region of 7-d-old primary leaves. UV-B reduced both the size of the elongation zone (basal 12mm compared to 14mm on the control), and also the SER of leaf tissue within the zone.

In both treatments the SER was lower within the basal 2mm of the leaf, then increased to a maximum at 4mm above the leaf base of $0.13\text{mm}\cdot\text{mm}^{-1}\cdot\text{hr}^{-1}$ in control plants, compared to $0.10\text{mm}\cdot\text{mm}^{-1}\cdot\text{hr}^{-1}$ in UV-B-grown plants. The SER then decreased and cessation of elongation occurred 14mm and 12mm above the leaf base of control and UV-B-grown plants respectively. UV-B significantly reduced ($p\leq 0.05$) the SER from the point of maximum elongation (4mm from the leaf base) through to the end of the elongation zone.

4.5.4 Spatial Distribution of Vertical Displacement Velocity (V_D) Within the Cell Elongation Zone

The V_D (*i.e.* the speed at which a certain segment is moving up the leaf blade) increased with distance from the leaf base, to the distal end of the elongation zone, where it became constant (Fig. 4.7b). UV-B significantly reduced ($p\leq 0.05$) the V_D in all regions beyond the basal 6mm of the leaf blade. Tissue was therefore being displaced more slowly through the elongation zone in UV-B grown plants. The final constant V_D was $0.7\text{mm}\cdot\text{hr}^{-1}$ in UV-B-grown plants compared with $0.95\text{mm}\cdot\text{hr}^{-1}$ in control plants, a reduction of *c.*30% by comparison. This constant V_D is a reflection of the leaf growth rate (Section 3.3.2) and is comparable to the mean growth rate over days 6-7 (Fig 3.2) of *c.* $0.7\text{mm}\cdot\text{hr}^{-1}$ in UV-B and *c.* $0.9\text{mm}\cdot\text{hr}^{-1}$ in control-grown plants.

4.6 Effects of UV-B on Cellular Differentiation

4.6.1 Tissue Preservation and Structure

Plate 4.3 shows the development of the primary leaf in transverse sections at the light microscope (LM) level. The thick tissue sections (0.5 μ m) used in the analysis of cellular differentiation at the LM level were taken from blocks fixed and embedded for transmission electron microscopy (TEM) (Sections 2.6-2.7). This provided a means of assessing both the fixation and orientation of tissue within the block before subsequent processing for analysis at the TEM level (see Chapter 5).

Plate 4.3a-d shows the changes in tissue structure from the leaf base to the leaf tip. The lack of shrinkage of cell contents from the cell wall is an indication of good fixation. Mesophyll cells in the basal region of the leaf are tightly packed together and contain a large amount of cytoplasm in cross-section with numerous small vacuoles, that may be inter-connected in the 3D cell (Plate 4.3a). As mesophyll cells develop (*i.e.* displaced towards the leaf tip) they become less packed with the formation of inter-cellular spaces, and there is an increase in transverse cell area accompanied by the formation of one large central vacuole, with all other cell contents becoming appressed against the cell wall (Plate 4.3d).

4.6.2 Volume Fractions of Tissue Types in the Primary Leaf

The volume fraction (V_V , *i.e.* the fractional volume of tissue occupied by each tissue type) of transverse leaf sections occupied by different tissue types varied along the length of the primary leaf (Fig. 4.8). The V_V of both epidermal and mesophyll tissue was similar in control and UV-B-grown plants, remaining relatively constant along the leaf blade (Fig. 4.8 a,c). The V_V of air spaces increased along the length of the leaf blade (Fig. 4.8d) as the V_V of vascular tissue decreased (Fig. 4.8b). An increase in the

V_v of air spaces within the basal region of the leaves grown under UV-B may be accounted for by slight decreases in the V_v of mesophyll and vascular tissue in this region. The average V_v of the whole leaf blade occupied by each tissue type was similar in both control and UV-B-grown plants, giving a ratio of volumes of mesophyll : vascular : epidermal : air of *c.* 10 : 1 : 5 : 4 (Fig 4.9).

4.6.3 Frequency of Cell Types in the Primary Leaf

The frequency of mesophyll, vascular and epidermal cells as a percentage of total cells was similar in both control and UV-B-grown plants, remaining relatively constant along the length of the leaf blade (Fig. 4.10). The frequency of each cell type, averaged for the whole leaf blade was similar in both control and UV-B-grown plants, giving a cell number ratio of mesophyll : vascular : epidermal of *c.* 8 : 7 : 5 (Fig. 4.11).

4.7 Cell Age Determination

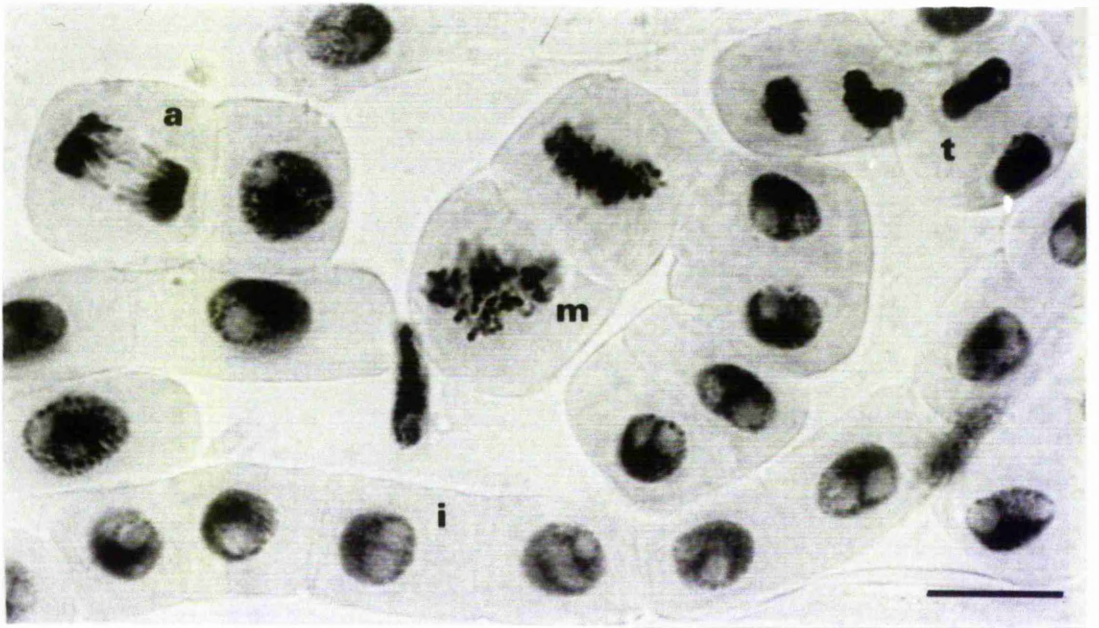
The distribution of cell ages along the leaf blade is similar in control and UV-B-grown plants, with a rapid ageing of cells over a short distance in the basal region of the leaf, followed by a linear increase in age towards the leaf tip (Fig. 4.12). From 10mm onwards, cells of UV-B-grown plants are *c.* 20% older than cells in the same position within control-grown plants. This is due to the reduced growth rate of UV-B-grown leaves (Section 3.4.2).

Plate 4.1 Light micrograph of meristematic cells undergoing mitosis

Tissue from the basal intercalary meristem of 7-d-old primary leaves grown under control conditions (Section 2.2) was fixed and stained as described in Section 2.5.4.

Abbreviations - i = interphase, m = metaphase, a = anaphase, t = telophase

Bar = 25 μ m



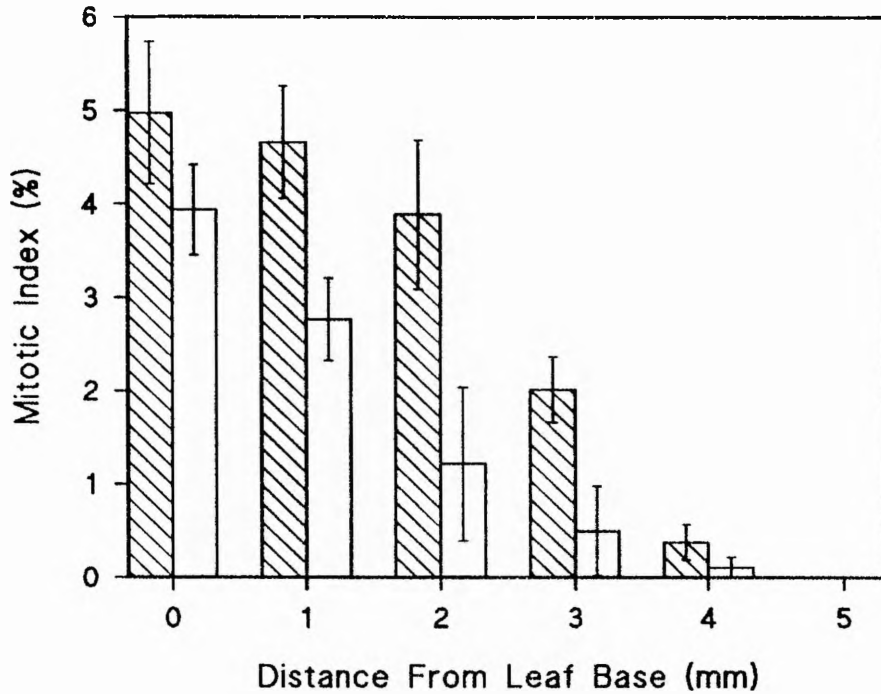


Fig. 4.2 Effect of UV-B radiation on the mitotic index of basal cells of 7-d-old primary leaves

Plants were grown under control (▨) and UV-B (□) conditions (Section 2.2). The mitotic index (*i.e.* the sum of cells in metaphase, anaphase and telophase, as a percentage of total cells) was measured as described in Section 2.5.4. Data points represent the mean of 5 independent growth studies, sampling 5 seedlings per replicate and scoring a total of 1600 cells per seedling. Error bars show \pm one standard error of the mean.

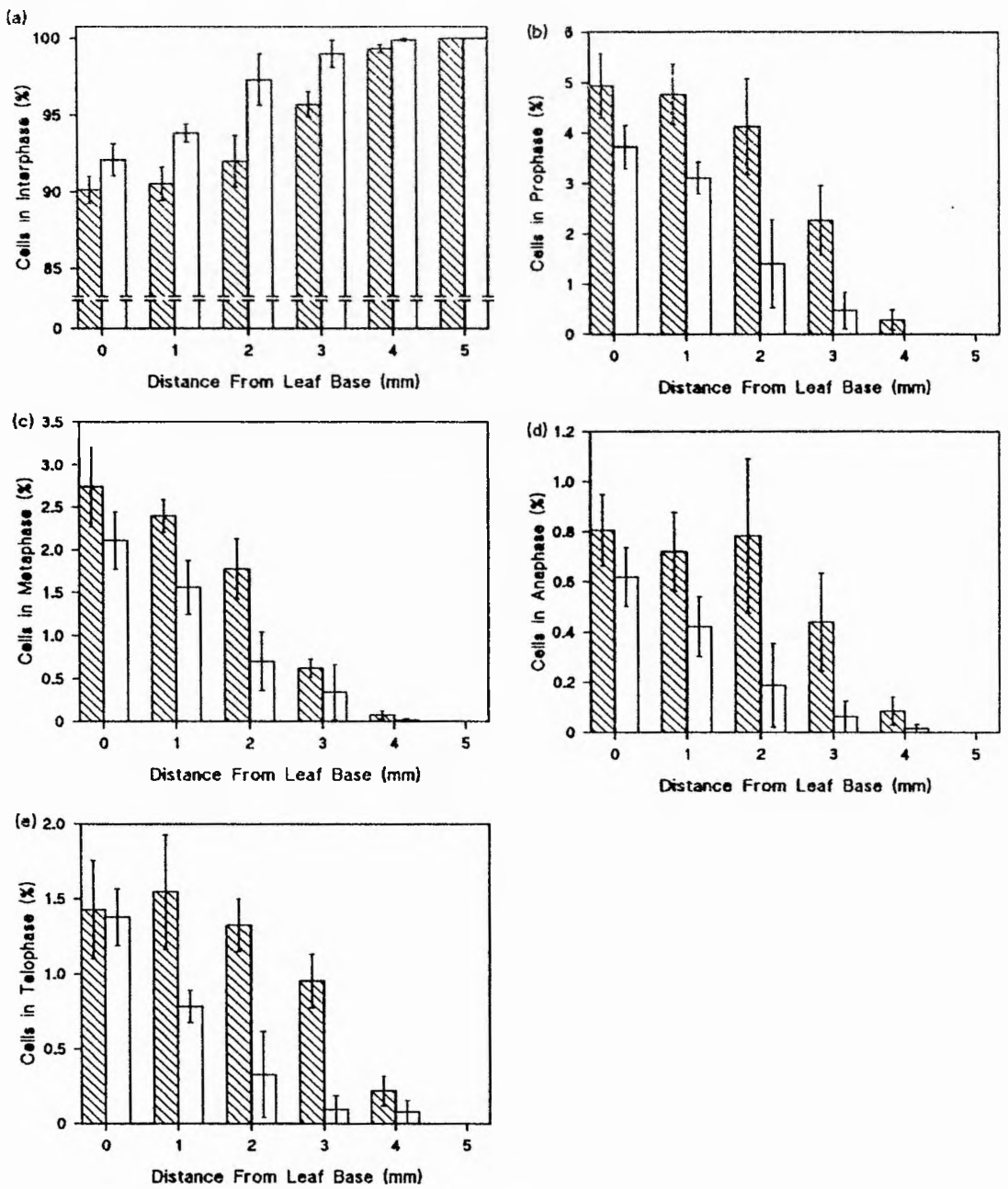


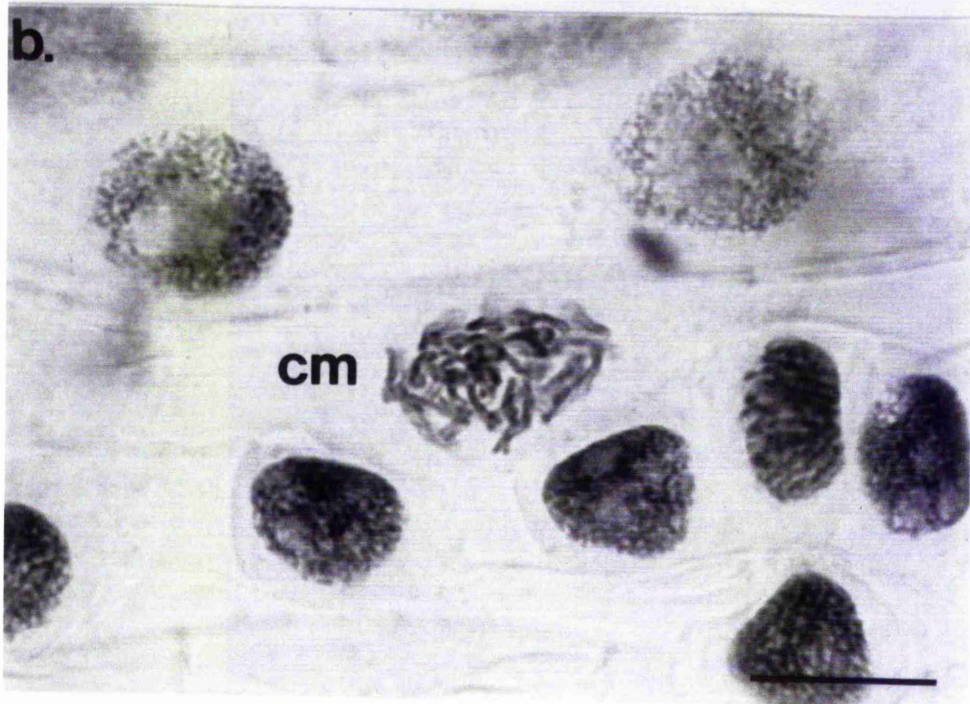
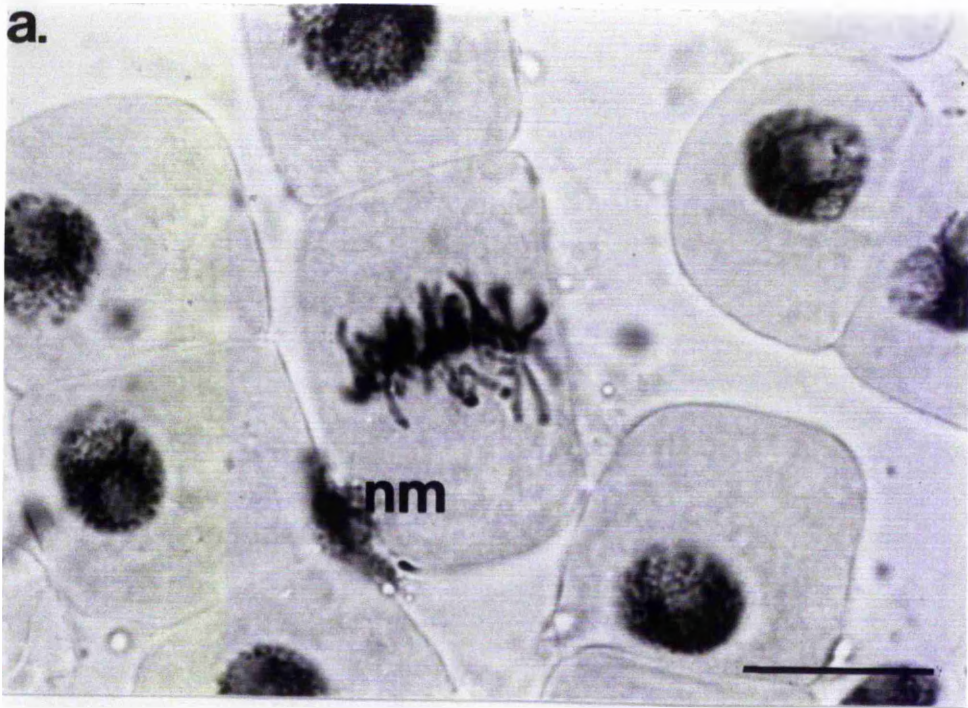
Fig. 4.3 Effect of UV-B radiation on the frequency of cells in (a) interphase, (b) prophase, (c) metaphase, (d) anaphase and (e) telophase in 7-d-old primary leaves Plants were grown under control (▨) and UV-B (□) conditions (Section 2.2). The frequency of cells in each stage of mitosis as a percentage of total cells was measured as described in Section 2.5.4. Data points represent the mean of 5 independent growth studies, sampling 5 seedlings per replicate and scoring a total of 1600 cells per seedling. Error bars show \pm standard error of the mean. N.B. Scales on Y ordinate are different for each figure.

Plate 4.2 Light micrographs of meristematic cells in metaphase, from control (a) and colchicine treated tissue (b)

Primary leaves were treated with either water or colchicine (Section 2.5.5), after which the basal intercalary meristem was fixed and stained as described in Section 2.5.4.

Abbreviations - nm = normal metaphase, cm = colchicine treated metaphase

Bars = 25 μ m



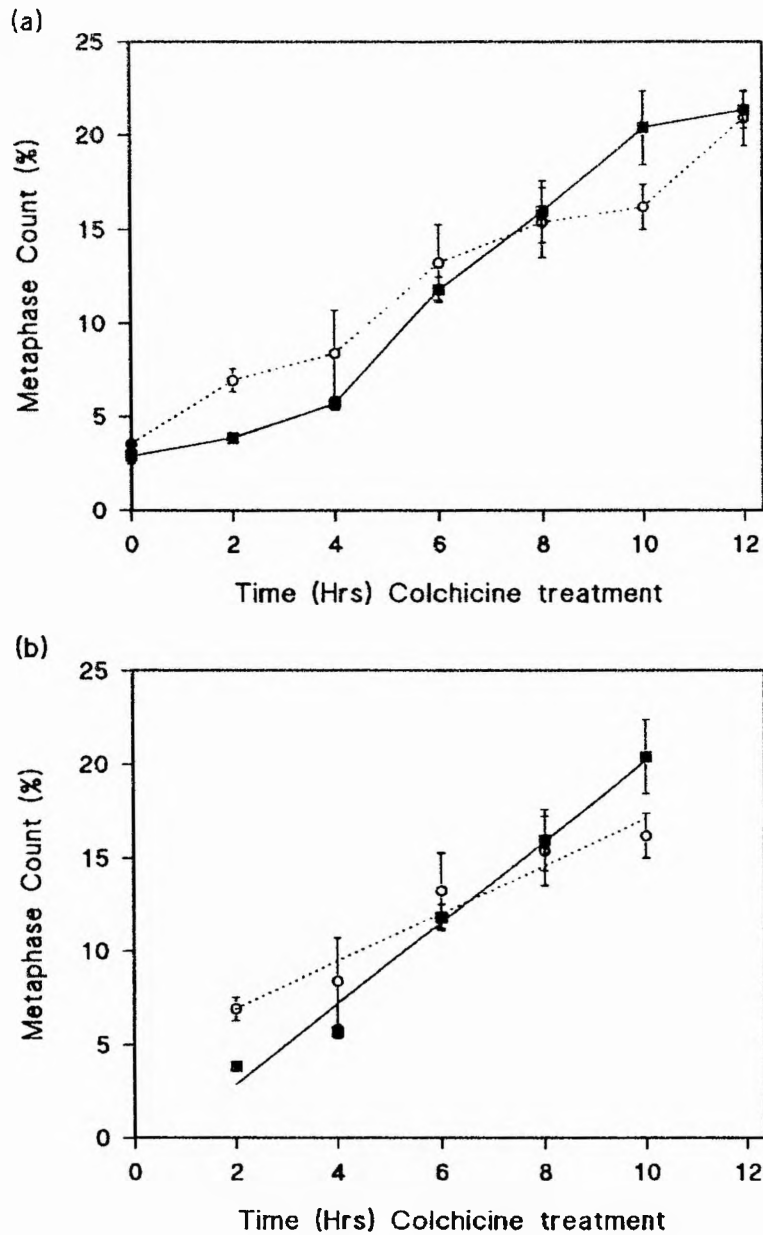


Fig. 4.4 Effect of UV-B radiation on the accumulation of meristematic cells in metaphase after colchicine treatment (a), and the linear regression of accumulation (b) Plants were grown under control (■) and UV-B (○) conditions (Section 2.2). Plants were treated with colchicine (Section 2.5.5), the tissue fixed and stained (Section 2.5.4) and the frequency of cells in metaphase as a proportion of the total cells calculated. Data points represent the mean of 3 independent growth studies, sampling 14 seedlings per replicate (2 seedlings per time point) and scoring a total of 1600 cells per seedling. The linear regression of metaphase accumulation was calculated omitting the first and last data points as explained in Section 4.4.2. Error bars show \pm one standard error of the mean.

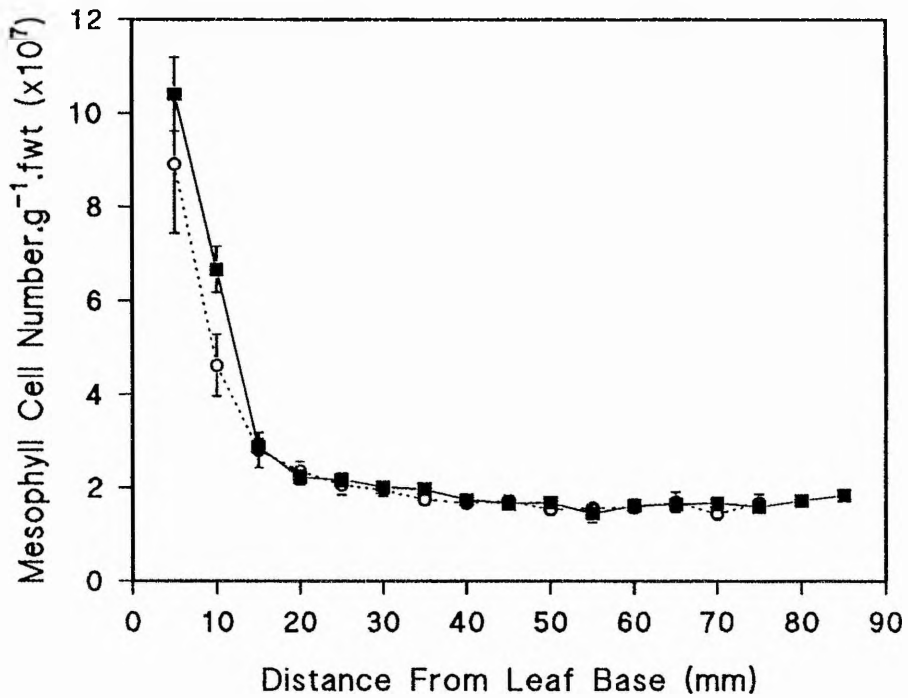


Fig. 4.5 Effect of UV-B radiation on mesophyll cell numbers along the length of 7-d-old primary leaves

Plants were grown under control (■) and UV-B (○) conditions (Section 2.2). Mesophyll cell numbers were measured and calculated as described in Section 2.5.9. Data points represent the mean of 5 independent growth studies, sampling 5 seedlings per replicate. Error bars show \pm one standard error of the mean.

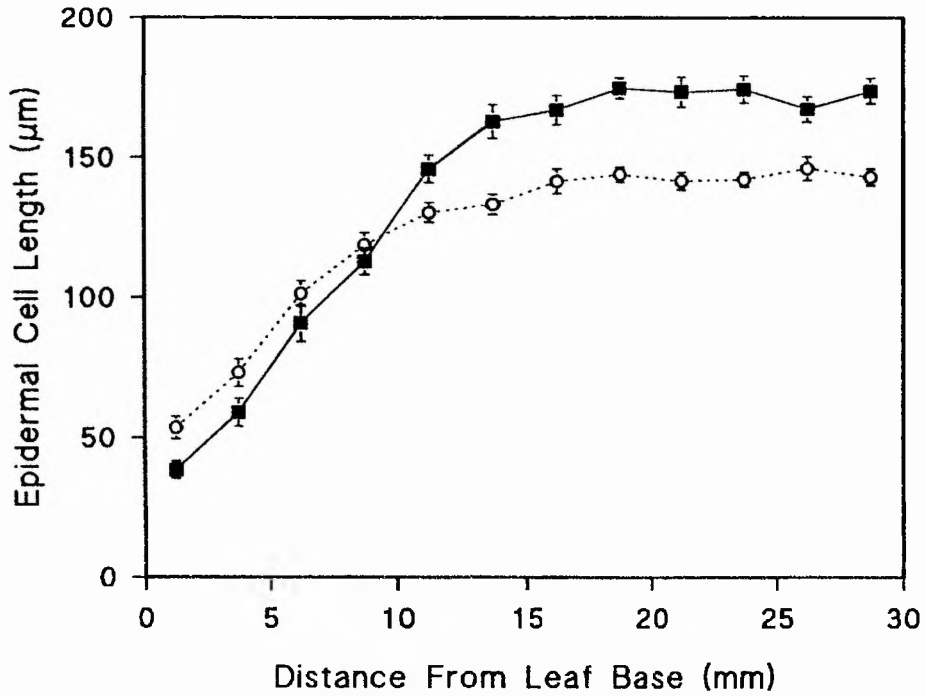


Fig. 4.6 Effect of UV-B radiation on the length of epidermal cells in the cell elongation zone of 7-d-old primary leaves

Plants were grown under control (■) and UV-B (○) conditions (Section 2.2). Epidermal cell length was measured as described in Section 2.5.8. Data points represent the mean of 5 independent growth studies, sampling 5 seedlings per replicate and counting 3 files of cells per seedling. Error bars show \pm one standard error of the mean.

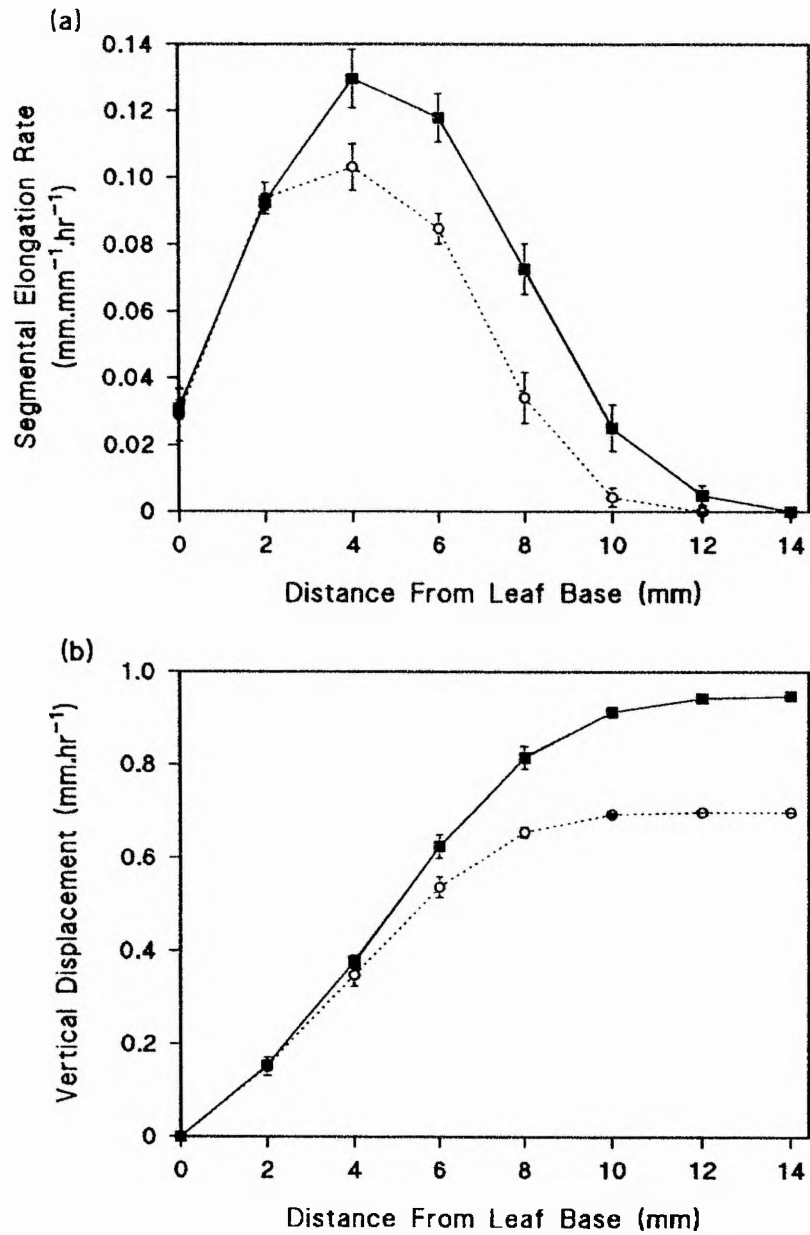


Fig. 4.7 Effect of UV-B radiation on the spatial distribution of segmental elongation rates (a) and velocity of displacement (b), within the cell elongation zone of 7-d-old primary leaves

Plants were grown under control (■) and UV-B (○) conditions (Section 2.2). SER and V_D were measured and calculated as described in Section 2.5.6. Data points represent the mean of 5 independent growth studies, sampling 10 seedlings per replicate. Error bars show \pm one standard error of the mean.

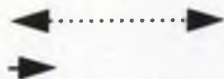
Plate 4.3 Light microscopy of primary leaf development

Tissue from 7-d-old primary leaves grown under control conditions (Section 2.2) was fixed and embedded as described in Sections 2.6.1-2.6.4. Transverse sections ($0.5\mu\text{m}$) were taken (a) 10mm (b) 30mm (c) 50 mm and (d) 80mm above the basal intercalary meristem and stained with methylene blue (Section 2.7.2).

Abbreviations - e = epidermis, m = mesophyll tissue, v = vascular bundle, a = air space,
s = stomatal pore

Bars = $50\mu\text{m}$

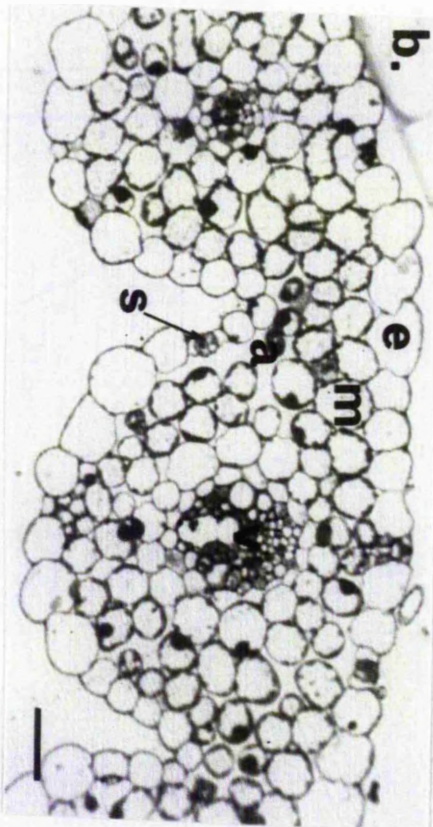
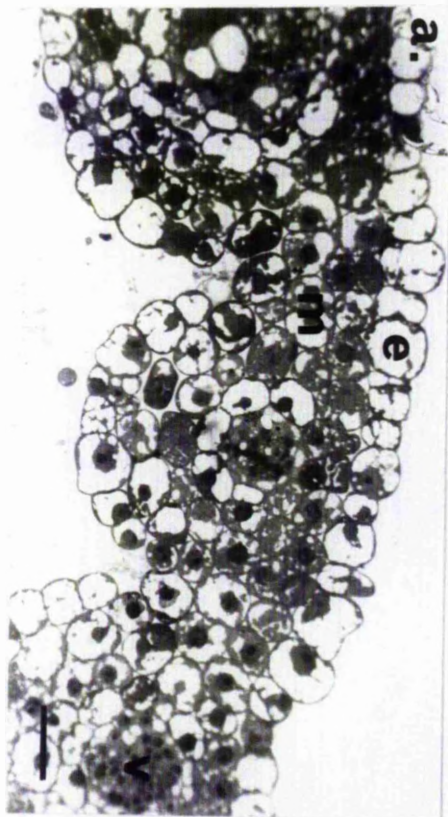
**Elongation
Division**

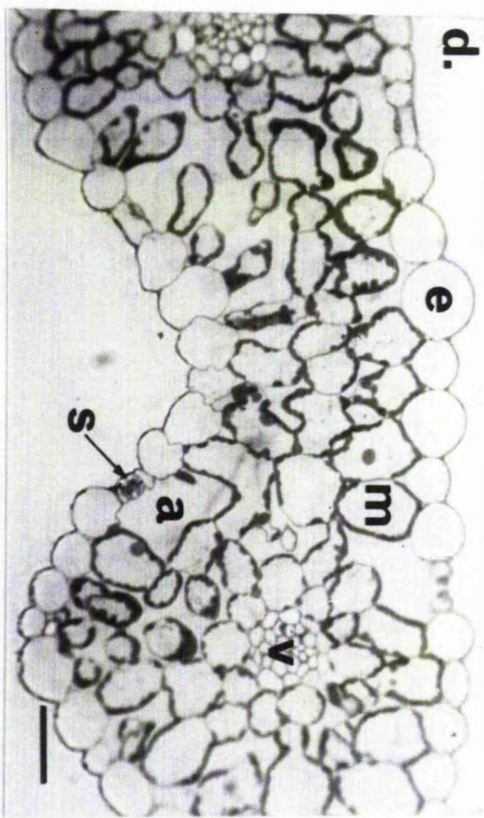
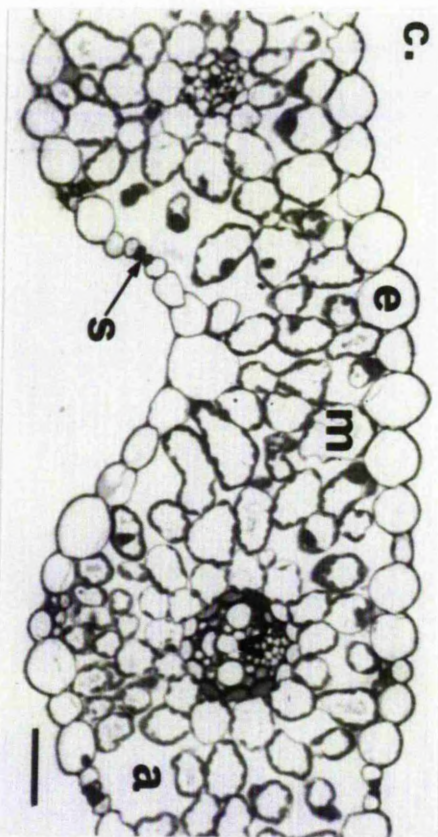
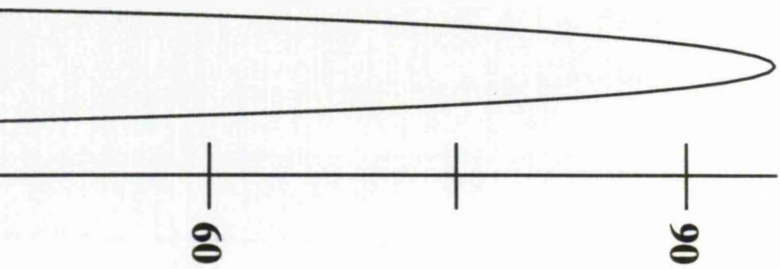


**Distance From
Leaf Base (mm)**



100





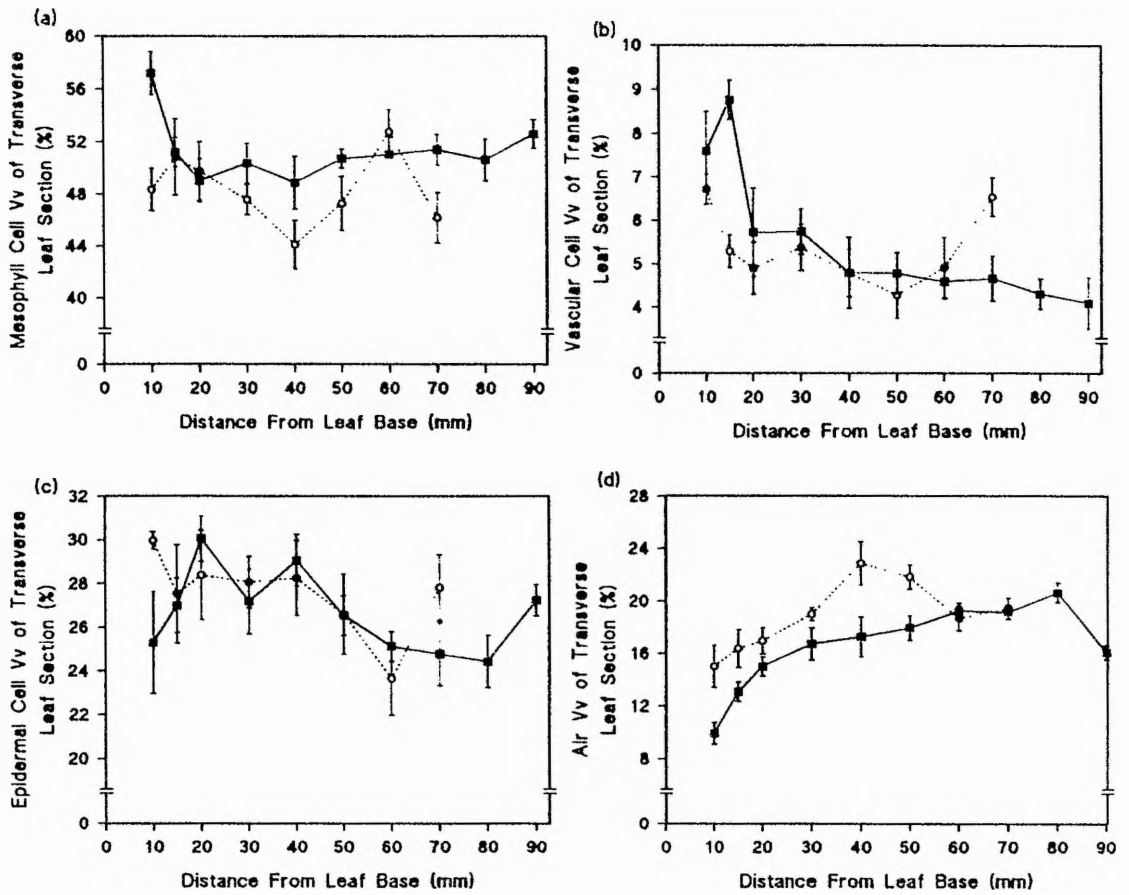


Fig. 4.8 Effect of UV-B radiation on the volume fraction of leaf tissue occupied by (a) mesophyll tissue, (b) vascular tissue, (c) epidermal tissue and (d) air spaces along the length of 7-d-old primary leaves

Plants were grown under control (■) and UV-B (○) conditions (Section 2.2). Tissue was fixed, embedded, sectioned and stained (Section 2.6-2.7) and volume fractions calculated from random micrographs (e.g. Plate 4.3a-d) as described in Section 2.8. Each data point represents the mean of 5 independent growth studies, sampling 10 seedlings per replicate. Error bars show \pm one standard error of the mean.

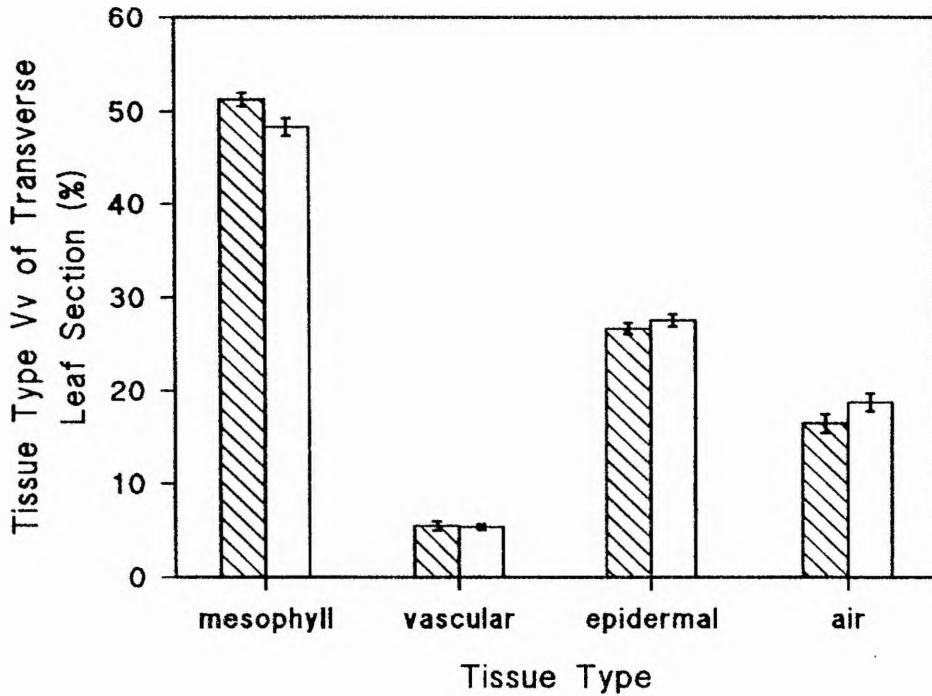


Fig. 4.9 Effect of UV-B radiation on the average volume fraction of tissue types within the 7-d-old primary leaf

Plants were grown under control (▨) and UV-B (□) conditions (Section 2.2). Tissue was fixed, embedded, sectioned and stained (Section 2.6-2.7) and average volume fractions calculated from random micrographs as described in Section 2.8. Each data point represents the mean of 5 independent growth studies, sampling 10 seedling per replicate. Error bars show \pm one standard error of the mean.

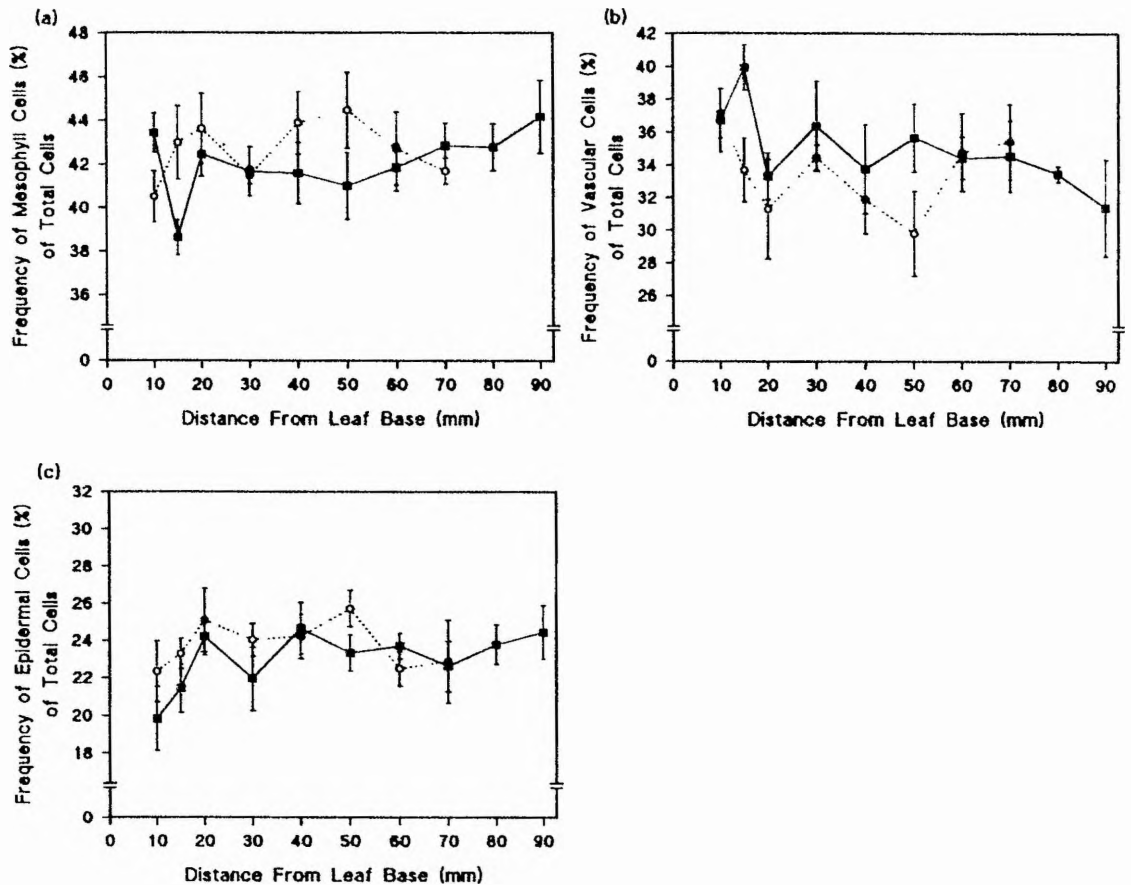


Fig. 4.10 Effect of UV-B radiation on the frequency of (a) mesophyll cells, (b) vascular cells and (c) epidermal cells in transverse sections along the length of 7-d-old primary leaves

Plants were grown under control (■) and UV-B (○) conditions (Section 2.2). Tissue was fixed, embedded, sectioned and stained (Section 2.6-2.7) and the frequency of each cell type as a percentage of total cells calculated from random micrographs (Section 2.8). Each data point represents the mean of 5 independent growth studies, sampling 10 seedling per replicate. Error bars show \pm one standard error of the mean.

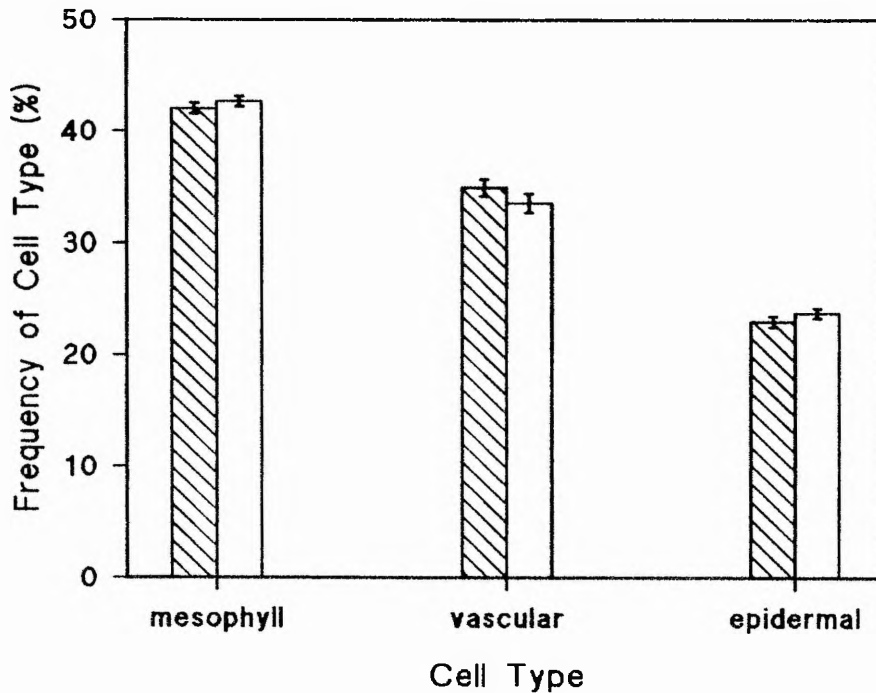


Fig. 4.11 Effect of UV-B radiation on the average frequency of cell types in the 7-d-old primary leaf

Plants were grown under control (▨) and UV-B (□) conditions (Section 2.2). Tissue was fixed, embedded, sectioned and stained (Sections 2.6-2.7), and the average frequency of each cell type calculated from random micrographs as described in Section 2.8. Each data point represents the mean of 5 independent growth studies, sampling 10 seedlings per replicate. Error bars show \pm one standard error of the mean.

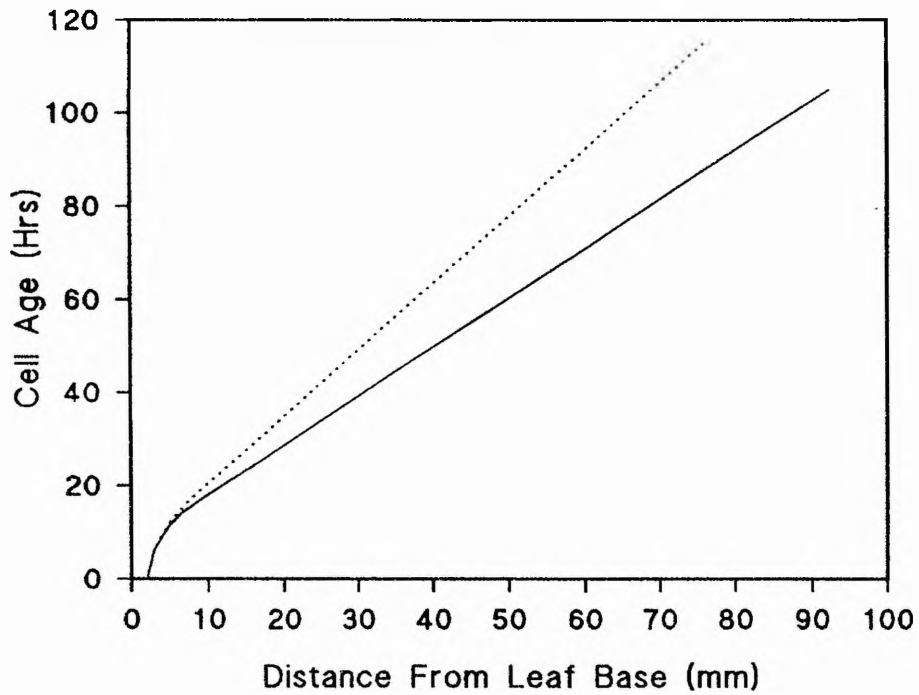


Fig. 4.12 Growth trajectory showing changes in cell age with distance from the leaf base of 7-d-old primary leaves

Plants were grown under control (-) and UV-B (· · ·) conditions (Section 2.2). Growth trajectories were calculated from V_D data (Fig. 4.7b) as described in Section 2.5.7.

DISCUSSION

A reduction in plant growth, *e.g.* plant height, leaf length, is a common response to UV-B, and has been reported in a wide range of species (See Section 1.6.1). In the majority of these studies, however, the response to UV-B at the cellular level in relation to altered growth is unknown. Within the primary leaf of wheat, the temporal and spatial separation of cell division and elongation provides a model system in which changes at the cellular level of plant growth can be measured. Both cell division and elongation occur within the basal region of the leaf blade, surrounded by the coleoptile which might be expected to have a role in protecting the sites of division and elongation from direct UV-B radiation. The purpose of this chapter was to determine which aspect of growth - cell division and/ or elongation - was affected by UV-B, resulting in the reduced plant growth reported in the previous chapter.

4.8 Effect of UV-B on Cell Division

Changes in cell division in response to UV-B have been reported in a variety of species, including *C.sativus* cotyledons (Tevini & Iwanzik, 1986), *Petroselinium crispum* cells (parsley; Logemann *et al.*, 1995) and *Petunia hybrida* leaf protoplasts (Staxén *et al.*, 1993). These changes in cell division may be the result of altered cell division rates (*i.e.* mitotic index) and/or duration (*i.e.* cell doubling time).

The results described in this chapter show all cell division to be located within the basal 5mm of the 7-d-old primary leaf blade, with the highest mitotic index occurring in the basal intercalary meristem of both control (*c.* 5%) and UV-B-grown plants (*c.* 4%). This is comparable to the mitotic index of *c.* 7% found by Ellis *et al.*,

(1983) for the primary leaf basal intercalary meristem of 7-d-old *Triticum aestivum* cv Maris Dove.

In the present study it was found that within the division zone of UV-B-grown plants, the frequency of mitotically active cells was reduced by *c.* 35% as compared to controls. Although this reduction in the proportion of cells dividing under UV-B could conceivably result in reduced growth this does not have to be the case. If the cells divided at a faster rate (reduced cell doubling time) under UV-B there could be no overall effect on plant growth rate. The results of this study, however, show that the meristematic cells of UV-B-grown plants had significantly longer cell doubling times (55.6 ± 2.85 hours) compared to controls (31.5 ± 6.02 hours). These changes in both the rate and duration of cell division in UV-B-grown plants can be related to the reduced growth rate reported in the previous chapter. Similar reductions in plant growth under UV-B, as a result of altered cell division, have been reported in *Rumex patientia* leaves (Dickson & Caldwell, 1978) and *C. sativus* cotyledons (Tevini & Iwanzik, 1986). The complex growth pattern of these dicot species; with clusters of cell division occurring throughout the tissue, however, made direct measurements of cell division, *e.g.* mitotic index and cell doubling time, impossible. In both studies, a reduction in cell numbers under UV-B led to the conclusion that cell division had been affected, even though other explanations, such as effects on cell elongation, were also feasible.

The majority of investigations into the effects of UV on cell division have used germicidal UV (*i.e.* UV-C $\lambda < 280\text{nm}$) and animal cells (Domon & Rauth, 1968; Carlson, 1976). In such studies irradiation of cells in the S phase of the cell cycle (see Section 4.2.1) was the most effective in delaying the onset of mitosis, and therefore the progression through the cycle. The S phase involves DNA synthesis and replication,

which are prime targets for UV radiation, as the absorbance maximum of DNA is c. 260nm (Davies, 1995). It has been suggested (see Staxén, Bergounioux & Bornman, 1993) that DNA repair of UV induced damage, prior to replication, results in the delayed progression through the cell cycle, and may be the cause of increased cell doubling times. Although these studies use UV-C and animal cells, as compared to UV-B and plant cells, the results can be related to the work in this chapter for two reasons. Firstly, although the maximum absorbance of DNA is 260nm, it still absorbs appreciably in the UV-B waveband (280-320nm)(Davies, 1995); and secondly, the cell cycle is a highly conserved process, with universal mechanisms observed in a wide range of taxonomic groups (Review: Francis, 1992).

In order to identify the mechanisms by which cell division responds to UV radiation in plants, the isolated cell, *e.g.* *P.hybrida* leaf protoplasts (Staxén *et al.*, 1993), *P.crispum* cell suspension culture (Logemann *et al.*, 1995), rather than the whole plant has been used as a model system. The limited number of studies in this area have shown similar results to those found in animal cells. For example, shortwave UV irradiation (maximum 254nm) of *H.vulgare* root meristem cells (Cieminis *et al.*, 1987) and UV (280-360nm) irradiation of *P.hybrida* leaf protoplasts (Staxén *et al.*, 1993) were both found to be most effective in delaying progression through the cell cycle when given to cells in the S phase. The study on *Petunia* protoplasts also found that cells irradiated during G1 and G2 phases delayed the cell cycle, indicating that additional mechanisms may be involved in the UV response. UV irradiation was also found to disrupt microtubule organisation of the *Petunia* protoplasts. It has been suggested (Staxén *et al.*, 1993) that this response is due to the absorbance of UV by tubulin at 280nm (Zaremba *et al.*, 1984); resulting in denaturation of the tubulin, which then loses its

ability to form dimers which normally polymerise to form the microtubules (the spindle fibres in dividing cells). This may delay progression through the cell cycle until new tubulin has been synthesised.

A recent molecular study of the effects of UV radiation on a *P. crispum* cell suspension culture found that the genes encoding a p34^{cdc2} protein kinase and a mitotic cyclin were transcriptionally repressed in UV irradiated cells (Logemann *et al.*, 1995). These proteins are of primary importance at the major checkpoints of the cell cycle, the transition of G₁ - S, and G₂ - M, and is another mechanism by which UV radiation could increase the cell doubling time.

It remains to be determined which, if any, of these processes is responsible for the observed effect of UV-B on cell division in the present study.

4.9 Effect of UV-B radiation on Cell Elongation

Changes in plant growth under UV-B as the result of altered elongation have been reported in a number of species, including *C. sativus* cotyledons (Ballaré *et al.*, 1991), *L. esculentum* hypocotyls (Ballaré *et al.*, 1995b) and *H. vulgare* leaves (Liu *et al.*, 1995). These changes may be the result of altered cell elongation rates and/ or duration, although in these studies no distinction was made between the two. The growth pattern of the primary wheat leaf (see Section 4.1.2.1), however, provides a system by which the effects of UV-B on cell elongation rates and duration can be measured separately.

During normal leaf development the rate of elongation of different tissue types is not entirely synchronised (MacAdam & Nelson, 1987; Dale, 1988; Kutshera, 1989), and the results described in this chapter show that in both control and UV-B-grown plants mesophyll cell elongation occurs over a larger section of the leaf blade than

epidermal elongation. Such differences in the elongation of different tissue types are the result of differences in the thickness and architecture of the cell wall. For example, the cell walls of epidermal cells have transverse and longitudinal orientated microfibrils and are thicker than those found in the ground tissue, e.g. mesophyll, in which the microfibrils are predominantly in transverse (Kutshera, 1988). This creates a mutual stress (tension and compression) between tissues, for example when the epidermis is separated from the ground tissue of *H. annuus* hypocotyls, the epidermis shrinks by 20% while the ground tissue expands (Kutschera, 1990). The epidermis, therefore, is considered to be the tissue that limits elongation (Dale, 1988; Kutshera, 1989).

In the grass leaf, elongation is a function of both the length of the epidermal elongation zone and the SER within the zone (Schnyder *et al.*, 1990; Skinner & Nelson, 1994). Elongation occurs in the region of the leaf blade enclosed by the coleoptile, and therefore the distribution of elongation can only be assessed by the use of the 'destructive' technique of hole marking (Section 2.5.6). Although this technique reduces the LER and SER, MacAdam and Nelson (1987) showed that all sections of the leaf blade were affected equally, and therefore the length of the elongation zone and spatial distribution of elongation would be unaltered.

The results of this chapter show the spatial distribution of SER within the primary wheat leaf is similar to that observed in *F. arundinacea* (Nelson & MacAdam, 1989), *Lolium perenne* (Schnyder *et al.*, 1990) and *Z. mays* (Ben-Haj-Salah & Tardieu, 1995). The maximum rate of elongation occurred just above the zone of cell division, after which the elongation rate decreased to zero, signifying the end of the elongation zone. Plants grown under UV-B had both a shorter zone of epidermal elongation (basal 12mm compared to 14mm) and a reduced rate of elongation within this zone, both of

which could result in reduced growth, as reported in the previous chapter. Measurements of epidermal cell lengths within the leaf blade showed that a constant cell length was reached 14mm and 12mm above the leaf base in control and UVB-grown plants respectively, thus confirming that the length of the elongation zone was accurately determined by hole marking.

Cell elongation is driven by both turgor pressure and cell wall extensibility (see Section 4.2.2). The limited number of studies into the mechanism by which UV-B reduces elongation suggest that reduced elongation rates are the result of altered cell wall extensibility, rather than changes in cell turgor. These alterations in wall extensibility in response to UV-B have been attributed to changes in indole-acetic acid (IAA) (Tevini & Iwanzik, 1986) and ferulic acid (Liu *et al.*, 1995), although other mechanisms may also be involved. Cell wall expansion is stimulated by IAA (see Section 4.2.2), which is a prime target for UV-B radiation as it absorbs at 290nm (Galston, 1950). This interaction between IAA and UV-B radiation results in the breakdown of IAA to produce a number of growth inhibitory IAA photoproducts (Tevini & Teramura, 1989). Tevini and Iwanzik (1986) showed that a reduction in *C.sativus* hypocotyl elongation was the result of IAA destruction in the tip of the stem. The other mechanism by which UV-B may reduce elongation rates has been suggested by Liu *et al.*, (1995) following an investigation into the effects of UV-B on ferulic acid. In the cell wall, especially those of grasses, simple phenolics such as ferulic acid are of primary importance in regulating cell expansion, as they form cross links with carbohydrates in the wall (Fry, 1986). Liu *et al.*, (1995) found that a reduction in elongation of the primary *H.vulgare* leaf grown under UV-B was accompanied by a two-fold increase in the concentration of insoluble, wall-bound ferulic acid in epidermal cells. Such an

increase in ferulic acid would result in more cross links to carbohydrates in the cell wall, and would therefore lead to a reduced cell elongation.

4.10 Consequences of Altered Cell Division and Elongation on the Growth of the Primary Leaf

In the previous chapter a *c.* 30% reduction was observed in the primary leaf length of 7-d-old UV-B-grown plants. Although reductions in plant growth in response to UV-B have previously been interpreted as the result of altered cell division and elongation (Dickson & Caldwell, 1978; Tevini & Iwanzik, 1986), this is the first known study to quantitatively analyse the response of cell division and elongation to UV-B. The results presented in this chapter have shown that both the rate and duration of cell division and elongation are altered in response to UV-B. In UV-B-grown plants the frequency of mitotically active cells is reduced (*c.* 35%) and the speed at which these cells divide is increased (*c.* 45%). Thus the supply of cells into the elongation zone is reduced in UV-B-grown plants, which, coupled to a reduction in the rate of elongation, results in the observed reduction in growth. Both cell division and elongation occur within the basal region of the leaf blade which is surrounded by the coleoptile. The observed changes may therefore be the result of direct effects of UV-B radiation at the sites of division and elongation. A certain amount of visible light is known to penetrate the coleoptile as light dependent chlorophyll synthesis occurs in the basal region of the leaf (see Chapter 6). Alternatively, effect may be indirect whereby fully expanded cells above the coleoptile absorb the UV-B and, via signal transduction cause a response in division and elongation.

Although the alterations in cell division and elongation under UV-B, resulting

in reduced plant growth, might appear to be a deleterious response to UV-B, a reduction in plant growth rate has been suggested to be a possible protective mechanism against UV-B (see Section 3.6). For example Ballaré *et al.*, (1995b) found that a delay of a few hours in *L.esculentum* seedling emergence was sufficient to allow the synthesis of flavonoids, which screen out the UV-B.

4.11 Effect of UV-B Radiation on Cellular Differentiation

The reduction in plant growth under UV-B (see Chapter 3) is the result of altered cell division and elongation, as discussed above. In addition, changes in cellular differentiation may also have a significant effect on plant morphology. For example, increased leaf thickness, as reported in the previous chapter (see Section 3.4.7) is a common response under UV-B, and may be the result of a thicker epidermis, which would protect the mesophyll cells from UV-B damage.

The work described in this chapter shows that the proportion of cell types in the primary leaf was similar in both control and UV-B-grown plants, with a ratio of mesophyll : vascular : epidermal cell numbers of *c.* 9 : 7 : 5, which is comparable to that found in a range of *Triticum* species (Jellings & Leech, 1982). The increased leaf thickness reported in Chapter 3, therefore, is not the result of an alteration in the ratio of each cell type. Different cell types, however, vary greatly in size, for example mesophyll cells are larger than vascular cells (see Plate 4.3), and the volume fraction of leaf occupied by each cell type is related more to cell size rather than to frequency. The increased leaf thickness, therefore, could be the result of an increase in volume fraction of a certain cell type. The results of this chapter show the ratio of mesophyll : vascular : epidermal : air volumes to be *c.* 50 : 5 : 25 : 20, and is similar to that

reported by Jellings and Leech (1984) for a range of *Triticum* species. The volume fraction of inter-cellular air space in the basal region of the leaf blade was slightly increased under UV-B, although the average volume fraction for the whole leaf blade was unchanged. Inter-cellular air space formation is due to greater epidermal expansion parallel to the leaf blade, relative to mesophyll expansion, normal to the blade (Maksymowych, 1973). The increase in leaf thickness appears therefore to be as a result of an increase in inter-cellular air spaces, with no effect of UV-B on either the ratio or volume fraction of leaf occupied by the different cell types. Increased leaf thickness has been suggested (Flint *et al.*, 1985) to be an adaptive response, increasing the optical path between the epidermis and sensitive cellular sites, *e.g.* the chloroplasts of mesophyll cells, and therefore reducing the flux of UV-B into the leaf tissue. In addition to the possible protective role via an increase in leaf thickness, changes in air spaces may also have important consequences for the photosynthetic capacity of the plant. For example, in the wheat leaf an increase in air space is associated with an increase in the mesophyll area exposed to air (Jellings & Leech, 1982) which is positively correlated to photosynthetic capacity (Nobel, Zaragoza & Smith, 1975). Effects of UV-B on photosynthetic capacity have varied in different species and is discussed in detail in Chapter 6.

4.12 Effect of Growth Under UV-B on the Cell Age Gradient Within The Primary Leaf

Recent evidence shows that the effects of UV-B may be dependent upon the developmental stage of the plant (Jordan *et al.*, 1994; Day *et al.*, 1996). As mentioned previously, the primary wheat leaf provides a gradient of both cell age and development. The gradient of cell age within the leaf blade was calculated from the V_D data (see

Section 2.5.7). As a result of the reduced growth rate in UV-B-grown plants, the cells were older at the same position within the leaf blade, as compared to controls, *e.g.* sampling tissue from 30mm from the leaf base in UV-B leaves, and at 40mm in control-grown leaves would give a comparison of cells the same age, *c.* 50 Hrs. These data allow for the altered growth under UV-B to be taken into account, and the effects of UV-B at the ultrastructural (Chapter 5) and the biochemical level (Chapter 6) can therefore be compared directly in cells of similar ages.

CHAPTER 5

Effects of UV-B Radiation on The Ultrastructural Development of Mesophyll Cells In the Wheat Primary Leaf

INTRODUCTION

In the developing grass leaf there is a progression in mesophyll cell metabolism, from heterotrophic in the leaf base, importing carbon from either the seed or more mature cells, to autotrophic towards the leaf tip, as the cells photosynthetic capacity develops (Dale, 1985; Tobin *et al.*, 1988; Merlo *et al.*, 1993). This metabolic transition is accompanied by changes in cell ultrastructure and metabolism. (see Sections 5.1.1.3, 5.1.2.3, 6.1). The developmental changes in ultrastructure are related to cell age, and therefore any factor that alters the cell age gradient, *e.g.* via a UV-B induced reduction in growth rate (see Section 3.4.2), may result - indirectly - in altered ultrastructure and metabolism. Few studies have investigated the effects of UV-B on cell ultrastructure, in contrast to the number of studies on the effects of UV-B on metabolism, *e.g.* photosynthesis (see Chapter 6).

The purpose of this chapter is firstly to quantify the effects of UV-B on the ultrastructural development of mesophyll cells using stereological analysis (see Section 2.8) of micrographs from light and transmission electron microscopy; and secondly, to test whether any changes in UV-B-grown plants are direct UV-B responses, or indirect UV-B responses, *i.e.* as a result of altered leaf growth. This introduction focuses on (a) mesophyll cell ultrastructure and development (with particular reference to chloroplasts and mitochondria), and (b) the principles of stereological analysis.

5.1 Mesophyll Cell Ultrastructure

The ground tissue of a leaf is composed of mesophyll cells, which constitute *c.* 50% of the total number of cells in the primary leaf of *T. aestivum* L. cv Maris Dove

(Jellings & Leech, 1982), *T.aestivum* L. cv Maris Huntsman (see Section 4.6.3). In the leaves of C₃ plants, mesophyll cells are the major site of photosynthesis, providing energy (ATP) and reductant (NADPH) that may be utilized for the assimilation of inorganic carbon to form carbohydrates, and the synthesis of a large number of other compounds including amino acids and lipids (Dennis & Turpin, 1990). The structure of mesophyll cells and the specialized membrane bound organelles they contain, *i.e.* chloroplasts and mitochondria, are well documented due to their importance in plant metabolism (for an overview of plant cell structure see Gunning & Steer, 1975).

5.1.1 The Chloroplast

5.1.1.1 Structure

Mature chloroplasts are typically lentiform, with average dimensions of 5 x 2 x 1-2 μm (Newcomb, 1990). They are bound by a double membrane (envelope) and have a complex internal membrane system of channels known as stromal and granal thylakoids, which are surrounded by a soluble phase, known as the stroma. Both the stromal and granal thylakoids are created from a single membrane folded back on itself. Stromal thylakoids are 'double membrane structures' that traverse the stroma. Granal thylakoids are flat, sac-like structures (granal sac) that form stacks, termed grana, which are interposed between stromal thylakoids. There are three distinct chloroplast compartments; the intermembrane space (between the inner and outer membranes of the envelope), the stroma, and the thylakoid space (granal and stromal) (see Fig. 5.1) (Newcomb, 1990; Anderson & Beardall, 1991). The thylakoid space contains numerous protein complexes, including photosystem II - light harvesting complex II (PSII-LHCII) (located predominantly on granal stacks) and photosystem I - light harvesting complex I (PSI-LHCI)(located on the stromal thylakoids) (Anderson, 1986). The stroma contains

starch, DNA and soluble proteins of the Calvin cycle *e.g.* Rubisco (E.C. 4.1.1.39). This highly organised internal structure is essential for chloroplast function, and therefore any changes in chloroplast ultrastructure may subsequently alter chloroplast metabolism.

5.1.1.2 Biogenesis

Chloroplasts are not synthesized *de novo*, but arise from proplastid division in leaf meristematic cells (see Figure 5.2) (Possingham, 1980). Proplastids are small, spherical organelles (0.5 - 1 μm diameter) surrounded by a double membrane (envelope), with few internal membrane structures (Thomson & Whatley, 1980). The proplastids increase in size and accumulate starch grains which they lose as they pass through an amoeboid stage. The inner membrane of the proplastid envelope then invaginates to form the first thylakoids, from which additional thylakoids proliferate. Granal stacks appear, the complexity (size and number) of which increases as the chloroplast matures and increases in size (Leech & Baker, 1983). Division of proplastids within the meristem keeps pace with cell division, thus maintaining the number of proplastids per cell (Leech, 1985). The increase in the number of chloroplasts per cell during development occurs as a result of chloroplast division in post-mitotic expanding cells (Boffey *et al.*, 1979; Tobin *et al.*, 1985).

5.1.1.3 Changes In Chloroplast Populations During Leaf Development

The growth pattern of the grass leaf (see Section 4.1.2.1), including *Z.mays* (Leech, Rumsby & Thomson, 1973), *H. vulgare* (Robertson & Laetsch, 1974) and *T.aestivum* (Boffey *et al.*, 1979; Tobin *et al.*, 1985), has provided an ideal system in which to study chloroplast and mesophyll cell development.

As mesophyll cells develop from the leaf base to the tip, both the size and number of chloroplasts per cell increase (Boffey *et al.*, 1979; Ellis *et al.*, 1985; Tobin

et al., 1985). Thus, chloroplasts occupy an increasing proportion of the mesophyll cell volume (Ellis & Leech, 1985; Tobin *et al.*, 1988). The number of chloroplasts per cell has been shown to be dependent on several factors, including mesophyll cell size (Pyke & Leech, 1987), ploidy level (Dean & Leech, 1982b; Jelling & Leech, 1984), genotype (Ellis & Leech, 1985) and environment (Jellings, Usher & Leech, 1983; Dietz, 1989). There is evidence to suggest that the factor controlling chloroplast replication is cell size, and that chloroplasts will only divide when there is space available in the cell. A linear relationship has been shown to exist between chloroplast number per cell and cell plan area (Ellis & Leech, 1985; Pyke & Leech, 1985), and cells containing chloroplasts with small face areas have a correspondingly higher density of chloroplasts, therefore maintaining a constant chloroplast area per cell (Pyke & Leech, 1991). Changes in chloroplast ultrastructure during mesophyll cell development, *e.g.* an increase in the number of granal sacs per granum, has been shown in a range of plants including *Z.mays* (Leech *et al.*, 1973; Baker & Leech, 1977) and *H.vulgare* (Robertson & Laetsch, 1974).

5.1.2 The Mitochondria

5.1.2.1 Structure

Plant mitochondria vary in form, but are generally spherical (0.5 - 1µm diameter) or rod-shaped (1 - 3µm in length). They are surrounded by two highly specialized membranes, an outer smooth membrane which forms an enclosing perimeter, and an inner membrane which has numerous inwardly directed invaginations, known as cristae. There are two distinct compartments present in the mitochondria; the intermembrane space (between inner and outer membrane), and the matrix which is enclosed by the inner membrane. The proteins involved in electron transport and oxidative

phosphorylation are located on the inner membrane, while the matrix contains ribosomes, DNA and soluble proteins, *e.g.* for the TCA cycle (Douce, 1985). As with chloroplasts, this highly organised internal structure is essential for mitochondrial function.

5.1.2.2 Biogenesis

Mitochondria are not synthesised *de novo*, but arise by division of pre-existing mitochondria (Manton, 1961). Very little is known about the control of mitochondrial division in plants. In the limited number of studies in which mitochondrial division has been investigated in plants, including, *P.sativum* (Solomos *et al.*, 1972) and *Anthoceros laevis* (Manton, 1961), the general consensus is that division begins with an inward furrowing of the inner membrane, which then fuses together, dividing the mitochondrion in two (Alberts *et al.*, 1996).

5.1.2.3 Changes In Mitochondria Populations During Leaf Development

Although the number of mitochondria per cell varies between plant species and tissue (Newcomb, 1990), there is evidence to relate mitochondrial numbers and ultrastructure to the metabolic activity of the tissue. The majority of studies investigating the relationship between changes in respiratory activity and mitochondria populations, have used plant tissue with characteristically high respiratory rates. For example, increased respiratory rates found in *P.sativum* (Solomos *et al.*, 1972) and *Arachis hypogaea* (peanut; Cherry, 1963) cotyledons during germination have been shown to be accompanied by increased differentiation of mitochondria, *e.g.* increased number of cristae per mitochondrion. Few studies have investigated changes in mitochondrial populations during leaf development, in contrast to the number of studies on developmental changes in chloroplast populations (see Section 5.1.1.3). In a study on

P.sativum leaf development, Geronimo & Beevers (1964) correlated a reduction in respiratory activity of older leaves, with a reduction in the number of cristae per mitochondrion, and suggested that the change in the surface area of the inner mitochondrial membrane, with which many mitochondrial enzymes are associated, e.g. ATP synthetase, may alter the activity and capacity of the mitochondrial electron transport chain. The mitochondrial population of the primary leaf of *T. aestivum* has also been shown to change during leaf development (W.J.Rogers, J.R.Thorpe & A.K.Tobin-unpublished data; Tobin & Rogers, 1992). In their study, Rogers, Thorpe & Tobin (unpublished) found that during leaf development, mitochondrial size increased, although the volume of cell occupied by mitochondria remained constant, suggesting a decrease in the number of mitochondria per cell with development (Tobin & Rogers, 1992).

5.1.3 Effects of UV-B on Cell Ultrastructure

Both the photosynthetic and respiratory capacity of a leaf may be influenced by the number and morphology of chloroplasts and mitochondria per mesophyll cell. Despite the association that exists between cell ultrastructure and metabolism, the effects of UV-B on ultrastructure are less well documented than the effects of metabolism. These limited studies have found qualitative changes in organelle ultrastructure, including the disorganisation of chloroplast membranes in *P.sativum* (Brandle *et al.*, 1977; He, Huang & Whitecross, 1994) and *B.vulgaris* (sugarbeet; Bornman *et al.*, 1983), and mitochondrial membranes in *P.sativum* (Brandle *et al.*, 1977) and *Z.mays* (Santos, Almeida & Salema, 1992).

5.2 Quantitative Analysis of Subcellular Compartmentation Using Stereology

Stereology is the three-dimensional interpretation of two-dimensional images that yield 3D information from 2D data (Reviews : Weibel, 1969; Weibel & Bolender, 1973; Briarty, 1975). The formulae and techniques of stereology can be used for quantitative image analysis *e.g.* cellular and subcellular volumes can be calculated from light and electron micrographs (Steer, 1981; Toth, 1982), and is commonly called morphometry (Weibel, 1969).

5.2.1 Stereological Parameters

Many structural parameters of tissues and cells can be quantified using stereological techniques (Weibel & Bolender, 1973; Briarty, 1975; Toth, 1982). In botanical research the most useful information is gained from three fundamental parameters:

- (1) V_V - volume fraction or volume density, *i.e.* the ratio of the volume of a component to the containing volume (*e.g.* chloroplast volume contained in the unit volume of cytoplasm).
- (2) S_V - surface area or surface density, *i.e.* the surface area of a component per unit containing volume (*e.g.* the area of cristae contained in the unit volume of mitochondrion).
- (3) N_V - numerical density, *i.e.* the number of particles (or features) per unit containing volume.

5.2.1.1 Volume Fraction

The fundamental principle on which all stereological measurements of V_V are based is derived from the work of the French geologist Delesse in 1847, which states that the areal density of profiles on sections is an unbiased estimate of the volume

density of structures (Weibel & Bolender, 1973):

$$\text{Area}_{\text{compartment}} / \text{Area}_{\text{total}} = \text{Volume}_{\text{compartment}} / \text{Volume}_{\text{total}}$$

$$A_A = V_V$$

The V_V of different tissues, cells and organelles can be calculated from area measurements taken from 2D electron and light micrographs. These area measurements have conventionally been estimated using planimetry, a cut-and-weigh method, and point counting (Weibel & Bolender, 1973), and more recently by the direct method of computer aided image analysis (see Section 2.8).

5.2.2 Sampling

Stereology is based on estimates of probability and will only give satisfactory results on an unbiased sample. Rigorous sampling procedures are therefore used to ensure randomness. To achieve random sampling of the tissue of interest, two major problems are encountered in collecting an unbiased set of micrographs. Firstly, the tissue or cell type under study may not be evenly distributed throughout the sample and therefore a simple random sample may contain only a small proportion of the tissue or cell type of interest. This problem is overcome by systematic random sampling, in which micrographs are taken over selected areas and, although not random with respect to the sample, this does fulfil the requirement of providing unbiased information on components within the selected area. It has been shown that a well-concieved procedure of systematic random sampling yields a smaller error than simple random sampling (Weibel & Bolender, 1973). The second problem encountered is that in using a low magnification to sample the maximum amount of tissue, the resolution of smaller structures may be lost. This problem can be overcome by separating the analysis into a series of stages using micrographs of increasing magnification. For example, large

scale features such as V_V of different cell types can be analysed at the LM level (x 500 magnification), smaller features such as the V_V of chloroplasts and mitochondria can be analysed at the EM level (x 5000 magnification). Information from the highest magnification can then be related to the whole tissue by using estimates at the lower magnifications.

In addition to the strict method of sampling, *e.g.* systematic random sampling, the size of the sample, *i.e.* the total number of micrographs examined to make the study statistically significant, must also be determined. A progressive method for determining sample size has been suggested by Bolender (1978). A trial sample is split into groups, *e.g.* 5 micrographs, and the mean and standard error calculated for successively larger groups, *e.g.* 10, 15, 20 micrographs. The decline in the standard error level with the increasing number of micrographs sampled, can then be used to calculate the approximate number of micrographs required for a particular standard error level (see Section 2.8).

5.2.3 Errors

In preparing tissue for stereological analysis a number of physical changes may occur in the processing of the original fresh tissue to the fixed tissue section. These changes may cause errors in stereological measurements, but they can be accommodated by the use of correction factors (Toth, 1982). It is well documented that in fixing and embedding tissue for EM, cells experience some degree of shrinkage (Kubinova, 1989), and compression of the resin during sectioning is another unavoidable problem. Parameters such as V_V , however, do not usually need correcting for the reduced tissue volume resulting from these factors (assuming uniform shrinkage and compression) as volume density, V_V ($\mu\text{m}^3 / \mu\text{m}^3$), is dimensionless. The basic stereological principles

used to determine V_V , assume that the measurements are made from sections of zero thickness (Weibel, 1979). Biological sections, however, are of finite thickness (60nm) and therefore opaque structures may be over represented, whereas translucent structures may be 'covered ' by opaque structures and underestimated. This is known as the Holmes effect (Toth, 1982), and states that a correction factor is needed only if the section thickness is more than 1/10th of the object diameter.

5.3 Chapter Aims

This chapter aims to quantify any changes in mesophyll cell ultrastructure under UV-B using light and transmission electron microscopy in conjunction with stereological analysis. As cell ultrastructure changes during normal leaf development, this must therefore be taken into account before assessing the response of ultrastructure to UV-B. The cell age gradient of the primary leaf determined in the previous chapter will be used to distinguish between direct effects on ultrastructure (*i.e.* data expressed on a cell age basis), and indirect effects in which differences in ultrastructure between control and UV-B-grown plants is the result of the altered growth under UV-B (*i.e.* data expressed as distance from leaf base).

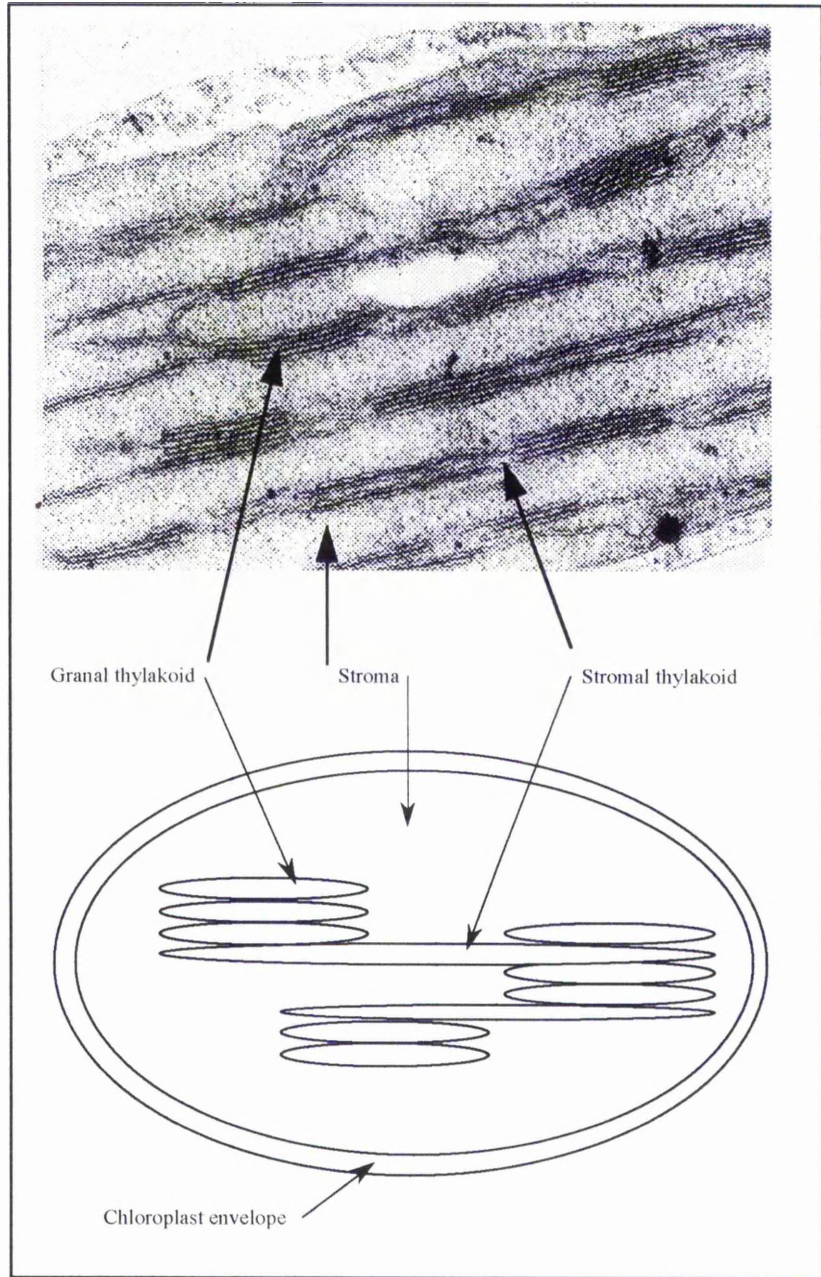


Fig. 5.1 Chloroplast Ultrastructure

Inset is a scanned electron micrograph of a mature chloroplast from wheat.

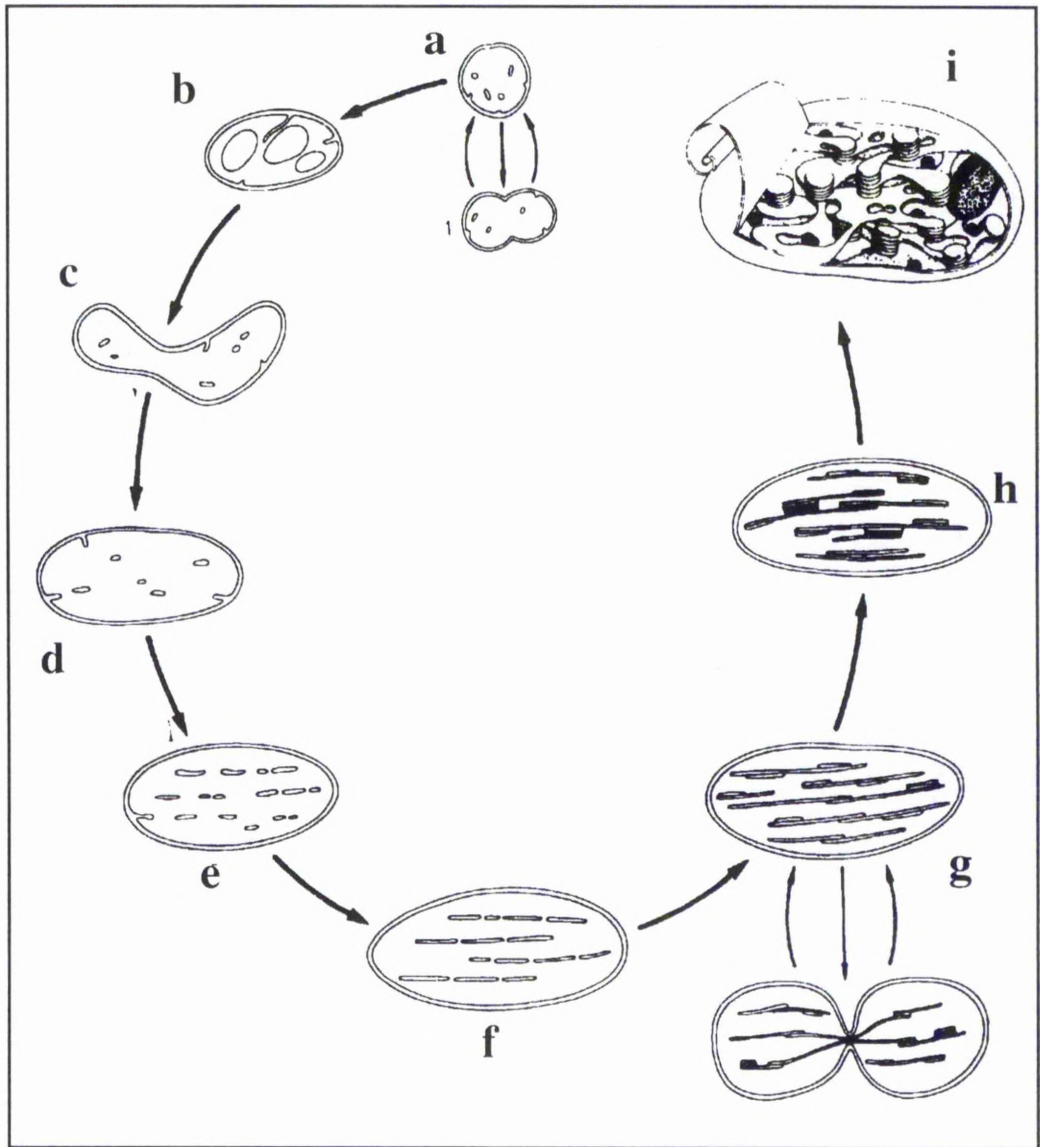


Fig. 5.2 Chloroplast Development

Diagram represents the development of a proplastid into a chloroplast.

a - proplastid; b - starch containing phase; c - amoeboid stage; d - before perforated membrane plates begin to extend; e-g - perforated membranes plates overlap; g - young chloroplasts divide, increase in size and in the complexity of their granal stacks (h); i - fully photosynthetic chloroplast (After Leech & Baker, 1983).

RESULTS

5.4 Effect of UV-B on Mesophyll Cell Structure

Mesophyll cell transverse area (TA) and volume fraction (V_V) occupied by the vacuole, was calculated from stereological analysis of random LM micrographs (*e.g.* Plate 5.1 a-d) taken along the length of the 7-d-old primary leaf blade (Section 2.6). Mesophyll cell ultrastructure, *e.g.* chloroplast and mitochondria TA and the V_V of mesophyll cell cytoplasm they occupy, and organelle ultrastructure, *e.g.* V_V of chloroplast occupied by stromal and granal thylakoids, was calculated from stereological analysis of random TEM micrographs (*e.g.* Plate 5.3a-f, 5.4a-f) taken along the length of the 7-d-old primary leaf blade (see Section 2.6). To allow comparisons to be made between control and UV-B-grown plants despite the difference in growth (see Section 3.4.2), data were expressed on both a spatial basis, *i.e.* relative to the position along the leaf, and on a temporal basis, *i.e.* relative to cell age, as calculated in the previous chapter (see Section 4.7).

5.5 LM Analysis

5.5.1 Mesophyll Cell Transverse Area

The TA of mesophyll cells increased along the length of the primary leaf, to a maximum TA of *c.* $900\mu\text{m}^2$, 40mm above the leaf base (*c.* 50 hours)(Fig. 5.3)(Plate 5.1a-d). Control and UV-B-grown plants showed similar changes in mesophyll TA, increasing 2-fold between 10mm above the leaf base to the leaf tip. On a spatial scale UV-B significantly increased mesophyll TA between 20-30mm above the leaf base (Fig. 5.3a), however, this difference was reduced when the data were expressed on a temporal scale

(Fig. 5.3b).

5.5.2 Vacuole Volume Fraction

The V_v of mesophyll cell occupied by vacuole was relatively constant along the length of the primary leaf, when expressed on either a spatial or temporal scale (Fig. 5.4a,b). There was no significant effect of UV-B on vacuole V_v , with an average V_v for the whole leaf blade of $70.1 \pm 0.7\%$, compared to $71.2 \pm 0.5\%$ in control-grown plants. Mesophyll cells in the basal region of the leaf contain numerous small vacuoles, that may be inter-connected in the 3D cell (Plate 5.1a). As mesophyll cells develop (*i.e.* displaced towards the leaf tip) and increase in transverse area (Section 5.5.1), the size of the vacuole increases at the same rate as the cell, forming one large central vacuole that occupies the same V_v of the cell as that of the small vacuoles in the mesophyll cells near the leaf base (Plate 5.1d).

5.6 TEM Analysis

5.6.1 Tissue Preservation

The tissue examined from both control and UV-B-grown plants showed good ultrastructural preservation, indicated by the lack of shrinkage of the cell contents from the cell wall (see Plate 5.2a), intact membranes, including the nuclear, chloroplast and mitochondrial envelopes (see Plate 5.2c), and chloroplast thylakoids and mitochondrial cristae (Plate 5.2b,c).

5.6.2 Effect of UV-B on Mesophyll Cell Ultrastructure

The V_v of mesophyll cell cytoplasm occupied by chloroplasts and mitochondria, and the transverse area of these organelles, were calculated using stereological analysis of random TEM micrographs (*e.g.* Plate 5.3i,ii a-f) taken along the length of the 7-d-old

primary leaf blade (see Section 2.8).

5.6.2.1 Chloroplast Volume Fraction

The V_V of cytoplasm occupied by chloroplasts increased three-fold along the length of the primary leaf (Fig. 5.5a,b). Control and UV-B-grown plants showed similar changes in chloroplastic V_V along the leaf blade when expressed on either a spatial (Fig. 5.5a) or a temporal (Fig. 5.5b) scale. There was an initial rapid 2-fold increase in V_V , within the basal 10mm of the leaf blade (0- 20 hours) from *c.* 25 - 50% , after which it continued to increase at a slower rate to give a final constant chloroplastic V_V of *c.* 75% from 40mm onwards (50+hours). UV-B significantly increased ($p \leq 0.05$) the chloroplastic V_V in the basal 5mm of the leaf blade only (0-15 hours). There was no significant difference in the chloroplastic V_V between control and UV-B-grown plants along the rest of the leaf blade. When expressed on a temporal scale these differences were no longer seen.

5.6.2.2 Chloroplast Transverse Area

Chloroplast transverse area (TA) increased at a linear rate along the length of the primary leaf (Fig.5.6a,b). In control-grown plants there was a 10-fold increase in chloroplast TA, from *c.* $1.6\mu\text{m}^2$ in the leaf base to *c.* $15.5\mu\text{m}^2$ in the tip. In UV-B-grown plants chloroplast TA increased 8-fold, from *c.* $1.8\mu\text{m}^2$ in the leaf base to *c.* $14.2\mu\text{m}^2$ in the tip. However, when compared on a spatial scale (*i.e.* distance from leaf base) there was no significant difference in chloroplast TA between control and UV-B-grown plants (Fig. 5.6a). When the data are expressed on a temporal scale (*i.e.* cell age) taking into account the different growth rates of control and UV-B grown plants, UV-B reduced the chloroplast TA in mesophyll cells aged 50 hours or more, by an average *c.* $2\mu\text{m}^2$, resulting in a maximum chloroplast TA of *c.* $14.2\mu\text{m}^2$, a reduction of *c.* 10% compared

to controls, *c.* $15.5\mu\text{m}^2$ (Fig. 5.6b).

5.6.2.3 Mitochondrial Volume Fraction

The V_V of mesophyll cell cytoplasm occupied by mitochondria decreased by a factor of 3 along the length of the primary leaf (Fig. 5.7). There was no effect of UV-B on mitochondrial V_V , which showed an initial rapid decrease in the basal 10mm of the leaf blade (0-20 hours), to half its original value, *c.* 6% to *c.* 3%. The V_V continued to decrease at a slower rate to give a final constant mitochondrial V_V of *c.* 2% from 40mm onwards (50+hours). Control and UV-B grown plants showed a similar distribution of mitochondrial V_V along the leaf blade when expressed on either a spatial (Fig. 5.7a) or temporal (Fig. 5.7b) scale.

5.6.2.4 Mitochondrion Transverse Area

Mitochondrion TA increased between the base and the tip of the primary leaf (Fig. 5.8). Control and UV-B-grown plants showed a similar distribution of TA, increasing by *c.* 30% within the basal 5mm of the leaf blade and then decreasing in the next 10mm to the original level found at the leaf base, indicating the zone of mitochondrial division to be between 5 and 15mm above the leaf base (*i.e.* above the zone of cell division, see Section 4.4.1). The TA then increased between 15mm and the leaf tip. The rate of increase in mitochondrion TA of UV-B-grown plants is lower than that of control-grown plants, a difference which is magnified when data are expressed on a temporal scale (Fig. 5.8b). When the data are expressed on a temporal scale, the 'zone of mitochondrial division' is larger in UV-B-grown plants, *c.* 10-30 hours, as compared to control-grown plants (*c.* 10-25 hours). In mesophyll cells aged 50 hours and more, UV-B decreased the average mitochondrion TA by *c.* $0.15\mu\text{m}^2$, resulting in a maximum mitochondrion TA of *c.* $0.59\mu\text{m}^2$, a reduction of *c.* 20% compared to

controls (*c.* $0.72\mu\text{m}^2$).

5.6.3 Effect of UV-B on Chloroplast Ultrastructure

The V_V of mesophyll cell chloroplasts occupied by granal and stromal thylakoids was calculated using stereological techniques of random TEM micrographs (e.g. Plate 5.4 i,ii a-d) taken along the length of the 7-d-old primary leaf blade (Section 2.6,2.8).

5.6.3.1 Granal Thylakoid Volume Fraction

The V_V of chloroplast occupied by granal thylakoids increased along the length of the primary leaf (Fig. 5.9). Control and UV-B-grown plants showed a similar distribution of granal V_V along the leaf, increasing between the leaf base and 15mm, then decreasing over the next 5mm, before increasing at a linear rate towards the leaf tip. UV-B-grown plants had a significantly greater ($p \leq 0.05$) granal V_V from 30mm onwards. However, when data are expressed on a temporal scale (Fig. 5.9b) this difference was lost, so that the granal V_V of mature chloroplasts was similar in control ($24.8 \pm 0.96\%$) and UV-B grown plants ($24.6 \pm 0.74\%$).

5.6.3.2 Stromal Thylakoid Volume Fraction

The V_V of chloroplast occupied by stromal thylakoids increased along the length of the primary leaf (Fig. 5.10). Control and UV-B-grown plants showed a similar distribution of stromal V_V along the leaf blade when expressed on both a spatial (Fig. 5.10a) and temporal (Fig. 5.10b) scale, increasing from *c.* 5% in the leaf base to *c.* 7-8% towards the leaf tip.

5.6.3.3 Granal Sac Number Per Granum

The number of granal sacs per granum increased 3-fold along the length of the primary leaf (Fig. 5.11). UV-B significantly increased ($p \leq 0.05$) the number of sacs per granum along the majority of the leaf blade when expressed on a spatial scale (Fig.

5.11a). However, when expressed on a temporal scale (Fig. 5.11b) there was no difference in the number of sacs per granum in chloroplasts in the top half of the leaf blade. The average number of granal sacs per granum in a mature chloroplast was *c.* 8.

5.7 Effect of UV-B on Chloroplast Number Per Mesophyll Cell

The number of chloroplasts per mesophyll cell was estimated from 3 representative merged confocal images (Plate 5.6) taken from a Z series of images through a mesophyll cell (Plate 5.5) (see Section 2.9). The number of chloroplasts per cell increased along the length of the primary leaf (Fig. 5.12). Both control and UV-B-grown plants showed a similar distribution in chloroplast numbers, increasing 2-fold between 10 and 40mm above the leaf base, after which a maximum number was maintained. UV-B significantly increased ($p \leq 0.05$) the number of chloroplasts per mesophyll cell along the whole of the leaf blade. In mature cells the average number of chloroplasts per cell in UV-B grown plants was significantly greater ($p \leq 0.05$) than control-grown plants, with an average of *c.* 165 chloroplasts per mature mesophyll cell, an increase of 15 chloroplasts per cell compared to controls. The maximum number of chloroplasts per mesophyll cell was reached at *c.* 50 hours.

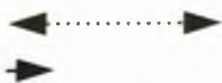
Plate 5.1 Light Microscopy Of Mesophyll Cell Development

Tissue from 7-d-old primary leaves grown under control conditions (Section 2.2) was fixed and embedded as described in Sections 2.6-2.7. Transverse sections ($0.5\mu\text{m}$) were taken 10, 30, 50 and 80mm above the basal meristem, corresponding to a cell age (Hrs) of (a) 18.1 (b) 39.2 (c) 60.3 and (d) 92.0. Sections stained with methylene blue (Section 2.7.2) and photographed at x500 magnification (Section 2.7.3) were used for the stereological determination of mesophyll cell TA and vacuole V_V (Section 2.8).

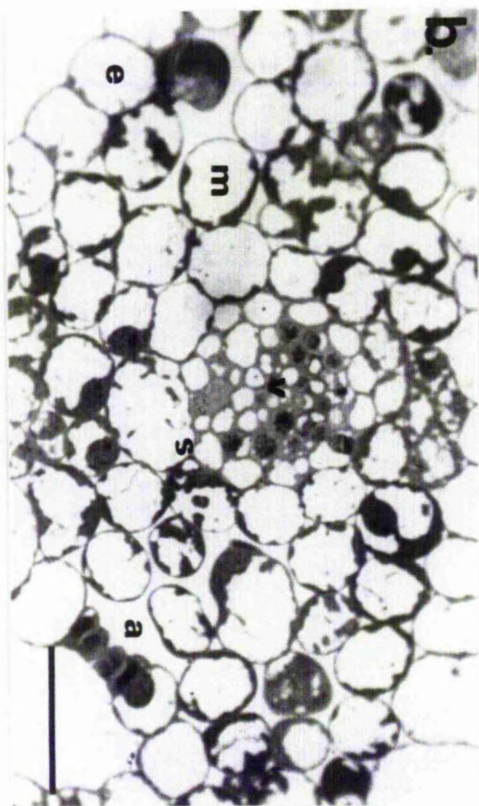
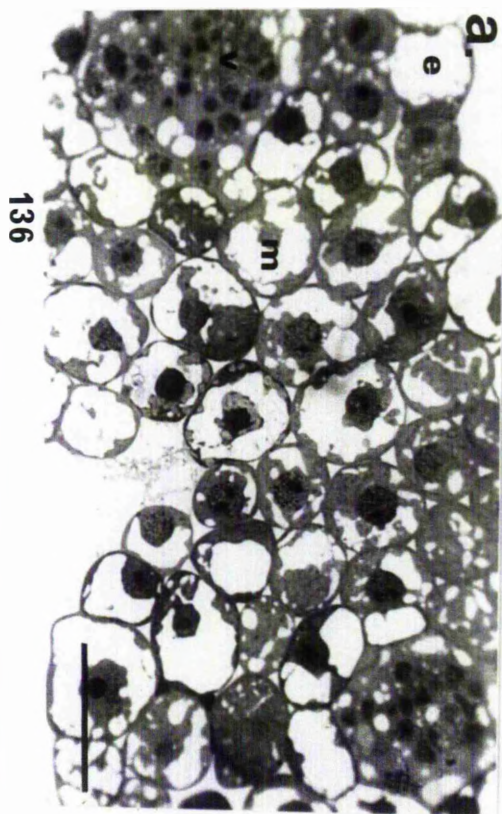
Abbreviations - e = epidermis, m = mesophyll tissue, v = vascular bundle

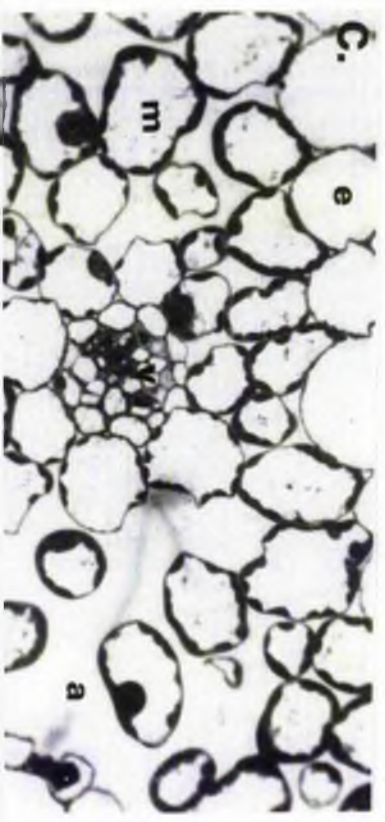
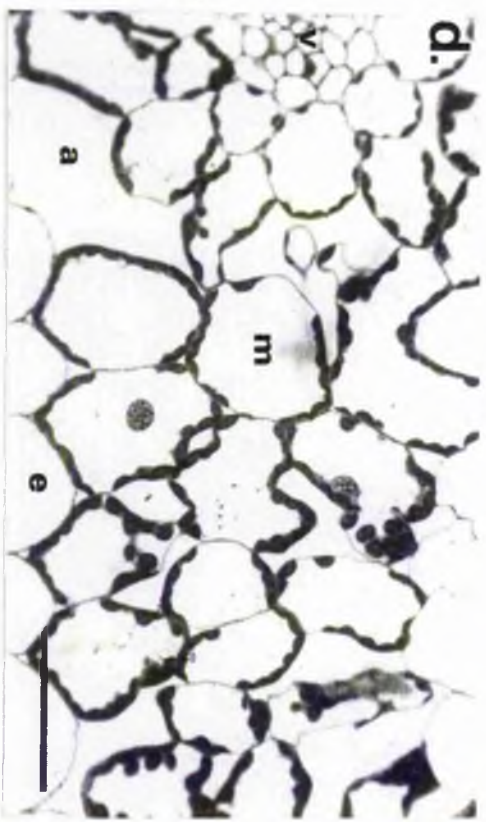
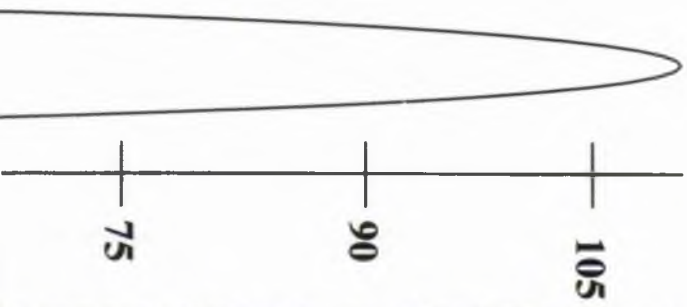
Bars = $50\mu\text{m}$

Elongation
Division



Cell Age
(Hours)





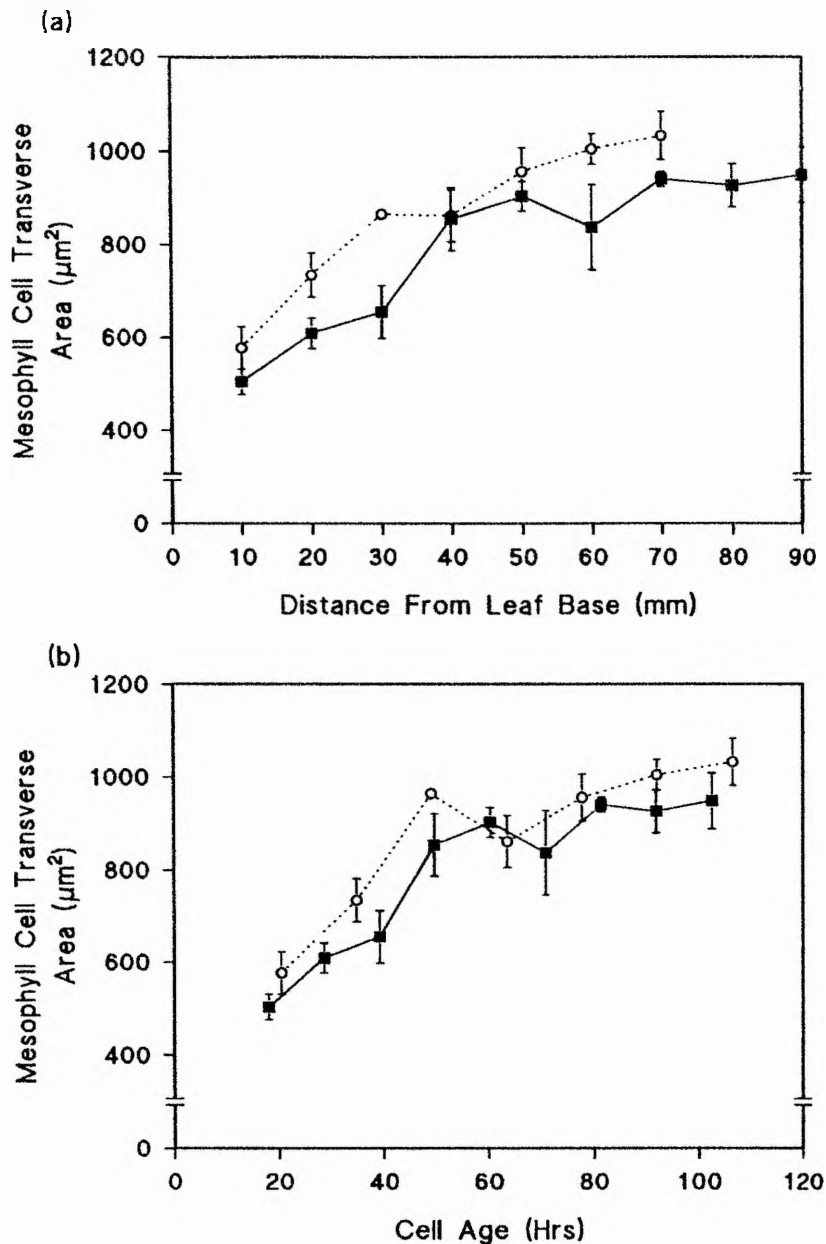


Fig. 5.3 Effect of UV-B radiation on mesophyll cell transverse area along the length of 7-d-old primary leaves, expressed on a (a) spatial and (b) temporal scale

Plants were grown under control (■) and UV-B (○) conditions (Section 2.2). Tissue was fixed, embedded, sectioned and stained (Section 2.6-2.7) and transverse areas calculated from random LM micrographs (e.g. Plate 5.1a-d) using stereology as described in Section 2.8. Each data point represents the mean of 5 independent growth studies, sampling 5 seedlings per replicate, from which a total of 20 micrographs were taken from 20 random blocks. Error bars show ± one standard error of the mean.

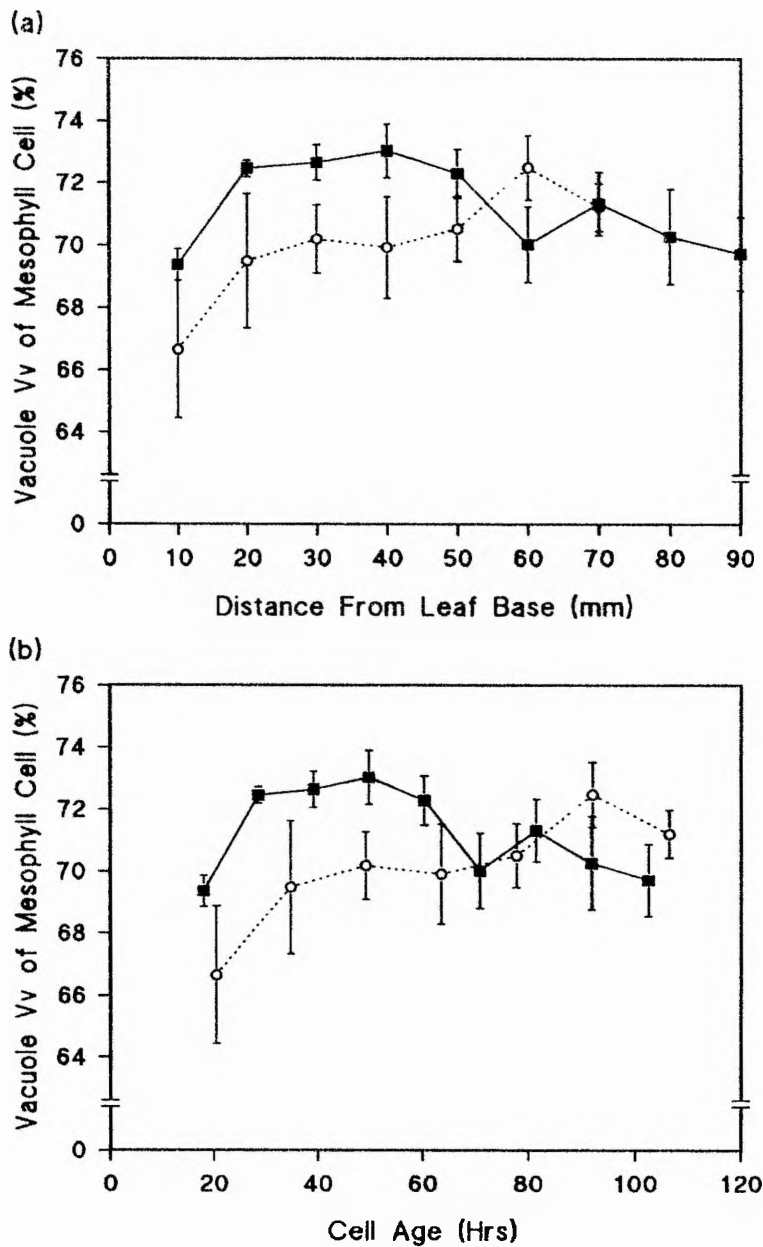


Fig. 5.4 Effect of UV-B radiation on the volume fraction of mesophyll cell occupied by vacuole along the length of 7-d-old primary leaves, expressed on a (a) spatial and (b) temporal scale

Plants were grown under control (■) and UV-B (○) conditions (Section 2.2). Tissue was fixed, embedded, sectioned and stained (Section 2.6-2.7) and volume fractions calculated from random LM micrographs (e.g. Plate 5.1a-d) using stereology as described in Section 2.8. Each data point represents the mean of 5 independent growth studies, sampling 5 seedlings per replicate, from which a total of 20 micrographs were taken from 20 random blocks. Error bars show \pm one standard error of the mean.

Plate 5.2 General Cell Ultrastructure Under The Transmission Electron Microscope

Tissue from 7-d-old primary leaves grown under control and UV-B conditions (Section 2.2) was fixed and embedded as described in section 2.6.1-2.6.4. Ultrathin transverse sections (60nm) were taken along the length of the leaf blade (Section 2.6.5), double stained with uranyl acetate and lead citrate (Section 2.6.6), and viewed at a range of magnifications under transmission electron microscopy (Section 2.6.7)

(a) Junction between 2 mesophyll cells, from UV-B treated tissue taken 20mm above leaf base. Note : narrow cytoplasmic channels (plasmodesmata) interconnecting adjacent mesophyll cells through the intervening wall.

(b) High magnification image of a vascular cell, from 20mm above leaf base of control-grown plants.

(c) High magnification image of a mesophyll cell, from 40mm above leaf base of UV-B-grown plants. Note : the double membranes enclosing the nucleus, chloroplast and mitochondrion, and the close association between these organelles.

Abbreviations - c = cytosol, cp = chloroplast, cr = cristae, cw = cell wall, g = golgi (dictyosome), m = mitochondrion, n = nucleus, ne = nuclear envelope, p = plasmodesmata, rer = rough endoplasmic reticulum

Bars = 0.5 μ m

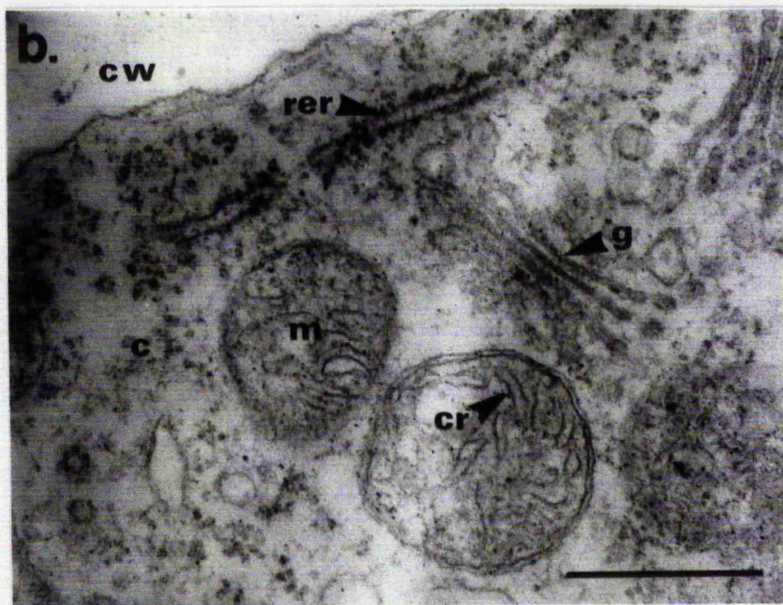
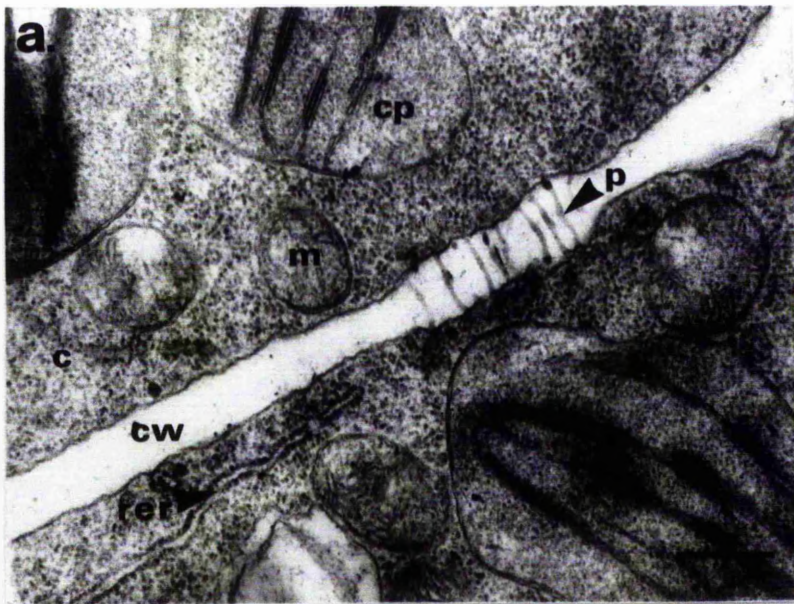


Plate 5.3 (i,ii) Transmission Electron Microscopy Of Mesophyll Cell Development

Tissue from 7-d-old primary leaves grown under UV-B conditions (Section 2.2) was fixed and embedded as described in section 2.6.1-2.6.4. Ultrathin transverse sections (60nm) were taken 5, 10, 20, 40, 50 and 70mm above the basal meristem, corresponding to a cell age (Hrs) of (i,a) 12 (i,b) 20 (i,c) 35 (ii,a) 60 (ii,b) 78 and (ii,c) 106 (see Section 4.7).

Sections, doubled stained with uranyl acetate and lead citrate (Section 2.6.6) and photographed at x5000 magnification (Section 2.6.7) were used for the stereological determination of TA and V_V (Section 2.8) of chloroplasts and mitochondria.

Abbreviations - a = air space, c = cytosol, cp = chloroplast, cw = cell wall, m = mitochondria, n = nucleus, v = vacuole

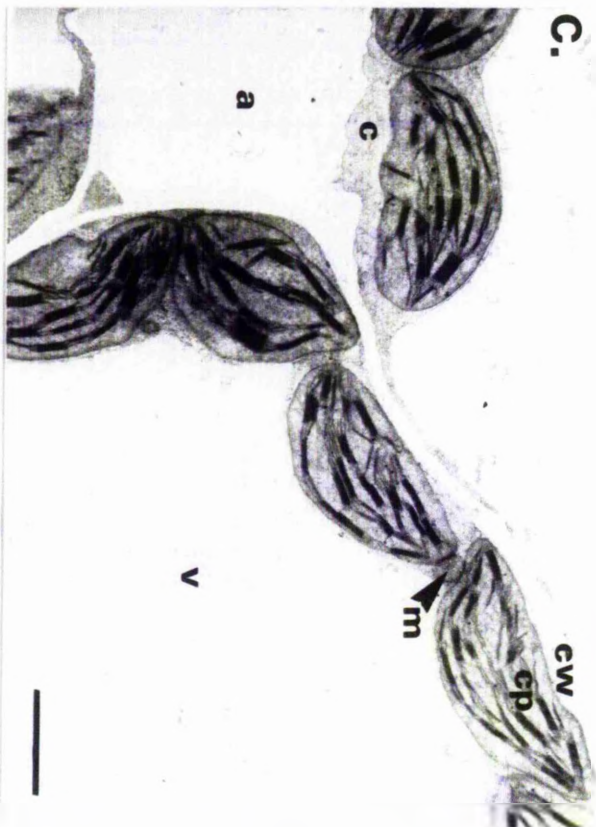
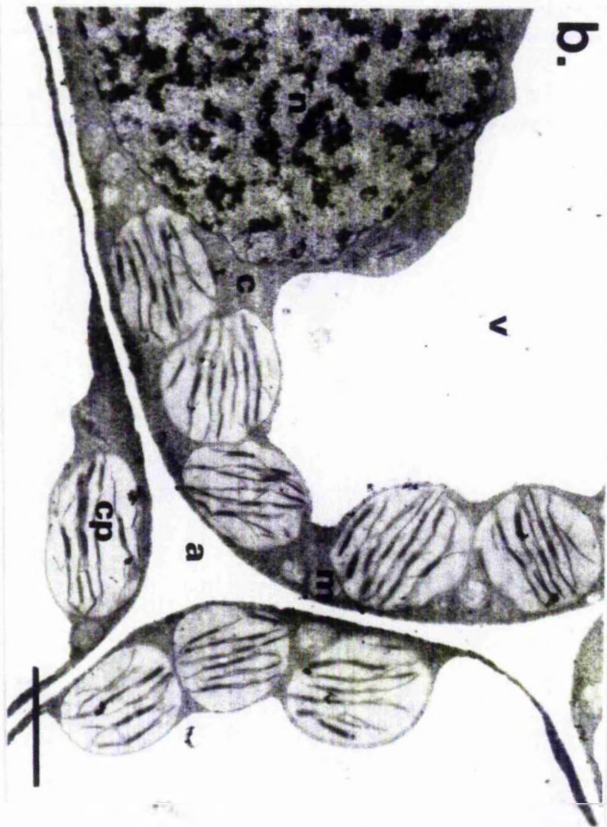
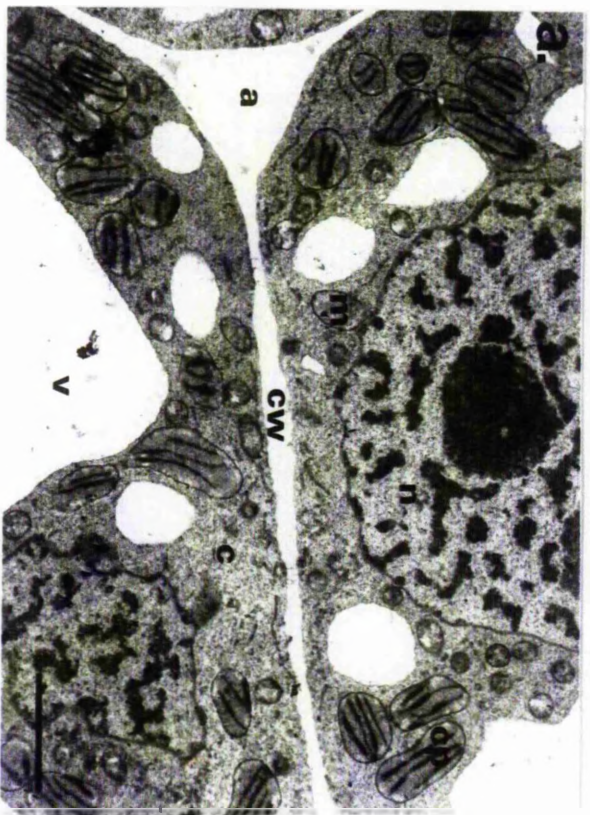
Bars = 2 μ m

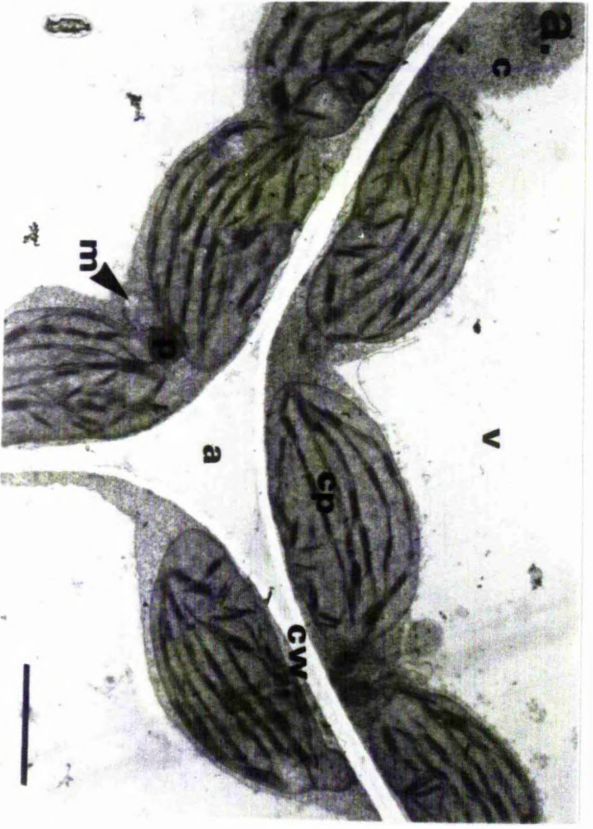
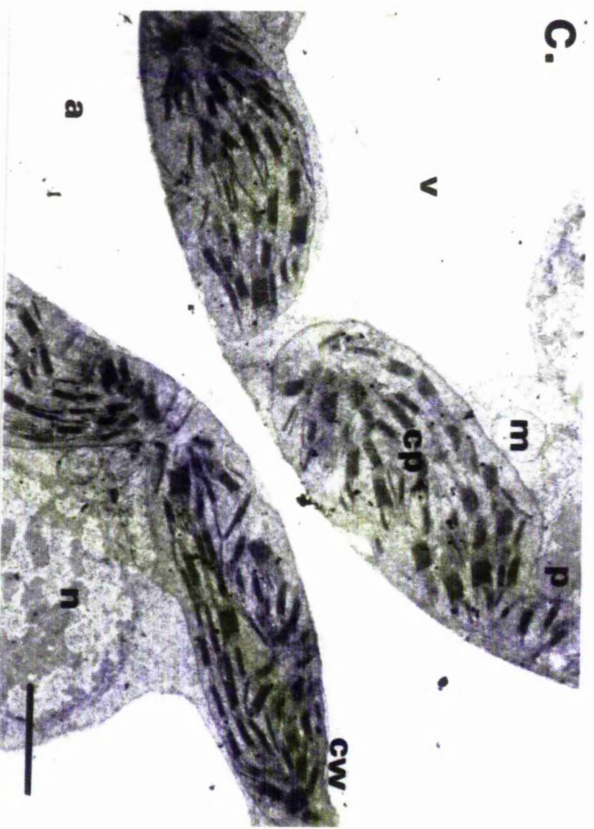
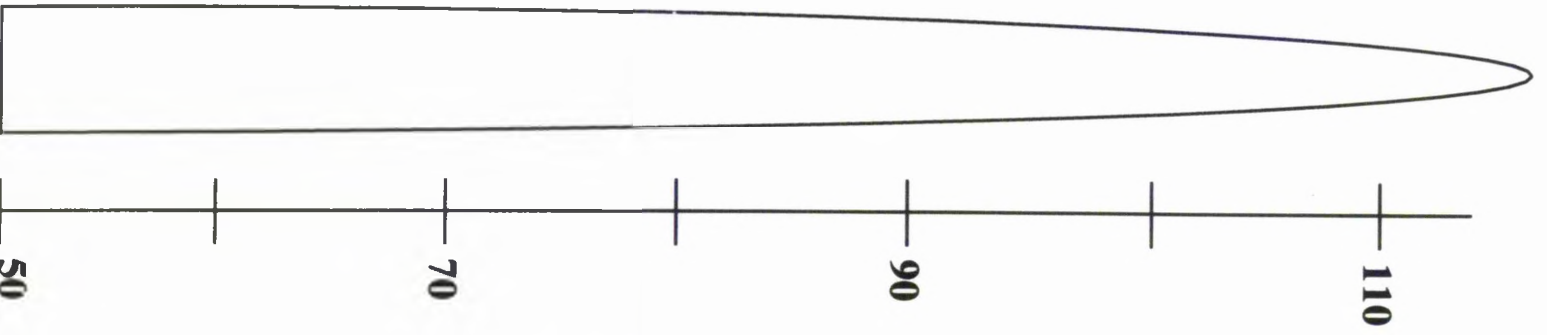
Elongation ← →

Division ← →



Cell Age
(Hours)





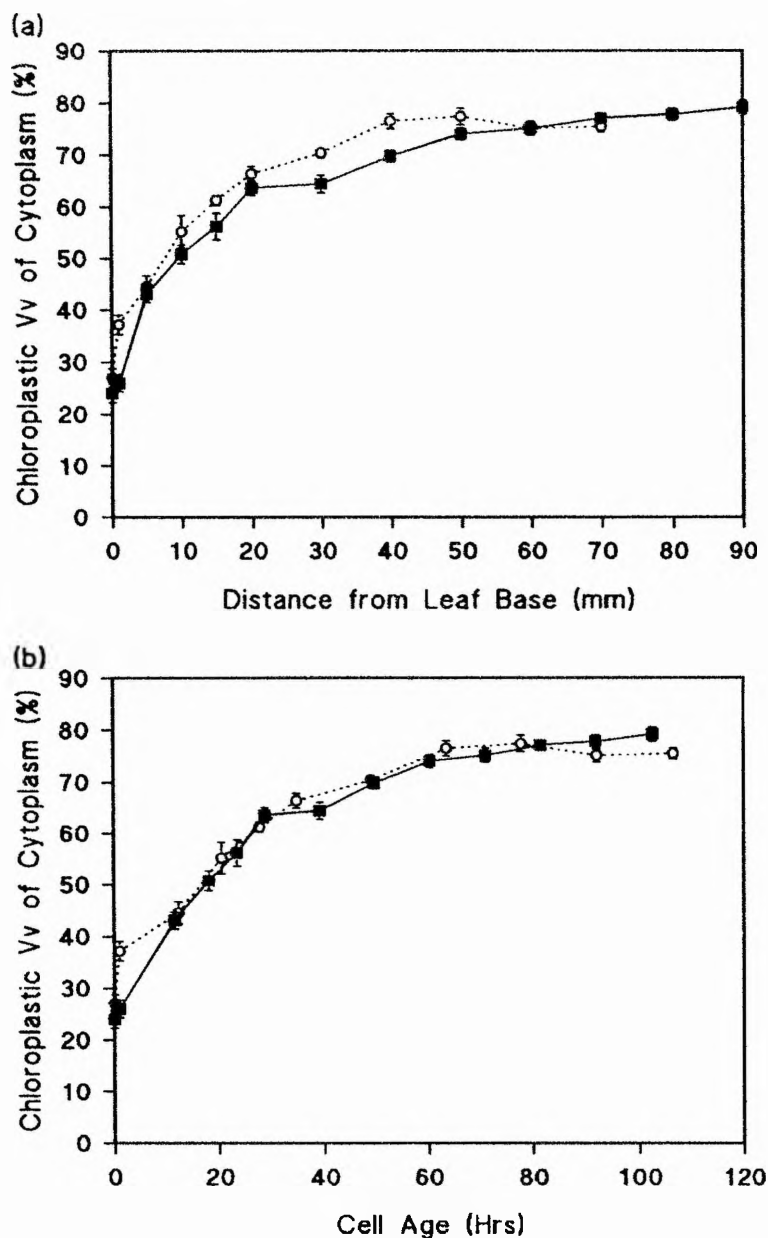


Fig. 5.5 Effect of UV-B radiation on the volume fraction of mesophyll cell cytoplasm occupied by chloroplasts along the length of 7-d-old primary leaves, expressed on a (a) spatial and (b) temporal scale

Plants were grown under control (■) and UV-B (○) conditions (Section 2.2). Tissue was fixed, embedded, sectioned and stained (Section 2.6) and volume fractions calculated from random TEM micrographs (e.g. Plate 5.3i,ii a -f) using stereology as described in Section 2.8. Each data point represents the mean of 5 independent growth studies, sampling 5 seedlings per replicate, from which a total of 20 micrographs were taken from 20 random blocks. Error bars show \pm one standard error of the mean.

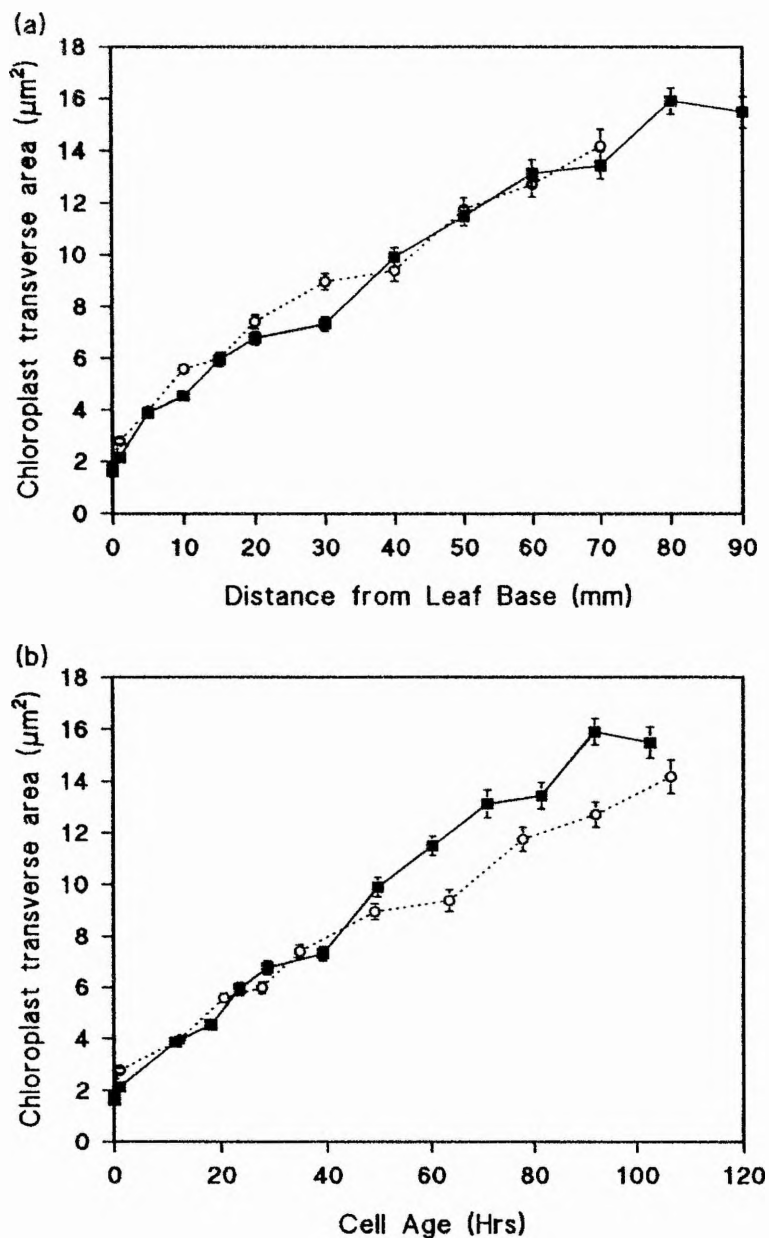


Fig. 5.6 Effect of UV-B radiation on mesophyll cell chloroplast transverse area along the length of 7-d-old primary leaves, expressed on a (a) spatial and (b) temporal scale. Plants were grown under control (■) and UV-B (○) conditions (Section 2.2). Tissue was fixed, embedded, sectioned and stained (Section 2.6) and transverse areas calculated from random TEM micrographs (e.g. Plate 5.3i,ii a-f) using stereology as described in Section 2.8. Each data point represents the mean of 5 independent growth studies, sampling 5 seedlings per replicate, from which a total of 20 micrographs were taken from 20 random blocks. Error bars show \pm one standard error of the mean.

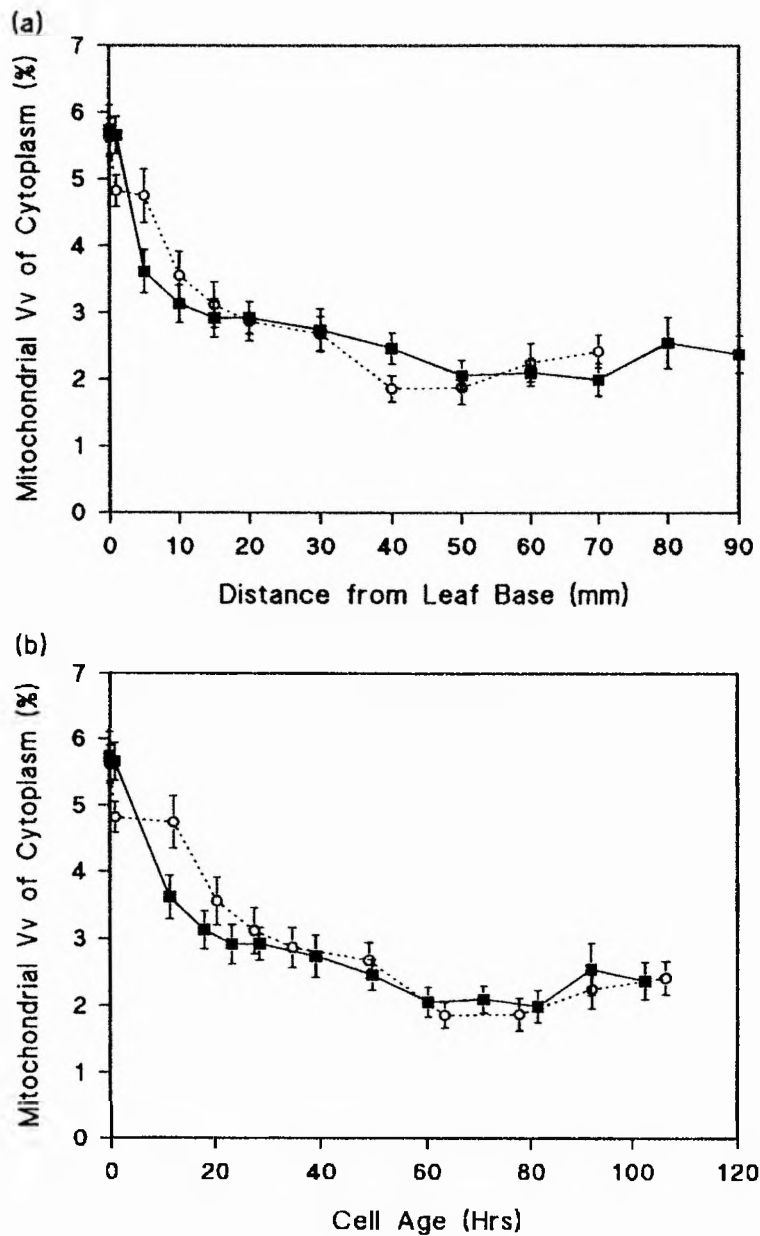


Fig. 5.7 Effect of UV-B radiation on the volume fraction of mesophyll cell cytoplasm occupied by mitochondria along the length of 7-d-old primary leaves, expressed on a (a) spatial and (b) temporal scale

Plants were grown under control (■) and UV-B (○) conditions (Section 2.2). Tissue was fixed, embedded, sectioned and stained (Section 2.6) and volume fractions calculated from random TEM micrographs (e.g. Plate 5.3i,ii a-f) using stereology as described in Section 2.8. Each data point represents the mean of 5 independent growth studies, sampling 5 seedlings per replicate, from which a total of 20 micrographs were taken from 20 random blocks. Error bars show \pm one standard error of the mean.

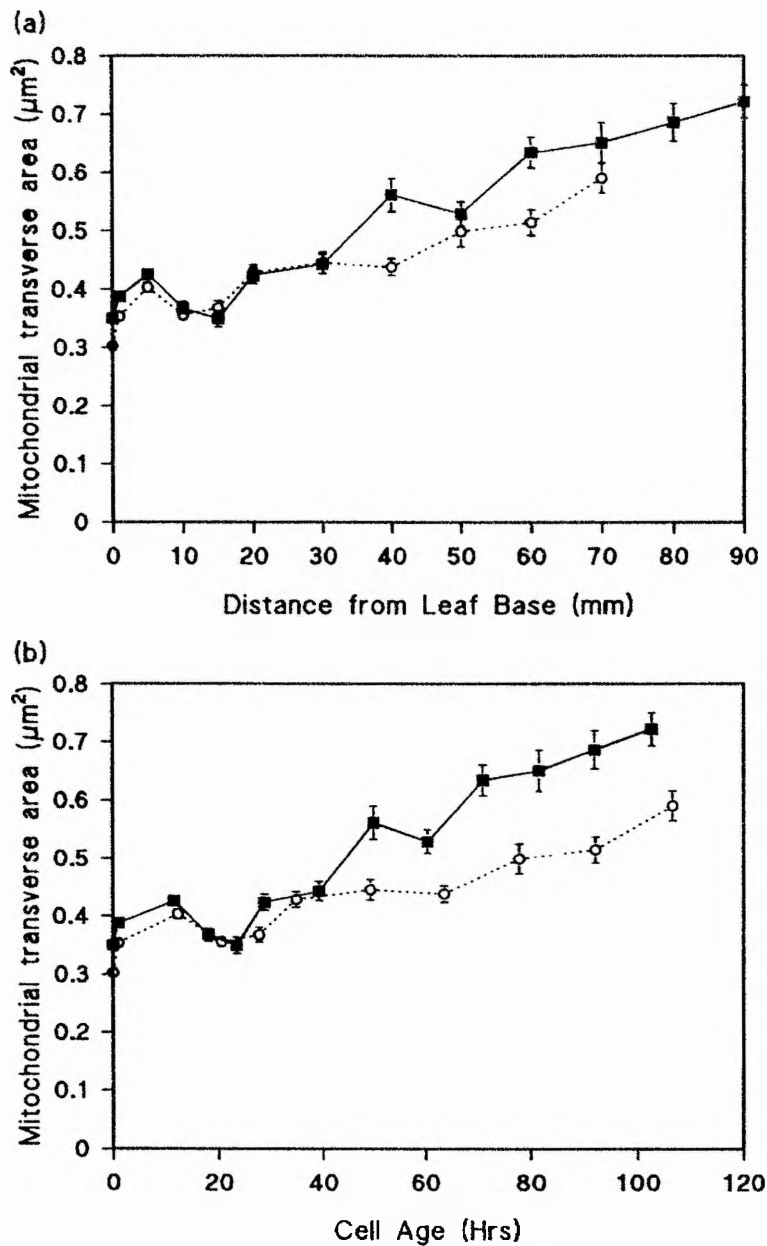


Fig. 5.8 Effect of UV-B radiation on mesophyll cell mitochondrial transverse area along the length of the 7-d-old primary leaves, expressed on a (a) spatial and (b) temporal scale

Plants were grown under control (■) and UV-B (○) conditions (Section 2.2). Tissue was fixed, embedded, sectioned and stained (Section 2.6) and transverse areas calculated from random TEM micrographs (e.g. Plate 5.3i,ii a-f) using stereology as described in Section 2.8. Each data point represents the mean of 5 independent growth studies, sampling 5 seedlings per replicate, from which a total of 20 micrographs were taken from 20 random blocks. Error bars show ± one standard error of the mean.

Plate 5.4 (i,ii) Transmission Electron Microscopy Of Chloroplast Development

Legend as for plate 5.3 i, ii.

Sections were photographed at x 29000 magnification (Section 2.6.7) and used for the stereological determination of granal and stromal V_V of the chloroplast (Section 2.8).

Abbreviations - c = cytosol, cp = chloroplast, cw = cell wall , g = grana, gt = granal thylakoid, m = mitochondria, p = plastoglobuli., st = stromal thylakoid, s = starch, v = vacuole

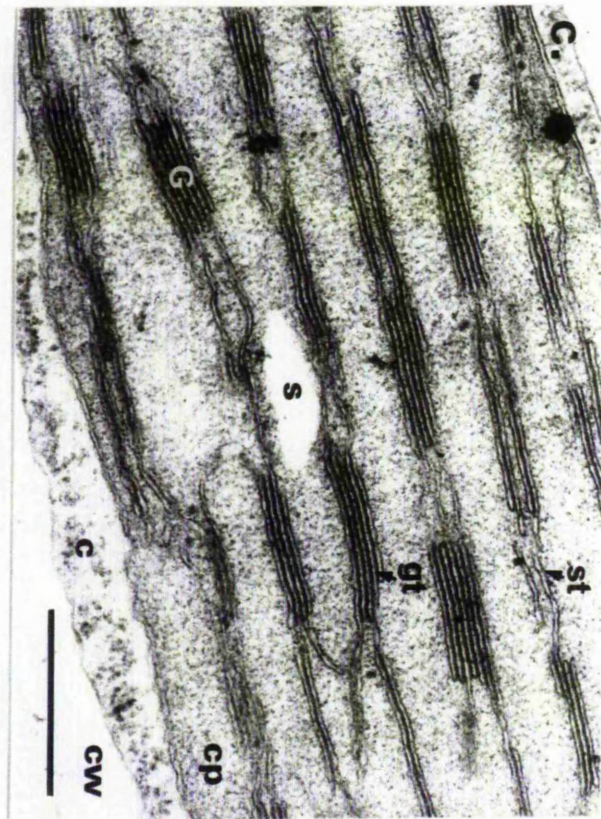
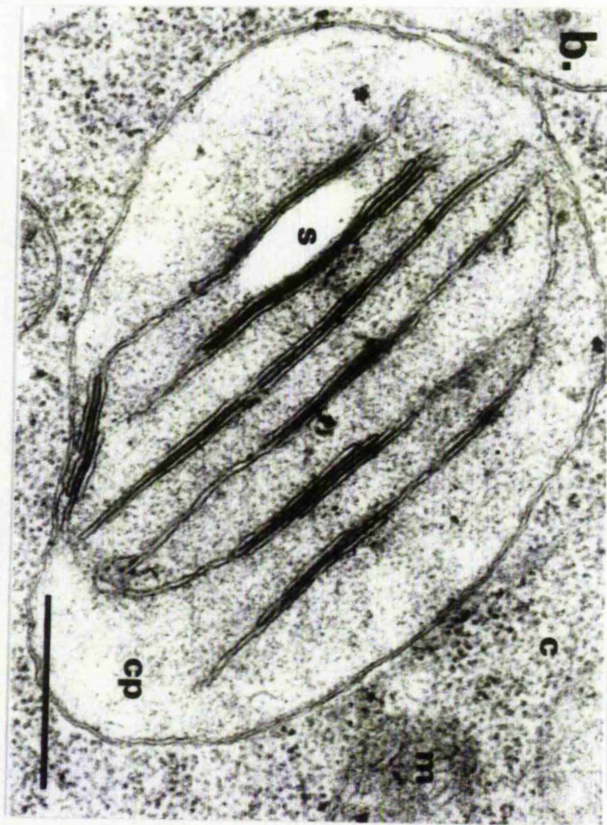
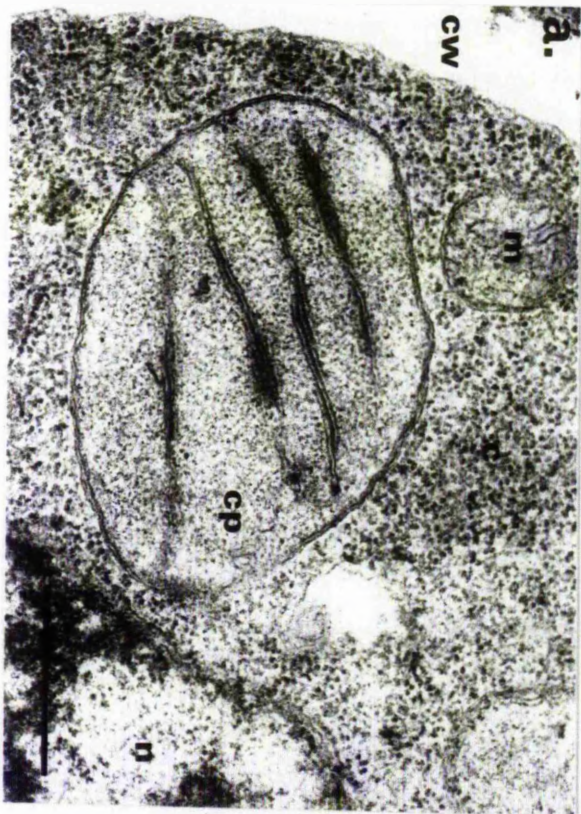
Bars =0.5 μ m

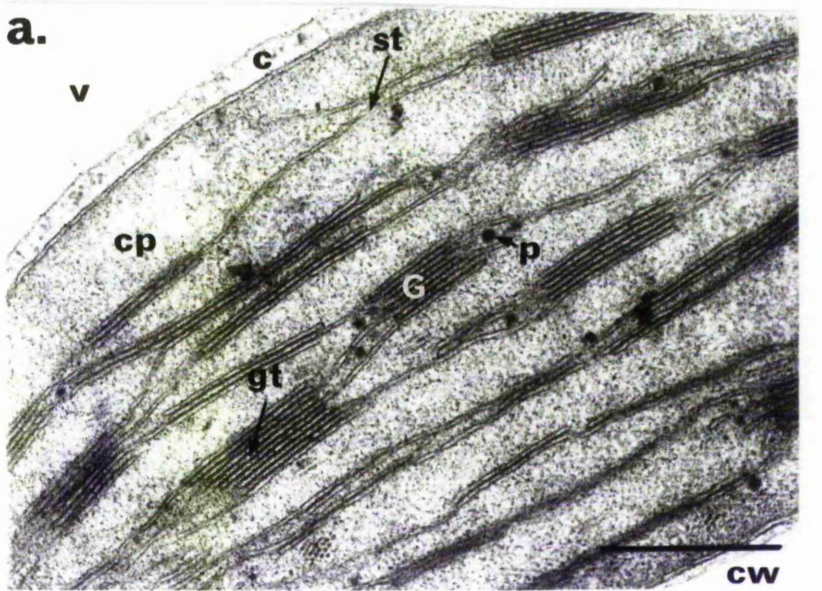
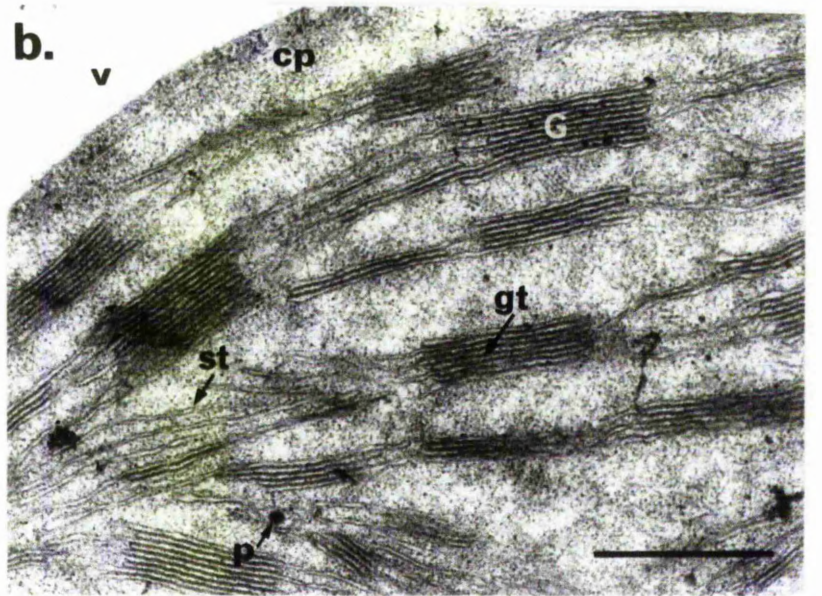
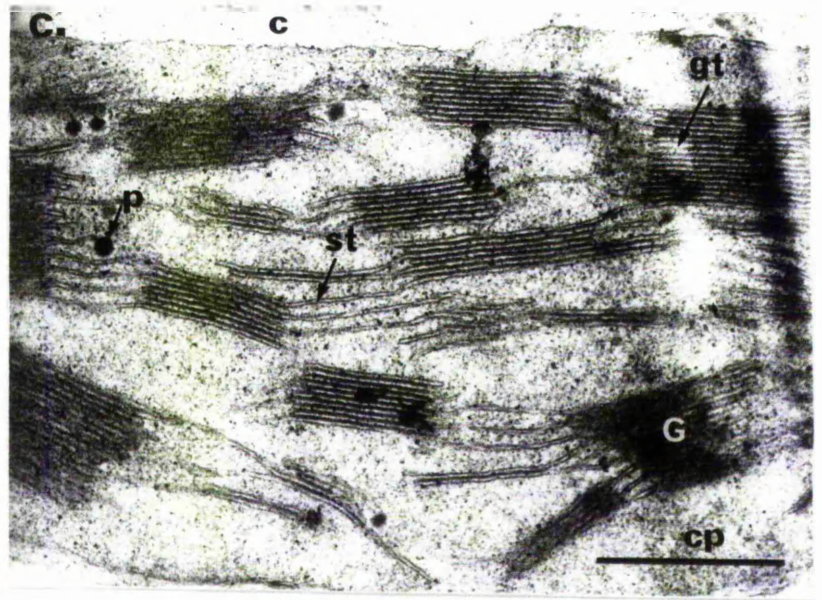
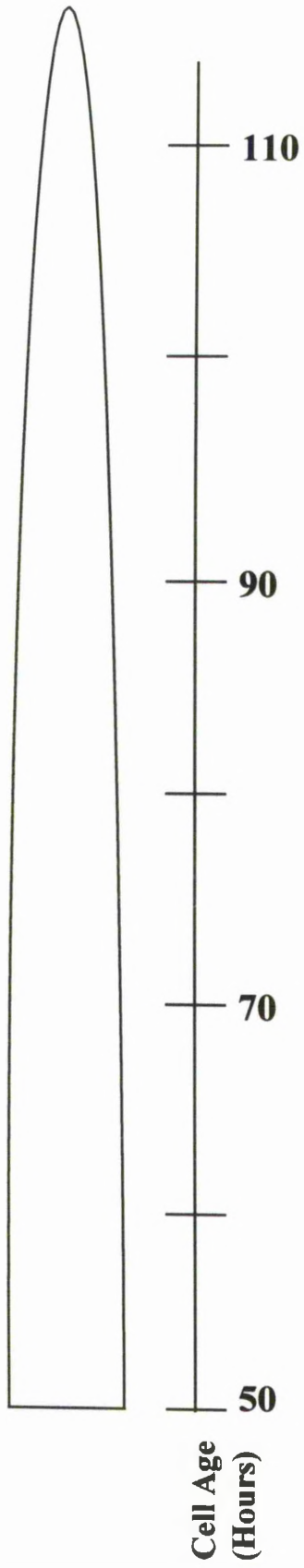
Elongation ← →

Division ← →



Cell Age
(Hours)





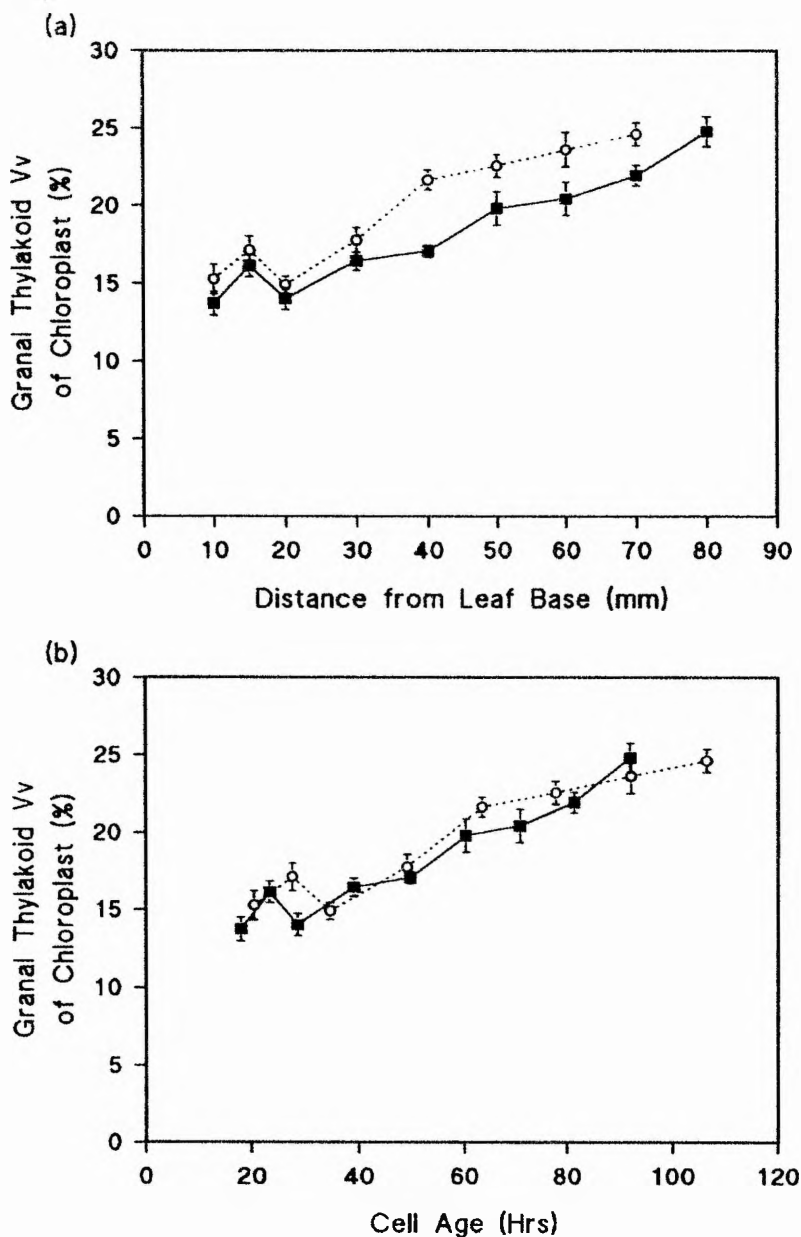


Fig. 5.9 Effect of UV-B radiation on the volume fraction of mesophyll cell chloroplast occupied by granal thylakoids along the length of 7-d-old primary leaves, expressed on a (a) spatial and (b) temporal scale

Plants were grown under control (■) and UV-B (○) conditions (Section 2.2). Tissue was fixed, embedded, sectioned and stained (Section 2.6) and volume fractions calculated from random TEM micrographs (e.g. Plate 5.4i,ii a-f) using stereology as described in Section 2.8. Each data point represents the mean of 5 independent growth studies, sampling 5 seedlings per replicate, from which a total of 20 micrographs were taken from 20 random blocks. Error bars show \pm one standard error of the mean.

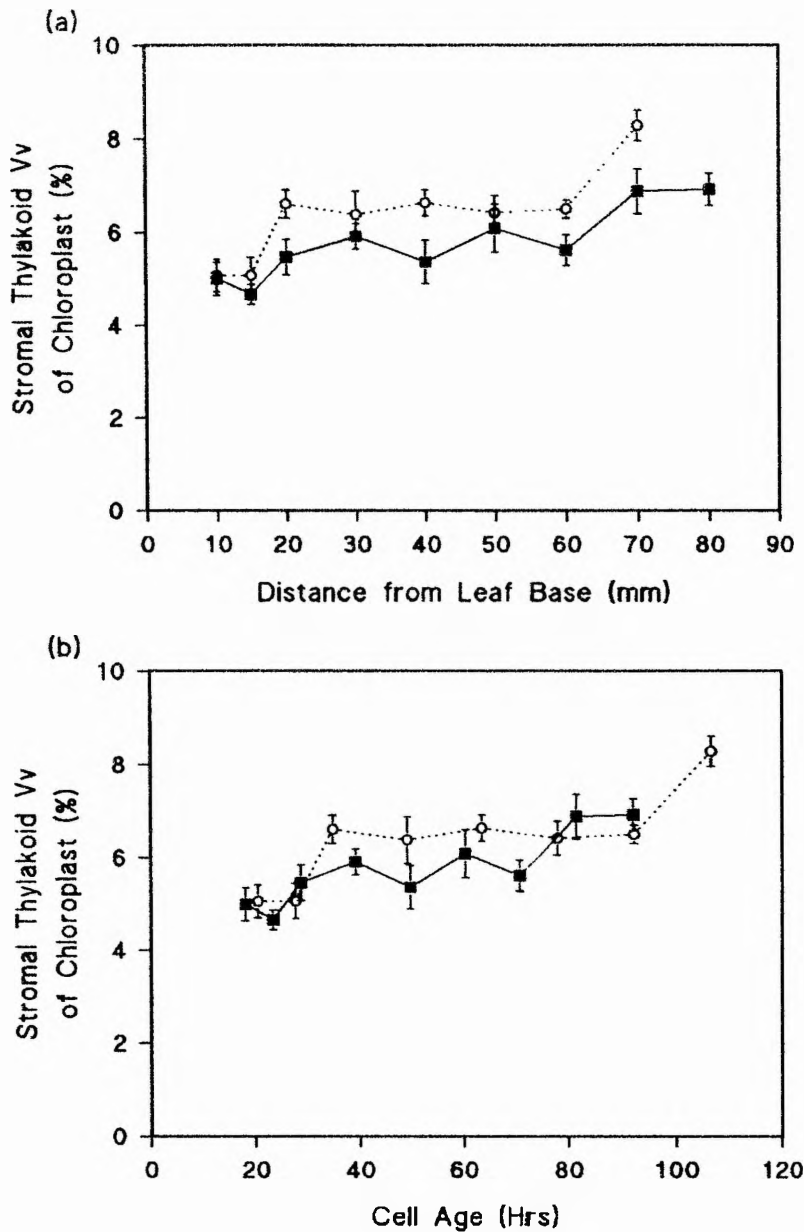


Fig. 5.10 Effect of UV-B radiation on the volume fraction of mesophyll cell chloroplast occupied by stromal thylakoids along the length of 7-d-old primary leaves, expressed on a (a) spatial and (b) temporal scale

Plants were grown under control (■) and UV-B (○) conditions (Section 2.2). Tissue was fixed, embedded, sectioned and stained (Section 2.6) and volume fractions calculated from random TEM micrographs (e.g. Plate 5.4i,ii a-f) using stereology as described in Section 2.8. Each data point represents the mean of 5 independent growth studies, sampling 5 seedlings per replicate, from which a total of 20 micrographs were taken from 20 random blocks. Error bars show \pm one standard error of the mean.

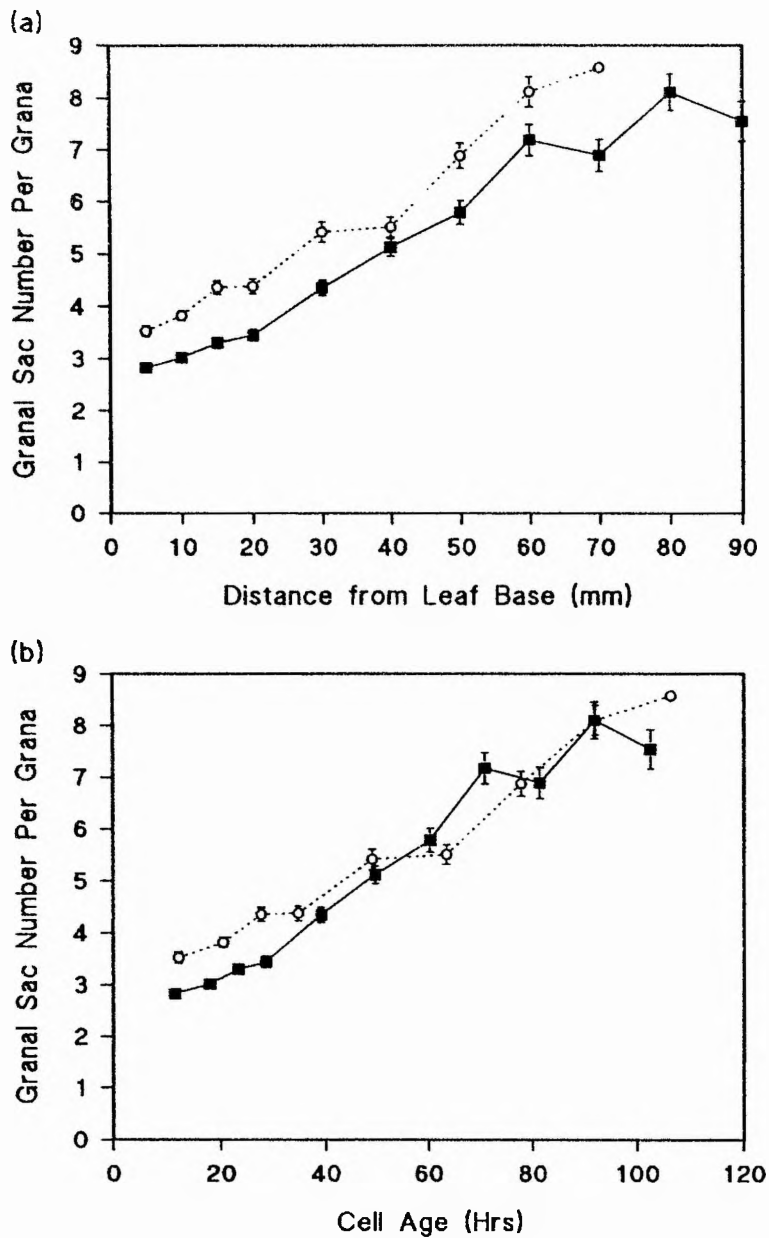


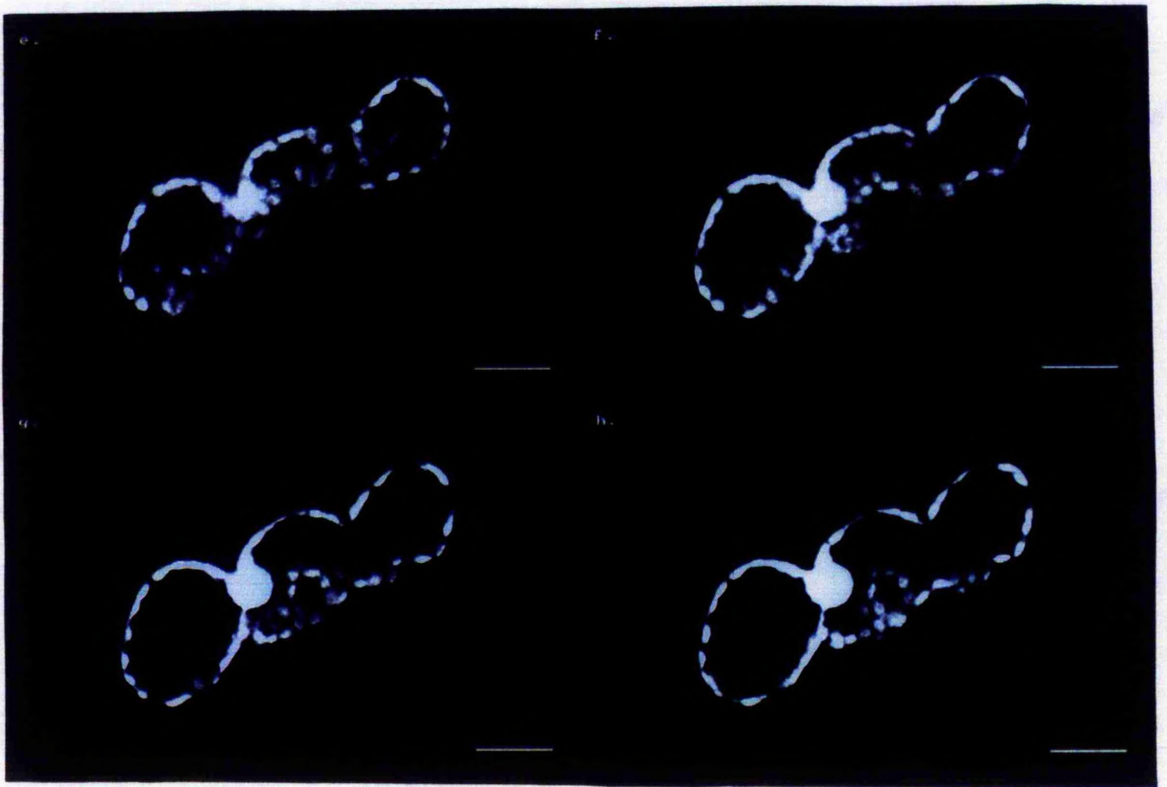
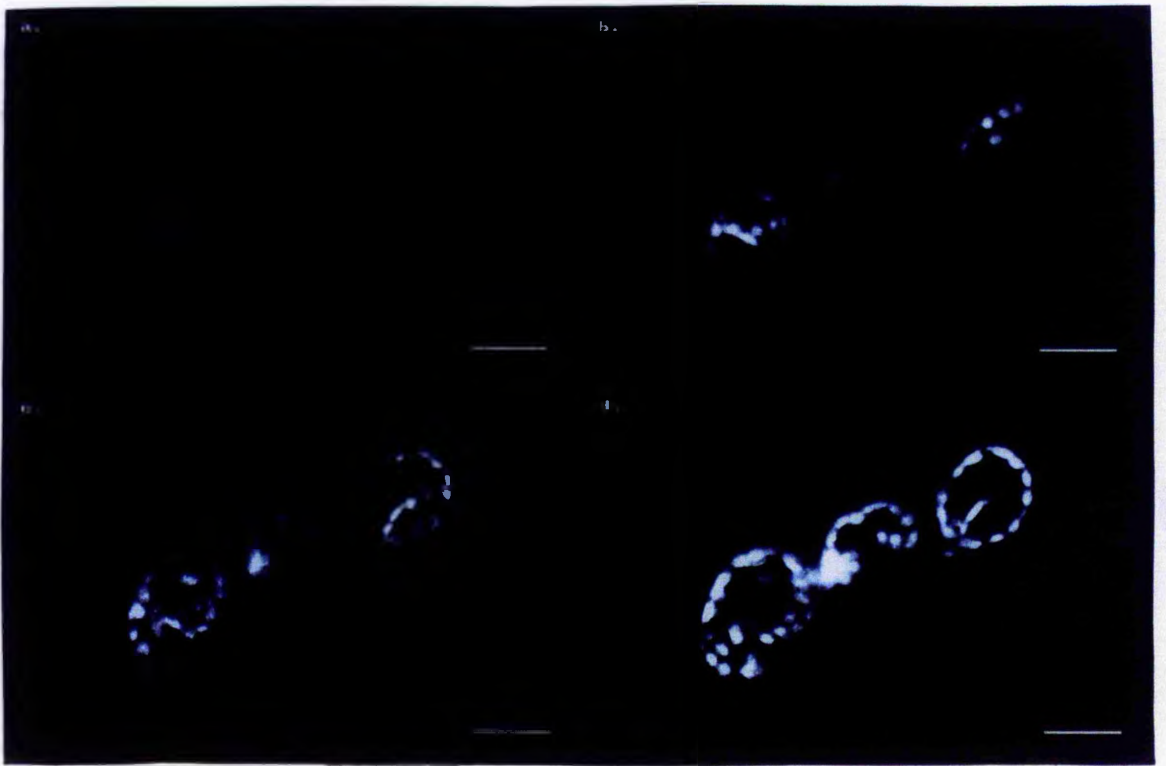
Fig. 5.11 Effect of UV-B radiation on the number of granal sacs per granum of mesophyll cell chloroplasts along the length of 7-d-old primary leaves, expressed on a (a) spatial and (b) temporal scale

Plants were grown under control (■) and UV-B (○) conditions (Section 2.2). Tissue was fixed, embedded, sectioned and stained (Section 2.6) and the number of granal sacs per granum calculated from random TEM micrographs (e.g. Plate 5.4i,ii a-f) as described in Section 2.8. Each data point represents the mean of 5 independent growth studies, sampling 5 seedlings per replicate, from which a total of 20 micrographs were taken from 20 random blocks. Error bars show \pm one standard error of the mean.

Plate 5.5 (i,ii) Confocal Microscopy Z Series Through a Mesophyll Cell

Tissue from 7-d-old primary leaves grown under control conditions (Section 2.2) was fixed and processed for confocal microscopy (Section 2.9). Images a - p represent a Z series of optical sections taken at 2 μ m interval through a mesophyll cell (Section 2.9.3), taken 40mm above the leaf base, equivalent to a cell age of 50 Hrs.

Bars = 20 μ m



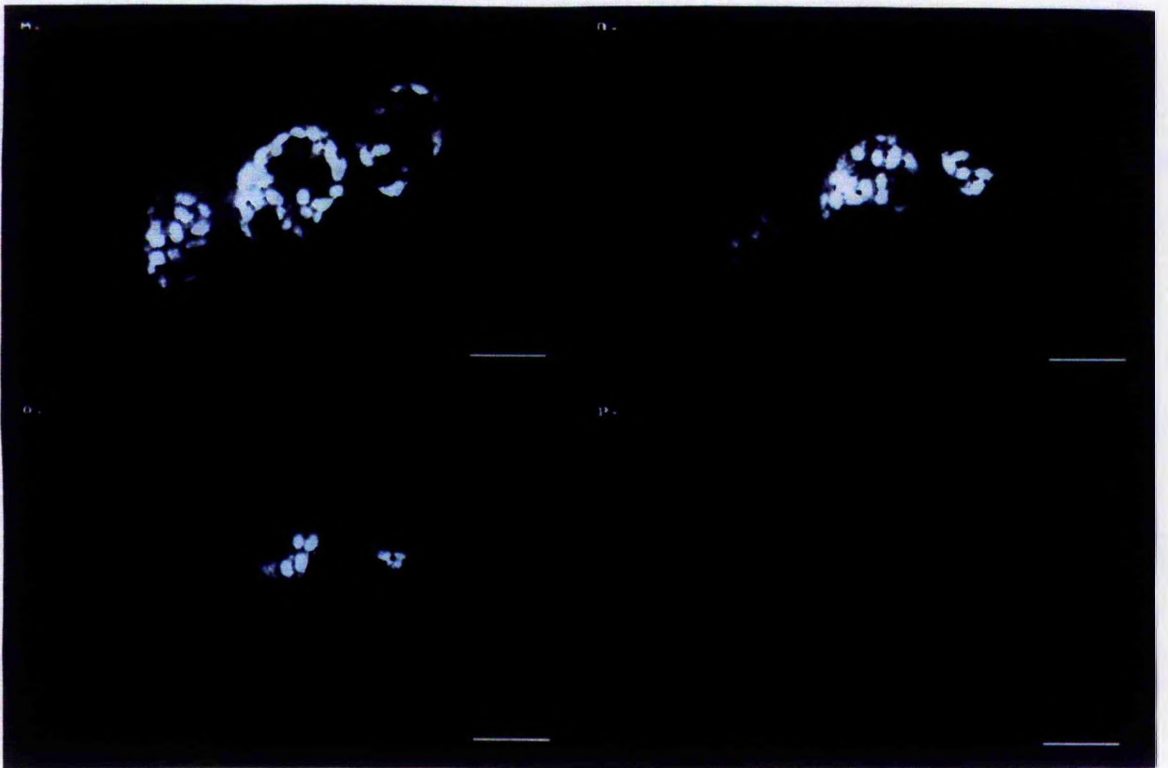
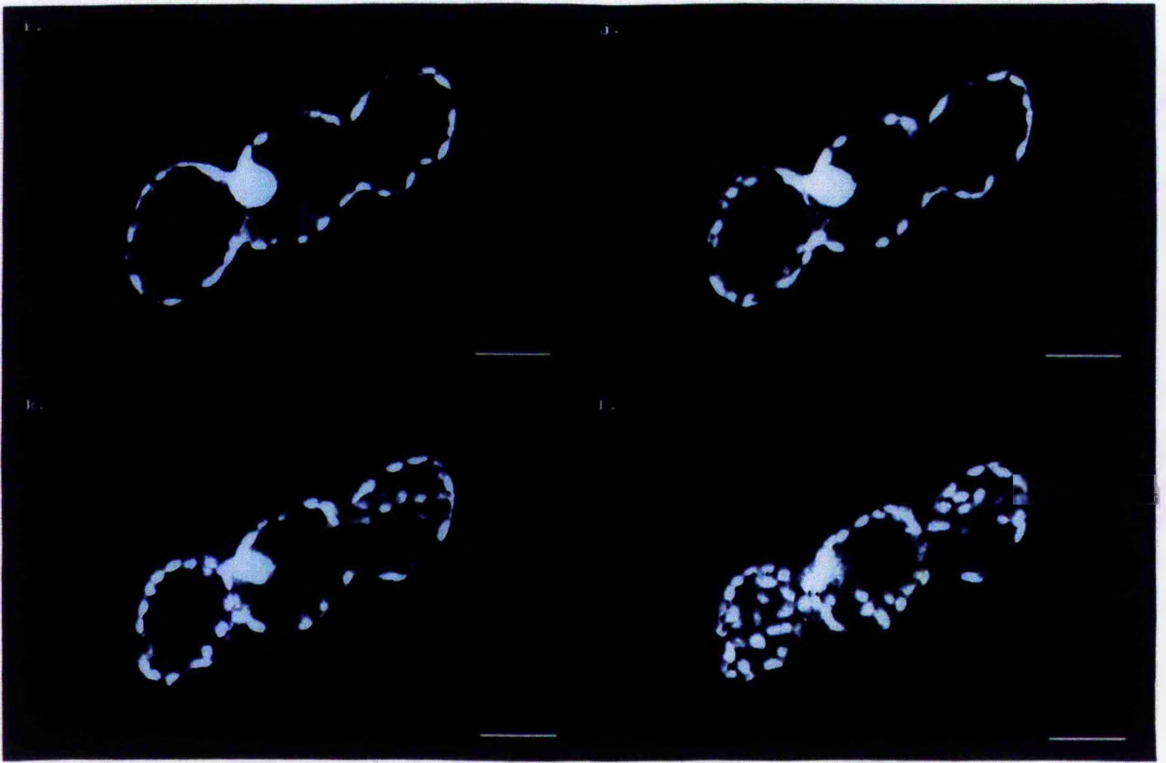
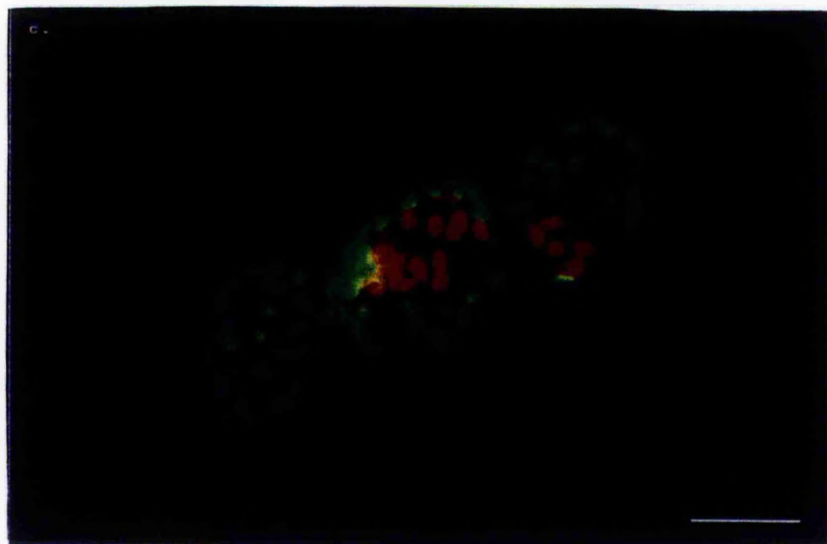
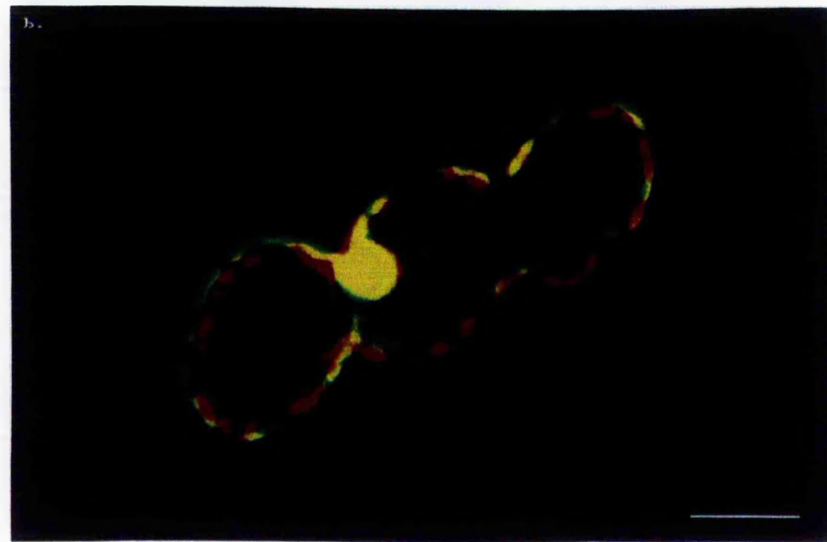


Plate 5.6 Merged Confocal Images From a Z series Through a Mesophyll Cell

Images a -c are representative merged images (N.B. false colour) taken from a confocal Z series (see Plate 5.5i,ii) through a mesophyll cell (Section 2.9.3). The average chloroplast number per mesophyll cell was estimated from 3 representative merged images per cell.

Bars = 20 μ m



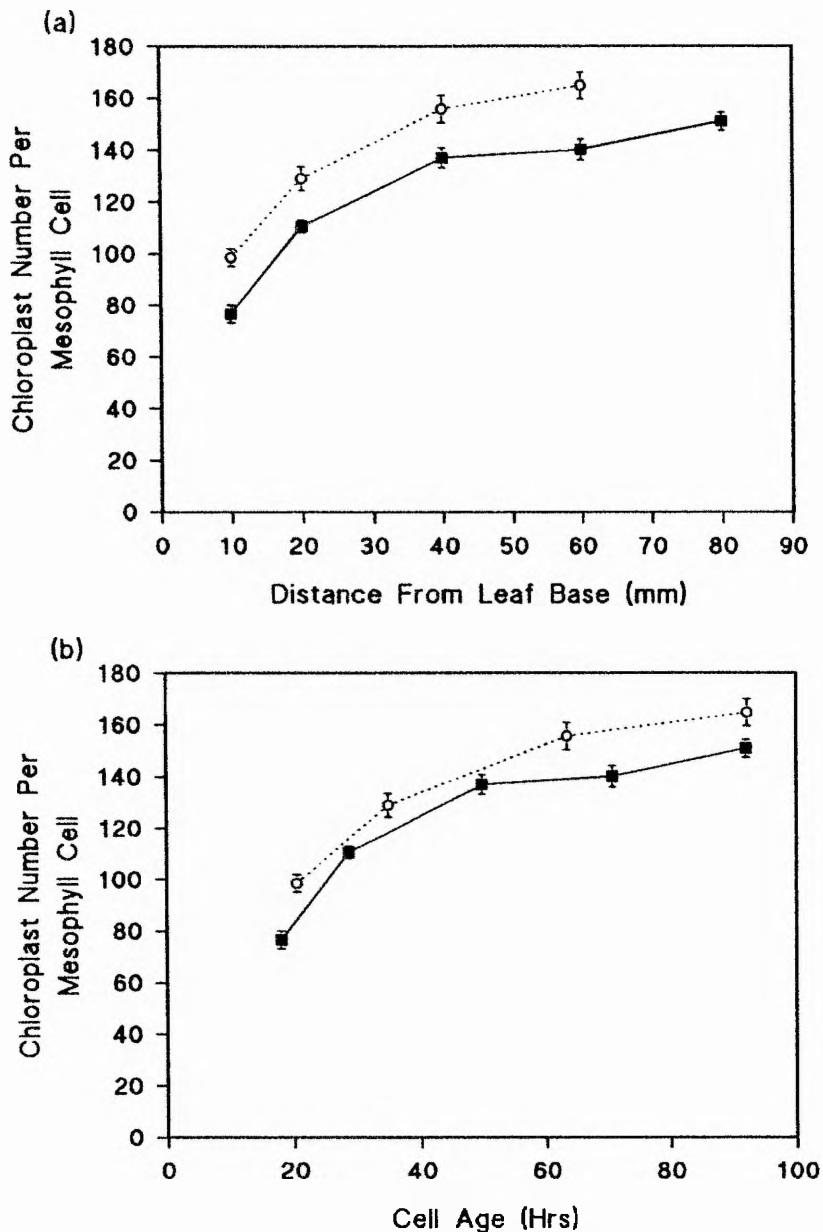


Fig. 5.12 Effect of UV-B radiation on chloroplast number per mesophyll cell along the length of 7-d-old primary leaves, expressed on a (a) spatial and (b) temporal scale

Plants were grown under control (■) and UV-B (○) conditions (Section 2.2). Tissue was fixed and processed for confocal microscopy (Section 2.9), and the number of chloroplasts per mesophyll cell calculated from merged images (*e.g.* Plate 5.6 a-c) taken from a Z series through the cell (*e.g.* Plate 5.5i,ii a-p). Each data point represents the mean of 3 independent growth studies, sampling 5 seedlings per replicate, from which a total of 20 random mesophyll cells were counted. Error bars show \pm one standard error of the mean.

DISCUSSION

Changes in cell ultrastructure, *e.g.* internal membrane disruption, in response to UV-B have been reported in a limited number studies. In the majority of these studies the response was assessed qualitatively and changes in cell ultrastructure during normal development were not taken into account. The gradient of cell age and development in the wheat primary leaf (see Section 4.1.2.1) provides a model system in which changes in cell ultrastructure during development can be assessed. The purpose of this chapter was to quantify changes in mesophyll cell ultrastructure in response to UV-B, while taking into account the changes in ultrastructure that occur during normal leaf development.

5.8 Mesophyll Cell Development in the Wheat Primary Leaf

Before being able to assess the effect of UV-B on the ultrastructural development of mesophyll cells, changes in ultrastructure during normal leaf development must be characterised. In the wheat primary leaf the temporal and spatial separation of cell division (basal 5mm) and elongation (basal 15mm), produces a gradient of mesophyll cell age and development (see Section 4.7) within which there are progressive changes in the structure and size of organelles. Stereological analysis (see Section 5.2) has been used to estimate organelle volumes within the developing mesophyll cell. The results in this chapter show that the vacuole occupies a V_V of 70% of the mesophyll cell throughout development, and therefore changes in the proportion of cell occupied by the chloroplasts and mitochondria were measured indirectly as a volume fraction of the cytoplasm.

The results of this study show that the chloroplast occupies an increasing proportion of the mesophyll cell during development. In meristematic mesophyll cells, the chloroplast V_V of the cytoplasm was *c.* 25%, increasing up to *c.* 75%, 40mm above the leaf base (*c.* 50 hours). This is similar to the chloroplast V_V found by Tobin *et al.*, (1985) in the developing wheat primary leaf (*T. aestivum* L. cv Maris Huntsman, as used in the present study), and by Winter, *et al.*, (1993) in mature mesophyll cells of the primary leaf of *H. vulgare*. This initial result suggests that the stereological techniques adopted in the present study produce data comparable to that of previous stereological work. The increased size of the chloroplast compartment during mesophyll cell development is due to an increase in both chloroplast size and number per cell (Boffey *et al.*, 1979; Leech, 1984; Tobin *et al.*, 1985). In the present study it was found that the number of chloroplasts per cell increased to a constant value of *c.* 150, 40mm above the leaf base (*c.* 50 hours), indicating chloroplast division to be occurring within this region of the leaf blade. This number of chloroplasts is comparable to that found by Boffey *et al.*, (1979), and Tobin *et al.*, (1985), in the mature mesophyll cells of the wheat primary leaf, *T. aestivum* L. cv. Maris Dove and cv. Maris Huntsman respectively. The TA of the chloroplast increases throughout the length of the primary leaf blade, *i.e.* during and after chloroplast division, from *c.* $1.6\mu\text{m}^2$ in the meristematic mesophyll cells, to *c.* $15\mu\text{m}^2$, 40mm from the leaf base (*c.* 50 hours). Similar increases in chloroplast size during development have been found by Ellis *et al.*, (1983) in the 7-d-old primary leaf of *T. aestivum* L. cv Maris Dove.

During chloroplast development the internal membrane system is structurally differentiated into grana stacks and stromal thylakoids. The work described in this chapter shows that the V_V of chloroplast occupied by thylakoids increases during

development from *c.* 20% , 10mm from the leaf base (*c.* 20 hours), to *c.* 30% at the leaf tip. This is the result of an increase in the V_V of both granal and stromal thylakoids during development. The granal thylakoids form granal sacs that stack together in increasing numbers to form grana. The number of sacs per granum increased at a linear rate throughout the leaf blade, to give an average of 8 sacs per granum in mature chloroplasts. A similar pattern of increased granal thylakoids per chloroplast and number of sacs per granum was found by Baker and Leech (1977) in the developing *Z.mays* primary leaf.

Changes in the chloroplast population of mesophyll cells during leaf development are accompanied by the acquisition of photosynthetic competence. The photosynthetic capacity of mesophyll cells, for example, has been shown to increase during leaf development in a number of species, including *H.vulgare* (Dale, 1972), *T.aestivum* (Tobin *et al.*, 1988), and *Prunus persica* (peach; Merlo *et al.*, 1993). This increase in photosynthesis can be related to changes in chloroplast structure. Granal stacking, for example, may increase the efficiency of light capture by increasing the density of light harvesting units (Anderson, Goodchild & Boardman, 1973). This relationship between ultrastructure and biochemistry highlights the importance of studying cellular ultrastructure. The changes found in this chapter can be related to the effects of UV-B on photosynthesis as discussed in Chapter 6.

The work described in this chapter also shows changes in the composition of mitochondrial populations in mesophyll cells during development. The TA of mitochondria increased within the basal 5mm of the leaf blade (*c.* 0-10 hours), and then decreased over the next 10mm to the original TA found in the leaf base. This distribution indicates that mitochondrial division is occurring between 5 and 15mm above

the leaf base (c. 10 - 20 hours), and corresponds to the increase in mitochondrial numbers in the basal 15mm of the wheat primary leaf (*T.aestivum* L. cv Maris Huntsman) found by Rogers, Thorpe and Tobin (unpublished)(Tobin & Rogers, 1992). Within this basal 15mm of the leaf blade the mitochondrial V_V is reduced, and is probably the result of the increased chloroplast V_V in this region. The TA of the mitochondria then increases at a linear rate towards the leaf tip, although the mitochondrial V_V remains constant. In order for larger mitochondria to occupy the same space, mitochondrial number per cell must be reduced. In a similar study on wheat primary leaf development, Rogers, Thorpe and Tobin (unpublished) found that a reduction in mitochondrial number during development was accompanied by a constant mitochondrial V_V , and suggested that mitochondrial fusion or autolysis was occurring. No direct evidence for the occurrence of either of these events is available in higher plants, although in an analogous study on the development of mitochondria in the flight muscle of ageing blowflies (Tribe & Ashurst, 1972), it was suggested that fusion of the mitochondria was occurring as they became compressed between tightly packed muscle fibres. A similar process may occur in mesophyll cells as the chloroplast compartment constrains the mitochondria in mature mesophyll cells and warrants further investigation.

Changes in mitochondrial populations have been shown to be related to the respiratory activity of the tissue (Simon & Chapman, 1961; Solomos *et al.*, 1972). The respiratory capacity has been shown to decrease during leaf development in a number of species including, *P.sativum* (Smillie, 1962; Geronimo & Beevers, 1964), *P.vulgaris* (Azcon-Bieto *et al.*, 1983) and *T.aestivum* (Tobin *et al.*, 1988). This reduction in respiratory activity could be related to changes in mitochondrial structure. In a study on *P.sativum* leaf development, for example, Geronimo & Beevers (1964) correlated a

reduction in respiration of older leaves with a reduction in the number of cristae per mitochondrion. As with the data relating changes in chloroplast populations with photosynthetic capacity, these studies showing a relationship between mitochondrial populations and respiratory capacity highlight the importance of studying cell ultrastructure. The changes found in this chapter can be related to the effects of UV-B on respiration as discussed in Chapter 6.

5.9 Changes in Mesophyll Cell Development Under UV-B

Despite the close relationship between cell ultrastructure and function, *e.g.* chloroplast development and photosynthetic capacity, there have only been a limited number of studies investigating the response of cellular ultrastructure to UV-B. In all of these studies, plants were grown under control conditions before being exposed to UV-B. The resulting response was dramatic, with the disruption of a number of organelles including the chloroplast, mitochondria, endoplasmic reticulum and nucleus.

The effects of UV-B on chloroplast ultrastructure reported in *P.sativum* (Brandle *et al.*, 1977; He *et al.*, 1994) and *Beta vulgaris* (sugarbeet; Bornman *et al.*, 1983, 1986) are cumulative, with increased damage occurring with increased exposure (time) to UV-B. The first sign of chloroplast damage is the dilation of thylakoid membranes, which may occur as rapidly as within 15 minutes of exposure to UV-B (Brandle *et al.*, 1977). This is followed by the disorientation of granal and stromal thylakoids, an accumulation of starch, and finally the disruption of the chloroplast envelope. UV-B induced structural changes of the chloroplast have been found to coincide with a reduction in PSII activity (Brandle *et al.*, 1977), and may be a contributing factor in reducing photosynthetic rates, a common response in UV-B grown plants (see Chapter 6).

Changes in mitochondrial structure in response to UV-B have been found in *Z.mays* (Santos *et al.*, 1992) and *P.sativum* (Brandle *et al.*, 1977). The effects of UV-B on mitochondria are similar to those found in chloroplasts, *i.e.* membrane disruption, with the mitochondria possessing fewer cristae. The various proteins involved in electron transport and oxidative phosphorylation are located on this inner membrane, and therefore changes in mitochondrial structure in response to UV-B may alter the respiratory capacity of the cell.

To date, the work described in this chapter is the only known study in which plants were exposed to UV-B (during the light period) throughout their development and the changes in ultrastructure then assessed. In comparison with the other studies, the results of this chapter show that the structural integrity of mesophyll cell organelles was maintained in UV-B-grown plants. Mature chloroplasts had a defined double membrane and well developed granal and stromal thylakoids, generally orientated parallel to the long axis of the chloroplast (Plate 5.4), and the mitochondria had a defined double membrane, and well developed cristae (Plate 5.2). A possible explanation for the different qualitative response in organelle ultrastructure found after continuous development under UV-B, compared to tissue grown under control conditions prior to UV-B exposure, is in the altered growth pattern of plants grown under UV-B. The work described in Chapter 3 shows that UV-B-grown plants had a reduced growth rate and a thicker leaf blade, both of which may play a role in protecting mesophyll cell organelles from UV-B damage. Increased leaf thickness has been suggested to be a possible protective mechanism by reducing light penetration into the leaf (Flint *et al.*, 1985), and Ballaré *et al.*, (1995b) found that a delay of a few hours in the emergence of *L.esculentum* seedlings was sufficient to allow the synthesis of flavonoids that

increase the screening capacity of the tissue (see Section 1.6.1).

Although on a qualitative basis there appears to be no gross change in cell ultrastructure in response to UV-B, quantitative changes in mesophyll cell ultrastructure in UV-B-grown plants were found. UV-B had no effect on either the TA of mesophyll cells, or the vacuole V_V , and therefore a direct comparison of the chloroplast V_V and mitochondrial V_V could be made between control and UV-B-grown plants. Differences in both the chloroplast and mitochondrial populations of developing mesophyll cells were found in UV-B-grown plants. Such changes, including a reduction in both chloroplast and mitochondrial TA, and an increase in chloroplast number per mesophyll cell, are direct UV-B responses, *i.e.* changes observed when data are expressed on a temporal basis, taking into account the UV-B induced reduction in growth (see Section 4.7).

The overall effect of UV-B on chloroplasts, was the production of more, smaller chloroplasts per cell, compared to control-grown plants. The reduction in chloroplast size and an increase in number during development indicates that UV-B is affecting both chloroplast division and expansion. All chloroplasts are derived from proplastids in the leaf meristem, the division of which keep pace with cell division to maintain the number of proplastids per cell (see Section 5.1.1.2). This is followed by chloroplast division in post-mitotic expanding cells, that increases the number of chloroplasts per cell (Possingham, 1980). A significant increase in the chloroplastic V_V within the basal 5mm of the leaf blade (*c.* 0 - 10 hours) suggests that UV-B may be having a direct effect on either proplastid and/or chloroplast division, resulting in the increased number of chloroplasts per mesophyll cell. Alterations in chloroplast numbers per cell, may also be an indirect effect, resulting from the UV-B induced change in mesophyll cell division

(see Section 4.4). During normal chloroplast development, proplastid division keeps pace with cell division to maintain a constant number of proplastids per cell. The cell cycle time of UV-B-grown plants was increased (see Section 4.4.2), and therefore even if proplastid/chloroplast division rate is unaltered by UV-B, this may result in a net increase in the number of chloroplasts per cell. It is interesting to note that the number of chloroplasts per cell is significantly increased in UV-B-grown plants, in cells *c.* 19 hours and older (10mm+ above the leaf base), a region of the leaf blade which is surrounded by the coleoptile and therefore not directly exposed to UV-B.

The results of this study also show that UV-B reduced the TA of chloroplasts in cells *c.* 50 hours and older, *i.e.* above the chloroplast division zone (0-40 hours), indicating a possible UV-B induced reduction in chloroplast expansion. Although chloroplast expansion is not fully understood, it is thought that chloroplasts expand to fill a predetermined area of the cell, and that changes in chloroplast numbers result in altered chloroplast expansion. For example, the work of Pyke & Leech (1991, 1992, 1994) found that in *A.thaliana* mutants with different chloroplast numbers, an increase in chloroplast number was accompanied by a reduction in chloroplast size, as each chloroplast had a reduced space available to expand into. The reduction in chloroplast TA found in UV-B-grown plants, may therefore be due to an indirect response of chloroplast expansion to UV-B, resulting from the UV-B induced increase in chloroplast number. In *T.aestivum* the correlation between chloroplast 'cover' and cell size has been shown to be much tighter than the correlation between chloroplast number and cell size (Leech & Pyke, 1988). In this study mesophyll cell size is similar in both control and UV-B grown plants, and therefore the proportion of cell area covered by chloroplast area may be similar for fewer, larger chloroplasts (control) as for more, smaller chloroplasts

(UV-B). The photosynthetic capacity of a leaf may be influenced by the morphology and number of the chloroplasts per cell, therefore any change, such as more, smaller chloroplasts per mesophyll cell, as observed in UV-B-grown plants, may alter photosynthesis, and is discussed in detail in Chapter 6.

Another factor that may influence the overall photosynthetic capacity of a leaf, is the photosynthetic competence of chloroplasts which is dependent upon the specialized organisation of the internal thylakoid membranes. Developing, unstacked thylakoids contain the core PSII and PSI complexes, cytochrome b/f complex, and ATP synthetase. As the thylakoids develop in the light there is a step-wise assembly of the functional complexes, including the interaction of chl a/b proteins of LHCII and LHCI with the PSII and PSII complexes, followed by the lateral rearrangement of thylakoid intrinsic protein complexes and concomitant membrane appression. In mature chloroplasts PSII-LHCII assemblies occur mainly in grana stacks, PSI-LHCI complexes on stromal thylakoids (Anderson, 1986). In this study, the V_V of the chloroplast occupied by granal thylakoids, and the number of granal sacs per granum was higher along the length of the leaf blade of UV-B-grown plants when expressed on a spatial scale, as compared to control-grown plants. These differences however, were lost when the data are expressed on a temporal scale, indicating that the changes observed in chloroplast ultrastructure of UV-B-grown plants, are a result of the altered growth of the primary leaf under UV-B, rather than a direct effect of UV-B.

The results of this study also shows UV-B to have a direct effect on developmental changes of the mitochondrial population in mesophyll cells. The distribution of mitochondrial TA along the length of the leaf blade (see Section 5.6.2.4), suggests that UV-B increased the region of mitochondrial division (cells aged *c.* 10 - 30

hours), as compared to control-grown plants (cells aged *c.* 10 - 25 hours). This increase in the 'mitochondrial division zone' of UV-B-grown plants results in the delayed onset of mitochondrial expansion and a reduction in the final maximum mitochondrion TA. Despite the reduction in mitochondrion TA, the V_v of cytoplasm occupied by the mitochondria of UV-B-grown plants, is similar to the V_v occupied by the larger mitochondria found in control-grown plants. This suggests that there are more, smaller mitochondria in UV-B-grown plants, which may possibly be the result of an increase in the rate of mitochondrial division, or a reduction in the rate of mitochondrial fusion. It is well established that plant tissue with high respiratory rates, *e.g.* *Arum* spadix, have a high mitochondrial number per cell. This correlation between mitochondrial numbers and respiratory rates, means that the observed changes in the mitochondrial population of UV-B-grown plants, which suggests a possible alteration in mitochondrial numbers, may effect the respiratory capacity of the primary leaf, and is discussed in detail in Chapter 6.

5.10 Summary

The work described in this chapter shows that although in contrast to previous studies (*e.g.* Brandle *et al.*, 1977; Bornman *et al.*, 1983,1986; Santos *et al.*, 1992; He *et al.*, 1994) no gross changes were observed in cell ultrastructure in response to UV-B, there were quantitative changes in both the chloroplast and mitochondrial populations. These quantitative changes, including a reduction in chloroplast and mitochondrion TA and an increase in chloroplast number per cell, are direct UV-B responses found when data are expressed on a cell age basis, taking into account the altered developmental gradient of UV-B-grown plants. The overall effect of UV-B on the chloroplast

population, was the production of more, smaller chloroplasts per mesophyll cell. The maximum number of chloroplasts per cell occurred later in UV-B-grown plants, but reached a maximum, smaller TA earlier than in control-grown plants, indicating that UV-B was prolonging/increasing chloroplast division, which resulted in a reduction in chloroplast expansion. The changing pattern of mitochondrial TA along the leaf blade suggests that mitochondrial division occurs for longer in UV-B-grown plants, and that the reduction in mitochondrion TA is the result of a delay in the onset of mitochondrial expansion. Although the TA of mitochondria is reduced under UV-B, the V_V of cytoplasm occupied is similar to that found in control-grown plants with larger mitochondria. This suggests there are more, smaller mitochondria per cell in UV-B-grown plants, which may be the result of a prolonged period of mitochondrial division, followed by a reduced period of mitochondrial expansion.

As the structure of a cell is intimately related to its function, the changes observed in the mesophyll cell ultrastructure of UV-B-grown plants may affect the metabolic activity of the cell. The aim of the following chapter is to determine what are the physiological consequences of these changes in ultrastructure.

CHAPTER 6

Effects of UV-B Radiation on the Metabolism of the Developing Primary Leaf of Wheat

INTRODUCTION

As a leaf develops a transition from heterotrophy to autotrophy occurs as a result of changes at the physiological, anatomical and metabolic levels (Merlo *et al.*, 1993)(as discussed in Chapter 5). The previous chapter described the changes in mesophyll cell ultrastructure of the primary leaf of wheat associated with this transition, and showed that the ultrastructural development of mesophyll cells was altered in UV-B-grown plants. Changes in cell ultrastructure during normal leaf development can be related to changes in metabolism. An increase in chloroplast size and number (Boffey *et al.*, 1979; Ellis *et al.*, 1983), and an increase in thylakoid stacking (Baker & Leech, 1977) during development, for example, can be correlated to an increase in photosynthetic capacity, although only a limited number of studies have directly linked ultrastructural changes to metabolism. The change in cell ultrastructure in response to UV-B, observed in the previous chapter, *e.g.* more, smaller chloroplasts per mesophyll cell (see Section 5.9), may therefore result in altered metabolism, *e.g.* reduced photosynthetic capacity.

The effects of UV-B radiation on metabolism, particularly carbon metabolism (*e.g.* photosynthesis), in mature leaf tissue is well documented (Reviews: Teramura, 1983; Bornman, 1989; Bornman & Sundby-Emanuelsson, 1995) (see Section 1.6.2). No studies, however, have investigated the effects of UV-B on the development of metabolism. The purpose of this chapter is firstly to investigate the effects of UV-B on the metabolic development of the primary leaf of wheat, and secondly, to relate any metabolic changes found in response to UV-B, to the UV-B induced changes in cell ultrastructure observed in the previous chapter. This introduction will give a brief outline of the major changes in metabolism, and the interaction between the different metabolic

pathways during normal leaf development.

6.1 Changes In Metabolism during Leaf Development

6.1.1 Photosynthesis

The rate of photosynthesis increases during leaf development. This is supported by measurements of light - and CO₂ - dependent - O₂ - evolution in the primary leaf of wheat (*T. aestivum* L. cv Maris Huntsman)(Tobin *et al.*, 1988), and the second leaf of *Z.mays* (Baker & Leech, 1977; Miranda, Baker & Long, 1981), which increases with development from the base to the tip of the leaf blade. Similarly, in the primary leaf of *H.vulgare*, the rate of ¹⁴CO₂ uptake in the light (per unit leaf area) is lowest within the basal region of the leaf and increases with development towards the leaf tip (Dale, 1972).

The change in photosynthetic capacity during development can be related to several factors, including changes in mesophyll cell ultrastructure, *e.g.* an increase in the size and number of chloroplasts per mesophyll cell (Boffey *et al.*, 1979; Tobin *et al.*, 1985)(see Chapter 5), and changes in the activity of Calvin cycle enzymes, *e.g.* Rubisco (Dean & Leech, 1982b). In the primary leaf of *H.vulgare* the concentration of Rubisco (per g. fresh weight) increases six-fold from the base to the tip of the leaf blade (Viro & Kloppstech, 1980). A similar pattern in the concentration of Rubisco in the primary wheat leaf (*T.aestivum* L. cv Maris Dove) was shown by Dean & Leech (1982b), in which the concentration of Rubisco per cell increased twenty-fold during leaf development. The expression of both the *rbc* L and *rbc* S transcripts, encoding the large (chloroplast encoded) and small (nuclear encoded) subunits of Rubisco, can also be correlated to the development of photosynthesis, with the expression of both transcripts

increasing from the base to the tip of the primary wheat leaf (*T.aestivum* L. cv Maris Dove) (Topping & Leaver, 1990).

6.1.2 Photorespiration

Photorespiration is the light-dependent release of CO₂ and uptake of O₂, that results from the oxygenase activity of Rubisco (Reviews: Keys *et al.*, 1978; Givan, Joy & Kleczkowski, 1988; Wallsgrave, Baron & Tobin, 1992).

The rate of photorespiration has been shown to increase during leaf development (Tobin *et al.*, 1988), and the activity of photorespiratory enzymes such as glycolate oxidase (peroxisomal), glycine decarboxylase (mitochondrial) and glutamine synthetase (chloroplastic isoform) increase in parallel with photosynthetic enzymes (Rogers *et al.*, 1991; Tobin *et al.*, 1985, 1988, 1989). A major determinant of the rate of photorespiration is the ratio of carboxylase to oxygenase activity of Rubisco (Gutteridge & Keys, 1985). There is no evidence to indicate that this ratio changes during development, and it has been suggested that the increase in photorespiration, which parallels the increase in photosynthesis, occurs as a result of an increase in the concentration of Rubisco (Tobin, 1992).

6.1.3 Respiration

The change in respiratory capacity with leaf development was first demonstrated by Kidd, West & Briggs (1921), in which they found the rates of 'dark' respiration in *Helianthus annuus* leaves to decrease with leaf age. This general decrease in respiratory rate during leaf growth has been found in a range of plants, including *P.sativum* (Smillie, 1962; Geronimo & Beever, 1964), *P.vulgaris* (Azcón-Bieto *et al.*, 1983) and *T.aestivum* L. cv. Maris Huntsman (Tobin *et al.*, 1988).

The altered respiratory capacity during development can be related to changes

in the activity of key respiratory enzymes. For example, in *Dianthus chinensis* leaves, the activity of enzymes of the oxidative pentose phosphate pathway (OPPP), e.g. glucose 6-phosphate dehydrogenase, and glycolysis, e.g. phosphofructokinase, are highest in the leaf primordia and decrease as the leaf develops (Croxdale, 1983; Croxdale & Outlaw, 1983). Alterations in the expression of specific mitochondrial genes encoding protein components of the respiratory chain also change during development. Topping & Leaver (1990) found that in the primary leaf of wheat (*T. aestivum* L. cv Maris Dove) the relative abundance of the genes encoding subunits I and II of the cytochrome-*c* oxidase (complex IV) and the α -subunit of the (F_1 - F_0) ATP-synthetase complex decrease 5 to 10-fold from the leaf base to 1cm above the leaf base, after which the abundance of each gene per cell remains constant. The abundance of the transcripts of these mitochondrial genes also decreases along the length of the leaf.

6.1.4 Amino Acid Metabolism

Amino acids are the structural units of proteins and are also a means of transporting nitrogen between different cells and organs. They are the precursors in the synthesis of a number of nitrogen-containing compounds, including chlorophyll and coenzyme A (Reviews: Mifflin & Lea, 1977; Bryan, 1990). Despite their importance, understanding of the biochemical pathways of amino acid metabolism is incomplete, and very little is known about changes during development (Sechley, Yamaya & Oaks, 1992).

The majority of the common amino acids are synthesised in the chloroplast (Mifflin & Lea, 1977; Emes & Tobin, 1993; Sechley *et al.*, 1992). The size and number of chloroplasts increases during leaf development (Boffey *et al.*, 1979; Ellis *et al.*, 1983), and therefore amino acid metabolism might be expected to increase in a similar way to

photosynthesis and photorespiration, which are influenced by changes in the chloroplast populations as discussed above.

Changes in the pool sizes of free amino acids during development have been found in the leaves of *Z.mays* (Chapman & Leech, 1977), and in *Cicer orientinum* (chickpea; Laurie & Stewart, 1993). Both studies report high concentrations of amino acids in younger leaf tissue, which decrease with tissue age. Laurie and Stewart (1993) found the high concentration of amino acids in the young leaves of *C.orientinum* to be due primarily to increased asparagine content, with the other amino acids remaining constant throughout development. In the study by Chapman and Leech (1977) the concentration of amino acids (mM) in both leaf tissue and chloroplasts of *Z.mays*, was highest in the leaf base and decreased towards the leaf tip. The decrease in concentration of amino acids in the chloroplasts was the result of an increase in chloroplast size during development, with the amount (mM) of amino acids per chloroplast remaining constant. Although measurements of free amino acid pool sizes give no indication of the flux of amino acids through the biosynthetic pathways, changes in pool sizes during development will reflect changes in the balance between synthesis, degradation and transport. Further analysis, e.g. using radiolabelled substrates, is required to determine changes in flux.

6.2 Interaction Between Different Metabolic Pathways During Leaf Development

Carbon and nitrogen metabolism are interdependent processes, neither of which can continue to operate to the detriment of the other (Huppe & Turpin, 1994). This metabolic integration results from the fact that both carbon and nitrogen metabolism, e.g. carbohydrate and amino acid biosynthesis, require energy (ATP), reductant (NADPH

and NADH), and carbon skeletons (Dennis & Turpin, 1990). The supply and demand of these will change during leaf development as metabolism changes from heterotrophic to autotrophic (Tobin, 1992).

In immature leaf cells energy, reductant and carbon skeletons are generated primarily by mitochondrial respiration, *i.e.* the reactions of the TCA cycle and the mitochondrial electron transport chain. As the leaf cells mature, the development of chloroplasts and of photosynthesis provides an additional source of ATP from photophosphorylation, and NADPH from the electron transport chain, while glycine oxidation of photorespiration provides a source of NADH and ATP (Dennis & Turpin, 1990). The role of the mitochondria, therefore, changes from bioenergetic; providing energy and reductant in immature cells, to biosynthetic in mature cells, providing carbon skeletons for the synthesis of amino acids (Douce, 1985).

6.3 Cell Ultrastructure and Metabolism

Despite the close association that exists between cell structure and function, as discussed in the previous chapter, few studies have related changes in metabolism during development directly to changes in cell ultrastructure.

It is well established that changes in chloroplast populations during development, *e.g.* an increase in chloroplast size (Ellis *et al.*, 1983) and number (Boffey *et al.*, 1979; Tobin *et al.*, 1985), and increased thylakoid stacking (Leech & Baker, 1983), can be correlated to an increase in photosynthetic capacity and efficiency during leaf development. Changes in mitochondrial populations, *e.g.* a reduction in the number of cristae per mitochondrion (Geronimo & Beevers, 1964), have been correlated to changes in respiratory capacity during leaf development. These studies highlight the fact that cell

structure is intimately related to its function, and therefore the changes observed in mesophyll cell ultrastructure of the primary leaf of wheat grown under UV-B (see Section 5.9), may result in changes in the metabolic development of the primary leaf grown under UV-B.

6.4 Chapter Aims

The aim of this chapter is to characterise changes in metabolism, particularly those pathways associated with the chloroplast, *i.e.* photosynthesis and amino acid synthesis, during mesophyll cell development, and to investigate the effects, if any, of UV-B on metabolic development. As metabolism changes during normal leaf development, the altered growth rate of UV-B-grown plants as compared to controls (see Section 3.4.2) must be taken into account, and therefore all data are expressed on a temporal (*i.e.* cell age), rather than a spatial (*i.e.* distance from the leaf base) scale (see Section 4.7). Any changes in metabolism during the development of control and UV-B-grown plants can then be related to the changes in ultrastructure of the primary wheat leaf reported in Chapter 5.

RESULTS

6.5 Effect of UV-B on The Chlorophyll Content of The Primary Leaf

The total chl concentration (per g.fresh weight) increased *c.* 11-fold along the length of both control and UV-B-grown primary leaves (Fig. 6.1 a,b). When the data are expressed on a spatial scale (*i.e.* distance from the leaf base) (Fig. 6.1a), UV-B significantly increased the total chl concentration from 20mm above the leaf base onwards. This difference, however, is lost when the data are expressed on a temporal scale (*i.e.* cell age) (Fig. 6.1b), which corrects for the different growth rates of control and UV-B-grown plants (as discussed in Chapter 4). The age-related increase in the total chl concentration is the result of an increase in both chl a (*c.* 9-fold increase)(Fig. 6.2a) and chl b (*c.* 10-fold increase)(Fig. 6.2b)(per g. fresh weight), and was similar in both control and UV-B-grown plants.

The chl concentration (per chloroplast) also increased with cell age along the length of the leaf. The concentration of both chl a and chl b (per chloroplast) was slightly lower in cells aged *c.* 40 hours and more, in UV-B-grown plants as compared to controls (Fig. 6.2c,d). The low chl concentration (per g.fresh weight) at the leaf base (*c.* 0-10Hrs) means that small differences in the amounts of chl a and chl b in control plants compared to UV-B-grown plants are amplified as a difference in the chl a:b ratio. In control-grown plants the chl a:b ratio in the youngest cells at the leaf base (*c.* 0-10 hours) was slightly higher (*c.* 3.6), but not significantly different than the ratio in UV-B grown plants (*c.* 2.8). In cells aged *c.* 20 hours and more, a constant chl a:b ratio of *c.* 3.0 was maintained in both control and UV-B grown plants (Fig. 6.3)

6.6 Effect of UV-B on Photosynthesis in the Primary Leaf

6.6.1 Photosynthetic Rate

The rate of photosynthesis (CO_2 - dependent O_2 evolution per leaf area) increases linearly with cell age along the length of the leaf, and is similar in both control and UV-B-grown plants. The linear increase in photosynthetic rate is related to the light level (PPFD) under which the plants were grown, with an increase between cells aged *c.* 10-100 hours of *c.* 5-fold at a PPFD of $79\mu\text{mole m}^{-2} \text{s}^{-1}$, rising to a maximum *c.* 40-fold increase, at a PPFD of $915\mu\text{mole quanta m}^{-2} \text{s}^{-1}$ (Fig. 6.7a,b,c). At a PPFD of $915\mu\text{mole m}^{-2} \text{s}^{-1}$, the rate of photosynthesis between cells aged *c.* 10-100 hours, increased *c.* 600-fold per mesophyll cell and *c.* 400-fold per chloroplast, in both control and UV-B-grown plants (Fig. 6.8a,b). There is, however, a slight decrease in the rate of photosynthesis per chloroplast between cells aged *c.* 40-80 hours in UV-B-grown plants (Fig. 6.8b).

6.6.2 Photosynthetic Efficiency

The relative quantum yield (QY), *i.e.* the maximum photosynthetic efficiency, was calculated by regression analysis of the initial slope (PPFD = 0 - $150\mu\text{mole .m}^{-2} \text{s}^{-1}$) of the light response curve (Fig. 6.4a, 6.5a), as described by Walker, (1988). The QY increases with cell age along the length of the primary leaf (Fig. 6.6a,b). Both control and UV-B-grown plants show a similar increase in QY, doubling between cells aged *c.* 30-90 hours.

6.7 Effect of UV-B on Dark Respiration in the Primary Leaf

The rate of dark respiration (per leaf area) decreases with cell age along the length of the leaf (Fig. 6.9). In UV-B-grown plants, the rate of dark respiration is slightly higher in cells aged *c.* 40 hours and more, as compared to control-grown plants.

Large standard errors on all data points, however, mean that such differences are probably not significant, with an average decrease of *c.* 5-fold in the rate of dark respiration between cells aged *c.* 10-100 hours in both control and UV-B-grown plants.

6.8 Effect of UV-B on the Carbohydrate Content of the Primary Leaf

6.8.1 Total Soluble Carbohydrate

The distribution of total soluble carbohydrate (TSC)(per g^{-1} fwt) along the length of the primary leaf was similar in control and UV-B-grown plants (Fig. 6.10a). In both, a maximum TSC concentration of *c.* 11mg g^{-1} fwt, occurs within the elongation zone of the leaf (*c.* 0-20 hours). The TSC concentration then rapidly decreases to a minimum of *c.* 3mg g^{-1} fwt between cells aged *c.* 40-60 hours, before increasing to give a concentration of *c.* 8mg g^{-1} fwt at the leaf tip (*c.* 100 hours). When the data are expressed on a per mesophyll cell basis (see Section 4.5.1), there is an overall increase in the concentration of TSC between the base and tip of the leaf, in control and UV-B-grown plants (Fig. 6.10b). In both, the concentration of TSC per cell doubles from the leaf base to the end of the elongation zone (*c.* 20 hours). The TSC concentration per cell then decreases between cells aged *c.* 20-40 hours, to a level similar to that found in the basal region of the leaf, before increasing with cell age towards the leaf tip.

6.8.2 Total Insoluble Carbohydrate

The distribution of total insoluble carbohydrate (TIC)(per g^{-1} fwt) along the length of the primary leaf was similar in control and UV-B-grown plants (Fig. 6.11a). In both, the TIC concentration increased from *c.* $4\text{-}5\text{ mg g}^{-1}$ fwt in cells aged *c.* 10 hours, to a maximum concentration of *c.* $6\text{-}7\text{mg g}^{-1}$ fwt in cells aged *c.* 30 hours. The TIC concentration then decreased to a minimum of *c.* 4mg g^{-1} fwt in cells aged *c.* 70

hours and more. When the data are expressed on a per mesophyll cell basis (see Section 4.5.1), there is an overall increase in the concentration of TIC between the base and tip of the leaf, in control and UV-B-grown plants (Fig. 6.11b). In both, the concentration of TIC per cell increased rapidly in cells aged *c.* 10-30 hours, after which there is a slight decrease in the concentration of TIC per cell, with increasing cell age towards the leaf tip.

6.9 Effect of UV-B on the Soluble Protein Content of the Primary Leaf

The distribution of soluble protein (per g^{-1} fwt) along the length of the primary leaf was similar in control and UV-B-grown plants (Fig. 6.12a). In both, a maximum protein concentration of *c.* $80mg\ g^{-1}$ fwt, occurs in the youngest cells at the leaf base. The protein concentration then rapidly decreases to a minimum of *c.* $40mg\ g^{-1}$ fwt towards the end of the elongation zone (*c.* 20 hours), before increasing at a linear rate towards the leaf tip (*c.* 100 hours). The rate at which the protein concentration increases from the end of the elongation zone to the leaf tip (cells aged *c.* 20-100 hours), is greater in UV-B-grown plants compared to controls. In UV-B-grown plants a final protein concentration of *c.* $80mg\ g^{-1}$ fwt, occurs in cells aged *c.* 70 hours and more, as compared to control-grown plants in which a final protein concentration of *c.* $70mg\ g^{-1}$ fwt occurs in cells aged *c.* 100 hours. When the data are expressed on a per mesophyll cell basis (see Section 4.5.1), there is a linear increase in the concentration of soluble protein in control (*c.* 4-fold) and UV-B-grown plants (*c.* 5-fold) between the base and tip of the leaf (Fig. 6.12b). The increased protein concentration in cells aged *c.* 10-40 hours, is similar in control and UV-B-grown plants. In cells aged *c.* 40-100 hours, the protein concentration is greater in UV-B-grown plants as compared

to controls.

6.10 Effect of UV-B on the Free Amino Acid Pools of the Primary Leaf

6.10.1 Total Free Amino Acid Pool

The distribution in the concentration of the total free amino acid pool (TFAA)(per g⁻¹ fwt) along the length of the primary leaf was similar in control and UV-B-grown plants (Fig. 6.13a). In both, a maximum TFAA concentration occurs within the elongation zone of the leaf (c. 0-20 hours), and then rapidly decreases to a minimum in cells aged between c. 30-60 hours, before increasing with cell age towards the leaf tip. The TFAA concentration (per g⁻¹ fwt) is higher in cells of all ages (c. 0-100 hours) in UV-B-grown plants as compared to controls. When the data are expressed on a per mesophyll cell basis (see Section 4.5.1), there is a linear increase in the concentration of TFAA in control (c. 4-fold) and UV-B-grown plants (c. 5-fold) between the base and tip of the leaf (Fig. 6.13b). The increased TFAA concentration in cells aged c. 10-30 hours, is similar in control and UV-B-grown plants. In cells aged c. 30-100 hours, the TFAA concentration is greater in UV-B-grown plants as compared to controls.

6.10.2 Abundant Amino Acids Pools

The most abundant amino acids found in the primary leaf of both control and UV-B-grown plants were Gln, Glu, Asn, Asp, Gly and Ser. These six amino acids occur in a ratio of 30 Glu: 10 Gln: 15 Asp: 3 Asn: 1 Gly: 5 Ser, and account for c. 65% of the total free amino acid pool (Figs. 6.14a-6.19a). The cell age related distribution of Glu, Gly and Ser (per g.fresh weight)(Figs. 6.14b, 6.18b, 6.19b) is similar in control and UV-B-grown plants. In both, the concentration of these amino acid is high in the leaf base, decreasing towards the end of the elongation zone (c. 20 hours), before increasing

with cell age to the leaf tip. The concentrations of Ser and Glu are increased in UV-B-grown plants as compared to controls, with the increase in Ser occurring throughout the leaf blade, and the increase in Glu occurring in cells aged *c.* 20 hours and more. The cell age related distribution of Gln, Asp and Asn (per g^{-1} fwt)(Figs. 6.15b, 6.16b, 6.17b) is similar in control and UV-B-grown plants. In both, the concentration of these amino acid is highest in the leaf base, decreasing towards the end of the elongation zone (*c.* 20 hours) to a constant level. The concentrations of Gln and Asp are increased in UV-B-grown plants as compared to controls, with the increase in Gln occurring throughout the leaf blade, and the increase in Asp occurring in cells aged *c.* 20 hours and more.

6.10.3 Other Protein Amino Acid Pools

The age related changes in the concentration of the other 10 protein amino acid pools detected which constitute *c.* 35% of the TFAA pool (Table. 6.1), is summarised in Table 6.2. The concentration (per g^{-1} fwt) of these 10 protein amino acid pools, displayed one of two cell age related distributions along the length of the leaf. The concentration of the His and Met pools are highest in the leaf base, and decrease to a constant level from the end of the elongation zone (*c.* 20 hours). The concentration of the other 8 protein amino acid pools (see Table 6.2) was high in the basal region of the leaf, decreasing towards the end of the elongation zone (*c.* 20 hours), before increasing with cell age to the leaf tip. The concentrations (per g^{-1} fwt) of the Thr, Ala, Tyr and Val free pools are increased in UV-B-grown plants as compared to control, with the concentration of the other protein amino acid pools similar in both control and UV-B-grown plants.

6.11 Effect of UV-B on the Incorporation of ^{14}C Into the Abundant Amino Acid Pools

The incorporation of ^{14}C into each of the six most abundant amino acids, expressed as a percentage of the total label in the six amino acids, was determined as described in Section 2.15. After the initial 10 minutes of labelling, the majority of the ^{14}C (*c.* 40%) was incorporated into the Asp pool, and the amount of label remained constant throughout the 120 minutes cold-chase period (Fig. 6.20a). The initial amount of ^{14}C label in the Glu pool was *c.* 25%, increasing to a constant level of *c.* 35% after 30 minutes of the cold-chase period (Fig. 6.20b). The initial amount of ^{14}C incorporated into the Ser and Gly pool of control-grown tissue was *c.* 25% and *c.* 3% respectively (Fig. 6.21a,c). The ^{14}C label in both the Ser and Gly pools decreased rapidly within the first 30 minutes of the cold-chase period, to a constant level of *c.* 5% and *c.* 2.5% respectively. In UV-B-grown tissue, both the initial amount of ^{14}C label and the amount of ^{14}C present throughout the 120 minutes cold-chase period, in the Ser pool was higher than that found in the control. The initial amount of ^{14}C incorporated into the Asn and Gln pools of control-grown tissue was *c.* 3% and *c.* 5% respectively (Figs. 6.20c, 6.21b). The label in both of these pools remained relatively constant throughout the 120 minutes cold-chase period. The amount of ^{14}C label in the Gln pool of UV-B-grown tissue increased throughout the 120 minutes cold-chase period as compared to the control.

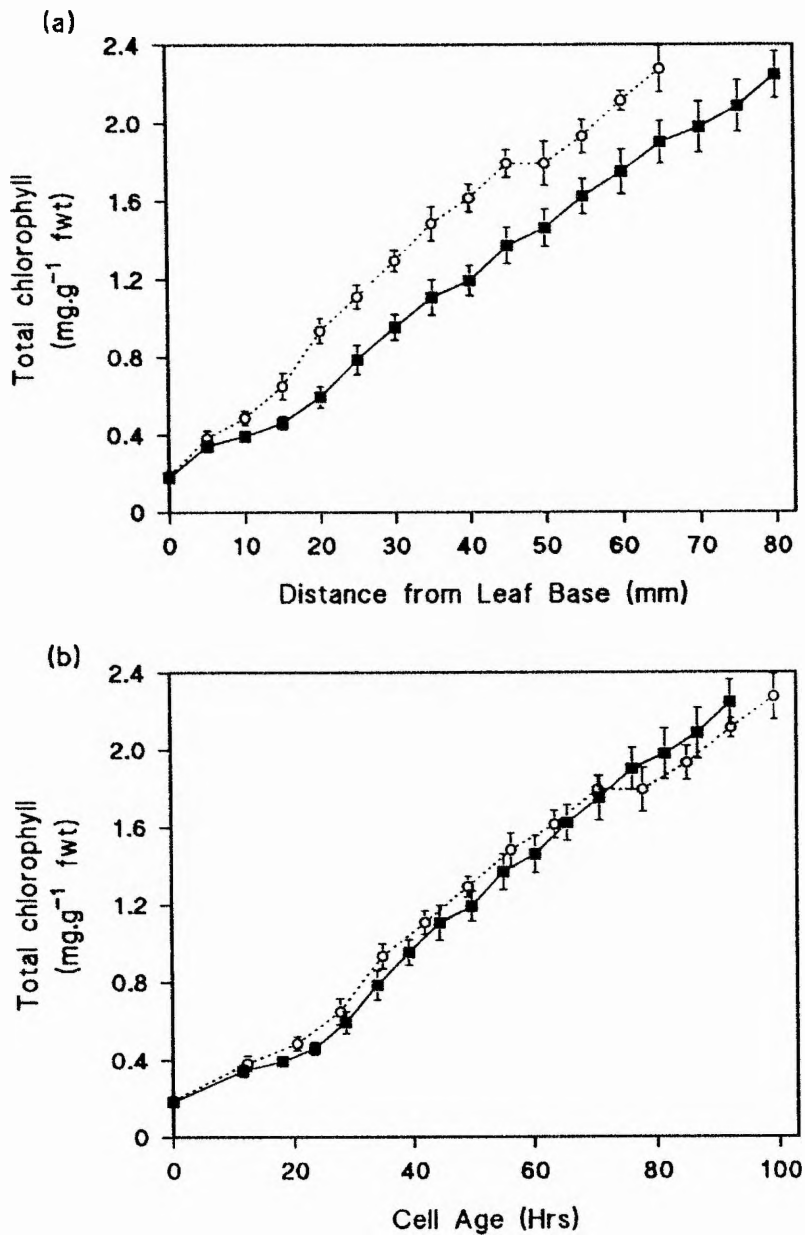


Fig. 6.1 Effect of UV-B radiation on the chlorophyll concentration along the length of 7-d-old primary leaves, expressed on a (a) spatial and (b) temporal scale

Plants were grown under control (■) and UV-B (○) conditions (Section 2.2). Chlorophyll was measured and calculated as described in Section 2.10. Each data point represents the mean of 5 independent growth studies, sampling 5 seedlings per replicate. Error bars show \pm one standard error of the mean.

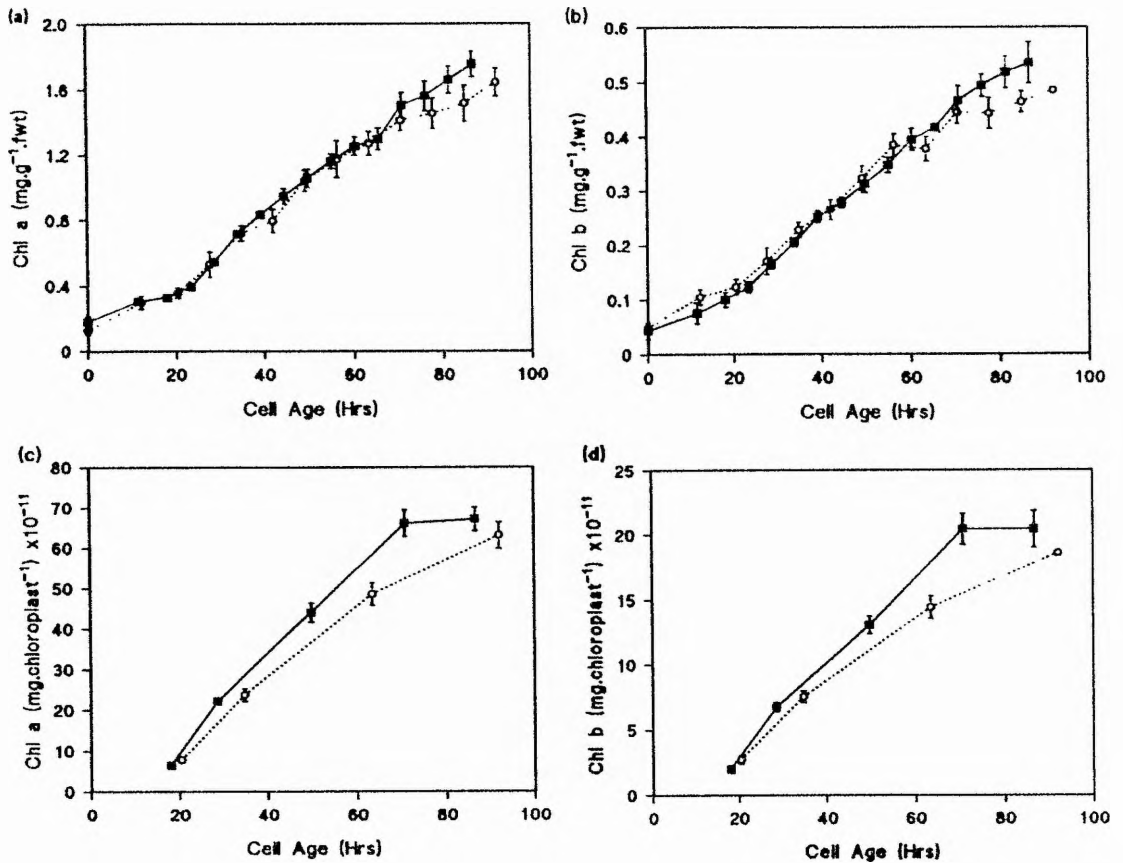


Fig. 6.2 Effect of UV-B radiation on the concentration of chlorophyll a and chlorophyll b, per g.fresh weight of tissue (a,b), and per chloroplast (c,d), in relation to cell age along the length of 7-d-old primary leaves

Plants were grown under control (■) and UV-B (○) conditions (Section 2.2). Chlorophyll a and b, were measured and calculated as described in Section 2.10. Each data point represents the mean of 5 independent growth studies, sampling 5 seedlings per replicate. Error bars show \pm one standard error of the mean.

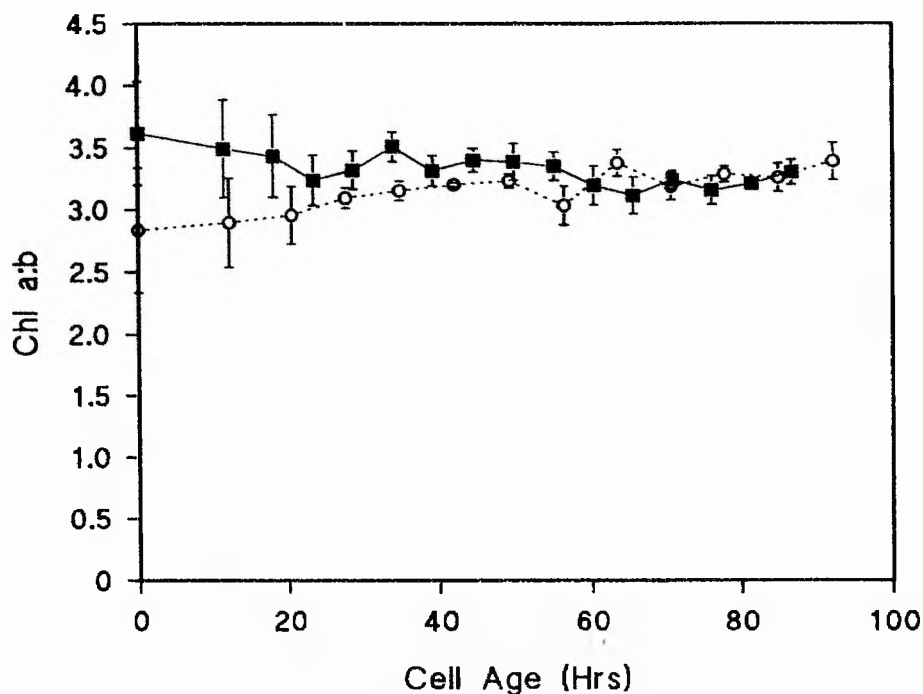


Fig. 6.3 Effect of UV-B radiation on the ratio of chlorophyll a:b, in relation to cell age along the length of the 7-d-old primary leaf

Plants were grown under control (■) and UV-B (○) conditions (Section 2.2). The chlorophyll a:b ratio was calculated from the chlorophyll a and b data, as described in Section 2.10. Each data point represents the mean of 5 independent growth studies, sampling 5 seedlings per replicate. Error bars show \pm one standard error of the mean.

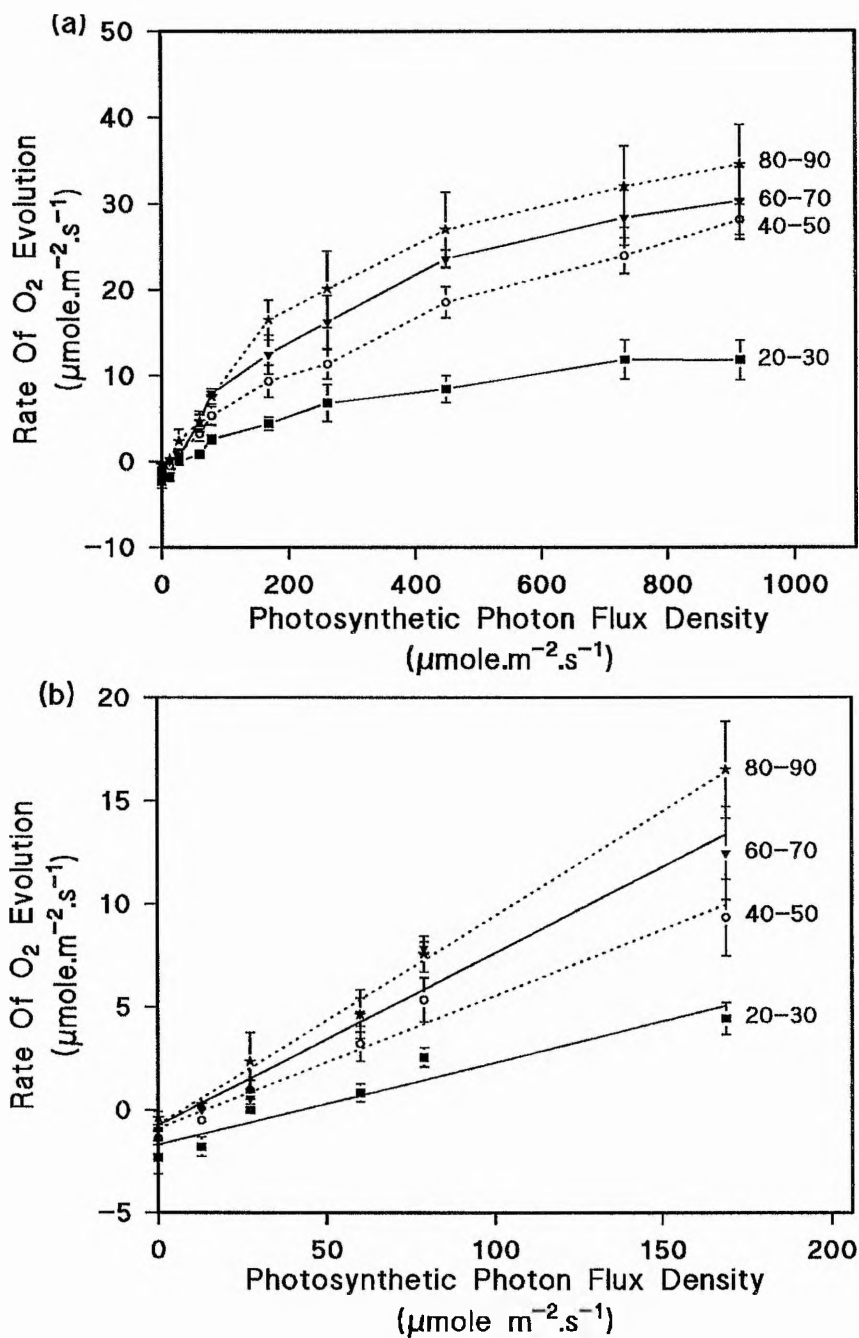


Fig. 6.4 Light response curve of photosynthetic O₂ evolution of leaf sections taken along the length of 7-d-old control-grown primary leaves (a), and the linear regression to the initial slope of the light response curves (b)

Plants were grown as described in Section 2.2. CO₂ - dependent O₂ evolution of transverse leaf sections taken at 20-30mm (■), 40-50mm (○), 60-70mm (▼) and 80-90mm (★) above the leaf base, was measured using a leaf disc electrode (Section 2.11.1-2.11.2) at a range of PPF and a saturating concentration of CO₂. Data points represent the mean of 3 independent growth studies, sampling 10 seedlings per replicate. Error bars show \pm one standard error of the mean.

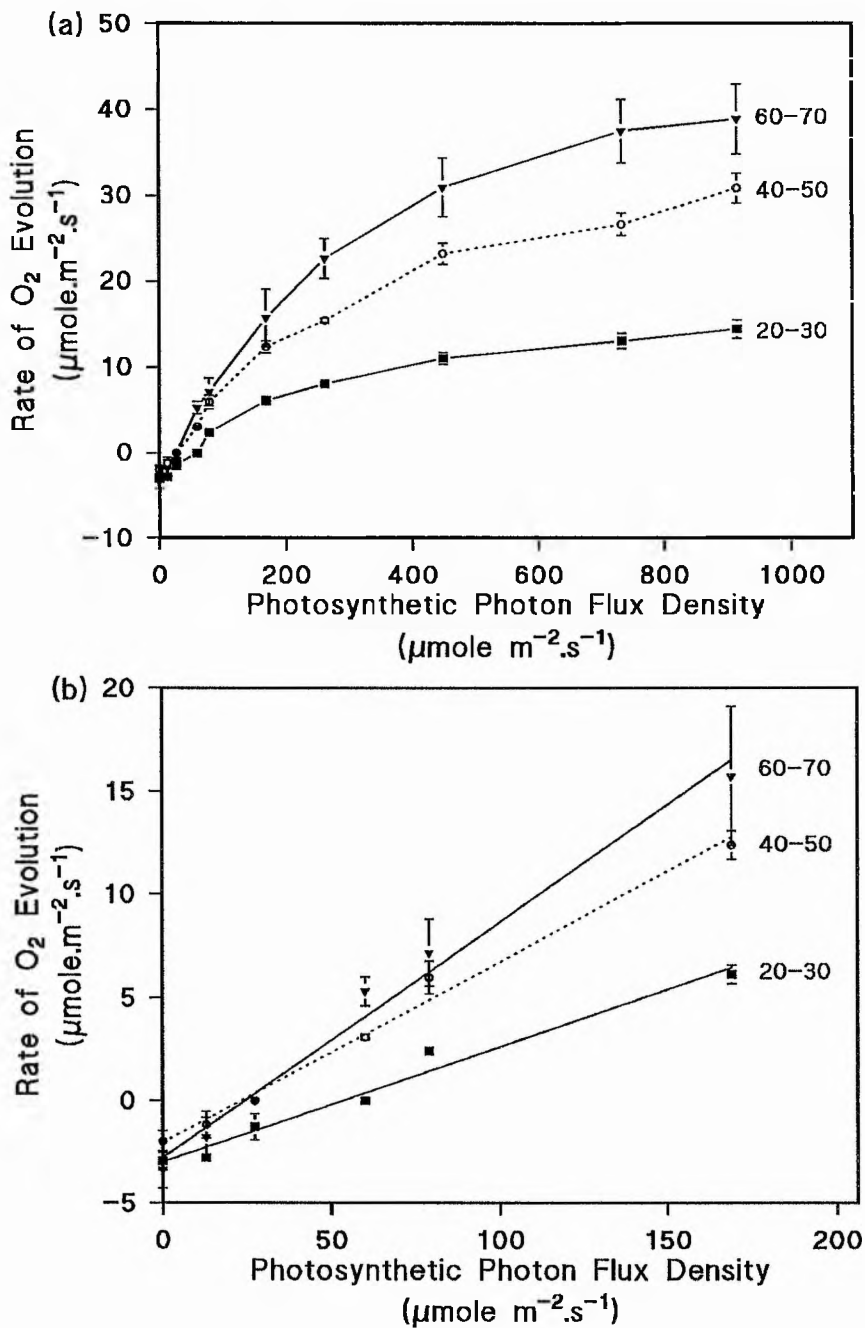


Fig. 6.5 Light response curve of photosynthetic O₂ evolution of leaf sections taken along the length of 7-d-old UV-B-grown primary leaves (a), and the linear regression to the initial slope of the light response curves (b)

Plants were grown as described in Section 2.2. CO₂-dependent O₂ evolution of transverse leaf sections taken at 20-30mm (■), 40-50mm (○) and 60-70mm above the leaf base, was measured using a leaf disc electrode (Section 2.11.1-2.11.2) at a range of PPF and a saturating concentration of CO₂. Data points represent the mean of 3 independent growth studies, sampling 10 seedlings per replicate. Error bars show \pm one standard error of the mean.

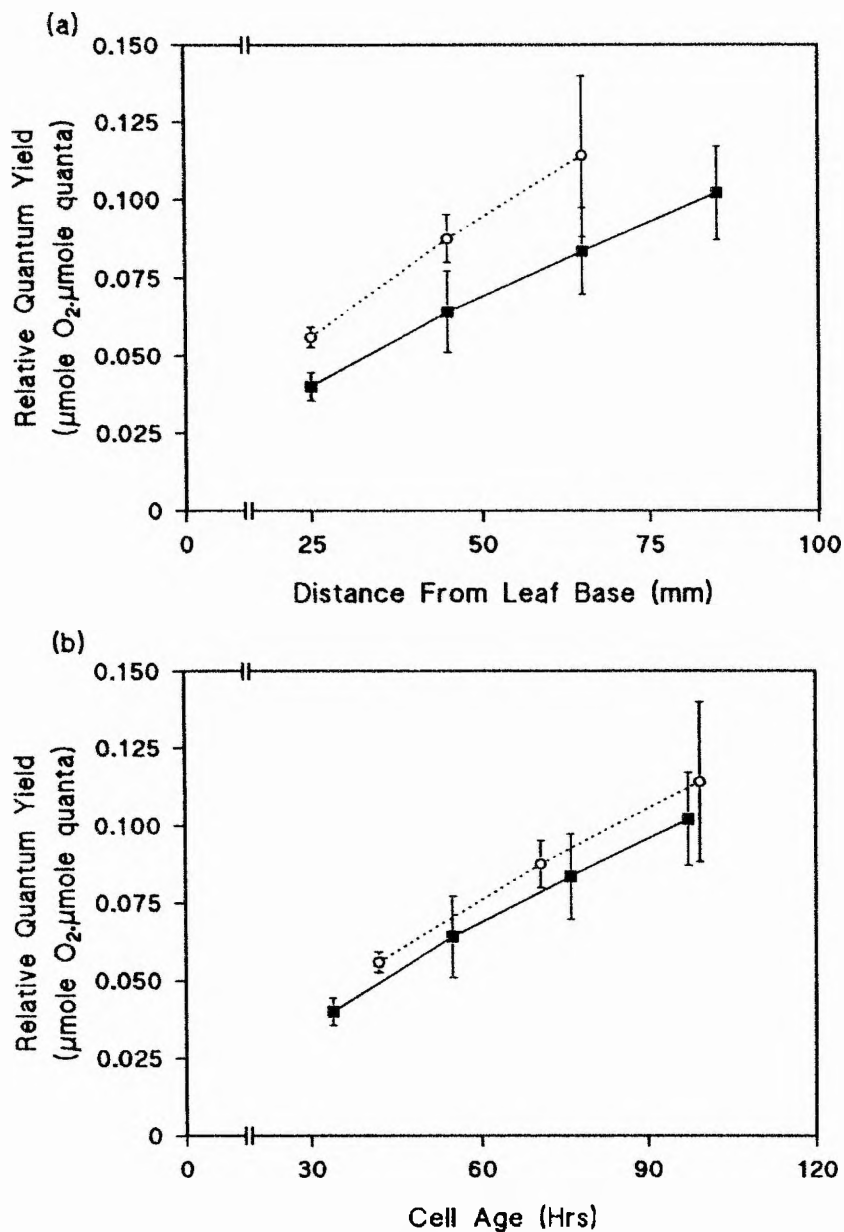


Fig. 6.6 Effect of UV-B radiation on the relative quantum yield in relation to cell age along the length of 7-d-old primary leaves, expressed on a (a) spatial, and (b) temporal scale

Plants were grown under control (■) and UV-B (○) conditions (Section 2.2). The relative quantum yield was calculated from the linear regression of the initial slope of the light response curves (Figs. 6.4b, 6.5b) as described in Section 6.6.2.

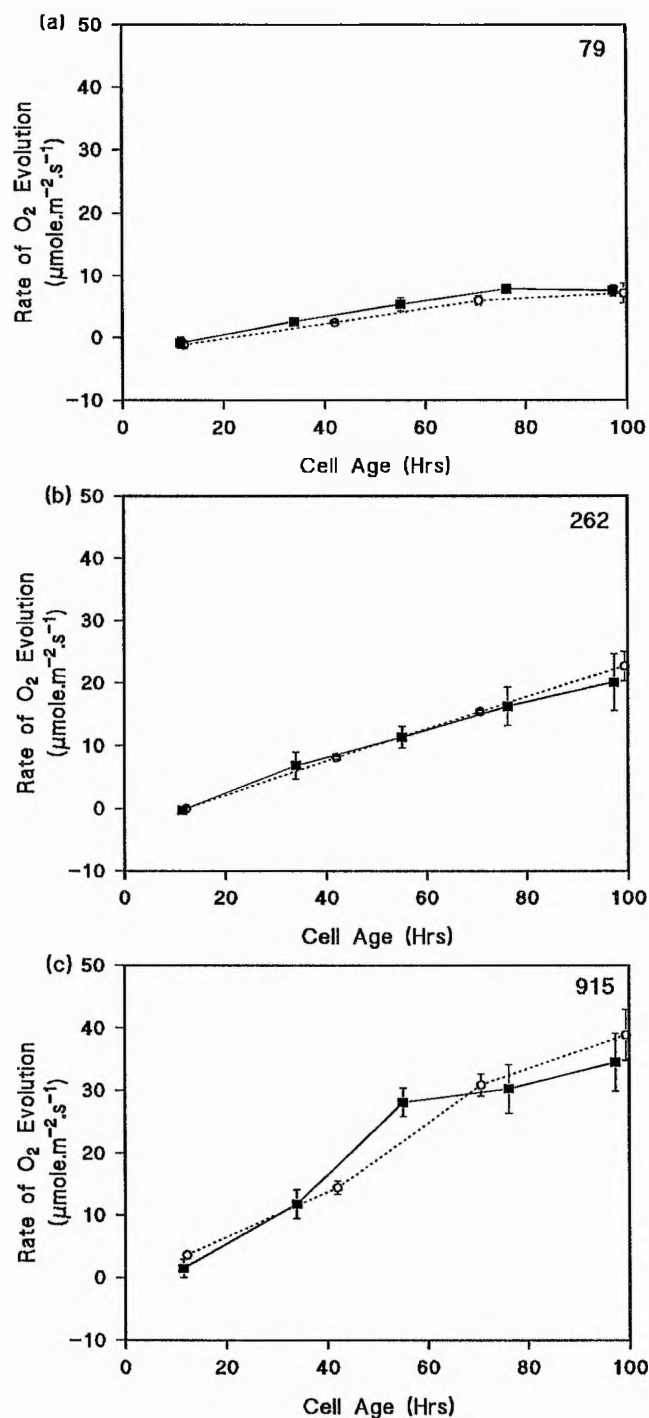


Fig. 6.7 Effect of UV-B radiation on the rate of CO₂ - dependent O₂ evolution in relation to cell age along the length of 7-d-old primary leaves, at a PPF of (a) 79, (b) 262 and (c) 915 $\mu\text{mole}\cdot\text{m}^{-2}\cdot\text{s}^{-1}$

Plants were grown under control (■) and UV-B (○) conditions (Section 2.2). CO₂ - dependent O₂ evolution was measured using a leaf disc electrode (Section 2.11.1-2.11.2) at saturating concentration of CO₂. Data points represent the mean of 3 independent growth studies, sampling 10 seedlings per replicate. Error bars show \pm one standard error of the mean.

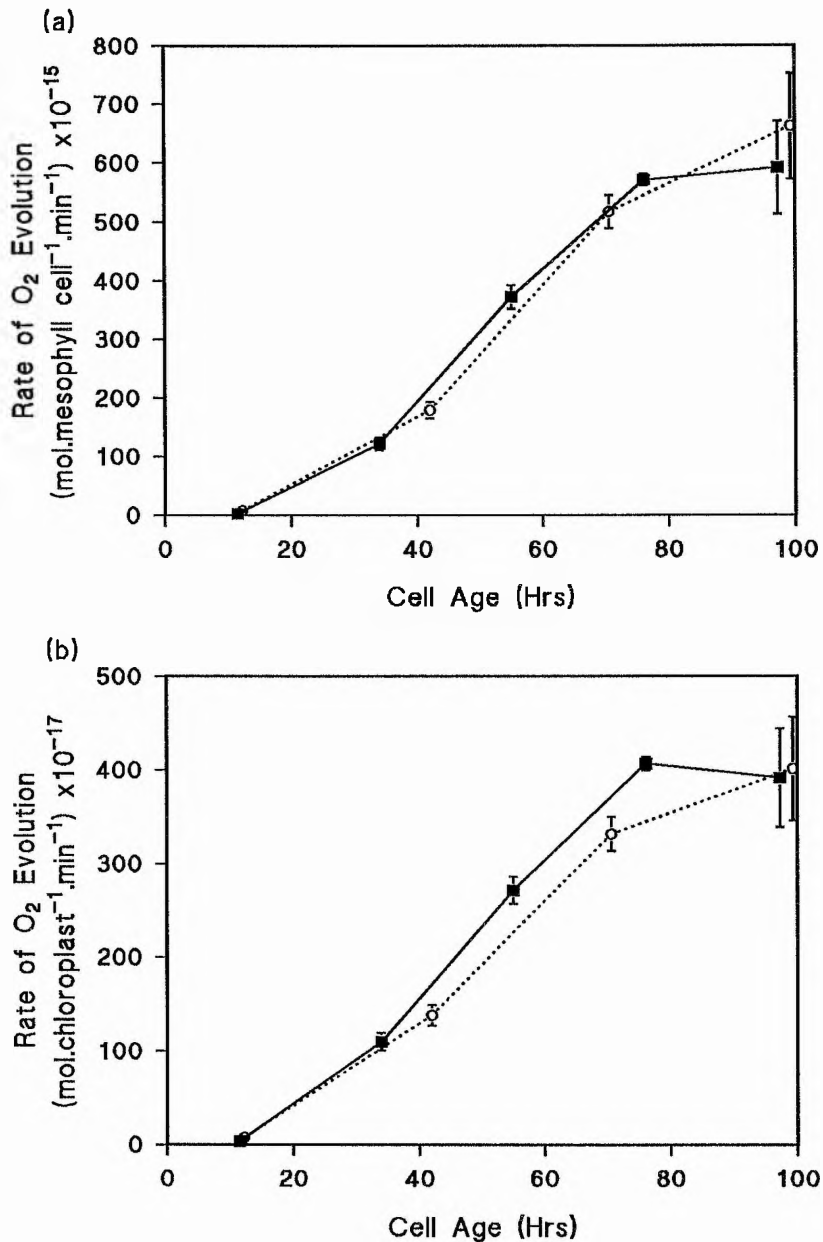


Fig. 6.8 Effect of UV-B radiation on the rate of CO_2 - dependent O_2 evolution per mesophyll cell (a), and per chloroplast (b), in relation to cell age along the length of 7-d-old primary leaves, at a PPF of $915 \mu\text{mol m}^{-2} \text{s}^{-1}$

Plants were grown under control (■) and UV-B (○) conditions (Section 2.2). CO_2 - dependent O_2 evolution was measured using a leaf disc electrode (Section 2.11.1-2.11.2) at saturating concentration of CO_2 . Data points represent the mean of 3 independent growth studies, sampling 10 seedlings per replicate. Error bars show \pm one standard error of the mean.

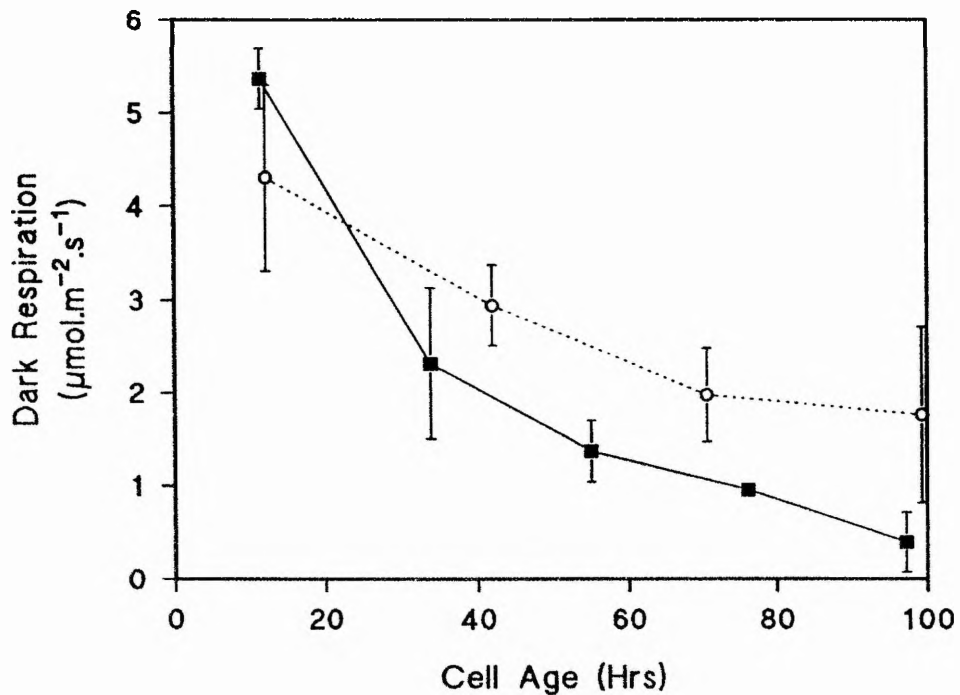


Fig. 6.9 Effect of UV-B radiation on the rates of dark respiration in relation to cell age along the length of 7-d-old primary leaves

Plants were grown under control (■) and UV-B (○) conditions (Section 2.2). Dark respiration was measured using a leaf disc electrode (Section 2.11.3). Data points represent the mean of 3 independent growth studies, sampling 10 seedlings per replicate. Error bars show \pm one standard error of the mean

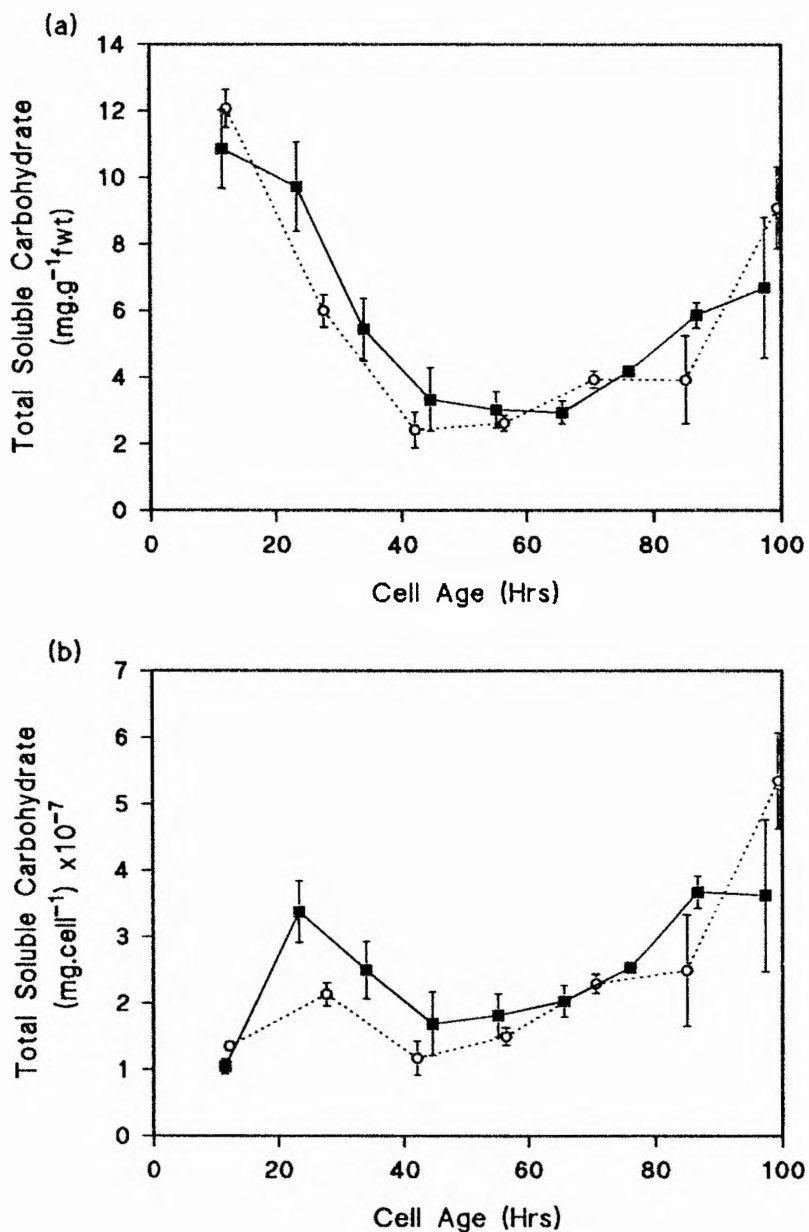


Fig. 6.10 Effect of UV-B radiation on the concentration of soluble carbohydrates per g. fresh weight tissue (a), and per cell (b), in relation to cell age along the length of 7-d-old primary leaves

Plants were grown under control (■) and UV-B (○) conditions (Section 2.2). Carbohydrates were extracted and determined using the anthrone reagent method (Section 2.12.3). Data points represent the mean of 5 independent growth studies, sampling 30 seedlings per replicate. Error bars show ± one standard error of the mean.

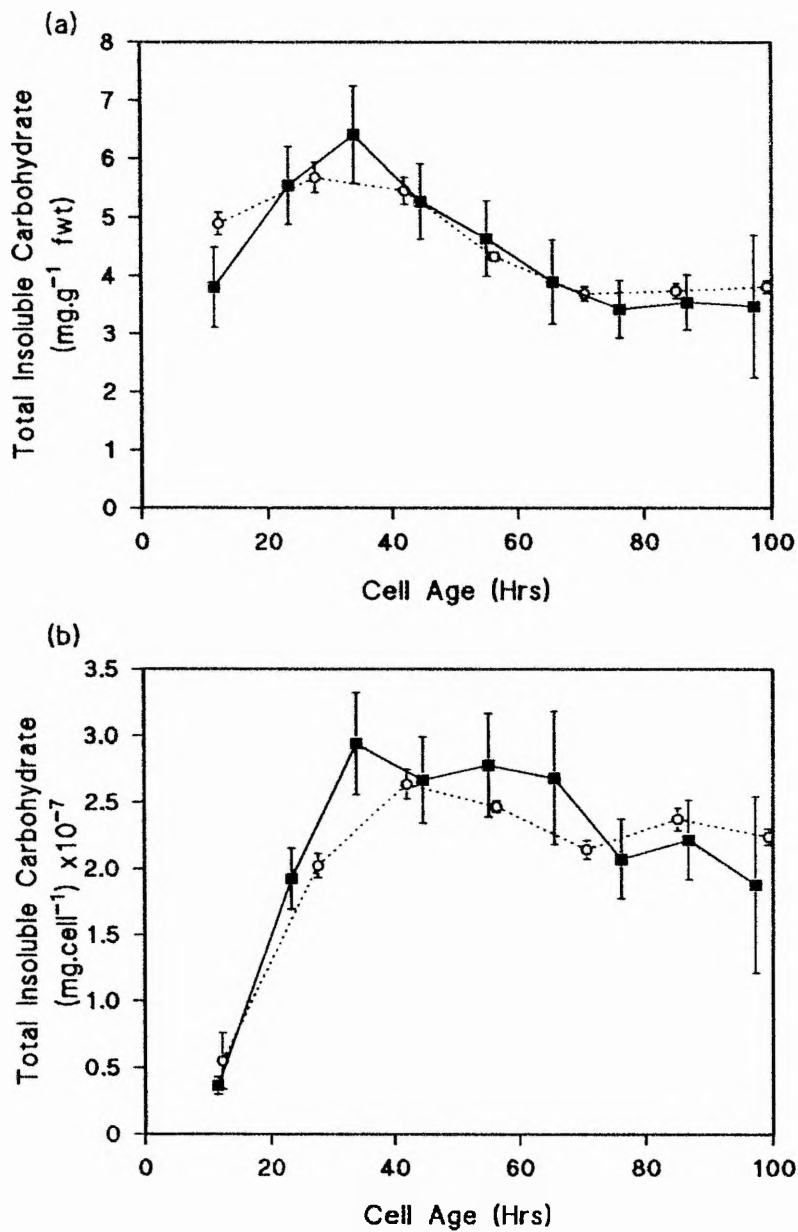


Fig. 6.11 Effect of UV-B radiation on the concentration of insoluble carbohydrates per g. fresh weight tissue (a), and per cell (b), in relation to cell age along the length of 7-d-old primary leaves

Plants were grown under control (■) and UV-B (○) conditions (Section 2.2). Carbohydrates were extracted and determined using the anthrone reagent method (Section 2.12.4). Data points represent the mean of 5 independent growth studies, sampling 30 seedlings per replicate. Error bars show ± one standard error of the mean.

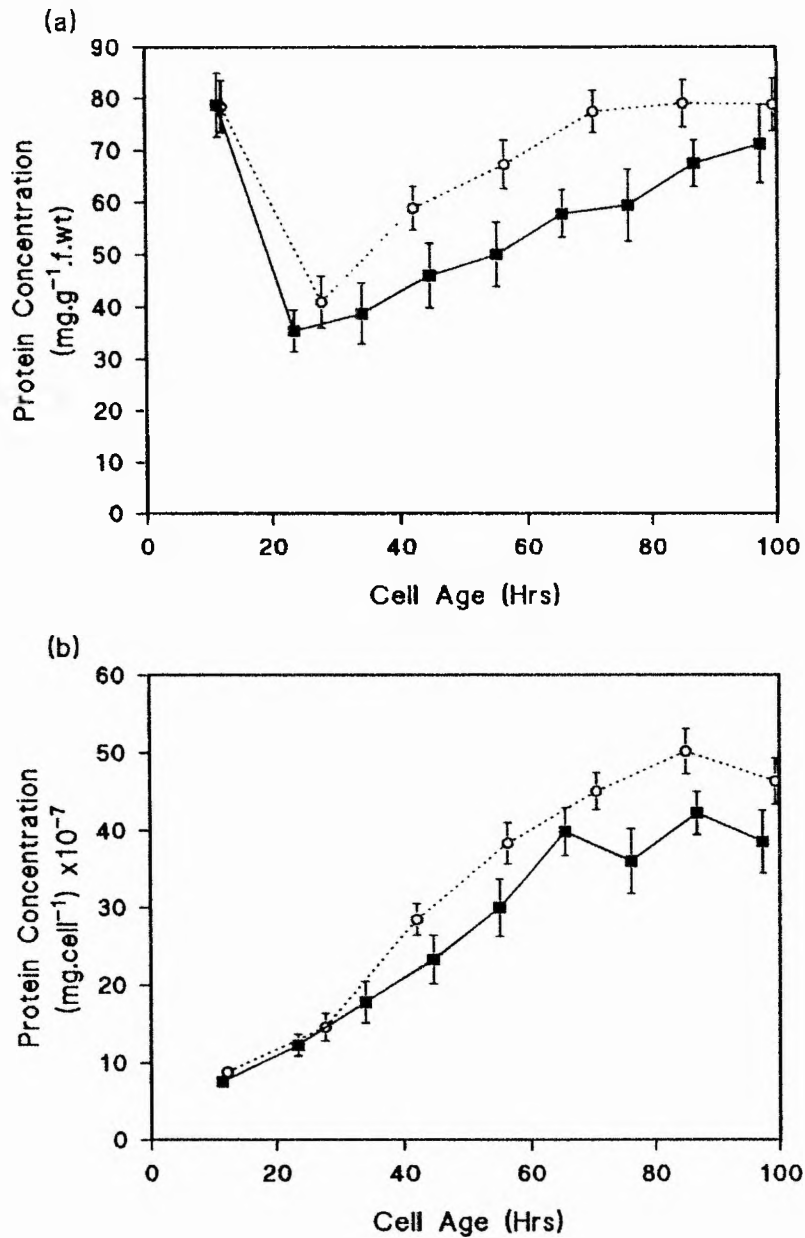


Fig. 6.12 Effect of UV-B radiation on the total soluble protein concentration per g. fresh weight tissue (a), and per cell (b), in relation to cell age along the length of 7-d-old primary leaves

Plants were grown under control (■) and UV-B (○) conditions (Section 2.2). Soluble protein was measured and calculated as described in Section 2.13. Each data point represents the mean of 5 independent growth studies, sampling 10 seedlings per replicate. Error bars show ± one standard error of the mean.

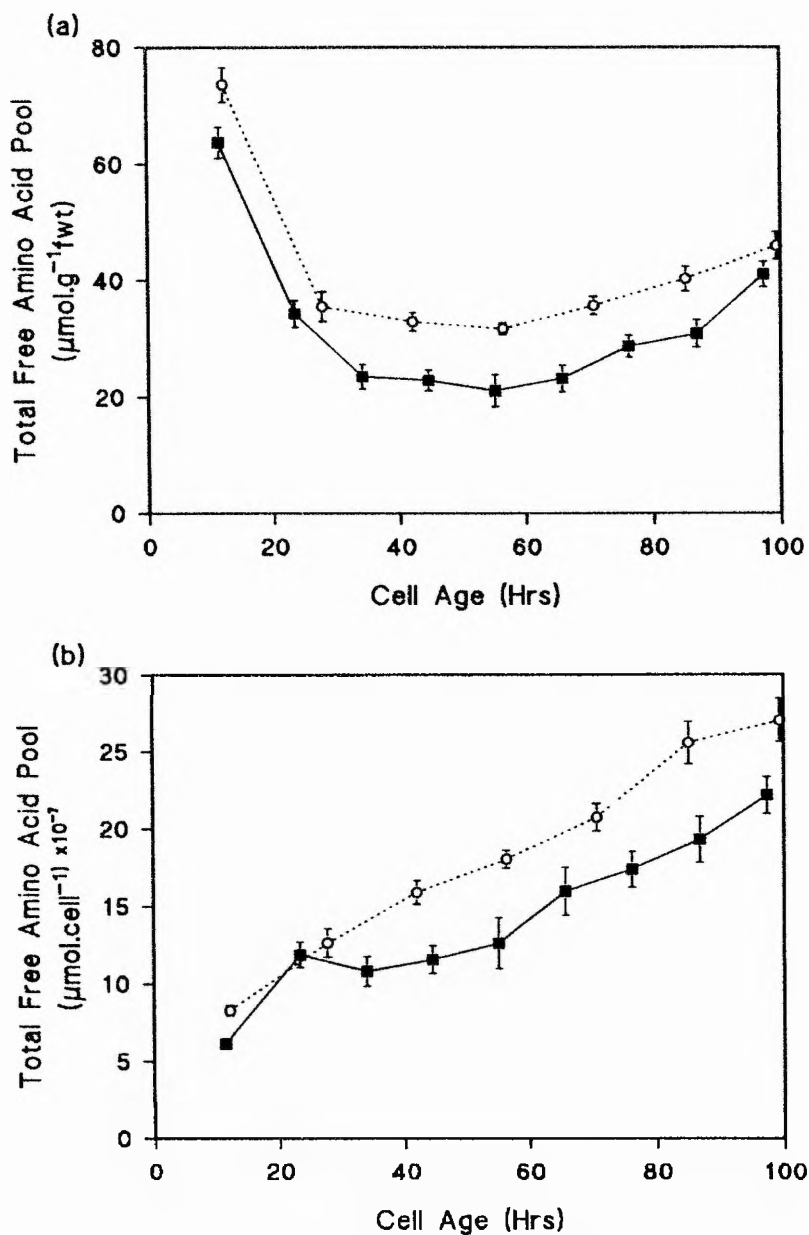


Fig. 6.13 Effect of UV-B radiation on the total free amino acid* pool per g.fresh weight tissue (a), and per cell (b), in relation to cell age along the length of 7-d-old primary leaves

Plants were grown under control (■) and UV-B (○) conditions (Section 2.2). The total free amino acid pool (* = common amino acids occurring in proteins, see Fig. 2.5) was determined using HPLC (Section 2.14). Data points represent the mean of 6 independent growth studies, sampling 5 seedlings per replicate. Error bars show \pm one standard error of the mean.

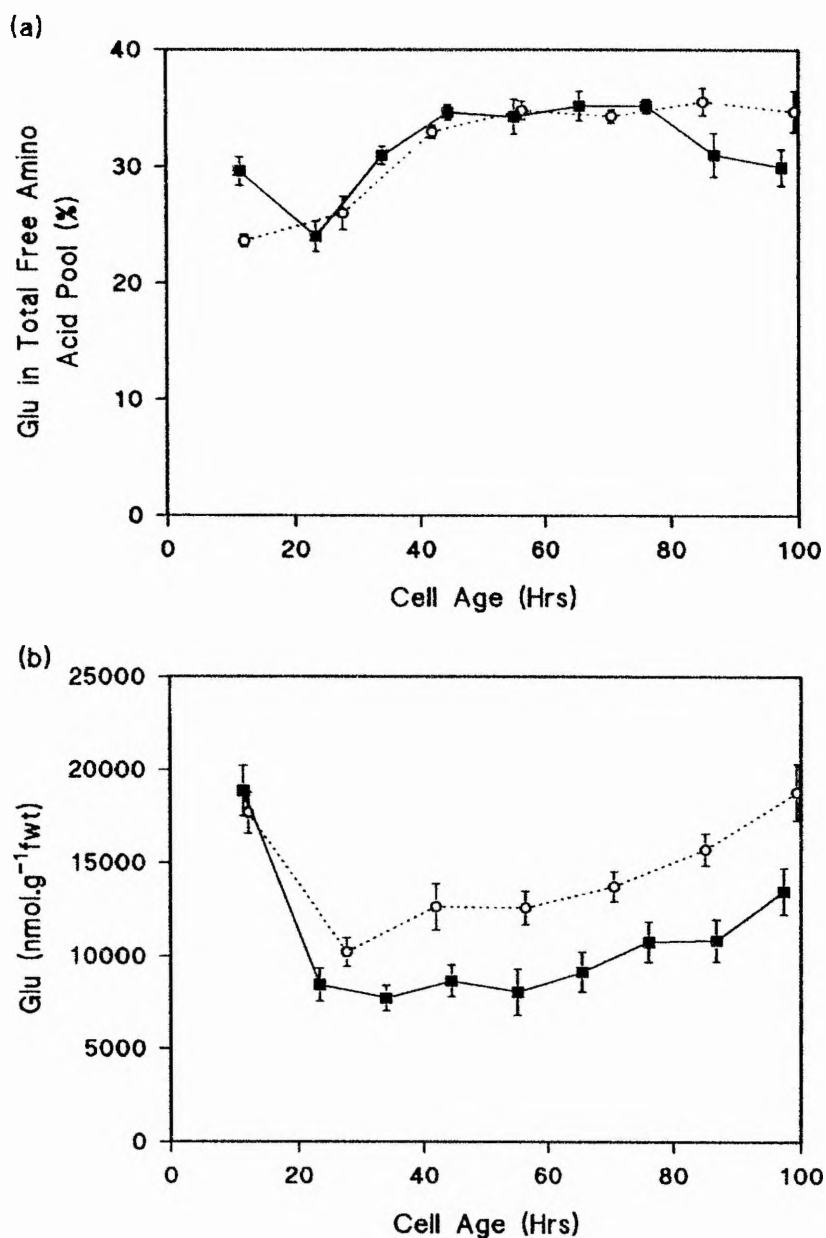


Fig. 6.14 Effect of UV-B radiation on (a) glutamate as percentage of the total free amino acid pool, and (b) the concentration of the free glutamate pool, in relation to cell age along the length of 7-d-old primary leaves

Plants were grown under control (■) and UV-B (○) conditions (Section 2.2). Amino acids were extracted from leaf tissue (Section 2.14.1) and the free glutamate pool determined using HPLC (Sections 2.14.5). Data points represent the mean of 6 independent growth studies, sampling 5 seedlings per replicate. Error bars show ± one standard error of the mean.

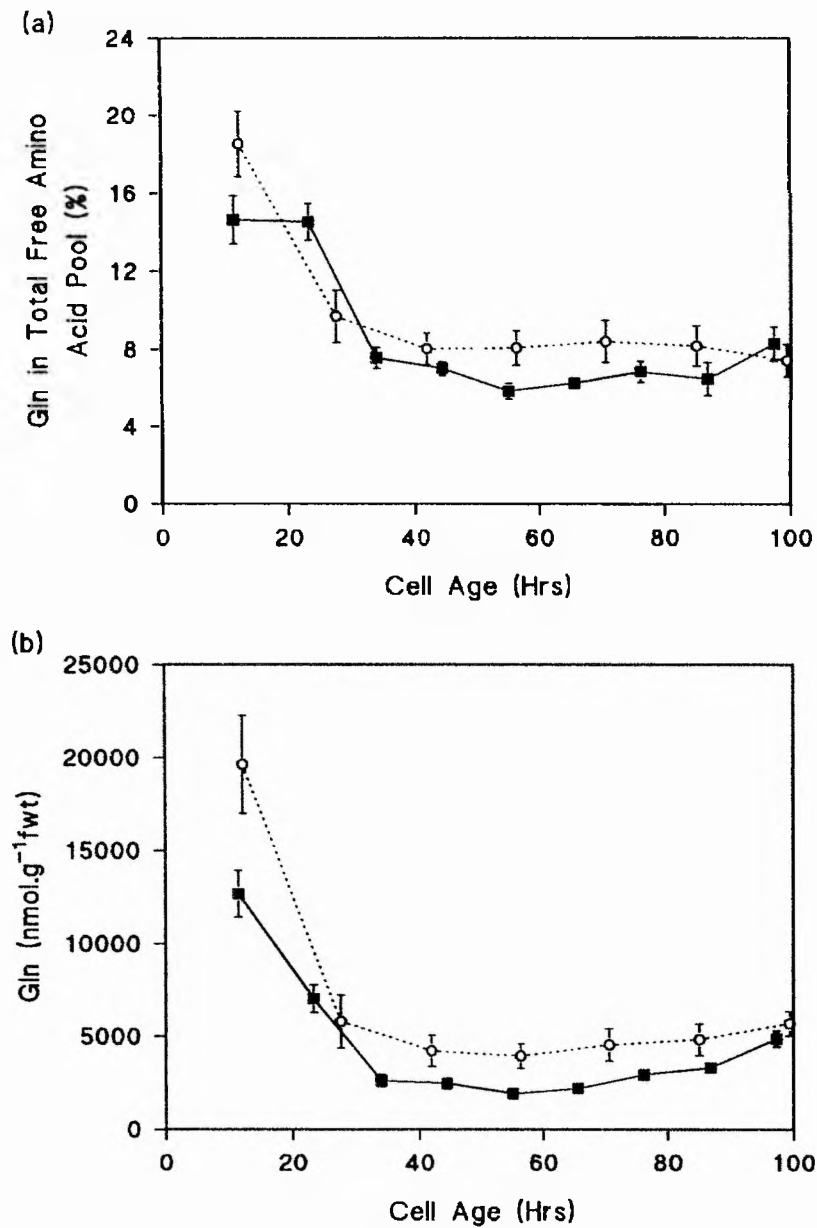


Fig. 6.15 Effect of UV-B radiation on (a) glutamine as a percentage of the total free amino acid pool, and (b) the concentration of the free glutamine pool, in relation to cell age along the length of 7-d-old primary leaves

Plants were grown under control (■) and UV-B (○) conditions (Section 2.2). Amino acids were extracted from leaf tissue (Section 2.14.1) and the free glutamine pool determined using HPLC (Sections 2.14.5). Data points represent the mean of 6 independent growth studies, sampling 5 seedlings per replicate. Error bars show ± one standard error of the mean.

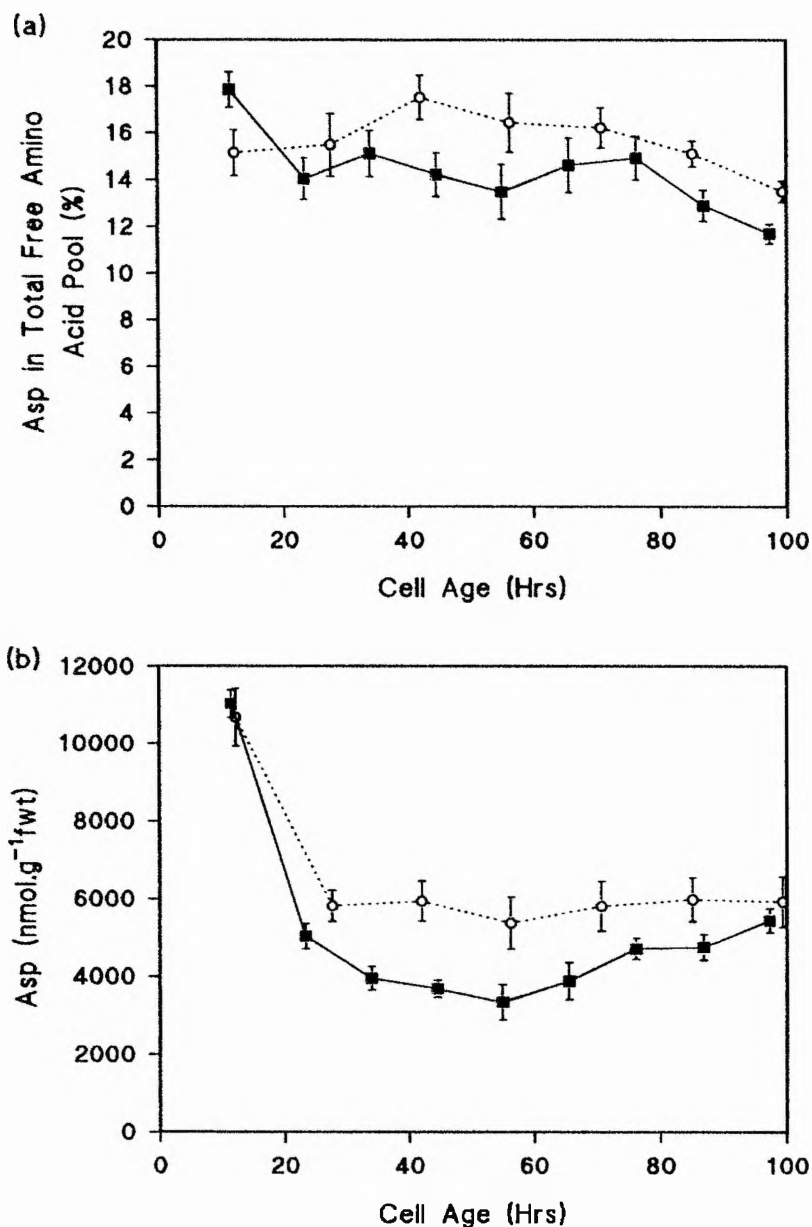


Fig. 6.16 Effect of UV-B radiation on (a) aspartate as a percentage of the total free amino acid pool, and (b) the concentration of the free aspartate pool, in relation to cell age along the length of 7-d-old primary leaves

Plants were grown under control (■) and UV-B (○) conditions (Section 2.2). Amino acids were extracted from leaf tissue (Section 2.14.1) and the free aspartate pool determined using HPLC (Section 2.14.5). Data points represent the mean of 6 independent growth studies, sampling 5 seedlings per replicate. Error bars show ± one standard error of the mean.

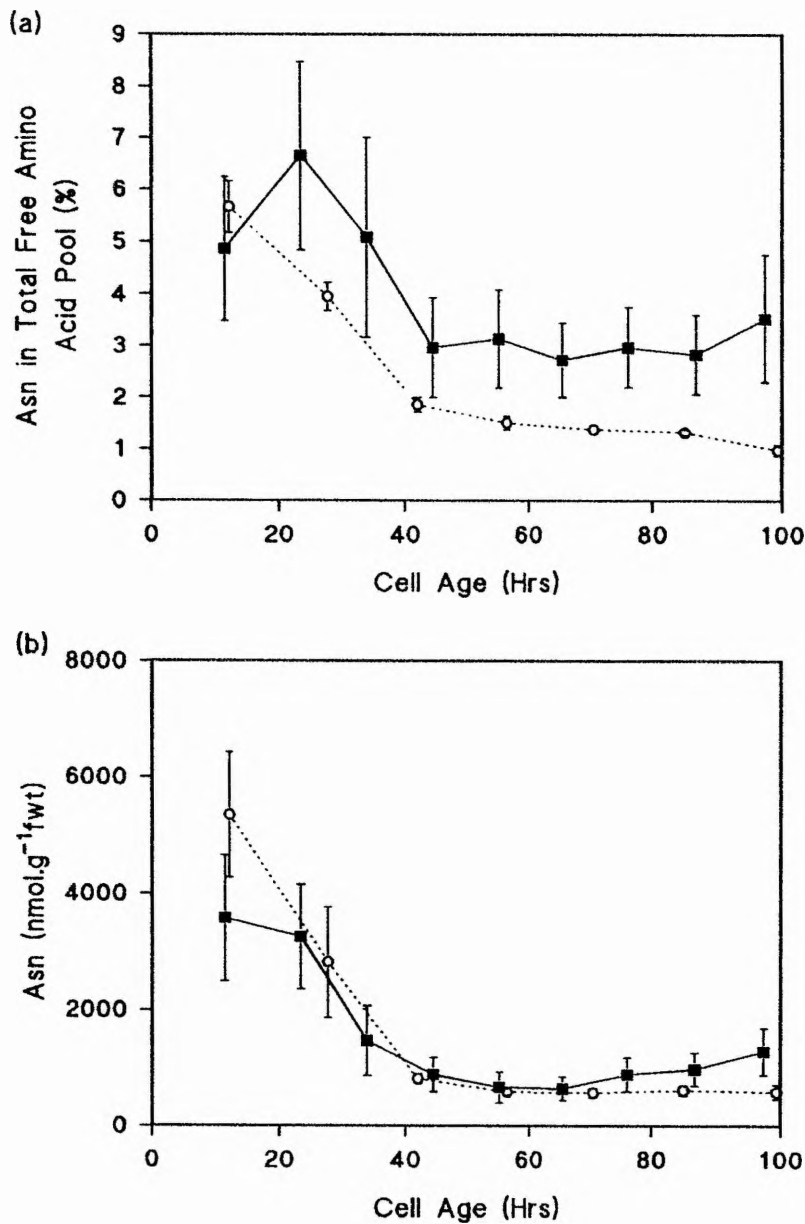


Fig. 6.17 Effect of UV-B radiation on (a) asparagine as a percentage of the total free amino acid pool, and (b) the concentration of the free asparagine pool, in relation to cell age along the length of 7-d-old primary leaves

Plants were grown under control (■) and UV-B (○) conditions (Section 2.2). Amino acids were extracted from leaf tissue (Section 2.14.1) and the free asparagine pool determined using HPLC (Section 2.14.5). Data points represent the mean of 6 independent growth studies, sampling 5 seedlings per replicate. Error bars show ± one standard error of the mean.

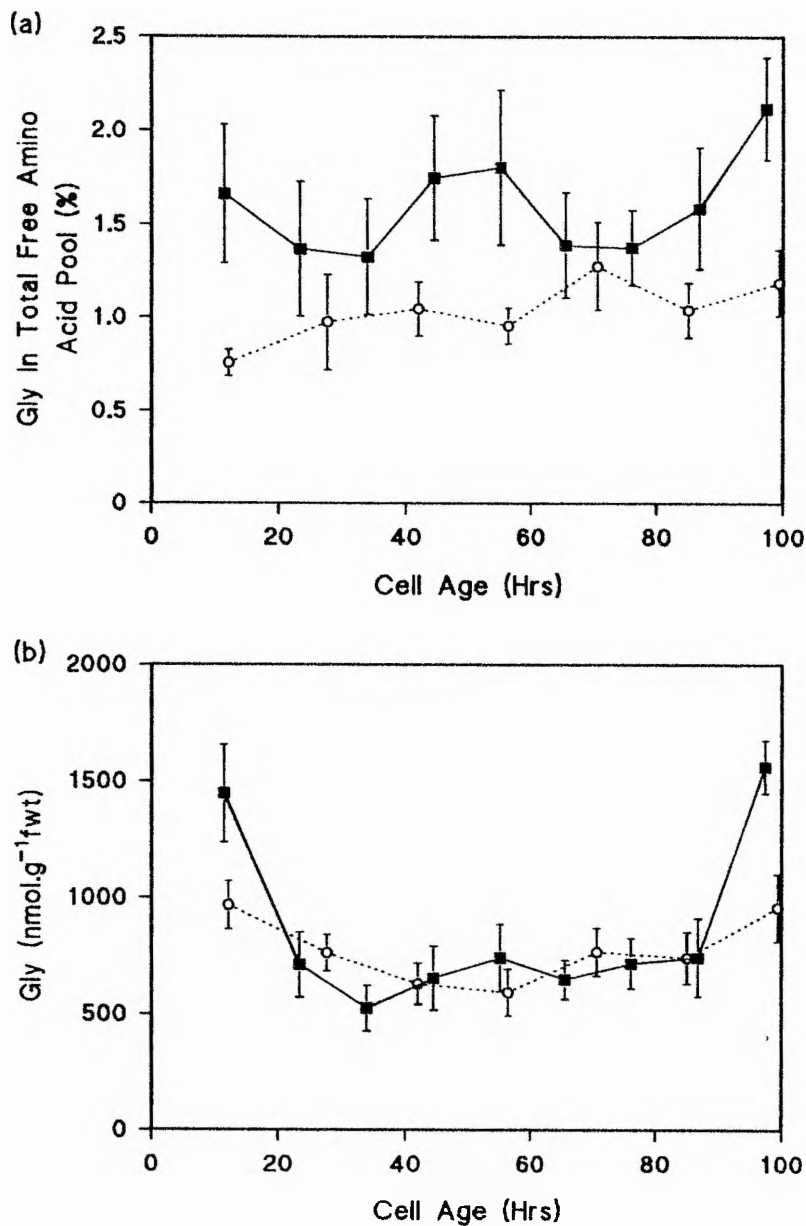


Fig. 6.18 Effect of UV-B radiation on (a) glycine as a percentage of the total free amino acid pool, and (b) the concentration of the free glycine pool, in relation to cell age along the length of 7-d-old primary leaves

Plants were grown under control (■) and UV-B (○) conditions (Section 2.2). Amino acids were extracted from leaf tissue (Section 2.14.1) and the free glycine pool determined using HPLC (Section 2.14.5). Data points represent the mean of 6 independent growth studies, sampling 5 seedlings per replicate. Error bars show \pm one standard error of the mean.

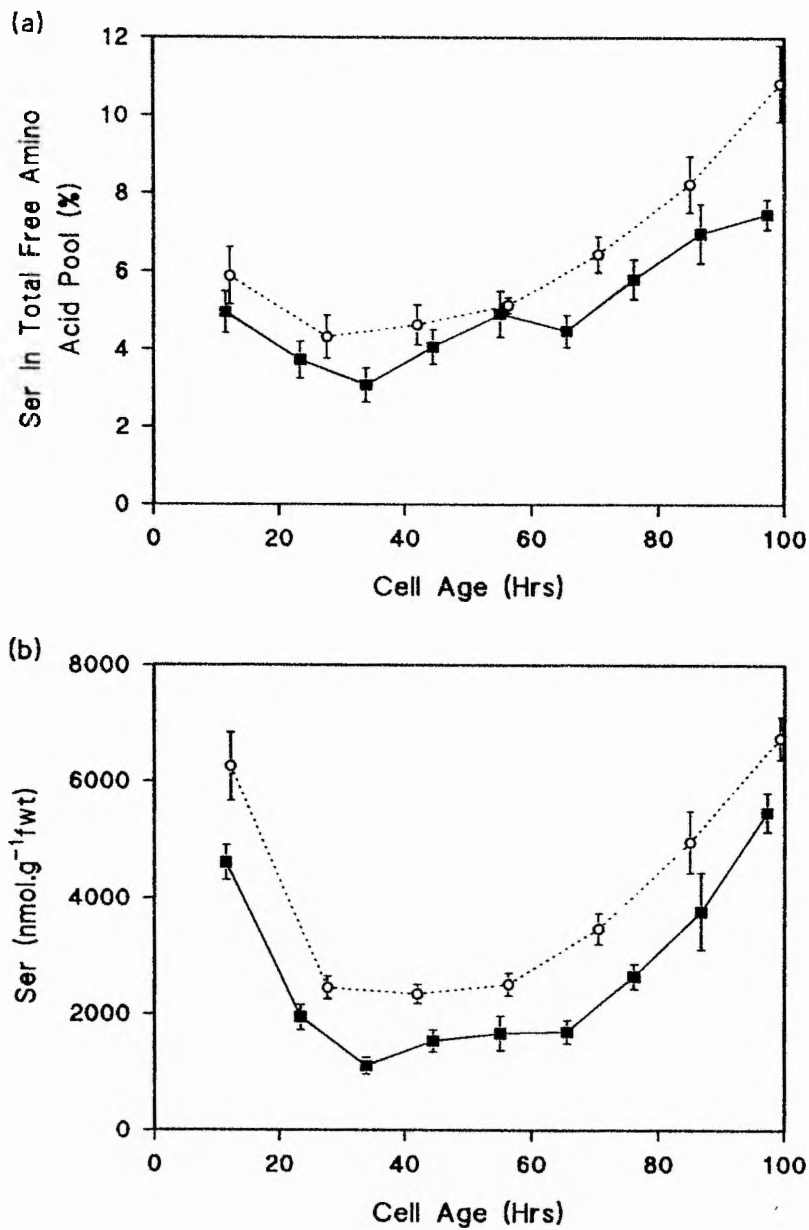


Fig. 6.19 Effect of UV-B radiation on (a) serine as a percentage of the total free amino acid pool, and (b) the concentration of the free serine pool, in relation to cell age along the length of 7-d-old primary leaves

Plants were grown under control (■) and UV-B (○) conditions (Section 2.2). Amino acids were extracted from leaf tissue (Section 2.14.1) and the free serine pool determined using HPLC (Section 2.14.5). Data points represent the mean of 6 independent growth studies, sampling 5 seedlings per replicate. Error bars show ± one standard error of the mean.

	Leaf Base (cell age ~ 10Hrs)		Mid-leaf (cell age ~ 50Hrs)		Leaf Tip (cell age ~ 100Hrs)	
	% of Total aa Pool		% of Total aa Pool		% of Total aa Pool	
	Control	UV-B	Control	UV-B	Control	UV-B
his	0.2087 ±0.0519	0.1922 ±0.0299	0.252 ±0.024	0.182 ±0.0224	0.1461 ±0.0284	0.12 ±0.0135
thr	1.999 ±0.086	2.0032 ±0.094	2.544 ±0.144	2.8478 ±0.1386	3.055 ±0.153	3.3293 ±0.2365
arg	0.2687 ±0.0414	0.2717 ±0.0397	0.427 ±0.0973	0.3322 ±0.0501	0.3186 ±0.0645	0.2858 ±0.0227
ala	9.175 ±0.394	9.3178 ±0.545	9.837 ±0.178	9.1048 ±0.2765	9.606 ±0.577	8.035 ±0.1855
tyr	0.4562 ±0.025	0.4822 ±0.039	1.1462 ±0.027	0.9548 ±0.0513	0.8868 ±0.047	1.0012 ±0.0726
met	0.699 ±0.0847	0.4688 ±0.0386	0.239 ±0.0121	0.1867 ±0.017	0.1772 ±0.0135	0.1763 ±0.0288
val	1.6912 ±0.082	1.8087 ±0.0919	1.4214 ±0.079	1.376 ±0.067	1.4181 ±0.0495	1.3785 ±0.0681
phe	0.5903 ±0.139	0.5028 ±0.425	0.5915 ±0.0632	0.4722 ±0.0496	0.5929 ±0.0374	0.5208 ±0.05795
iso	0.6669 ±0.0463	0.6 ±0.0492	0.7994 ±0.0561	0.645 ±0.052	0.7134 ±0.0166	0.441 ±0.083
leu	0.5562 ±0.0435	0.4725 ±0.0515	0.5897 ±0.0473	0.5245 ±0.0741	0.6356 ±0.0694	0.5538 ±0.0859

Table 6.1 Changes in Amino Acids as a Percentage of The Total Free Amino Acid Pool

Plants were grown under control and UV-B conditions (Section 2.2). Amino acids were extracted from leaf tissue (Section 2.14.1) and the free amino acid pools determined using HPLC (Section 2.14.5). Data represents the mean of 6 independent growth studies, sampling 5 seedlings per replicate. Error bars show ± one standard error of the mean.

	Leaf Base (cell age ~ 10Hrs)		Mid-leaf (cell age ~ 50Hrs)		Leaf Tip (cell age ~ 100Hrs)	
	aa nmol.g ⁻¹ .fwt		aa nmol.g ⁻¹ .fwt		aa nmol.g ⁻¹ .fwt	
	Control	UV-B	Control	UV-B	Control	UV-B
his	213.57 ±49.6	243.3 ±39.51	99.36 ±19.32	103.72 ±13.29	87.56 ±5.31	91.56 ±8.32
thr	1437.93 ±73.59	1685.07 ±95.67	700.03 ±91.83	1087.58 ±74.59	1627.52 ±110.74	1630.95 ±139.68
arg	186.91 ±24.26	220.69 ±28.04	112.67 ±15.44	121.52 ±15.04	176.01 ±30.98	144.14 ±22.18
ala	6477.18 ±200.57	7521.26 ±528.55	2553.44 ±268.36	3318.08 ±104.14	4839.91 ±226.19	4433.62 ±400.28
tyr	311.55 ±18.91	384.39 ±31.95	287.96 ±35.29	345.62 ±25.22	427.34 ±44.24	482.62 ±52.0
met	523.24 ±61.69	397.32 ±48.66	67.84 ±6.97	69.72 ±3.99	98.53 ±3.34	78.39 ±8.08
val	1033.76 ±49.66	1277.46 ±81.91	316.63 ±36.72	438.34 ±19.66	614.7 ±25.6	582.11 ±21.59
phe	449.78 ±93.52	453.99 ±48.34	166.05 ±23.86	186.87 ±10.5	317.96 ±30.24	281.25 ±34.93
iso	417.71 ±29.08	429.77 ±25.63	179.05 ±21.41	208.65 ±10.11	310.83 ±22.95	228.86 ±21.14
leu	391.29 ±24.51	377.19 ±38.43	145.77 ±18.8	185.01 ±16.17	291.33 ±29.53	246.88 ±41.37

Table 6.2 Changes in Amino Acids (nmol.g⁻¹.fwt) in The Total Free Amino Acid Pool

Plants were grown under control and UV-B conditions (Section 2.2). Amino acids were extracted from leaf tissue (Section 2.14.1) and the free amino acid pools determined using HPLC (Section 2.1.4.5). Data represents the mean of 6 independent growth studies, sampling 5 seedlings per replicate. Error bars show ± one standard error of the mean.

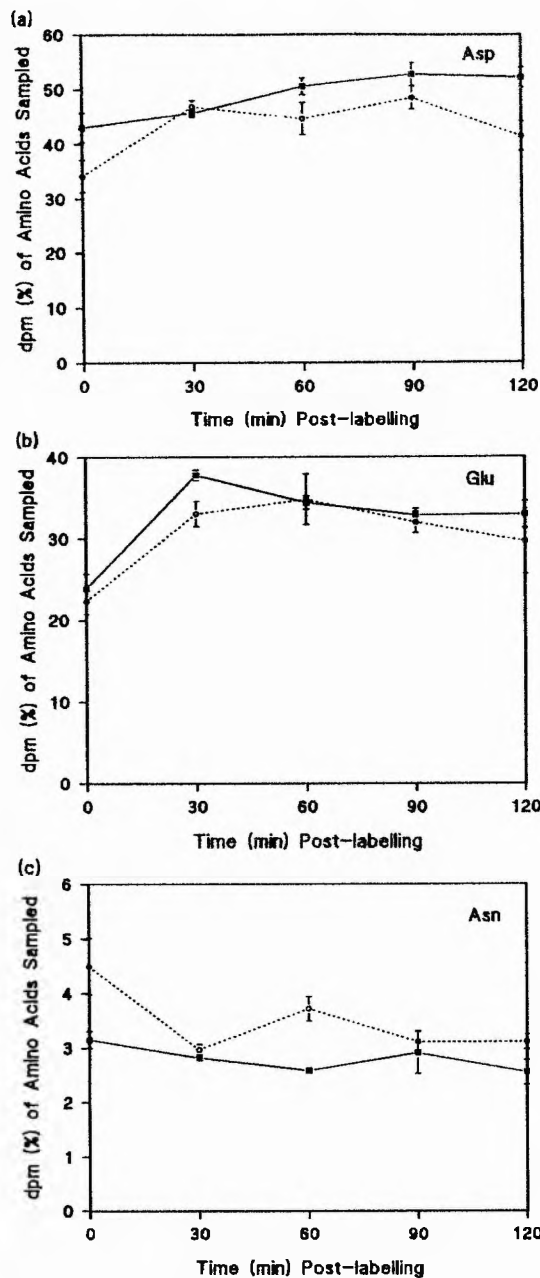


Fig. 6.20 Changes in the ^{14}C post-labelling content of the (a) aspartate, (b) glutamate and (c) asparagine free pools

Plants were grown under control (■) and UV-B (○) conditions (Section 2.2). Leaf tissue was exposed to $^{14}\text{CO}_2$ for 10 minutes, and the amount of ^{14}C label in amino acid free pools was measured for 120 minutes post-labelling, as described in Section 2.15. Data points represent the mean of 3 independent growth studies, sampling 18 seedlings per replicate. Error bars show \pm one standard error of the mean.

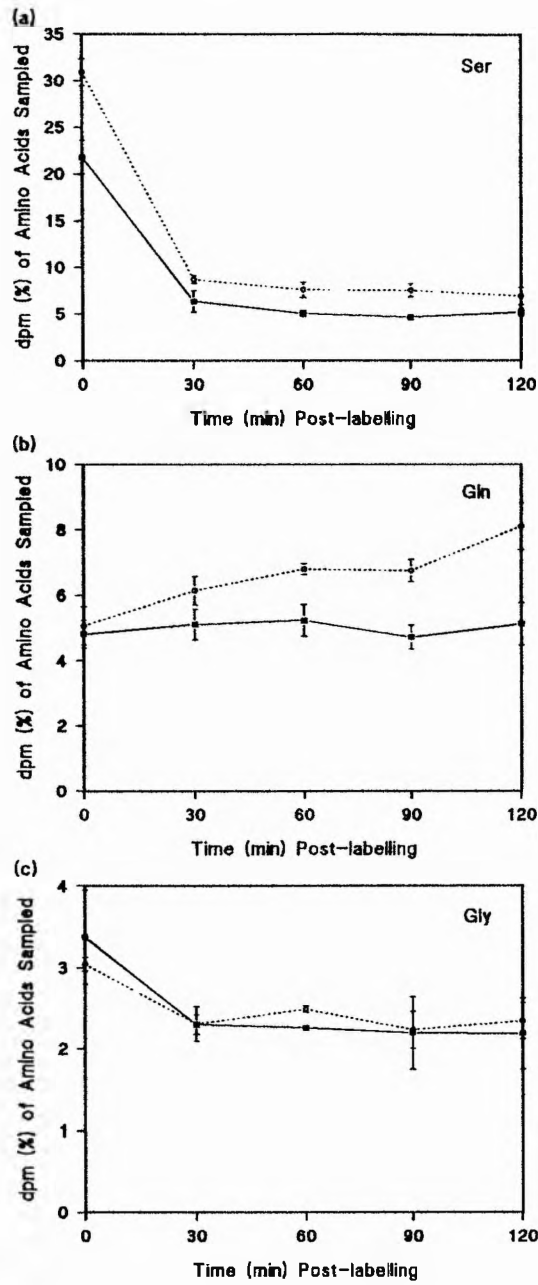


Fig. 6.21 Changes in the ^{14}C post-labelling content of the (a) serine, (b) glutamine and (c) glycine free pools

Plants were grown under control (■) and UV-B (○) conditions (Section 2.2). Leaf tissue was exposed to $^{14}\text{CO}_2$ for 10 minutes, and the amount of ^{14}C label in amino acid free pools was measured for 120 minutes post-labelling, as described in Section 2.15. Data points represent the mean of 3 independent growth studies, sampling 18 seedlings per replicate. Error bars show \pm one standard error of the mean.

DISCUSSION

Alterations in plant metabolism, especially carbon metabolism, *e.g.* reduced photosynthetic activity, in response to UV-B have been reported in a wide range of species including *P.sativum* (Day & Vogelmann, 1995) and *G.max* (Teramura *et al.*, 1984)(see Section 1.6.2). In the majority of these studies, however, the effects of UV-B on metabolism have only been investigated in tissue of one specific developmental stage, *e.g.* mature tissue. Changes in metabolism during 'normal' development, resulting from a number of highly co-ordinated changes at the ultrastructural (see Section 5.1.1.3 - 5.1.2.3) and biochemical levels (see Sections 6.1), were not taken into account in any previous studies.

The results of the previous chapter showed changes in the ultrastructural development of the primary leaf, *e.g.* more, smaller chloroplasts per mesophyll cell, in response to UV-B. As a cell structure is related to its function (see Chapter 5), it was suggested that such changes in ultrastructure may result in altered metabolism. The purpose of this chapter was to determine the effects of UV-B on the development of metabolism, and to relate any changes in the metabolism of the developing control and UV-B-grown plants to the ultrastructural changes observed in the previous chapter.

6.12 Changes in Carbon Metabolism During Leaf Development

The developing grass leaf provides a model system, in which a gradient exists along the leaf blade, whereby both the age and developmental stage of a cell is a function of its position relative to the origin, *i.e.* basal meristem (as discussed in Section 4.1.2.1). This simple model system has been used to investigate changes in metabolism

during development, and changes in a number of different aspects of carbon metabolism, including photosynthesis (Dale, 1972; Baker & Leech, 1977), photorespiration (Tobin *et al.*, 1988) and carbohydrate metabolism (Schnyder & Nelson, 1987; Allard & Nelson, 1991), are well characterised. The results described in this chapter show that developmental changes in dark respiration, photosynthesis and carbohydrate metabolism in control-grown plants are comparable to the observations of other studies on *T. aestivum* L. cv Maris Huntsman (Tobin *et al.*, 1988), *Z. mays* (Baker & Leech, 1977) and *F. arundinacea* (Allard & Nelson, 1991).

The rate of respiration is controlled primarily by the rates of reactions supplying electrons to the respiratory chain and by the rates of reactions consuming or producing ATP (Douce & Neuburger, 1990). A number of factors, including substrate supply, adenylates and enzyme levels (Farrar, 1985) will influence the rates of these reactions, and therefore changes in any of these factors during development may result in altered rates of respiration.

Plants can oxidize a range of substances, including lipids and proteins, however in most plants respiration is dominated by the oxidation of carbohydrates via glycolysis and the TCA cycle (Dennis & Turpin, 1990). The results of this chapter show the concentration of carbohydrates (total soluble + total insoluble) in control-grown plants (per g⁻¹ fwt), to be greatest within the elongation zone (*c.* 0-20 hours) of the leaf blade. This is due to the high cell number within this region (see Section 4.5.1), with an overall increase in the concentration of carbohydrate per mesophyll cell from the base to the tip of the leaf blade. Similar high levels of carbohydrates (per g⁻¹ fwt); predominantly fructans which are the major form of stored carbohydrates in temperate C₃ grasses (Meirer & Reid, 1982), have also been reported in the elongation zone of

T.aestivum L. cv. Caldwell (Spollen & Nelson, 1988), and *F.arundinacea* (Volenec & Nelson, 1984a). Carbohydrates are the principle products of CO₂ assimilation. In this study the high carbohydrate concentration (per g.fresh weight), and a rapid increase in carbohydrate per cell, within the elongation zone (c. 0-20 hours) of the leaf blade in which the rate of photosynthesis is low (see Section 6.6.1), indicates that carbohydrates are being imported into this region from either the seed or mature leaf tissue. The results of this study also show the rate of dark respiration (per leaf area) in control-grown plants to be highest in the basal region of the leaf, where the high energy demanding processes of cell division and elongation occur (see Chapter 4), and then decreases c. 10-fold with cell age towards the leaf tip. Similar decreases in respiration with tissue age have been demonstrated in *P.sativum* (Smillie, 1962; Geronimo & Beevers, 1964), *P.vulgaris* (Azcón-Bieto *et al.*, 1983), *F.arundinacea* (Volenec & Nelson, 1984b) and *P.persica* (Merlo *et al.*, 1993). Despite the high rates of respiration in the elongation zone of the leaf (c. 0-20 hours), both the carbohydrate concentration per cell increases, and the level of carbohydrates (per g⁻¹ fwt) are greatest within this region, which implies that the basal region of the leaf blade is a carbon sink.

The decline in the rates of respiration during leaf development have been associated with a decrease in the rate of glycolysis. Azcón-Bieto *et al.*, (1983) found that the O₂ uptake rates of *P.vulgaris* leaf slices in the presence of sucrose and the uncoupler, FCCP, decreased with leaf age. The activity of enzymes associated with glycolysis and OPPP have also been found to change during leaf development. The activity of the glycolytic enzyme, PFK was found to be highest in the young leaf primordia of *Dianthus chinensis*, and decreased with leaf age (Croxdale, 1983). The activity of the OPPP enzyme, G6PDH, has also been shown to decrease with leaf age in *D.chinensis*

(Croxdale & Outlaw, 1983). The highest activity of G6PDH was found in leaf primordia in which the activity of PFK had already begun to decline, and Croxdale & Pappas (1987) suggested that in very young leaf cells, oxidation of carbohydrates is by glycolysis, and that the OPPP becomes more important in the later stages of development. There is also evidence to indicate that the reduction in respiration during development may be the result of changes in mitochondrial electron transport activity. Azcón-Bieto *et al.*, (1983) found the decreased rate of dark respiration of leaf slices and isolated mitochondria from *P.vulgaris* during development, was largely due to a decline in the activity and capacity of the phosphorylating cytochrome pathway, and that the capacity of the non-phosphorylating pathway remained constant. During development mitochondria become less tightly coupled in respect to oxidative phosphorylation, therefore resulting in a decrease in the electron transport capacity. Further evidence of changes in capacity of mitochondrial electron transport during development, comes from the work of Geronimo & Beevers (1964), in which they found that mitochondria isolated from older leaves of *P.sativum* had fewer cristae, and suggested that such a change in the inner membrane surface area might affect the activity and capacity of the cytochrome chain.

The results of the previous chapter showed a linear increase in mitochondrial TA in mesophyll cells aged *c.* 25Hrs and more. Despite the increase in mitochondrial TA, the V_v of cytoplasm occupied by mitochondria remained constant, and it was suggested that during leaf development autolysis and/or fusion was possibly resulting in fewer, larger mitochondria per cell. It is well established that the respiratory capacity of a tissue is related to mitochondrial numbers, *e.g.* *Arum* spadix with high respiratory rates are composed of cells with numerous mitochondria (Mewcomb, 1990). The reduction

in dark respiration (per leaf area) during leaf development, may therefore be related to a possible reduction in the number of mitochondria per cell, and this needs to be investigated further.

With the decrease in rate of dark respiration, there is the concurrent increase in the rate of photosynthesis during leaf development. In meristematic cells, proplastids (chloroplast precursors) are unable to synthesise ATP (Webber *et al.*, 1984), and are dependent upon respiration for a supply of energy. As the chloroplasts develop there is an increase in the supply of ATP from photophosphorylation and mitochondrial ATP synthesis decreases (Hampp & Wellburn, 1980). This transition in the supply of ATP, from the mitochondria to the chloroplast, signifies a change in the metabolic status of the cell from heterotrophic to autotrophic.

In this study the rate of photosynthesis (per leaf area) increased *c.* 30-fold during mesophyll cell development from the base to the tip of the leaf blade of control-grown plants. Similar increases in the rate of photosynthesis during leaf development have been observed in *T. aestivum* L. cv. Maris Huntsman (Tobin *et al.*, 1988) and *Z. mays* (Baker & Leech, 1977). The acquisition of photosynthetic competence during leaf development can be related to several factors, including changes in the chloroplast population, *e.g.* an increase in chloroplast size and number per cell (see Chapter 5), and photosynthetic enzymes, *e.g.* Rubisco (Dean & Leech, 1982b). The increased photosynthetic capacity during leaf development found in this study can be related to the *c.* 3-fold increase in the proportion of mesophyll cell occupied by chloroplasts, due to an increase in both chloroplast size (*c.* 9-fold; see Section 5.6.2.2), and number per mesophyll cell (see Section 5.7). The results of this chapter show that the increase in photosynthesis (per leaf area) during leaf development is the result of an increase in both the number of

chloroplasts per cell, resulting in an increase in photosynthesis per cell, and also an increase in the photosynthetic capacity of individual chloroplasts during development. Dean & Leech (1982b) found the concentration of Rubisco per mesophyll cell increased 20-fold along the length of the primary leaf of wheat (*T. aestivum* L. cv Maris Dove), and in an accompanying study to the present one, the concentration of both the large and small subunits of Rubisco were shown to increase from the base to the tip of the leaf (Personal communication, M.A. Bond). Rubisco has been shown to constitute up to 50% of total soluble proteins in the leaf (Ellis, 1979), and the c. 4-fold increase in total soluble protein (per mesophyll cell) from the base to the tip of the leaf, reported in this chapter may be the result of the increased concentration of Rubisco associated with the increased photosynthetic capacity.

A close association has also been shown to exist between chl levels and photosynthetic development (Baker & Leech, 1977; Viro & Kloppstech, 1980). In this study both chl a and chl b (per g⁻¹ fwt & per chloroplast) increased c. 10-fold along the length of the leaf blade of control-grown plants. Similar increases in chl (per plastid) during leaf development have been found along the length of the primary leaf of wheat (*T. aestivum* L. cv. Maris Dove) (Boffey *et al.*, 1980), and barley (*H. vulgare*) (Barkdardottir *et al.*, 1987), with increases in chl levels of 8-fold and 9-fold respectively. The location of chl a and chl b within the chloroplast means that changes in the ratio of chl a:b during development can be related to changes in chloroplast ultrastructure and the increased photosynthetic capacity. Chlorophyll a and chl b are distributed between PSI (chl a & b) which is located predominantly on the unstacked, stromal thylakoids, and PSII (mainly chl b) found predominantly on the stacked, granal thylakoids (Anderson, 1986). The ratio of chl a:b was highest in the leaf base, c. 3.6,

and decreased within the elongation zone to *c.* 3.2, after which the ratio remained constant. As the chloroplast develops there is a *c.* 3-fold increase in the number of granal sacs per granum (see Section 5.6.3.3), suggesting an increase in PSII relative to PSI. A similar pattern in the ratio of chl a:b during leaf development has been reported previously in *T. aestivum* L. cv Maris Dove by Boffey *et al.*, (1980), and in the same study a chl a:b ratio of 3.4 was found for mature tissue which is comparable to that found in this study.

In addition to the increase in the rate of photosynthesis during leaf development, the results of this chapter also show that photosynthetic efficiency increases with development. The quantum yield (QY), which is derived from the regression of the initial slope of the light response curve, is a measure of the maximum photosynthetic efficiency, *i.e.* the efficiency of light energy conversion into photosynthate (Walker, 1990). The results of this chapter show that the QY doubles along the length of the leaf blade, and this can be related to the linear increase in granal stacking (*c.* 3-fold) during leaf development as reported in the previous chapter, which may increase the efficiency of light capture by increasing the density of light harvesting units (Anderson *et al.*, 1973). In a study by Baker & Leech (1977), the initial slope of the light response curve of leaf sections taken along the length of the *Z. mays* leaf increased with development. As QY is derived from the regression of the slope, the data suggest that the photosynthetic efficiency increased during development, which is in agreement with the increased QY reported by Baker & Ort (1992), also during *Z. mays* leaf development.

6.13 Effects of UV-B on Carbon Metabolism During Leaf Development

A reduction in photosynthesis is a frequently observed response to UV-B and has been reported in a variety of species including *P.sativum* (Day & Vogelmann, 1995), *O.sativa* (Teramura, Ziska & Szein, 1991), and *G.max* (Teramura *et al.*, 1984). Although there is no general consensus on the mechanisms involved, alterations in photosynthetic capacity under UV-B have been shown to be the result of direct responses, *i.e.* changes in photosynthetic enzymes, *e.g.* Rubisco (Vu *et al.*, 1984), and disruption of the PSII reaction centre (Strid *et al.*, 1990), and/or indirect responses, *i.e.* changes in stomatal number and function (Day & Vogelmann, 1995; Dai *et al.*, 1995), photosynthetic pigments (Deckmyn *et al.*, 1994), and tissue and cell structure (He *et al.*, 1994)(see Section 1.6.2). As with a number of other parameters, such as plant growth (see Chapter 3), the response of photosynthesis to UV-B varies between species and cultivars. For example, the photosynthetic capacity of wheat has been shown to be both sensitive (*T.aestivum* L. cv. Obelisk)(Rozema *et al.*, 1991), and resistant (*T.aestivum* L. cv. Bannock)(Beyschlag *et al.*, 1988) to UV-B. A major factor determining the effect of UV-B on photosynthesis is the interaction with other environmental variables, for example both light (Mirecki & Teramura, 1984) and nutrients (Murali & Teramura, 1985) have been shown to modify the response of photosynthesis to UV-B (as discussed in Section 1.7.1). Differences in growth conditions must therefore be taken into account when comparing the response of photosynthesis to UV-B between different studies.

The previous chapter showed that the mesophyll cells of UV-B grown plants contained more, smaller chloroplasts than control-grown plants, and it is suggested that such an alteration might affect photosynthetic capacity. The work described in this chapter shows that in UV-B-grown plants, the rate of photosynthesis (per chloroplast)

was reduced in mesophyll cells aged *c.* 40 hours and more. However, as the mesophyll cells of UV-B-grown plants contain more chloroplasts per cell as compared to control-grown plants (see Section 5.7), when the rate of photosynthesis is expressed on a per cell basis and per g^{-1} fwt tissue, UV-B has no overall effect on the photosynthetic rate of the developing primary leaf. The results of this study also show that UV-B has no effect on the relative quantum yield during the development of the primary leaf of wheat, and that the 'maximum' rate and efficiency of photosynthesis, found in older tissue towards the leaf tip, was similar in both control and UV-B-grown plants. Similar insensitivity in both the rate and the efficiency of photosynthesis to UV-B has been reported previously in *T. aestivum* L. cv. Bannock (Beyschlag *et al.*, 1988; Teramura, Sullivan & Ziska, 1990), and other species in which photosynthesis has been shown to be tolerant to UV-B include *L. styraciflua* (Dillenburg *et al.*, 1995), *Manihot esculentum* (cassava; Ziska *et al.*, 1993) and *P. vulgaris* (Deckmyn & Impens, 1995).

Despite the alteration in mesophyll cell ultrastructure, *e.g.* more, smaller chloroplast per mesophyll cell, reported in the previous chapter, the work described in this chapter shows that although UV-B reduces the rate of photosynthesis per chloroplast, when the difference in chloroplast number per cell is taken into account UV-B has no overall effect on the developmental changes in either the rate or efficiency of photosynthesis. A possible explanation for this observation, may be made from the reports by Leech and co-workers from a number of studies on chloroplast division in different varieties of *T. aestivum* (Ellis & Leech, 1985) and the *arc* (accumulation and replication of chloroplasts) mutants of *A. thaliana* (Pyke & Leech, 1991, 1992, 1994). In these studies Leech and co-workers found that it was the 'cover' of cells by chloroplasts that was the critical factor in determining the chloroplast content, which in turn would

influence the photosynthetic capacity of the cell. For example, the *arc* mutants of *A.thaliana* show varying numbers of chloroplasts per mesophyll cell of a given size, however, the ratio of total chloroplast area to cell area remains virtually constant over a seven-fold range of chloroplast numbers per cell (Pyke & Leech, 1991). Leech and co-workers suggested that as chloroplast cover will influence the efficiency of light harvesting, a mechanism exists (as yet unidentified) that means during development chloroplasts will grow and divide until the 'optimum' cover is achieved in each photosynthetic cell. Mesophyll cells with more, smaller chloroplasts, e.g. UV-B grown plants of this study (see Section 5.9), may therefore have a similar photosynthetic capacity to mesophyll cells with fewer, larger chloroplasts, e.g. control plants of this study (see Section 5.8).

During normal leaf development a close association has been found to exist between photosynthesis and chl concentration (see Section 6.12 (Viro & Kloppstech, 1980)). In this study the concentration of both chl a and b (per chloroplast) in UV-B-grown plants was reduced in mesophyll cells aged *c.* 20 hours and more. However, as with the photosynthesis data, the fact that there are more chloroplasts per mesophyll cell in UV-B-grown plants (see Section 5.9), there is no overall effect of UV-B on the developmental increase in either chl a or chl b (per g⁻¹ fwt), and the maximum concentration of chl a and chl b found in older tissue towards the tip of the leaf blade was similar in both control and UV-B-grown plants. Similar insensitivity of both chl a and chl b to UV-B has been reported in *C.sativus* (Takeuchi *et al.*, 1989) and arctic grass species *C.pupurea* (Gwynn-Jones & Johanson, 1996).

Chlorophyll has been identified as being one of the primary targets of UV-B within the photosynthetic apparatus (Bornman, 1989), which may result in an reduction

in both the rate and efficiency of photosynthesis. Chlorophyll b content has been shown to be more readily reduced by UV-B than chl a (Tevini *et al.*, 1983). This may be the result of the spatial distribution of chl within LHCI-PSI and LHCII-PSII (Renger *et al.*, 1989; Strid *et al.*, 1990). Although UV-B may exert a differential effect on chl a and chl b, the overall common response to UV-B is a reduction in total chl which has been reported for a variety of species including *P.vulgaris* (Tevini *et al.*, 1981; Deckmyn & Impens, 1995) and *P.sativum* (Vu, Allen & Garrard, 1984). Recent data from molecular studies suggest that there are no specific effects of UV-B on the enzymes involved in chl biosynthesis, but instead the increased degradation of chl under UV-B is correlated to a down-regulation in the expression of genes critical for chl binding proteins, *e.g.* *cab* (Jordan *et al.*, 1991; Strid & Porra, 1992). In addition to altering chl concentrations, UV-B has also been shown to result in a shift in the distribution of chl to the abaxial mesophyll surface, deeper in the leaf tissue (Day & Vogelmann, 1995). The UV-B fluxes are relatively low in this region of the leaf tissue (Bornman & Vogelmann, 1991), and therefore the redistribution of chl may be regarded as a UV-B induced protective mechanism. The distribution of chl a and chl b between LHCI-PSI and LHCII-PSII, means that the ratio of chl a:b may give an indication of the ratio of PSI:PSII. In this study the ratio of chl a:b in UV-B grown plants was constant along the length of the leaf blade at *c.* 3.0, which is similar to the ratio found in control-grown plants. The fact that there are no UV-B induced changes in the ratio of chl a:b is consistent with the similar developmental increases in the number of granal sacs per granum found in both control and UV-B-grown plants (see Section 5.6.3.3), and suggests that UV-B is having no effect on the development of either PSI or PSII.

The primary CO₂ fixing enzyme of C₃ photosynthesis, Rubisco, which may represent up to 50% of total soluble leaf protein, has also been shown to be a primary target of UV-B, which may result in altered photosynthesis. Both Rubisco content and enzyme activity may be inhibited by UV-B exposure (Vu *et al.*, 1984; Jordan *et al.*, 1992, 1994), and reductions in Rubisco content have been correlated to reductions in total soluble leaf protein (Vu *et al.*, 1984; He *et al.*, 1993). In an accompanying study to the present one, UV-B had no effect on the Rubisco content along the length of the primary leaf of wheat (personal communication, M.A.Bond), which is consistent with the unchanged photosynthesis (per leaf area) and chlorophyll content (per g⁻¹ fwt) of UV-B-grown plants reported in this chapter. Despite the unchanged Rubisco content, the results of this chapter show that UV-B increased the concentration of total soluble leaf protein in mesophyll cells aged *c.* 20 hours and more. A similar increase in soluble leaf protein was reported by Tevini *et al.*, (1981) in *H.vulgare*, *Z.mays*, *P.vulgaris* and *R.sativus* grown under UV-B, and it was suggested that the increased protein may be a reflection of increased synthesis of aromatic amino acids, which are the precursors for flavonoid biosynthesis. Although in the present study there is no evidence to show increased synthesis of the aromatic amino acid precursors of flavonoids, UV-B was found to increase the free pool of protein amino acids and this may be related to the increased protein concentration (see Section 6.9).

Carbon metabolism consists of numerous, highly co-ordinated processes, of which photosynthesis is only one aspect. The ultrastructural changes, *e.g.* more, smaller chloroplasts per mesophyll cell, found in response to UV-B in the previous chapter, may therefore affect other aspects of carbon metabolism. Additional studies were undertaken to relate ultrastructural changes, with any UV-B induced changes in carbon partitioning,

e.g. carbohydrate status and amino acid metabolism of the developing primary leaf.

Changes in the concentration of carbohydrate have been detected in response to UV-B (Takeuchi *et al.*, 1989; Santos *et al.*, 1993; He *et al.*, 1994). In a study by Takeuchi *et al.*, (1989), the total content of sugars in *C.sativus* cotyledons irradiated with UV-B for 8 days was *c.* 40% of control levels, and was the result of significant reductions in glucose, fructose and sucrose. A similar reduction in soluble sugars, paralleled by an increase in starch, was reported by He *et al.*, (1994) in the leaves of *P.sativum* irradiated with UV-B for 3+ days. He *et al.*, (1994) related the changes in carbohydrates to the disruption of chloroplast ultrastructure under UV-B (*i.e.* dilation of thylakoid membranes, see Section 5.9), and suggested that the increased starch was due to the cells lack of ability to mobilise the starch as a result of membrane damage leading to the loss or destruction of mobilizing enzymes, which would severely inhibit photosynthesis and lead to a reduction in soluble sugars. The results of this chapter show that UV-B had no effect on concentration of either soluble or insoluble carbohydrates (per g⁻¹ fwt & per cell) along the developmental gradient of the primary leaf of wheat. As carbohydrates are among the principle products of CO₂ assimilation, the unchanged carbohydrate concentrations are consistent with the observation that UV-B had no effect on the photosynthetic activity (per leaf area) of the primary leaf of wheat. Carbohydrate is the major respiratory substrate in plants, and therefore forms the link between photosynthesis and respiration.

Compared to the large number of studies into the effects of UV-B on photosynthesis, there has only been a limited number of studies investigating the response of respiration to UV-B. The rate of dark respiration has been shown to be unaffected by UV-B in the majority of these studies, on a variety of species including,

G.max (Teramura *et al.*, 1980; Teramura *et al.*, 1984), *L.styraciflua* (Dillenburg *et al.*, 1995), *C.sativus* (Takeuchi *et al.*, 1989) and *M.esculentum* (Ziska *et al.*, 1993). As stated previously, the respiratory capacity of a tissue has been shown to be closely correlated to mitochondrial numbers. The results of the previous chapter showed a UV-B induced reduction in the average mitochondrial TA in mesophyll cells aged *c.* 50 hours and more (see Section 5.6.2.4). Despite the reduction in mitochondrial TA, the V_v of cytoplasm occupied by mitochondria was similar in both control and UV-B-grown plants (see Section 5.6.2.3), and it was suggested that there are more, smaller mitochondria in UV-B-grown plants. The results described in this chapter show that the developmental changes in the rate of dark respiration, *i.e.* highest in younger cells at the leaf base and decreasing with cell age towards the leaf tip, was similar in both control and UV-B-grown plants. The rate of dark respiration in UV-B-grown plants, however, was slightly higher throughout the length of the leaf blade as compared to controls, and might be a result of the possible increase in mitochondrial numbers in UV-B-grown plants. The large standard errors of the dark respiration data probably means that the differences between control and UV-B-grown plants are not significant. However, the possible link between changes in mitochondrial populations and dark respiration induced by UV-B warrents further investigation.

6.14 Changes in Amino Acid Free Pools During Leaf Development

Developing wheat leaves receive most of their nitrogen as nitrate, which is transported from the roots via the xylem and thus the starting point for amino acid biosynthesis is via the GS/GOGAT cycle (Sechley *et al.*, 1992). The synthesis of gln and glu, and their subsequent metabolism to other amino acids requires energy (ATP) and reducing power (Fd_{red} , NADH) supplied by either photosynthetic or respiratory processes, and carbon-skeletons, which are predominantly intermediates of respiratory metabolism (Dennis & Turpin, 1990). Changes in both nitrogen and carbon assimilation during development may therefore be paralleled to changes in amino acid metabolism.

Plant cells contain appreciable amounts of free amino acids, and changes in the size of amino acid pools have been observed during leaf development in *Z.mays* (Chapman & Leech, 1977) and *C.arietinum* (Laurie & Stewart, 1993). Although pool sizes do not reflect amino acid flux, they do represent the balance between amino acid synthesis and utilization. Changes in pool sizes during leaf development therefore may be related to the changing metabolic status of the cell. The results of this study show the pool size of free amino acids to be greatest in the elongation zone of the leaf (*c.* 0-20 hours), and then to decrease with cell age along the length of the leaf blade. The high free amino acid pool size of the elongation zone is a result of the high cell number within this region (see Section 4.5.1), and the concentration of free amino acids per mesophyll cell increases linearly (*c.* 4-fold) from the base to the tip of the leaf. The changing pool size of free amino acids (per g^{-1} fwt) during primary wheat leaf development, is in agreement with the observations in *Z.mays* (Chapman & Leech, 1977) and *C.arietinum* (Laurie & Stewart, 1993), in which the concentration of free amino acids decreased with tissue age. In this study glutamate, glutamine, aspartate,

asparagine, serine and alanine were the most abundant amino acids present along the length of the leaf blade, and constituted *c.* 65% of the total free amino acid pool. A similar pattern in amino acid pool sizes was reported by Chapman & Leech (1977), with asparagine, aspartate, serine, glutamate, alanine and glycine constituting *c.* 88% of the total free amino acid pool throughout *Z.mays* leaf development. The change in the total amino acid pool size during *C.arietinum* leaf development reported by Laurie & Stewart (1993) however, was the result of a change in the size of the asparagine pool whilst the level of other amino acids remained constant. Amides such as asparagine and glutamine are used as nitrogen transport compounds (Ireland, 1990), and the high amino acid content (including asparagine and glutamine) found in the young leaf tissue of *C.arietinum* (Laurie & Stewart, 1993), *Z.mays* (Chapman & Leech, 1977) and *T.aestivum* may reflect the import of nitrogen into the developing leaf for protein synthesis. Gastal, Nelson & Coutts (1992) found that the rates of nitrogen deposition in tall fescue (*F.arundinacea*) were maximal in the elongation zone of the leaf blade, the same region in which the soluble protein concentration was highest (Volenc & Nelson, 1984b). The results of this chapter show that the highest levels of soluble proteins (per g^{-1} fwt) are present in the elongation zone of the leaf blade, and therefore the high levels of amino acids (per g^{-1} fwt) in this region of the leaf may be a reflection of the high demand for amino acids for protein synthesis.

The changes in amino acid pool sizes found during wheat leaf development indicate an alteration in the balance between amino acid synthesis and/or utilization. Although it remains to be determined which process is specifically responsible for the changing pool sizes during development, ^{14}C flux measurements (see Section 6.11) will give some indication as to whether UV-B is altering the flow of photosynthetically

assimilated carbon into and between the amino acid free pools.

6.15 Effect of UV-B on Amino Acid Free Pools During Leaf Development

Amino acids are the organic product of inorganic nitrate assimilation. In addition to their structural role in proteins, amino acids are involved in transporting nitrogen around the plant, are the precursors in the synthesis of chlorophyll and other nitrogen containing compounds, and serve as a source of carbon and nitrogen in the production of secondary metabolites (Reviews: Sechley *et al.*, 1992; Huppe & Turpin, 1994). Despite their obvious importance and the fact that amino acids provide a link between nitrogen and carbon metabolic pathways (see Section 6.1.4), very few studies have investigated the effects of UV-B on nitrogen metabolism. The majority of these studies have been on phytoplankton (Döhler, 1992; Goes *et al.*, 1995a,b), and to date there are only two known studies on the response of higher plant nitrogen metabolism to UV-B, those of Saralabai, Thamizhchelvan & Santhaguru (1989) on the angiosperm *Crotolaria juncea*, and Appenroth *et al.*, (1993) on *Spirodela polyrhiza*. These studies have shown UV-B to alter various aspects of nitrogen metabolism, ranging from the rate of nitrogen uptake (Döhler, 1992), the activity of the key enzymes of nitrate assimilation, including nitrate reductase (NR), nitrite reductase (NiR) and glutamine synthetase (GS)(Appenroth *et al.*, 1993; Sinha *et al.*, 1995), and the pool sizes of amino acids (Döhler, 1992; Goes *et al.*, 1995; Braune & Döhler, 1996).

The results described in this chapter show that the total amino acid pool size was increased along the length of the primary leaf grown under UV-B. This increase is a result of selective changes in the pool sizes of specific amino acids under UV-B, which were either unchanged or increased from the levels found in control-grown plants. The

most abundant amino acids were the same in both control and UV-B-grown plants. However, UV-B increased the levels of three of the six most abundant amino acids, glutamate, aspartate and serine, and as these constitute a large proportion of the total pool, will be the main cause of the increased pool size. Similar increases in the pool sizes of glutamate and aspartate in response to UV-B have also been found in a variety of marine phytoplankton (Döhler, 1992; Goes *et al.*, 1995a,b). In this study the soluble protein content of UV-B-grown plants was greater than that of controls, and therefore the increased free amino acid pool under UV-B may be a reflection of an increased demand for amino acids for protein synthesis. As stated previously, the developing wheat leaf receives most of its nitrogen as nitrate from the root, and the starting point for amino acid biosynthesis is via the GS/GOGAT cycle (Sechley *et al.*, 1992). UV-B induced changes in the activity of enzymes associated with nitrogen assimilation have been found in response to UV-B, including the stimulation of NR activity in cyanobacteria (Sinha *et al.*, 1995), *C. juncea* (Saralabai *et al.*, 1989) and marine diatoms (Döhler, 1990), and the inhibition of GS activity in cyanobacteria (Sinha *et al.*, 1995), marine diatoms (Döhler, 1985) and *S. polyrhiza* (Appenroth *et al.*, 1993). Such changes in the activity of NR and GS in response to UV-B could result in an alteration in amino acid free pools, however it remains to be determined if the activity of any of the enzymes associated with nitrogen assimilation are altered in the primary leaf of wheat grown under UV-B.

The synthesis of amino acids requires energy (ATP), reducing power (NADH) and carbon-skeletons, which are supplied by either photosynthetic or respiratory processes. The results of this chapter show that UV-B has no effect on the rates of either photosynthesis or respiration, and therefore the potential supply of energy and

reductant for amino acid synthesis is the same in control and UV-B-grown plants. Most of the carbon-skeletons used in amino acid synthesis are intermediates of respiratory metabolism, with pyruvate, oxaloacetate (OAA) and α -ketoglutarate, from glycolysis and the TCA cycle serving as the major withdrawal points for organic carbon. Significant amounts of phosphoenolpyruvate (PEP) and acetyl Co-A are also used in amino acid synthesis, and the carbon-skeletons for the photorespiratory synthesis of glycine and serine are provided by the Calvin cycle (see Fig. 6.22).

6.15.1 The Incorporation of ^{14}C Into Amino Acid Free Pools

The higher levels of soluble protein found in UV-B-grown plants suggests that there might be an increase in flux, both into and out of the amino acid pools. In order to compare the flow of carbon into the most abundant amino acid pools of control and UV-B-grown plants, leaves were exposed to $^{14}\text{CO}_2$ for 10 minutes and the incorporation of ^{14}C into the amino acid pools measured over a cold chase period of 120 minutes (see Section 2.15.2). The total amount of ^{14}C label incorporated into the total free amino acid pool was comparable in control and UV-B-grown plants (*c.* 5%; data not shown). This suggests control and UV-B-grown plants have a similar rate of photosynthetic carbon assimilation, and is consistent with the unchanged photosynthetic capacity and efficiency of UV-B-grown plants as compared to controls reported previously in this chapter.

6.15.1.1 Glycine and Serine

Glycine and serine are products of photorespiration, and the accumulation of ^{14}C into the glycine and serine pools, via carbon-skeletons of the Calvin cycle, shows that the plants were actively photorespiring. The ^{14}C label found in glycine and serine pools of control and UV-B-grown plants decreased rapidly over time to a constant 'basal' level,

indicating a rapid turnover of both pools. The initial level of ^{14}C label found in serine of UV-B-grown plant was slightly higher than that found in the control, however the label decreased more quickly under UV-B which suggests that UV-B may be stimulating serine utilization.

6.15.1.2 Aspartate

After the initial 10 minutes of labelling the majority of the ^{14}C incorporated into the abundant amino acids was found in the aspartate pool, in both control and UV-B-grown plants. This rapid incorporation of ^{14}C into the aspartate pool may be due to the fact that the carbon-skeleton of aspartate is OAA, which can be formed via a one-step reaction involving PEP and CO_2 . The level of ^{14}C in the aspartate pool remained constant throughout the chase period, indicating a slow turnover rate, with no effect of UV-B.

6.15.1.3 Glutamate

The accumulation of ^{14}C in the glutamate pool increased to a maximum level 30 minutes into the chase period, in both control and UV-B grown plants. The longer time period taken for the maximum level of ^{14}C to be incorporated into the glutamate pool compared to that of the aspartate pool may be due to the fact that the incorporation of ^{14}C from CO_2 into α -ketoglutarate, the carbon-skeleton of glutamate is via five reactions (see Fig. 6.22), as compared to the one-step incorporation of ^{14}C into OAA. The free glutamate pool size is greater in UV-B grown plants, however the rate at which ^{14}C label increases in the glutamate pool during the initial 30 minutes is slower under UV-B as compared to control-grown plants. This suggests that the larger free glutamate pool size found in UV-B grown-plants is not due to an increase in the rate of glutamate formation, but due to a decrease in the rate of utilization.

6.15.1.4 Asparagine

The level of ^{14}C label found in the asparagine pool of control-grown plants remained constant throughout the chase period. The initial level of ^{14}C in the asparagine pool of UV-B-grown plants was slightly higher than that found in the control, however this decreased to a basal level similar to control-grown plants 30 minutes into the chase period. The relatively constant level of ^{14}C label in the asparagine pool indicates a slow turnover rate, with no effect of UV-B.

6.15.1.5 Glutamine

The incorporation of ^{14}C into the glutamine pool of control-grown plants remained constant throughout the chase period and indicates a slow turnover of the pool, as compared to the ^{14}C label in the glutamine pool of UV-B-grown plants which increased throughout the chase period, indicating an increased flow of ^{14}C labelled carbon-skeletons into glutamine. This difference in the ^{14}C labelling pattern of the glutamine pool of control and UV-B-grown plants suggests that UV-B is increasing the flow of photosynthetically assimilated carbon via glycolysis or the TCA cycle into the synthesis of amino acids.

6.15.1.6 Consequences of UV-B Radiation on the flow of Carbon Into Amino Acid Free Pools

The incorporation of ^{14}C into the total amino acid free pool, and the direct measurements of photosynthesis and carbohydrate status, suggests that UV-B is having no effect on the primary assimilation of carbon and its partitioning into carbohydrates. However, the changes observed in the flux of photosynthetically assimilated ^{14}C into amino acid free pools, suggests UV-B is affecting carbon partitioning at the amino acid level. The changing pattern of ^{14}C label incorporated in the major amino acids suggests

UV-B is altering the flow of carbon, for example, the flux of ^{14}C through the serine and glutamate free pools indicates UV-B is increasing the rate of serine utilization and decreasing glutamate utilization.

6.16 Summary

The work described in this chapter shows that different aspects of carbon metabolism vary in their response to UV-B. For example, UV-B has no effect on the photosynthetic capacity and efficiency, dark respiration, and carbohydrate status of the primary leaf. However, changes in the development of amino acid metabolism in the primary leaf were observed. Alterations in the metabolic development of the primary leaf of UV-B-grown plants, found in this chapter, can be correlated to the changes in the mesophyll cell ultrastructure of UV-B-grown plants found in the previous chapter. For example, the smaller chloroplasts of UV-B-grown plants (see Section 5.9) had a reduced photosynthetic rate, as compared to the larger chloroplasts of control plants. However, the increased number of chloroplasts per mesophyll cell found in UV-B-grown plants (see Section 5.9), resulted in no overall difference in the rate of photosynthesis (per leaf area) between control and UV-B-grown plants. The effect of UV-B on the developmental changes in amino acid metabolism, was to increase the size of the total free amino acid pool. Such a change in amino acid free pools, may be the result of alterations in carbon and/or nitrogen metabolism in response to UV-B. The results of this chapter suggest that although UV-B has no effect on photosynthetic carbon assimilation and its subsequent partitioning into carbohydrates, the partitioning of carbon into amino acid free pools suggest that UV-B is altering some aspect of carbon/nitrogen metabolism. Whether this is a direct effect of UV-B on nitrogen metabolism or an

indirect effect, *i.e.* via changes in the supply of ATP, NADPH or carbon skeletons from photosynthesis or respiration is yet to be determined.

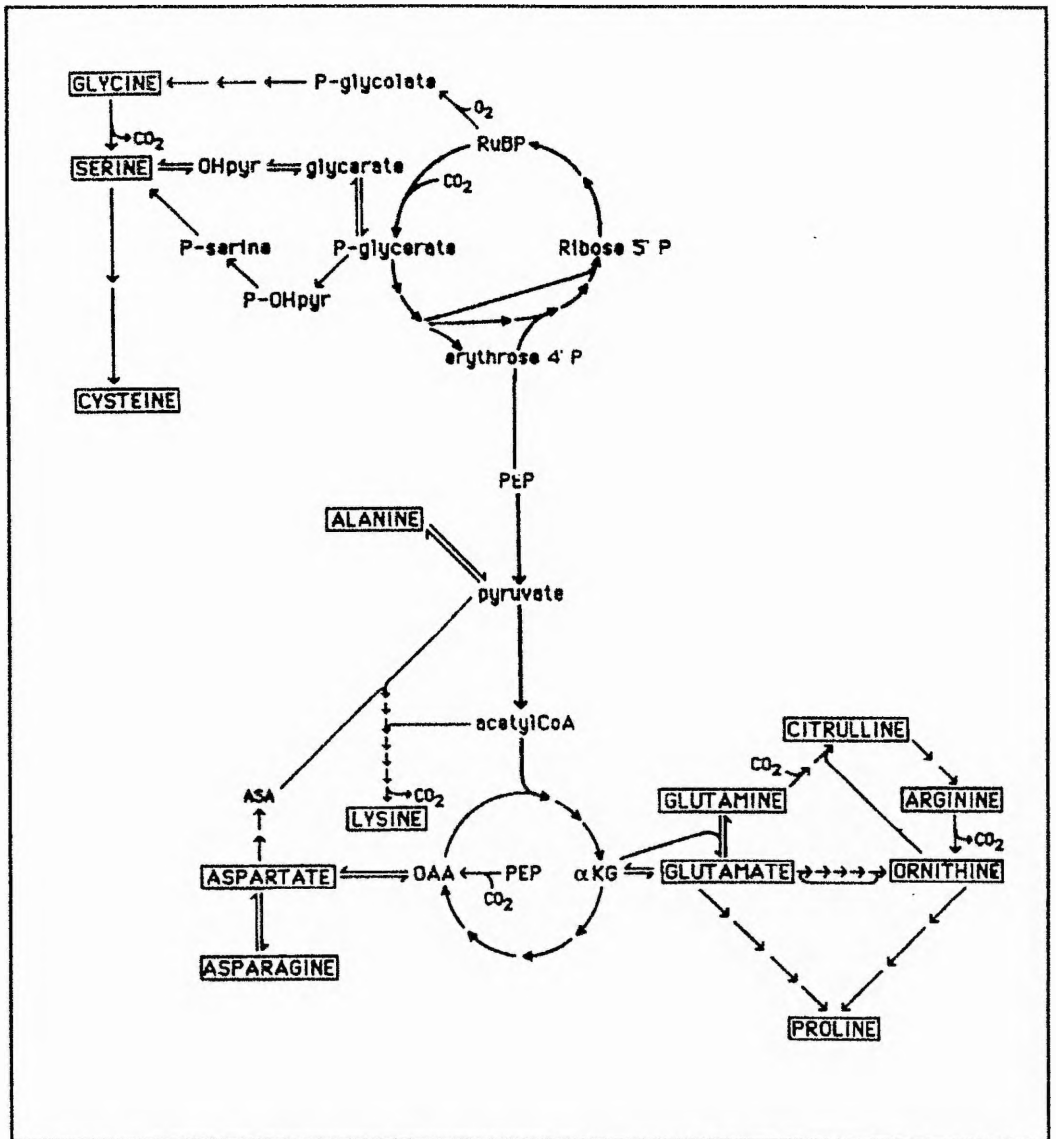


Fig. 6.22 Carbon Flow in Amino Acid Biosynthesis

Each arrow represents a separate reaction.

PEP- phophoenol pyruvate; OAA - oxaloacetic acid; α KG - α ketoglutarate, OHpyr - hydroxy pyruvate; P-OHpyr - phosphohydroxy pyruvate; ASA - aspartate semialdehyde; RuBP - ribulose-1,5-bisphosphate (After Ireland, 1990).

CHAPTER 7
General Discussion

The aim of this thesis was to determine the effects of UV-B radiation on the development of the primary leaf of wheat, at the cellular, subcellular and metabolic levels. The majority of research investigating the effects of UV-B radiation on leaves has used tissue harvested at a specific developmental stage. Although such studies provide information about the ultimate effects of UV-B, they do not take into account possible differences in UV-B responses during leaf development. For this study the primary leaf of wheat, in which a gradient of cell age and development occurs from the base to the tip of the leaf blade, provided a simple model system in which to investigate the effects of UV-B on leaf development. This system allowed for the comparison of UV-B effects on a range of cell developmental stages, and also for direct comparisons to be made between cells of the same age in control and UV-B-grown plants.

7.1 Changes in Leaf Morphology in Response to UV-B

The results of this study show that UV-B alters the morphology of the primary leaf of wheat, resulting in a shorter, broader, thicker leaf blade (see Section 3.6). Similar changes in leaf morphology have been frequently observed in a variety of plant species, including *A. sativa* (Barnes *et al.*, 1988), *T. aestivum* L. cv Bannock (Barnes *et al.*, 1990) and *C. sativus* (Takeuchi *et al.*, 1989). The UV-B induced changes in leaf morphology found in this study may have adaptive consequences by affecting the degree to which sensitive cellular targets, *e.g.* chloroplasts of mesophyll cells, are exposed to UV-B. A reduction in leaf growth rate, which delays the emergence of the primary leaf from the coleoptile, has been suggested (Wellmann, 1983; Ballaré *et al.*, 1995b) to play a protective role by minimizing the exposure of the leaf to UV-B until it has accumulated UV-B screening pigments, *e.g.* flavonoids. Similarly, increased leaf thickness induced

by UV-B has also been suggested to protect against UV-B damage, by lengthening the optical path between the leaf epidermis and the mesophyll tissue (Bornman & Vogelmann, 1991). Flavonoid analysis and measurements of the flux of UV-B into the leaf using quartz-fibre optic microprobes (Cen & Bornman, 1993), would enable the determination of whether such adaptive mechanisms also occur in the primary leaf of UV-B-grown wheat.

7.2 UV-B Induced Changes in Cell Division and Elongation Alter Leaf Morphology

Both cell division and elongation contribute to leaf growth. The spatial and temporal distribution of these processes in the primary leaf provide a system in which the specific mechanism(s) involved in the observed reduction in leaf growth under UV-B could be identified.

The UV-B induced reduction in growth rate was found to be the result of altered cell division and elongation. Changes in cell division, measured as an increase in cell number have been reported previously in *R.patientia* leaves (Dickson & Caldwell, 1978) and *C.sativus* cotyledons (Tevini & Iwanzik, 1986). The growth pattern of the primary leaf used in this study allowed for the distinction between cell division rates (mitotic index) and duration (cell doubling time). Both were altered by UV-B, resulting in fewer mitotically active cells (see Section 4.4.1), with significantly longer CDTs (see Section 4.4.2), which may account in part for the reduced growth rate. Analysis of the duration of individual cell cycle phases, as described by Moses, Ougham & Francis (1997), would lead to further understanding of the specific mechanisms involved in the UV-B alteration of cell division. For example, it has been suggested (see Staxén *et al.*, 1993) that DNA repair of UV induced damage, prior to replication, may result in a longer S

phase and a delay in the progression through the cell cycle. The results of my study also show that plants grown under UV-B had a shorter zone of elongation, and a reduced rate of elongation within this zone (see Section 4.5.4). Similar changes in cell elongation in response to UV-B, resulting in reduced growth rates have been reported in a number of plants, including *H.vulgare* leaves (Liu *et al.*, 1995) and *L.esculentum* hypocotyls (Ballare *et al.*, 1995b).

It is interesting to note that both cell division and elongation occur within the basal 20mm of the leaf blade. This region of the leaf is surrounded by the coleoptile, which has been suggested to protect against UV-B (Hausstätter, Rohde & Weissenböck, 1996). Therefore, are the changes observed in cell division and elongation the result of direct effects, induced by UV-B penetrating the coleoptile, or indirect effects, in response to older cells above the coleoptile 'sensing' the UV-B? The synthesis of chlorophyll within the basal 20mm of the leaf blade indicates that a certain amount of visible light reaches this region (see Section 6.5), and therefore it is possible that UV-B radiation may have a direct effect at the leaf base. This could be investigated further with the use of fibre optics (Cen & Bornman, 1993) to quantify the transmission of monochromatic UV-B radiation (λ 310nm) through the coleoptile. A number of substances that are related to cell division and elongation, including auxins (John *et al.*, 1990) and sucrose (Van't Hof, 1973; Francis, 1992) have been shown to be susceptible to UV-B (Takeuchi *et al.*, 1989; Ros & Tevini, 1995). Changes in the concentration and/or supply of such substances to the basal region of the leaf may result in altered cell division and elongation. The results of my study show that the concentration of soluble carbohydrates is highest within the elongation zone of the leaf (see Section 6.8.1). The rate of photosynthesis within this region is low, and therefore it was concluded that

carbohydrates are imported from either the seed or mature, photosynthesising tissue. It is possible that changes in the supply of sucrose from mature tissue above the coleoptile, exposed directly to UV-B, may mediate an indirect response in cell division and elongation. This could be investigated further by exposing plants to $^{14}\text{CO}_2$ and following the incorporation of ^{14}C into the sucrose pools in the basal region of the leaf.

From the spatial distribution of cell division and elongation, the cell age gradient along the length of the leaf was calculated. All other parameters measured, *e.g.* ultrastructure and metabolism, could therefore be compared directly in cells of the same age in control and UV-B-grown plants.

7.3 Changes in the Development of Cell Structure in Response to UV-B

The importance of analysing data on a cell age basis is highlighted in the changes found in the ultrastructural development of control and UV-B-grown plants. When the data are expressed on a spatial basis (distance from leaf base), which does not account for the different growth rates of control and UV-B-grown plants, there appears to be no UV-B induced changes in ultrastructural development. However, when the data are expressed on a temporal basis (cell age), which compensates for the difference in growth rates, UV-B induced changes in the development of both chloroplast and mitochondrial populations of mesophyll cells are found. These 'direct' UV-B induced changes include the production of more, smaller chloroplasts per cell, and smaller mitochondria which occupy the same volume fraction of the cell as the larger mitochondria of control-grown plants, thus suggesting the production of more, smaller mitochondria per cell (see Section 5.9). Therefore, in addition to the UV-B induced alteration in cell division rates, the results of my study also suggest that UV-B may be

altering organelle division. To date this is the first known report of changes in organelle numbers in response to UV-B radiation, and the specific mechanism by which UV-B alters organelle development clearly warrants further investigation.

The production of more, smaller chloroplasts per cell in response to UV-B may be due to alterations in either proplastid or chloroplast division (see Section 5.9). Although the genetic factors controlling the division and rate of accumulation of chloroplasts during cell development are unknown, a mechanism exists in which changes in chloroplast division are compensated for by changes in the size of individual chloroplasts. This results in a similar chloroplast compartment size per unit mesophyll cell volume, *i.e.* the V_V of mature mesophyll cell occupied by chloroplasts is constant. The production of more, smaller chloroplasts in response to UV-B, as compared to the fewer, larger chloroplasts per cell of control-grown plants, is therefore in agreement with this general model. The recent identification of a number of chloroplast development mutants in *A.thaliana* (Pyke & Leech, 1991, 1992, 1994; Pyke *et al.*, 1994; Robertson, Rutherford & Leech, 1996), provides a system in which the control mechanisms responsible for chloroplast replication may be identified. These mutants, *e.g.* *arc5* which does not affect proplastid division but functions at a later stage of chloroplast division, could be used to identify the mechanism(s) involved in the UV-B induced alteration in chloroplast size and number per cell. The results of my study also suggest a prolonged period of mitochondrial division, resulting in more mitochondria per cell, in response to UV-B. As such changes are derived from data on mitochondrial volume fractions and transverse areas, quantification of changes in the number of mitochondria per cell is needed before proceeding with further investigations into the specific mechanisms by which UV-B affects mitochondrial division.

7.4 Changes in Metabolic Development in Response to UV-B

As a cell's structure is intimately related to its function the changes observed in the ultrastructural development of mesophyll cells in response to UV-B were suggested to have possible consequences on the metabolic development of the primary leaf.

Despite the relevance of chloroplast content to photosynthetic efficiency, up until recently only general statements regarding the relationship between chloroplasts and photosynthesis existed (see Boffey, 1992). The recent discovery of chloroplast development mutants in *A.thaliana* (see Section 7.3) however, may enable the manipulation of chloroplast size and number, so that their contribution to photosynthetic efficiency can be assessed independently. It was suggested that the UV-B induced changes observed in the chloroplast population of mesophyll cells in this study may alter the photosynthetic capacity of the leaf (see Section 5.9). A reduction in photosynthesis is a frequently observed response to UV-B and has been reported in a variety of species (see Section 1.6.2). Such alterations in photosynthetic capacity have been shown to be the result of a number of UV-B induced responses, including changes in the PSII reaction centre (Bornman, 1989) and photosynthetic pigments (Takeuchi *et al.*, 1989; Strid *et al.*, 1990). The total chlorophyll content was significantly higher in UV-B-grown plants when expressed on a spatial basis, however when the difference in growth rate between control and UV-B-grown plants was taken into account UV-B had no effect on chlorophyll content (see Section 6.5). Similarly, UV-B significantly increased the number of thylakoids per granum, a parameter that was used to assess the development of PSI and PSII, throughout leaf development when expressed on a spatial basis, but this difference was lost when expressed in relation to cell age.

These data highlight again the importance of taking into account developmental

changes induced by UV-B, before analysing any response to UV-B. The results of my study also show that although the rate of photosynthesis per chloroplast was reduced in UV-B grown plants, when the increase in the number of chloroplast per cell was taken into account and data expressed on a leaf area basis, there was no difference in photosynthetic rate between control and UV-B-grown plants (see Section 6.6.1). This is in agreement with the analysis of photosynthesis in *arc* mutants of *A.thaliana* (excluding the pale chloroplast mutant, *arc1*), in which the difference in the number of chloroplasts were compensated for by altered chloroplast size, *i.e.* mutants with similar chloroplast compartment size per unit mesophyll cell, in which no major differences in photosynthesis was found between mutants (Personal communication, K.A.Pyke, RHBNC, University of London). Therefore despite the UV-B induced alterations observed in chloroplast development, UV-B had no effect on the overall rate of photosynthesis, which is consistent with the observation that UV-B also had no effect on either the rate of photosynthetic carbon assimilation or the carbohydrate status of the primary leaf. The effects of UV-B on photosynthetic activity could be investigated further using more sensitive techniques, *e.g.* fluoresence analysis.

Although the rate of photosynthetic carbon assimilation was similar in UV-B and control-grown plants, UV-B altered the partitioning of carbon into amino acid free pools and increased the concentration of the total free amino acid pools throughout development (see Section 6.10.1). Considering the importance of nitrogen metabolism, this is one area of UV-B research in higher plants in which there are suprisingly few studies. The changes observed in amino acid metabolism in this study clearly warrent further investigation. Key enzymes of nitrogen metabolism, *e.g.* NR ,NiR and GS have all been identified as UV-B sensitive targets in a limited number of studies investigating

the effects of UV-B on the nitrogen metabolism of phytoplankton (Appenroth *et al.*, 1993; Sinha *et al.*, 1995). The effects of UV-B radiation on the activity of these enzymes, and the flux of ^{15}N and ^{14}C to amino acids would be a starting point in which to investigate the response of nitrogen metabolism in higher plants to UV-B.

7.5 Conclusions

The altered morphology of the primary leaf of wheat, grown under UV-B, was identified as being the result of changes in the rate and duration of both cell division and elongation. The growth pattern of the primary leaf enabled the cell age gradient within the leaf blade of control and UV-B-grown plants to be determined. This allowed for the distinction between 'indirect' UV-B responses, resulting from the altered development of UV-B-grown plants as compared to controls, and 'direct' UV-B responses between cells of the same age in control and UV-B-grown plants. The effects of UV-B on the development of cell structure and function was found to vary with the developmental stage of the plant. In conclusion, this thesis has shown that the sensitivity of the primary leaf of wheat to UV-B varies with development. This highlights the importance of considering leaf age in the design of experiments investigating the effects of environmental stresses, for example, UV-B, CO_2 and nitrogen nutrition, on plant growth.

CHAPTER 8
REFERENCES

Abbatt, J.P.D. & Molina, M.J. (1993) State of stratospheric ozone depletion. *Annual Review of Energy and the Environment* **18**, 1-29

Alberts, B., Bray, D., Lewis, J., Raff, M., Roberts, K. & Watson, J.D. (1996) *Molecular Biology of the Cell*. 3rd Edition. Garland Publishing Inc. New York & London

Albrechtová, J. & Kubínova, L. (1991) Quantitative analysis of the structure of etiolated barley leaf using stereological methods. *Journal of Experimental Botany* **42** (243), 1311-1314

Allard, G. & Nelson, C.J. (1991) Photosynthate partitioning in basal zones of tall fescue leaf blades. *Plant Physiology* **95**, 663-668

Allen, D.J., McKee, I.F., Farage, P.K. & Baker, N.R. (1997) Analysis of limitations to CO₂ assimilation on exposure of leaves of two *Brassica napus* cultivars to UV-B. *Plant, Cell and Environment* **20**, 633-640

Ambach, W., Blumthaler, M. & Wendler, G. (1991) A comparison of ultraviolet radiation measured at an arctic and an alpine site. *Solar Energy* **47** (2), 121-126

Anderson, J.M. (1986) Photoregulation of the composition, function, and structure of thylakoid membranes. *Annual Review of Plant Physiology* **37**, 93 - 136

Anderson, J.W. & Beardall, J. (1991) *Molecular activities of plant cells - An introduction to plant biochemistry*. Blackwell Scientific Publications, Oxford

Anderson, J.M., Goodchild, D.J. & Boardman, N.K. (1973) Composition of the photosystems and chloroplast structure in extreme shade plants. *Biochimica et Biophysica Acta* **325**, 573-585

Appenroth, K.J., Augsten, H., Mattner, A., Teller, S. & Döhler, G. (1993) Effect of UV-B irradiation on enzymes of nitrogen metabolism in turions of *Spirodela polyrhiza* (L.) *Schleiden. Journal of Photochemistry and Photobiology B: Biology* **18**, 215-220

Amon, D.I. (1949) Copper enzymes in isolated chloroplasts. Polyphenoloxidase in *Beta vulgaris*. *Plant Physiology* **24**, 1-15

Attridge, T.H. (1990) *Light and Plant Responses*. Edward Arnold, London.

Azcón-Bieto, J., Lambers, H. & Day, D.A. (1983) Respiratory properties of developing bean and pea leaves. *Australian Journal of Plant Physiology* **10**, 237-245

Baker, N.R. & Leech, R.M. (1977) Development of photosystem I and photosystem II activities in leaves of light-grown Maize (*Zea mays*). *Plant Physiology* **60**, 640-644

Baker, N.R. & Ort, D.R. (1992) Light and crop photosynthetic performance In: *Topics in Photosynthesis- Vol 12* (ed. J. Barber), Crop photosynthesis: spatial and temporal determinants (eds. N.R.Baker & H.Thomas), pp. 289-312. Elsevier, Amsterdam

Balakumar, T., Vincent, V.H.B. & Paliwal, K. (1993) On the interaction of UV-B radiation (280-315nm) with water stress on crop plants. *Physiologia Plantarum* **87**, 217-222

Ballaré, C.I., Barnes, P.W. & Flint, S.D. (1995a) Inhibition of hypocotyl elongation by ultraviolet-B radiation in de-etiolating tomato seedlings. I. The photoreceptor. *Physiologia Plantarum* **93**, 584-592

Ballaré, C.J., Barnes, P.W., Flint, S.D. & Price, S. (1995b) Inhibition of hypocotyl elongation by ultraviolet-B radiation in de-etiolating tomato seedlings. II. Time-course, comparisons with flavonoid responses, and adaptive significance. *Physiologia Plantarum* **93**, 593-601

Ballaré, C.L., Barnes, P.W. & Kendrick, R.E. (1991) Photomorphogenic effects of UV-B radiation on hypocotyl elongation in wild type and stable-phytochrome-deficient mutant seedlings of cucumber. *Physiologia Plantarum* **83**, 652-658

Ballaré, C.L., Scopel, A.L., Stapleton, A.E. & Yanovsky, M.J. (1996) Solar ultraviolet-B radiation affects seedling emergence, DNA integrity, plant morphology, growth rate, and attractiveness to herbivore insects in *Datura ferox*. *Plant Physiology* **112**, 161-170

Barkdardottir, R.B., Jensen, B.F., Kreiberg, J.D., Nielsen, P.S. & Gausing, K. (1987) Expression of selected nuclear genes during leaf development in barley. *Developmental Genetics* **8**, 495-511

Barnes, P.W., Ballaré, C.L. & Caldwell, M.M. (1996) Photomorphogenic effects of UV-B radiation on plants: consequences for light competition. *Journal of Plant Physiology* **148**, 15-20

Barnes, P.W., Flint, S.D. & Caldwell, M.M. (1990) Morphological responses of crop and weed species of different growth forms to ultraviolet-B radiation. *American Journal of Botany* **77**(10), 1354-1360

Barnes, P.W., Jordan, P.W., Gold, W.G., Flint, S.D. & Caldwell, M.M. (1988) Competition, morphology and canopy structure in wheat (*Triticum aestivum* L.) and wild oat (*Avena fatua* L.) exposed to enhanced ultraviolet-B radiation. *Functional Ecology* **2**, 319-330

Beggs, C.J., Stolzer-Jehle, A. & Wellmann, E. (1985) Isoflavonoid formation as an indicator of UV-stress in bean (*Phaseolus vulgaris* L.) leaves. *Plant Physiology* **79**, 630-634

Ben-Haj-Salah, H. & Tardieu, F. (1995) Temperature affects expansion rate of maize leaves without change in spatial distribution of cell length. *Plant Physiology* **109**, 861-870

- Beyschlag, W., Barnes, P.W., Flint, S.D. & Caldwell, M.M.** (1988) Enhanced UV-B irradiation has no effect on photosynthetic characteristics of wheat (*Triticum aestivum* L.) and wild oat (*Avena fatua* L.) under greenhouse and field conditions. *Photosynthetica* **22** (4), 516-525
- Blumthaler, M. & Ambach, W.** (1990) Indication of increasing solar ultraviolet-B radiation flux in Alpine regions. *Science* **248**, 206-208
- Boffey, S.A.** (1992) Chloroplast Replication. In: *Topics in Photosynthesis- Vol 12* (ed. J. Barber) Crop photosynthesis: spatial and temporal determinants (eds. N.R. Baker & H. Thomas), pp. 361-380. Elsevier, Amsterdam
- Boffey, S.A., Ellis, J.R., Selldén, G. & Leech, R.M.** (1979) Chloroplast division and DNA synthesis in light-grown wheat leaves. *Plant Physiology* **64**, 502-505
- Boffey, S.A., Selden, G. & Leech, R.M.** (1980) Influence of cell age on chlorophyll formation in light-grown and etiolated wheat seedlings. *Plant Physiology* **65**, 680-684
- Bolender, R.P.** (1978) Correlation of morphometry and stereology with biochemical analysis of cell fractions. *International Reviews of Cytology* **55**, 247-289
- Bomman, J.F.** (1989) Target sites of UV-B radiation in photosynthesis of higher plants. *Journal of Photochemistry and Photobiology, B: Biology*, **4**, 145-158
- Bomman, J.F., Björn, L.O. & Akerlund, H.E.** (1984) Action spectrum for inhibition by ultraviolet radiation of photosystem II activity in spinach thylakoids. *Photochemistry and Photobiophysics* **8**, 305-313
- Bomman, J.F., Evert, R.F. & Mierzwa, R.J.** (1983) The effect of UV-B and UV-C radiation on sugar beet leaves. *Protoplasma* **117**, 7-16

Bomman, J.F., Evert, R.F., Mierzwa, R.J. & Bomman, C.H. (1986) Fine structural effects of UV radiation on leaf tissue of *Beta vulgaris*. In: *Stratospheric Ozone Reduction, Solar Ultraviolet Radiation and Plant Life*, Vol. **G8** (eds. R.C. Worrest & M.M. Caldwell), pp. 199-209. NATO ASI Series. Springer-Verlag, Berlin.

Bomman, J.F. & Sundby-Emanuelsson, C. (1995) Response of plants to UV-B radiation: some biological and physiological effects. In: *Environmental and Plant Metabolism-Flexibility and Acclimation* (ed. N.Smirnoff), pp 245-262. Environmental Plant Biology Series, BIOS Scientific Publishers, UK

Bomman, J.F. & Vogelmann, T.C. (1991) Effect of UV-B radiation on leaf optical properties measured with fibre optics. *Journal of Experimental Botany* **42** (237), 547-554

Bradford, M. (1976) A rapid and sensitive method for the quantification of microgram quantities of protein utilizing the principle of protein-dye binding. *Analytical Biochemistry* **72**, 248-252

Brandle, J.R., Campbell, W.F., Sisson, W.B. & Caldwell, M.M. (1977) Net photosynthesis, electron transport capacity, and ultrastructure of *Pisum sativum* L. exposed to ultraviolet-B radiation. *Plant Physiology* **60**, 165-169

Brasseur, G. & Solomon, S. (1986) *Aeronomy of the middle atmosphere*. Dordrecht, Reidel

Braune, W. & Döhler, G. (1996) Impact of UV-B radiation on ¹⁵N-ammonium and ¹⁵N-nitrate uptake by *Haematococcus lacustris* (Volvocales) II. The influence of a recovery period. *Journal of Plant Physiology* **149**, 349-357

Brett, C.T. & Waldron, K.W. (1996) *Physiology and biochemistry of plant cell walls*. Topics in Plant Functional Biology: 1 (eds. M. Black & B. Charlwood), Chapman & Hall, London

Briarty, L.G. (1975) Stereology: methods for quantitative light and electron microscopy. *Science Progress, Oxford* **62**, 1-32

Britt, A.B. (1995) Repair of DNA damage induced by ultraviolet radiation. *Plant Physiology* **108**, 891-896

Britt, A.B. (1996) DNA damage and repair in plants. *Annual Review of Plant Physiology and Plant Molecular Biology* **47**, 75-100

Bryan, J.K. (1990). In: *The Biochemistry of Plants* (eds. B.J.Miflin & P.J.Lea), Vol **16**, pp. 161-195. Academic Press, London

Caldwell, M.M. (1971) Solar UV radiation and the growth and development of higher plants. In: *Photophysiology*, Vol **6** (ed. A.C.Giese), pp 131-177. Academic Press, New York, NY.

Caldwell, M.M. (1994) Modification of the cellular heat sensitivity of cucumber by growth under supplemental ultraviolet-B radiation. *Plant Physiology* **104**, 395-399

Caldwell, M.M., Camp, L.B., Warner, C.W. & Flint, S.D. (1986) Action spectra and their key role in assessing biological consequences of solar UV-B radiation change. In: *Stratospheric ozone reduction, solar ultraviolet radiation and plant life*. Vol **G8** (eds R.C. Worrest & M.M. Caldwell), pp. 87-111 NATO ASI Series. Springer-Verlag, Berlin.

Caldwell, M.M., Flint, S. & Searles, P.S. (1994) Spectral balance and UV-B sensitivity of soybean: a field experiment. *Plant, Cell and Environment* **17**, 267-276

Caldwell, M.M., Robberecht, R. & Flint, S.D. (1983) Internal filters: prospects for UV-acclimation in higher plants. *Physiologia Plantarum* **58**, 445-450

Caldwell, M.M., Teramura, A.H. & Tevini, M. (1989) The changing solar ultraviolet climate and the ecological consequences for higher plants. *Trends in Ecology and Evolution* **4** (12), 363-367

Caldwell, M.M., Teramura, A.H., Tevini, M., Bomman, J.F., Björn, L.O. & Kulandaivelu, G. (1995) Effects of increased solar ultraviolet radiation on terrestrial plants. *Ambio* **24** (3), 166-173

Carlson, J.G. (1976) Mitotic effects of monochromatic ultraviolet radiation at 225, 265 and 280nm on eleven stages of the cell cycle of the grasshopper neuroblast in culture. 1. Overall retardation from the stage irradiated to nuclear membrane breakdown. *Radiation Research* **68**, 57-74

Cen, Y.P. & Bomman, J.F. (1990) The response of bean plants to UV-B radiation under different irradiance of background visible light. *Journal of Experimental Botany* **41**, 1489-1495

Cen, Y.P. & Bomman, J.F. (1993) The effect of exposure to enhanced UV-B radiation on the penetration of monochromatic and polychromatic UV-B radiation in leaves of *Brassica napus*. *Physiologia Plantarum* **87**, 249-255

Chapman, D.J. & Leech, R.M. (1977) Changes in pool sizes of free amino acids and amides in leaves and plastids of *Zea mays* during leaf development. *Plant Physiology* **63**, 567-572

Cherry, J.H. (1963) Nucleic acid, mitochondria and enzyme changes in the cotyledons of peanut seeds during germination. *Plant Physiology* **38**, 440-446

Chipperfield, M.P., Lee, A.M. & Pyle, J.A. (1996) Model calculations of ozone depletion in the Arctic polar vortex for 1991/92 to 1994/95. *Geophysical Research Letters* **23** (5), 559-562

Cieminis, K.G.K., Rancėlienė, V.M., Prijalgauskienė, A.J., Tiunaitienė, N.V., Rudzianskaitė, A.M. & Janėys, Z.J. (1987) Chromosome and DNA damage and their repair in higher plants irradiated with short-wave ultraviolet light. *Mutation Research* **181**, 9-16

Coohill, T.P. (1989) Ultraviolet action spectra (280-380nm) and solar effectiveness spectra for higher plants. *Photochemistry and Photobiology* **50**, 451-457

Coohill, T.P. (1991) Action spectra again? *Photochemistry and Photobiology* **54**, 859-870

Cosgrove, D.J. (1987) Wall relaxation in growing stems: comparison of four species and assessment of measurement techniques. *Planta* **171**, 266-278

Croxdale, J.G. (1983) Quantitative measurements of hexokinase activity in the shoot apical meristem, leaf primordia, and leaf tissues of *Dianthus chinensis* L. *Plant Physiology* **73**, 66-70

Croxdale, J.G. & Outlaw, W.H. (1983) Glucose-6-phosphate dehydrogenase activity in the shoot apical meristem, leaf primordia, and leaf tissue of *Dianthus chinensis* L. *Planta* **157**, 289-297

Croxdale, J.G. & Pappas, T. (1987) Activity of glyceraldehyde-3-phosphate dehydrogenase-NADP in developing leaves of light-grown *Dianthus chinensis* L. *Plant Physiology* **84**, 1427-1430

Cutter, E.G. (1971) *Plant Anatomy: Experiment and Interpretation*. Part 2. Organs. Edward Arnold, London

Dai, Q., Peng, S., Chavez, A.Q. & Vergara, B.S. (1995) Effects of UVB radiation on stomatal density and opening in rice (*Oryza sativa* L.). *Annals of Botany* **76**, 65-70

Dale, J.E. (1972) Growth and photosynthesis in the first leaf of barley. The effect of time and the application of nitrogen. *Annals of Botany* **36**, 967-979

Dale, J.E. (1985) The carbon relations of the developing leaf. In: *Control of Leaf Growth*. Society for Experimental Biology Seminar Series, No.27 (eds. N.R.Baker, W.J. Davies & C.K.Ong), pp. 135-153. Cambridge University Press, Cambridge

Dale, J.E. (1988) The control of leaf expansion. *Annual Review of Plant Physiology and Plant Molecular Biology* **39**, 267-295

Dale, J.E. (1992) How do leaves grow? Advances in cell and molecular biology are unravelling some of the mysteries of leaf development. *BioScience* **42**, 423-432

Davies, R.J.H. (1995) Ultraviolet Radiation Damage in DNA. *Biochemical Society Transactions* **23**, 407-418

Day, T.A. (1993) Relating UV-B radiation screening effectiveness of foliage to absorbing-compound concentration and anatomical characteristics in a diverse group of plants. *Oecologia* **95**, 542-550

Day, T.A. & Vogelmann, T.C. (1995) Alterations in photosynthesis and pigment distributions in pea leaves following UV-B exposure. *Physiologia Plantarum* **94**, 433-440

Day, T.A., Howells, B.W. & Ruhland, C.T. (1996) Changes in growth and pigment concentrations with leaf age in pea under modulated UV-B radiation field treatments. *Plant, Cell and Environment* **19**, 101-108

Dean, C. & Leech, R.M. (1982a) Genome expression during normal leaf development. I. Cellular and chloroplast numbers and DNA, RNA, and protein levels in tissue of different ages within a seven-day-old wheat leaf. *Plant Physiology* **69**, 904-910

Dean, C. & Leech, R.M. (1982b) Genome expression during normal leaf development. II. Direct correlation between Ribulose bisphosphate carboxylase content and nuclear ploidy in a polyploid series of wheat. *Plant Physiology* **70**, 1605-1608

Deckmyn, G. & Impens, I. (1995) UV-B increases the harvest index of bean (*Phaseolus vulgaris* L.). *Plant, Cell and Environment* **18**, 1426-1433

Deckmyn, G., Martens, C. & Impens, I. (1994) The importance of the ratio UV-B/photosynthetic active radiation (PAR) during leaf development as determining factor of plant sensitivity to increased UV-B irradiance: effects on growth, gas exchange and pigmentation of bean plants (*Phaseolus vulgaris* cv. Label). *Plant, Cell and Environment* **17**, 295-301

Dennis, D.T. & Turpin, D.H. (1990) *Plant Physiology, Biochemistry and Molecular Biology*. Longman Scientific and Technical, Singapore

Dickson, J.G. & Caldwell, M.M. (1978) Leaf development of *Rumex patientia* L. (Polygonaceae) exposed to UV irradiation (280-320nm). *American Journal of Botany* **65** (8), 857-863

Dietz, K-J. (1989) Leaf and chloroplast development in relation to nutrient availability. *Journal of Plant Physiology* **134**, 544-550

Dillenburg, L.R., Sullivan, J.H. & Teramura, A.H. (1995) Leaf expansion and development of photosynthetic capacity and pigments in *Liquidambar styraciflua* (Hamamelidaceae) - effects of UV-B radiation. *American Journal of Botany* **82**(7), 878-885

Doemer, P.W. (1994) Cell cycle regulation in plants. *Plant Physiology* **106**, 823-827

Döhler, G. (1985) Effect of UV-B radiation (290-320nm) on the nitrogen metabolism of several marine diatoms. *Journal of Plant Physiology* **118**, 391-400

- Döhler, G.** (1990) Effect of UV-B (290-320nm) radiation on uptake of ¹⁵N-nitrate by marine diatoms. In: *Inorganic nitrogen in plants and microorganisms. Uptake and metabolism* (ed. W.R. Ullrich), pp. 349-354. Springer Verlag, Berlin
- Döhler, G.** (1992) Impact of UV-B radiation on uptake of ¹⁵N-ammonia and ¹⁵N-nitrate by phytoplankton of the Wadden Sea. *Marine Biology* **112**, 485-489
- Domon, M. & Rauth, A.M.** (1968) Ultraviolet irradiation of mouse L cells: effects on DNA synthesis and progression through the cell cycle. *Radiation Research* **35**, 350-368
- Douce, R.** (1985) *Mitochondria in Higher Plants. Structure, Function, and Biogenesis.* Academic Press, Orlando
- Douce, R. & Neuberger, M.** (1990). Metabolite exchange between the mitochondrion and the cytosol. In: *Plant Physiology, Biochemistry and Molecular Biology* (eds. D.T.Dennis & D.H.Turpin), pp. 173-190. Longman Scientific and Technical, Singapore
- Ellis, J.R., Jellings, A.J. & Leech, R.M.** (1983) Nuclear DNA content and the control of chloroplast replication in wheat leaves. *Planta* **157**, 376-380
- Ellis, J.R. & Leech, R.M.** (1985) Cell size and chloroplast size in relation to chloroplast replication in light-grown wheat leaves. *Planta* **165**, 120-125
- Ellis, R.J.** (1979) The most abundant protein in the world. *Trends in Biochemical Science* **4**, 241-244
- Emes, M.J. & Tobin, A.K.** (1993) Control of metabolism and development in higher plant plastids. *International Review of Cytology* **145**, 149-216
- Estelle, M.** (1992) The plant hormone auxin: insight in sight. *Bioessays* **14** (7), 439-444

- Evans, H.J. Neary, G.J. & Tonkinson, S.M.** (1957) The use of colchicine as an indicator of mitotic rate in broad bean root meristems. *Journal of Genetics* **55**, 487-502
- Farman, J.C., Gardiner, B.G. & Shanklin, J.D.** (1985) Large losses of total ozone in Antarctica reveal seasonal ClO_x/NO_x interactions. *Nature* **315**, 207-210
- Farrar, J.F.** (1985) The respiratory source of CO₂. *Plant, Cell and Environment* **8**, 427-438
- Fitter, A.H. & Hay, R.K.M.** (1987) *Environmental Physiology of Plants*. Academic Press, London.
- Flint, S.D., Jordan, P.W. & Caldwell, M.M.** (1985) Plant protective responses to enhanced UV-B radiation under field conditions: Leaf optical properties and photosynthesis. *Photochemistry and Photobiology* **41**, 95-99
- Francis, D.** (1992) The cell cycle in plant development. *New Phytologist* **122**, 1-20
- Francis, D. & Halford, N.G.** (1995) The plant cell cycle. *Physiologia Plantarum* **93**, 365-374
- Fry, S.C.** (1986) Cross-linking of matrix polymers in the growing cell walls of angiosperms. *Annual Review of Plant Physiology* **37**, 165-186
- Galston, H.W.** (1950) Riboflavin, light, and the growth of plants. *Science* **111**, 619-624
- Gastal, F., Nelson, C.J. & Coutts, J.H.** (1992) Leaf growth of tall fescue: The role of nitrogen nutrition. *Proceedings of the 14th Meeting of the European Grassland Federation* **14**, 418-420
- Geronimo, J. & Beevers, H.** (1964) Effects of aging and temperature on respiratory metabolism of green leaves. *Plant Physiology* **39**, 786-793

Giller, Y.E. (1991) UV-B effects on the development of photosynthetic apparatus, growth and productivity of higher plants. *Impact of Global Climatic Changes on Photosynthesis and Plant Productivity*.

Givan, C.V., Joy, K.W. & Kleczkowski, L.A. (1988) A decade of photorespiratory nitrogen cycling. *Trends in Biochemical Sciences* **13** (11), 433-437

Gleason, J.F., Bhartia, P.K., Herman, J.R., McPeters, R., Newman, P., Stolarski, R.S., Flynn, L., Labow, G., Larko, D., Seftor, C., Wellemeyer, C., Komhyr, W.D., Miller, A.J. & Planet, W. (1993) Record low global ozone in 1992. *Science* **260**, 523-526

Goes, J.I., Handa, N., Taguchi, S. & Hama, T. (1995a) Changes in the patterns of biosynthesis and composition of amino acids in a marine phytoplankter exposed to ultraviolet-B radiation: Nitrogen limitation implicated. *Photochemistry and Photobiology* **62** (4), 703-710

Goes, J.I., Handa, N., Taguchi, S., Hama, T. & Saito, H. (1995b) Impact of UV radiation on the production patterns and composition of dissolved free and combined amino acids in marine phytoplankton. *Journal of Plankton Research* **17** (6), 1337-1362

Gold, W.G. & Caldwell, M.M. (1983) The effects of ultraviolet-B radiation on plant competition in terrestrial ecosystems. *Physiologia Plantarum* **58**, 435-444

Greenberg, B.M., Gaba, V., Canaani, O., Malkin, S., Mattoo, A.K. & Edelman, M. (1989) Separate photosensitizers mediate degradation of the 32-kDa photosystem II reaction center protein in the visible and UV spectral regions. *Proceedings of the National Academy of Science USA* **86**, 6617-6620

Gribben, J. (1989) Centenary unlocks the history of the ozone hole. *New Scientist* **121**, 24

Grime, J.P., Hodgson, J.G. & Hunt, R. (1990) *The abridged comparative plant ecology*. Unwin Hyman, London.

Gunning, B.E.S. & Steer, M.W. (1975) *Plant Cell Biology: An Ultrastructural Approach*. Edward Arnold, London

Gutteridge, S. & Keys, A.J. (1985) Photosynthetic mechanisms and the Environment In: *Topics in Photosynthesis, Vol 6* (eds. J.Barber & N.R.Baker), pp. 259-285. Elsevier, Amsterdam

Gwynn-Jones, D. & Johanson, U. (1996) Growth and pigment production in two subarctic grass species under four different UV-B irradiation levels. *Physiologia Plantarum* **97**, 701-707

Hampp, R. & Wellburn, A.R. (1980) Translocation and phosphorylation of adenine nucleotides by mitochondria and plastids during greening. *Zeitschrift für Pflanzenphysiologie* **98**,289-303

Hart, J.W. (1988) *Light and Plant Growth*. *Topics in Plant Physiology: 1* (eds. M. Black & J. Chapman). Unwin Hyman, London

Haussühl, K., Rohde, W. & Weissenböck, G. (1996) Expression of chalcone synthase genes in coleoptiles and primary leaves of *Secale cereale* L. after induction by UV radiation: Evidence for a UV-protective role of the coleoptile. *Botanical Acta* **109**, 229-238

He, J., Huang, L.-K. & Whitecross, M.L. (1994) Chloroplast ultrastructure changes in *Pisum sativum* associated with supplementary ultraviolet (UV-B) radiation. *Plant, Cell and Environment* **17**, 771-775

Huppe, H.C. & Turpin, D.H. (1994) Integration of carbon and nitrogen metabolism in plant and algal cells. *Annual Review of Plant Physiology and Plant Molecular Biology* **45**, 577-607

Ireland, I. (1990) Amino acid and ureide biosynthesis. In: *Plant Physiology, Biochemistry and Molecular Biology* (eds. D.T. Dennis & D.H. Turpin) pp. 407-421, Longman Scientific and Technical, Singapore

Jansen, M.A.K., Depka, B., Trebst, A. & Edelman, M. (1993) Engagement of specific sites in the plastoquinone niche regulates degradation of the D1 protein in photosystem II. *The Journal of Biological Chemistry* **268**, 21246-21252

Jellings, A.J. & Leech, R.M. (1982) The importance of quantitative anatomy on the interpretation of whole leaf biochemistry in species of *Triticum*, *Hordeum* and *Avena*. *New Phytologist* **92**, 39-48

Jellings, A.J. & Leech, R.M. (1984) Anatomical variation in first leaves of nine *Triticum* genotypes, and its relationship to photosynthetic capacity. *New Phytologist* **96**, 371-382

Jellings, A.J., Usher, M.B. & Leech, R.M. (1983) Chloroplast size in tall and short phenotypes of *Poa flabellata* on South Georgia. *British Antarctic Survey Bulletin* **59**, 41-46

John, P.C.L., Sek, F.J. & Lee, M.G. (1989) A homolog of the cell cycle control protein p34cdc2 participates in the division cycle of *Chlamydomonas*, and a similar protein is detectable in higher plants and remote taxa. *The Plant Cell* **12**, 1185-1193

Jordan, B.R. (1993) The molecular biology of plants exposed to ultraviolet-B radiation and the interaction with other stresses. In: *Interacting Stresses on Plants in a Changing Climate* (eds. M.B. Jackson & C.R. Black), pp. 153-170. Springer-Verlag, Berlin

- Jordan, B.R.** (1996) The effects of ultraviolet-B radiation on plants: a molecular perspective. *Advances in Botanical Research* **22**, 97-162
- Jordan, B.R., Chow, W.S., Strid, Å. & Anderson, J.M.** (1991) Reduction in *cab* and *psb* A RNA transcripts in response to supplementary ultraviolet-B radiation. *Federation of European Biochemical Societies*. **284** (1), 5-8
- Jordan, B.R., He, J., Chow, W.S. & Anderson, J.M.** (1992) Changes in mRNA levels and polypeptide subunits of ribulose 1,5-bisphosphate carboxylase in response to supplementary ultraviolet-B radiation. *Plant, Cell and Environment* **15**, 91-98
- Jordan, B.R., James, P.E., Strid, Å. & Anthony, R.G.** (1994) The effect of ultraviolet-B radiation on gene expression and pigment composition in etiolated and green pea leaf tissue: UV-B-induced changes are gene-specific and dependent upon the developmental stage. *Plant, Cell and Environment* **17**, 45-54
- Kaminski, A., Ausin, R.B., Ford, M.A. & Morgan, C.L.** (1990) Flag leaf anatomy of *Triticum* and *Aegilops* species in relation to photosynthetic rate. *Annals of Botany* **66**, 359-365
- Kerr, R.A.** (1988) Ozone hole bodes ill for the globe. *Science* **241**, 785-786
- Kerr, J.B. & McElroy, C.T.** (1993) Evidence for large upward trends of ultraviolet-B radiation linked to ozone depletion. *Science* **262**, 1032-1034
- Keys, A.J., Bird, I.F., Cornelius, M.J., Lea, P.J., Wallsgrove, R.M. & Miflin, B.J.** (1978) Photorespiratory nitrogen cycle. *Nature* **275**, 741-743
- Kidd, F., West, C. & Briggs, G.E.** (1921) A quantitative analysis of the growth of *Helianthus annuus*. I. The respiration of the plant and of its parts throughout the life cycle. *Proceedings of the Royal Academy of London. Series B (Biology)* 368-384

- Komberg, A. & Baker, T.A.** (1992) *DNA replication*, pp. 771-791. W.H. Freeman, New York
- Kripke, M.L.** (1994) Ultraviolet radiation and immunology: Something new under the Sun - Presidential address. *Cancer Research* **54**, 6102-6105
- Krizek, D.T.** (1975) Influence of ultraviolet radiation on germination and early seedling growth. *Physiologia Plantarum* **34**, 182-186
- Kubinova, L.** (1989) Stereological analysis of the leaf of barley. *Acta Stereology* **8**, 19-26
- Kutshera, U.** (1989) Tissue stresses in growing plant organs. *Physiologia Plantarum* **77**, 157-163
- Kutshera, U.** (1990) Cell-wall synthesis and elongation growth in hypocotyls of *Helianthus annuus* L. *Planta* **181**, 316-323
- Larcher, W.** (1995) *Physiological Plant Ecology*. Springer, London.
- Laurie, S. & Stewart, G.R.** (1993) Effects of nitrogen supply and high temperature on the growth and physiology of chickpea. *Plant, Cell and Environment* **16**, 609-621
- Leech, R.M.** (1984) Chloroplast development in Angiosperms: current knowledge and future prospects. In: *Topics in Photosynthesis*, Vol. 5, Chloroplast Biogenesis (eds. N.R. Baker & J. Barber), pp. 1-21. Elsevier, Amsterdam.
- Leech, R.M.** (1985) The synthesis of cellular components in leaves. In: *Control of Leaf Growth*. Society for Experimental Biology Seminar Series, No.27 (eds. N.R. Baker, W.D. Davies & C. Ong), pp. 93-114, Cambridge University Press, Cambridge

- Leech, R.M. & Baker, N.R.** (1983) The development of photosynthetic capacity in leaves. In: *The Growth and Functioning of Leaves* (eds. J.E. Dale & F.L. Milthorpe), pp 271-307. Cambridge University Press, Cambridge
- Leech, R.M. & Pyke, K.A.** (1988) Chloroplast division in higher plants with particular reference to wheat. In: *Division and Segregation of organelles*. Society for Experimental Biology Seminar Series No. 35 (eds. S.A. Boffey & D. Lloyd), pp. 39-62. Cambridge University Press, Cambridge
- Leech, R.M., Rumsby, M.G. & Thomson, W.W.** (1973) Plastid differentiation, acyl lipid, and fatty acid changes in developing green maize leaves. *Plant Physiology* **52**, 240-245
- Lockhart, J.A.** (1965) An analysis of irreversible plant cell elongation. *Journal of Theoretical Biology* **8**, 264-275
- Logemann, E., Wu, S-C., Schröder, J., Schmelzer, E., Somssich, I.E. & Hahlbrock, K.** (1995) Gene activation by UV light, fungal elicitor or fungal infection in *Petroselinum crispum* is correlated with repression of cell cycle-related genes. *The Plant Journal* **8** (6), 865-876
- Liu, L. & McClure, J.W.** (1995) Effects of UV-B on activities of enzymes of secondary phenolic metabolism in barley primary leaves. *Physiologia Plantarum* **93**, 734-739
- Liu, L., Gitz, D.C. & McClure, J.W.** (1995) Effects of UV-B on flavonoids, ferulic acid, growth and photosynthesis in barley primary leaves. *Physiologia Plantarum* **93**, 725-733
- Lyndon, R.F.** (1983) The mechanism of leaf initiation. In: *The Growth and Functioning of Leaves* (eds. J.E. Dale & F.L. Milthorpe), pp. 3-24. Cambridge University Press, Cambridge
- Lyndon, R.F.** (1990) *Plant Development: The Cellular Basis*. Topics in Plant Physiology: 3 (eds. M. Black & J. Chapman). Unwin Hyman, London

- MacAdam, J.W. & Nelson, C.J.** (1987) Specific leaf weight in zones of cell division, elongation and maturation in tall fescue leaf blades. *Annals of Botany* **59**, 369-376
- MacAdam, J.W., Nelson, C.J. & Sharp, R.E.** (1992a) Peroxidase activity in the leaf elongation zone of tall fescue. I. Spatial distribution of ionically bound peroxidase activity in genotypes differing in length of the elongation zone. *Plant Physiology* **99**, 872-878
- MacAdam, J.W., Nelson, C.J. & Sharp, R.E.** (1992b) Peroxidase activity in the leaf elongation zone of tall fescue. II. Spatial distribution of apoplastic peroxidase activity in genotypes differing in length of the elongation zone. *Plant Physiology* **99**, 879-885
- McFarland, M. & Kaye, J.** (1992) Chlorofluorocarbons and ozone. *Photochemistry and Photobiology* **55**, 911-929
- Mackerness, S.A-H., Butt, P.J., Jordan, B.R. & Thomas, B.** (1996) Amelioration of ultraviolet-B-induced down regulation of mRNA levels for chloroplast proteins, by high irradiance, is mediated by photosynthesis. *Journal of Plant Physiology* **148**, 100-106
- Madronich, S. & De Gruijl, F.R.** (1994) Stratospheric ozone depletion between 1979 and 1992: Implications for biologically active ultraviolet-B radiation and non-melanoma skin cancer incidence. *Photochemistry and Photobiology* **59** (5), 541-546
- Maksymowych, R.** (1973) *Analysis of Leaf Development*. Cambridge University Press, Cambridge
- Manney, G.L., Froidevaux, L., Waters, J.W., Zurek, R.W., Read, W.G., Elson, L.S., Kumer, J.B., Mergenthaler, J.L., Roche, A.E., O'Neill, A., Harwood, R.S., MacKenzie, I. & Swinbank, R.** (1994) Chemical depletion of ozone in the Arctic lower stratosphere during winter 1992-93. *Nature* **370**, 429-434

- Manton, I.** (1961) Some problems of mitochondrial growth. *Journal of Experimental Botany* **12** (36), 421-429
- Meirer, H. & Reid, J.S.G.** (1982) Reserve Polysaccharides other than starch in higher plants. In: *Carbohydrates. Encyclopedia of Plant Physiology* (New Series) Vol **13A** (eds. F.A.Loewus & W.Tanner), pp. 418-471. Springer-Verlag, Berlin
- Melis, A., Nemson, J.A. & Harrison, M.A.** (1992) Damage to functional components and partial degradation of photosystem II reaction centre proteins upon chloroplast exposure to ultraviolet-B radiation. *Biochimica et Biophysica Acta* **1109**, 312-320
- Merlo, L., Ferretti, M., Ghisi, R. & Passera, C.** (1993) Developmental changes of enzymes of malate metabolism in relation to respiration, photosynthesis and nitrate assimilation in peach leaves. *Physiologia Plantarum* **89**, 71-76
- Mifflin, B.J. & Lea, P.J.** (1977) Amino acid metabolism. *Annual Review of Plant Physiology* **28**, 299-329
- Milthorpe, F.L. & Moorby, J.** (1974) *An introduction to crop physiology*. Cambridge University Press, Cambridge
- Miranda, V., Baker, N.R. & Long, S.P.** (1981) Limitations of photosynthesis in different regions of the *Zea mays* leaf. *New Phytologist* **89**, 165-178
- Mirecki, R.M. & Teramura, A.H.** (1984) Effects of ultraviolet-B irradiance on soybean. V. The dependence of plant sensitivity on the photosynthetic photon flux during and after leaf expansion. *Plant Physiology* **74**, 475-480
- Molina, M.J. & Rowland, F.S.** (1974) Stratospheric sink for chlorofluoromethanes: chlorine atom-catalysed destruction of ozone. *Nature* **249**, 810-812

- Morris, D.L.** (1948) Quantitative determination of carbohydrates with Dreywood's anthrone reagent. *Science* **107**, 254-255
- Moses, L., Ougham, H.J. & Francis, D.** (1997) The effect of the *slow-to-green* mutation on cell division during leaf initiation and early leaf growth in *Lolium temulentum*. *New Phytologist* **135**, 51-57
- Murali, N.S. & Teramura, A.H.** (1985) Effects of ultraviolet-B irradiance on soybean. VII. Biomass and concentration and uptake of nutrients at varying P supply. *Journal of Plant Nutrition* **8** (2), 177-192
- Nelson, C.J., Asay, K.H. & Sleper, D.A.** (1977) Mechanisms of canopy development in tall fescue genotypes. *Crop Science* **17**, 449-452
- Nelson, C.J. & MacAdam, J.W.** (1989) Cellular dynamics in the leaf growth zone. *Current Topics in Plant Biochemistry and Physiology* **8**, 207-223
- Newcomb,** (1990) Mitochondrial Structure. In: *Plant Physiology, Biochemistry and Molecular Biology* (eds. D.T. Dennis & D.H. Turpin) pp. 103-105, Longman Scientific and Technical, Singapore
- Nobel, P.S., Zaragoza, L.J. & Smith, W.K.** (1975) The relationship between mesophyll surface area, photosynthetic rate and illumination level during development of leaves of *Plectranthus parviflorus* Henckel. *Plant Physiology* **55**, 1067-1070
- Nogués, S. & Baker, N.R.** (1995) Evaluation of the role of damage to photosystem II in the inhibition of CO₂ assimilation in pea leaves exposed to UV-B radiation. *Plant, Cell and Environment* **18**, 781-787
- Noorudeen, A.M. & Kulandaivelu, G.** (1982) On the possible site of inhibition of photosynthetic electron transport by ultraviolet (UV-B) radiation. *Physiologia Plantarum* **55**, 161-166

- Ougham, H.J., Jones, T.W.A. & Evans, M.L.L.** (1987) Leaf development in *Lolium temulentum* L. : Progressive changes in soluble polypeptide complement and isoenzymes. *Journal of Experimental Botany* **38** (195), 1689-1696
- Pang, Q. & Hays, J.B.** (1991) UV-B-inducible and temperature sensitive photoreactivation of cyclobutane pyrimidine dimers in *Arabidopsis thaliana*. *Plant Physiology* **95**, 536-543
- Pearce, F.** (1996) Big freeze digs a deeper hole in the ozone layer. *New Scientist* **149** (2021), 7
- Pines, J.** (1994) Arresting developments in cell-cycle control. *Trends in Biochemical Sciences* **19**(4), 143-145
- Possingham, J.V.** (1980) Plastid replication and development in the life cycle of higher plants. *Annual Review of Plant Physiology* **31**, 113-129
- Prasil, O., Adir, N., & Ohad, I.** (1992) Dynamics of photosystem II: mechanisms of photoinhibition and recovery processes. In: *The Photosystems. Structure, Function and Molecular Biology* (ed. J. Barber), pp. 295-348. Elsevier, London.
- Prather, M., Midgley, P., Sherwood Rowland, F. & Stolarski, R.** (1996) The ozone layer: the road not taken. *Nature* **381**, 551-554
- Prather, M. J. & Watson, R.T.** (1990) Stratospheric ozone depletion and future levels of atmospheric chlorine and bromine. *Nature* **344**, 729-734
- Proffitt, M.H., Margitan, J.J., Kelly, K.K., Loewenstein, M., Podolske, J.R. & Chan, K.R.** (1990) Ozone loss in the Arctic polar vortex inferred from high-altitude aircraft measurements. *Nature* **347**, 31-36

- Pyke, K.A. & Leech, R.M.** (1985) Variation in ribulose 1,5 bisphosphate carboxylase content in a range of winter wheat genotypes. *Journal of Experimental Botany* **36** (171), 1523-1529
- Pyke, K.A. & Leech, R.M.** (1987) The control of chloroplast number in wheat mesophyll cells. *Planta* **170**, 416-420
- Pyke, K.A. & Leech, R.M.** (1991) Rapid image analysis screening procedure for identifying chloroplast number mutants in mesophyll cells of *Arabidopsis thaliana* (L.) Heynh. *Plant Physiology* **96**, 1193-1195
- Pyke, K.A. & Leech, R.M.** (1992) Chloroplast division and expansion is radically altered by nuclear mutations in *Arabidopsis thaliana*. *Plant Physiology* **99**, 1005-1008
- Pyke, K.A. & Leech, L.M.** (1994) *arc6*, A fertile *Arabidopsis* mutant with only mesophyll cell chloroplasts. *Plant Physiology* **106**, 1169-1177
- Quastler, H. & Sherman, F.G.** (1959) Cell population kinetics in the intestinal epithelium of the mouse. *Experimental Cell Research* **17**, 420-438
- Rayle, D.L. & Cleland, R.E.** (1977) Control of plant cell enlargement by hydrogen ions. *Current Topics in Developmental Biology* **11**, 187-214
- Renger, G., Völker, M., Eckert, H.J., Fromme, R., Hohm-Veit, S. & Gräber, P.** (1989) On the Mechanism of Photosystem II deterioration by UV-B irradiation. *Photochemistry and Photobiology* **49** (1), 97-105
- Reynold, E.S.** (1963) The use of lead citrate at high pH as an electron opaque stain in electron microscopy. *Journal of Cell Biology* **17**, 208-212
- Robertson, D. & Laetsch, W.M.** (1974) Structure and function of developing barley plastids. *Plant Physiology* **54**, 148-159

Robertson, E.J., Rutherford, S.M. & Leech, R.M. (1996) Characterization of chloroplast division using the Arabidopsis mutant *arc5*. *Plant Physiology* **112**, 149-159

Rogers, W.J., Jordan, B.R., Rawsthorne, S. & Tobin, A.K. (1991) Changes to the stoichiometry of glycine decarboxylase subunits during wheat (*Triticum aestivum* L.) and pea (*Pisum sativum* L.) leaf development. *Plant Physiology* **96**, 952-956

Ros, J. & Tevini, M. (1995) Interaction of UV-radiation and IAA during growth of seedlings and hypocotyl segments of sunflower. *Journal of Plant Physiology* **146**, 295-302

Rozema, J., van de Staay, J., Costa, V., Pereira, J.T., Broekman, R., Lenssen, G. & Stroetenga, M. (1991) A comparison of the growth, photosynthesis and transpiration of wheat and maize in response to enhanced ultraviolet-B radiation. In: *Impact of Global Climatic Changes on Photosynthesis and Plant Productivity*, (ed. Y.P. Arbol?) pp 163-174

Salawitch, R.J., Wofsy, S.C., Gottlieb, E.W., Lait, L.R., Newman, P.A., Schoeberl, M.R., Loewenstein, M., Podolske, J.R., Strahan, S.E., Proffitt, M.H., Webster, C.R., May, R.D., Fahey, D.W., Baumgardner, D., Dye, J.E., Wilson, J.C., Kelly, K.K., Elkins, J.W., Chan, K.R. & Anderson, J.G. (1993) Chemical loss of ozone in the Arctic polar vortex in the winter of 1991-1992. *Science* **261**, 1146-1149

Salisbury, F.B. & Ross, C.W. (1985) *Plant Physiology*. Wadsworth Publishing Company, California.

Sancar, A. (1994) Structure and function of DNA photolyase. *Biochemistry* **33**, 2-9

Santos, I., Almeida, J.M. & Salema, R. (1993) Plants of *Zea mays* L. developed under enhanced UV-B radiation. I. Some ultrastructural and biochemical aspects. *Journal of Plant Physiology* **141**, 450-456

Saralabai, V.C., Thamizhchelvan, P. & Santhaguru, K. (1989) Influence of ultraviolet-B radiation on fixation and assimilation of nitrogen in *Crotolaria juncea* L. *Indian Journal of Plant Physiology* **32**, 65-67

Schnyder, H. & Nelson, C.J. (1987) Growth rates and carbohydrate fluxes in the growth zone of tall fescue leaf blades. *Plant Physiology* **85**, 548-553

Schnyder, H. & Nelson, C.J. (1988) Diurnal growth of tall fescue leaf blades. I. Spatial distribution of growth, deposition of water, and assimilate import in the elongation zone. *Plant Physiology* **86**, 1070-1076

Schnyder, H. & Nelson, C.J. (1989) Growth rates and assimilate partitioning in the elongation zone of tall fescue leaf blades at high and low irradiance. *Plant Physiology* **90**, 1201-1206

Schnyder, H., Nelson, C.J. & Coutts, J.H. (1987) Assessment of spatial distribution of growth in the elongation zone of grass leaf blades. *Plant Physiology* **85**, 290-293

Schnyder, H., Seo, S., Rademacher, L.F. & Kühbauch, W. (1990) Spatial distribution of growth rates and of epidermal cell lengths in the elongation zone during leaf development in *Lolium perenne* L. *Planta* **181**, 423-431

Schoeberl, M.R. & Hartman, D.L. (1991) The dynamics of the stratospheric polar vortex and its relation to springtime ozone depletions. *Science* **251**, 46-52

Sechley, K.A., Yamaya, T. & Oaks, A. (1992) Compartmentation of nitrogen assimilation in higher plants. *International Review of Cytology* **134**, 85-163

Sekmeyer, G. & McKenzie, R.L. (1992) Increased ultraviolet radiation in New Zealand (45°S) relative to Germany (48°N). *Nature* **359**, 135-137

- Setlow, R.B. (1974)** The wavelengths in sunlight effective in producing skin cancer: a theoretical analysis. *Proceedings of the National Academy of Science USA* **71** (9), 3363-3366
- Sharman, B.C. (1942)** Developmental anatomy of the shoot of *Zea mays* L. *Annals of Botany* **1**, 245-282
- Silk, W.K. & Wagner, K.K. (1980)** Growth sustaining water potential distributions in the primary corn root. *Plant Physiology* **66**, 859-863
- Simon, E.W. & Chapman, J.A. (1961)** The development of mitochondria in *Arum* spadix. *Journal of Experimental Botany* **12** (36), 414-420
- Sinha, R.P., Kumar, H.D., Kumar, A. & Häder, D-P. (1995)** Effects of UV-B irradiation on growth, survival, pigmentation and nitrogen metabolism enzymes in cyanobacteria. *Acta Protozoologica* **34**, 187-192
- Skinner, R.H. & Nelson, C.J. (1994)** Epidermal cell division and the coordination of leaf and tiller development. *Annals of Botany* **74**, 9-15
- Smillie, R.M. (1962)** Photosynthetic and respiratory activities of growing pea leaves. *Plant Physiology* **37**, 716-721
- Solomon, S. (1988)** The mystery of the Antarctic ozone hole. *Review of Geophysics* **26**, 131-148
- Solomon, S. (1990)** Progress towards a quantitative understanding of Antarctic ozone depletion. *Nature* **347**, 347-354
- Solomon, S. & Albritton, D.L. (1992)** Time-dependant ozone depletion potentials for short- and long-term forecasts. *Nature* **357**, 33-37

- Solomos, T., Malhotra, S.S., Prasad, S., Malhotra, S.K. & Spencer, M.** (1972) Biochemical and structural changes in mitochondria and other cellular components of pea cotyledons during germination. *Canadian Journal of Biochemistry* **50**, 725-737
- Spollen, W.G. & Nelson, C.J.** (1988) Characterisation of fructan from mature leaf blades and elongation zones of developing leaf blades of wheat, tall fescue, and Timothy. *Plant Physiology* **88**, 1349-1353
- Spurr, A.R.** (1969) A low-viscosity epoxy resin embedding medium for electron microscopy. *Journal of Ultrastructural Research* **26**, 31-35
- Staxén, L., Bergounioux, C. & Bomman, J.F.** (1993) Effect of ultraviolet radiation on cell division and microtubule organization in *Petunia hybrida* protoplasts. *Protoplasma* **173**, 70-76
- Stapleton, A.E., Thorber, C.S. & Walbot, V.** (1997) UV-B component of sunlight causes measurable damage in field-grown maize (*Zea mays* L.): developmental and cellular heterogeneity of damage and repair. *Plant, Cell and Environment* **20**, 279-290
- Steer, M.W.** (1981) *Understanding Cell Structure*. Cambridge University Press, Cambridge
- Steeves, T.A. & Sussex, I.M.** (1989) *Patterns in plant development*. 2nd Edition. Cambridge University Press, Cambridge
- Steinmetz, V. & Wellmann, E.** (1986) The role of solar UV-B in growth regulation of cress (*Lepidium sativum* L.) seedling. *Photochemistry and Photobiology* **43**, 189-193
- Steinmüller, D.** (1986) On the effect of ultraviolet radiation (UV-B) on leaf surface structure and on the mode of action of cuticular lipid biosynthesis in some crop plants. *Karler. Beitr. Entw. Ökophysiol* **6**, 1-174

- Stolarski, R.S., Bloomfield, P., McPeters, R.D. & Herman, J.R.** (1991) Total ozone trends deduced from Nimbus TOMS data. *Geophysical Research Letters* **18**, 1015-1018
- Stolarski, R.S., Krueger, A.J., Schoeberl, M.R., McPeters, R.D., Newman, P.A. & Alpert, J.C.** (1986) Nimbus 7 satellite measurements of the springtime Antarctic ozone decrease. *Nature* **322**, 808-811
- Strid, Å.** (1993) Alteration in expression of defence genes in *Pisum sativum* after exposure to supplementary ultraviolet-B radiation. *Plant Cell Physiology* **34**, 475-489
- Strid, Å. & Porra, R.J.** (1992) Alterations in pigment content in leaves of *Pisum sativum* after exposure to supplementary UV-B. *Plant and Cell Physiology* **33**(7), 1015-1023
- Strid, Å., Chow, W.S. & Anderson, J.M.** (1990) Effects of supplementary ultraviolet-B radiation on photosynthesis in *Pisum sativum*. *Biochimica et Biophysica Acta* **1020**, 260-268
- Takeuchi, Y., Akizuki, M., Shimizu, H., Kondo, N. & Sugahara, K.** (1989) Effect of UV-B (290-320nm) irradiation on growth and metabolism of cucumber cotyledons. *Physiologia Plantarum* **76**, 425-430
- Taylor, R.M., Nikaido, O., Jordan, B.R., Rosamond, J., Bray, C.M. & Tobin, A.K.** (1996) Ultraviolet-B-induced DNA lesions and their removal in wheat (*Triticum aestivum* L.) leaves. *Plant, Cell and Environment* **19**, 171-181
- Teramura, A.H.** (1980) Effects of ultraviolet-B irradiances on soybean. I. Importance of photosynthetically active radiation in evaluating ultraviolet-B irradiance effects on soybean and wheat growth. *Physiologia Plantarum* **48**, 333-339
- Teramura, A.H.** (1983) Effects of ultraviolet-B radiation on the growth and yield of crop plants. *Physiologia Plantarum* **58**, 415-427

Teramura, A.H. & Caldwell, M.M. (1981) Effects of ultraviolet-B irradiances on soybean. IV. Leaf ontogeny as a factor in evaluating ultraviolet-B irradiance effects on net photosynthesis. *American Journal of Botany* **68** (7), 934-941

Teramura, A.H., Biggs, R.H. & Kossuth, S. (1980) Effects of ultraviolet-B irradiances on soybean. II. Interaction between ultraviolet-B and photosynthetically active radiation on net photosynthesis, dark respiration, and transpiration. *Plant Physiology* **65**, 483-488

Teramura, A.H., Perry, M.C., Lydon, J., McIntosh, M.S. & Summers, E.G. (1984) Effects of ultraviolet-B irradiation on plants during mild water stress. III. Effects on photosynthetic recovery and growth in soybean. *Physiologia Plantarum* **60**, 484-492

Teramura, A.H. & Sullivan, J.H. (1991) Potential impacts of increased solar UV-B on global plant productivity. In: *Photobiology*. (ed. E.Riklis), pp. 625-634, Plenum Press, New York

Teramura, A.H., Sullivan, J.H. & Lydon, J. (1990) Effects of UV-B radiation on soybean yield and seed quality: a 6-year field study. *Physiologia Plantarum* **80**, 5-11

Teramura, A.H., Sullivan, J.H. & Ziska, L.H. (1990) Interaction of elevated ultraviolet-B radiation and CO₂ on productivity and photosynthetic characteristics in wheat, rice, and soybean. *Plant Physiology* **94**, 470-475

Teramura, A.H., Tevini, M. & Iwanzik, W. (1983) Effects of ultraviolet-B irradiation on plants during mild water stress. I. Effects on diurnal stomatal resistance. *Physiologia Plantarum* **57**, 175-180

Teramura, A.H., Ziska, L.H. & Sztein, A.E. (1991) Changes in growth and photosynthetic capacity of rice with increased UV-B radiation. *Physiologia Plantarum* **83**, 373-380

Tevini, M. (1993) Effects of enhanced UV-B radiation on terrestrial plants. In: *UV-B Radiation and Ozone Depletion: Effects on Humans, Animals, Plants, Microorganisms and Materials* (ed. M. Tevini), pp. 125-153. Lewis Publishers, CRC Press, USA

Tevini, M. (1994) UV-B effects on terrestrial plants and aquatic organisms. In: *Progress in Botany*, Vol **55**, pp. 174-190. Springer-Verlag, Berlin

Tevini, M. & Iwanzik, W. (1986) Effects of UV-B radiation on growth and development of cucumber seedling. In: *Stratospheric ozone reduction, solar ultraviolet radiation and plant life*. Vol **G8** (eds. R.C.Worrest & M.M. Caldwell), pp. 271-285. Springer-Verlag, Berlin.

Tevini, M. & Teramura, A.H. (1989) UV-B effects on terrestrial plants. *Photochemistry and Photobiology* **50** (4), 479-487

Tevini, M., Iwanzik, W. & Teramura, A.H. (1983) Effects of UV-B radiation on plants during mild water stress. II. Effects on growth, protein, and flavonoid content. *Zeitschrift fur Pflanzenphysiologie* **110**, 459-467

Tevini, M., Iwanzik, W. & Thoma, U. (1981) Some effects of enhanced UV-B irradiation on the growth and composition of plants. *Planta* **153**, 388-394

Thomson, W.W. & Whatley, J.M. (1980) Development of non-green plastids. *Annual Review of Plant Physiology* **31**, 375-394

Tobin, A.K. (1992) Carbon and nitrogen metabolism: interactions during leaf development. In: *Topics in Photosynthesis- Vol 12* (ed. J. Barber), Crop photosynthesis: spatial and temporal determinants (eds. N.R.Baker & H.Thomas), pp. 381-412. Elsevier, Amsterdam

- Tobin, A.K. & Rogers, W.J.** (1992) Metabolic regulation of organelles during leaf development. In: *Plant Organelles*. Society for Experimental Biology Seminar Series, No. 50 (ed. A.K.Tobin), pp. 293-323, Cambridge University Press, Cambridge
- Tobin, A.K., Ridley, S.M., & Stewart, G.R.** (1985) Changes in the activities of chloroplast and cytosolic isoenzymes of glutamine synthetase during normal leaf growth and plastid development in wheat. *Planta* **163**, 544-548
- Tobin, A.K., Sumar, N. Patel, M., Moore, A.L. & Stewart, G.R.** (1988) Development of photorespiration during chloroplast biogenesis in wheat leaves. *Journal of Experimental Botany* **39**, 833-843
- Tobin, A.K., Thorpe, J.R., Hylton, C.M. & Rawsthorne, S.** (1989) Spatial and temporal influences on the cell-specific distribution of glycine decarboxylase in leaves of wheat (*Triticum aestivum* L.) and pea (*Pisum sativum* L.). *Plant Physiology* **91**, 1219-1225
- Topping, J.F. & Leaver, C.J.** (1990) Mitochondrial gene expression during wheat leaf development. *Planta* **182**, 399-407
- Toth, R.** (1982) An introduction to morphometric cytology and its application to botanical research. *American Journal of Botany* **69**(10), 1694-1706
- Tribe, M.A. & Ashurst, E.A.** (1972) Biochemical and structural variations in the flight muscle mitochondria of aging blowflies, *Calliphora erythrocephala*. *Cell Science* **10**, 443-469
- Utrilla, L., Sans, J. & De la Torre, C.** (1989) Colchicine-resistant assembly of tubulin in plant mitosis. *Protoplasma* **152**, 101-108
- van de Staaij, J.W.M., Ernst, W.H.O., Hakvoort, H.W.J. & Rozema, J.** (1995) Ultraviolet-B (280-320nm) absorbing pigments in the leaves of *Silene vulgaris* : their role in UV-B tolerance. *Journal of Plant Physiology* **147**, 75-80

- Van't Hof, J., Hoppin, D.P. & Yagi, S.** (1973) Cell arrest in G1 and G2 of the mitotic cycle of *Vicia faba* root meristems. *American Journal of Botany* **60** (9), 889-895
- Viro, M. & Kloppstech, K.** (1980) Differential expression of the genes for ribulose-1,5-bisphosphate carboxylase and light-harvesting chlorophyll a/b/ protein in the developing barley leaf. *Planta* **150**, 41-45
- Volenec, J.J. & Nelson, C.J.** (1981) Cell dynamics in leaf meristems of contrasting tall fescue genotypes. *Crop Science* **21**, 381-385
- Volenec, J.J. & Nelson, C.J.** (1983) Responses of tall fescue leaf meristems to N fertilization and harvest frequency. *Crop Science* **23**, 720-724
- Volenec, J.J. & Nelson, C.J.** (1984a) Carbohydrate metabolism in leaf meristems of tall fescue. I. Relationship to genetically altered leaf elongation rates. *Plant Physiology* **74**, 590-594
- Volenec, J.J. & Nelson, C.J.** (1984b) Carbohydrate metabolism in leaf meristems of tall fescue. II. Relationship to Leaf elongation rates modified by nitrogen fertilization. *Plant Physiology* **74**, 595-600
- Vu, C.V., Allen, L.H. & Garard, L.A.** (1984) Effects of enhanced UV-B radiation (280-320nm) on ribulose-1,5-bisphosphate carboxylase in pea and soybean. *Environmental and Experimental Botany* **24** (2), 131-143
- Walker, D.** (1990) *The use of the oxygen electrode and fluorescence probes in simple measurements of photosynthesis*. Oxygraphic Limited, Sheffield.
- Wallsgrave, R.M., Baron, A.C. & Tobin, A.K.** (1992) Carbon and nitrogen cycling between organelles during photorespiration. In: *Plant Organelles*. Society for Experimental Biology Seminar Series No. 50 (ed. A.K.Tobin), pp. 79-96. Cambridge University Press, Cambridge.

Wareing, P.F. & Phillips, I.D.J. (1981) *Growth and Differentiation in Plants*. Pergamon Press, Oxford.

Wamer, C.W. & Caldwell, M.M. (1983) Influence of photon flux density in the 400-700nm waveband on inhibition of photosynthesis by UV-B (280-320 nm) irradiation in soybean leaves: separation of indirect and immediate effects. *Photochemistry and Photobiology* **38**, 341-346

Webber, A.N., Baker, N.R., Platt-Aloia, K.A. & Thomson, W.W. (1984) Appearance of a state 1-state 2 transition during chloroplast development in the wheat leaf: energetic and structural considerations. *Physiologia Plantarum* **60**, 171-179

Webster, C.R., May, R.D., Toohey, D.W., Avallone, L.M., Anderson, J.G., Newman, P., Lait, L., Schoeberl, M.R., Elkins, J.W. & Chan, K.R. (1993) Chlorine chemistry on polar stratospheric cloud particles in the Arctic winter. *Science* **261**, 1130-1134

Weibel, E.R. (1969) Stereological principles for morphometry in electron microscopic cytology. *International Reviews of Cytology* **26**, 235-302

Weibel, E.R. & Bolender, R.P. (1973) Stereological techniques for electron microscopic morphometry. In: *Principles and Techniques of Electron Microscopy, Biological Applications, Vol (3)* (ed. M.A.Hayat), pp. 237-296. Van Nostrand Reinhold Company, New York

Wellmann, E. (1983) Photomorphogenesis. In: *Encyclopedia of Plant Physiology* (New Series) Vol. **16B** (eds. W.Shropshire & H.Mohr), pp. 745-756. Springer-Verlag, Berlin

Winter, H., Robinson, D.G. & Heldt, H.W. (1993) Subcellular volumes and metabolite concentrations in barley leaves. *Planta* **191**, 180-190

Wirth, M. & Renger, W. (1996) Evidence of large scale ozone depletion within the arctic polar vortex 94/95 based on airborne LIDAR measurements. *Geophysical Research Letters* **23** (8), 813-816

Witkin, E.M. (1976) Ultraviolet mutagenesis and inducible DNA repair in *Escherichia Coli*. *Bacteriology Review* **40**, 869-907

Witkowski, E.T.F. & Lamont, B.B. (1991) Leaf specific mass confound leaf density and thickness. *Oecologia* **88**, 486-493

www.nasa.gov (1997) unpublished

Zarema, T.G., LeBon, T.R., Millar, D.B., Smejkal, R.M. & Hawley, R.J. (1984) Effects of ultraviolet light on the in vivo assembly of microtubules. *Biochemistry* **23**, 1073-1080

Ziska, L.H., Teramura, A.H., Sullivan, J.H. & McCoy, A. (1993) Influence of ultraviolet-B (UV-B) radiation on photosynthetic and growth characteristics in field-grown cassava (*Manihot esculentum* Crantz). *Plant, Cell and Environment* **16**, 73-79